

# Survey of Period Variations of Superhumps in SU UMa-Type Dwarf Novae. IX: The Ninth Year (2016–2017)

Taichi KATO,<sup>1\*</sup> Keisuke ISOGAI,<sup>1</sup> Franz-Josef HAMBACH,<sup>2,3,4</sup>  
Tonny VANMUNSTER,<sup>5</sup> Hiroshi ITOH,<sup>6</sup> Berto MONARD,<sup>7,8</sup> Tamás TORDAI,<sup>9</sup>  
Mariko KIMURA,<sup>1</sup> Yasuyuki WAKAMATSU,<sup>1</sup> Seiichiro KIYOTA,<sup>10</sup>  
Ian MILLER,<sup>11</sup> Peter STARR,<sup>12</sup> Kiyoshi KASAI,<sup>13</sup> Sergey Yu. SHUGAROV,<sup>14,15</sup>  
Drahomir CHOCHOL,<sup>15</sup> Natalia KATYSHEVA,<sup>14</sup> Anna M. ZASTROJNYKH,<sup>16</sup>  
Matej SEKERÁŠ,<sup>15</sup> Yuliana G. KUZNYETSOVA,<sup>17</sup> Eugenia S. KALINICHEVA,<sup>18</sup>  
Polina GOLYSHEVA,<sup>14</sup> Viktoriia KRUSHEVSKA,<sup>17</sup> Yutaka MAEDA,<sup>19</sup>  
Pavol A. DUBOVSKY,<sup>20</sup> Igor KUDZEJ,<sup>20</sup> Elena P. PAVLENKO,<sup>21,22</sup>  
Kirill A. ANTONYUK,<sup>21</sup> Nikolaj V. PIT,<sup>21</sup> Aleksei A. SOSNOVSKIJ,<sup>21</sup>  
Oksana I. ANTONYUK,<sup>21</sup> Aleksei V. BAKLANOV,<sup>21</sup> Roger D. PICKARD,<sup>23,24</sup>  
Naoto KOJIGUCHI,<sup>25</sup> Yuki SUGIURA,<sup>25</sup> Shihei TEI,<sup>25</sup> Kenta YAMAMURA,<sup>25</sup>  
Katsura MATSUMOTO,<sup>25</sup> Javier RUIZ,<sup>26,27,28</sup> Geoff STONE,<sup>29</sup>  
Lewis M. COOK,<sup>30</sup> Enrique de MIGUEL,<sup>31,32</sup> Hidehiko AKAZAWA,<sup>33</sup>  
William N. GOFF,<sup>34</sup> Etienne MORELLE,<sup>35</sup> Stella KAFKA,<sup>29</sup>  
Colin LITTLEFIELD,<sup>36</sup> Greg BOLT,<sup>37</sup> Franky DUBOIS,<sup>38</sup>  
Stephen M. BRINCAT,<sup>39</sup> Hiroyuki MAEHARA,<sup>40</sup> Takeshi SAKANOI,<sup>41</sup>  
Masato KAGITANI,<sup>41</sup> Akira IMADA,<sup>42,43</sup> Irina B. VOLOSHINA,<sup>14</sup>  
Maksim V. ANDREEV,<sup>44,45</sup> Richard SABO,<sup>46</sup> Michael RICHMOND,<sup>47</sup>  
Tony RODDA,<sup>48</sup> Peter NELSON,<sup>49</sup> Sergey NAZAROV,<sup>21</sup>  
Nikolay MISHEVSKIY,<sup>29</sup> Gordon MYERS,<sup>50</sup> Denis DENISENKO,<sup>14</sup>  
Krzysztof Z. STANEK,<sup>51</sup> Joseph V. SHIELDS,<sup>51</sup> Christopher S. KOCHANEK,<sup>51</sup>  
Thomas W.-S. HOLOIEN,<sup>51</sup> Benjamin SHAPPEE,<sup>52</sup> José L. PRIETO,<sup>53,54</sup>  
Koh-ichi ITAGAKI,<sup>55</sup> Koichi NISHIYAMA,<sup>56</sup> Fujio KABASHIMA,<sup>56</sup>  
Rod STUBBINGS,<sup>57</sup> Patrick SCHMEER,<sup>58</sup> Eddy MUYLLAERT,<sup>59</sup>  
Tsuneo HORIE,<sup>60</sup> Jeremy SHEARS,<sup>61,23</sup> Gary POYNER,<sup>62</sup>  
Masayuki MORIYAMA,<sup>63</sup>

<sup>1</sup> Department of Astronomy, Kyoto University, Kyoto 606-8502, Japan

<sup>2</sup> Groupe Européen d'Observations Stellaires (GEOS), 23 Parc de Levesville, 28300 Bailleul l'Evêque, France

<sup>3</sup> Bundesdeutsche Arbeitsgemeinschaft für Veränderliche Sterne (BAV), Munsterdamm 90, 12169 Berlin, Germany

<sup>4</sup> Vereniging Voor Sterrenkunde (VVS), Oude Bleken 12, 2400 Mol, Belgium

<sup>5</sup> Center for Backyard Astrophysics Belgium, Walhostraat 1A, B-3401 Landen, Belgium

<sup>6</sup> Variable Star Observers League in Japan (VSOLJ), 1001-105 Nishiterakata, Hachioji, Tokyo 192-0153, Japan

<sup>7</sup> Bronberg Observatory, Center for Backyard Astrophysics Pretoria, PO Box 11426,

- Tiegerpoort 0056, South Africa
- <sup>8</sup> Kleinkaroo Observatory, Center for Backyard Astrophysics Kleinkaroo, Sint Helena 1B, PO Box 281, Calitzdorp 6660, South Africa
- <sup>9</sup> Polaris Observatory, Hungarian Astronomical Association, Laborc utca 2/c, 1037 Budapest, Hungary
- <sup>10</sup> VSOLJ, 7-1 Kitahatsutomi, Kamagaya, Chiba 273-0126, Japan
- <sup>11</sup> Furzehill House, Ilston, Swansea, SA2 7LE, UK
- <sup>12</sup> Warrumbungle Observatory, Tenby, 841 Timor Rd, Coonabarabran NSW 2357, Australia
- <sup>13</sup> Baselstrasse 133D, CH-4132 Muttenz, Switzerland
- <sup>14</sup> Sternberg Astronomical Institute, Lomonosov Moscow State University, Universitetsky Ave., 13, Moscow 119992, Russia
- <sup>15</sup> Astronomical Institute of the Slovak Academy of Sciences, 05960 Tatranska Lomnica, Slovakia
- <sup>16</sup> Institute of Physics, Kazan Federal University, Ulitsa Kremlevskaya 16a, Kazan 420008, Russia
- <sup>17</sup> Main Astronomical Observatory of National Academy of Sciences of Ukraine, 27 Akademika Zabolotnoho St., Kyiv 03143, Ukraine
- <sup>18</sup> Faculty of Physics, Lomonosov Moscow State University, Leninskie gory, Moscow 119991, Russia
- <sup>19</sup> Kaminishiyamamachi 12-14, Nagasaki, Nagasaki 850-0006, Japan
- <sup>20</sup> Vihorlat Observatory, Mierova 4, 06601 Humenne, Slovakia
- <sup>21</sup> Federal State Budget Scientific Institution “Crimean Astrophysical Observatory of RAS”, Nauchny, 298409, Republic of Crimea
- <sup>22</sup> V. I. Vernadsky Crimean Federal University, 4 Vernadskogo Prospekt, Simferopol, 295007, Republic of Crimea
- <sup>23</sup> The British Astronomical Association, Variable Star Section (BAA VSS), Burlington House, Piccadilly, London, W1J 0DU, UK
- <sup>24</sup> 3 The Birches, Shobdon, Leominster, Herefordshire, HR6 9NG, UK
- <sup>25</sup> Osaka Kyoiku University, 4-698-1 Asahigaoka, Osaka 582-8582, Japan
- <sup>26</sup> Observatorio de Cantabria, Ctra. de Rocamundo s/n, Valderredible, 39220 Cantabria, Spain
- <sup>27</sup> Instituto de Física de Cantabria (CSIC-UC), Avenida Los Castros s/n, E-39005 Santander, Cantabria, Spain
- <sup>28</sup> Agrupación Astronómica Cantabria, Apartado 573, 39080, Santander, Spain
- <sup>29</sup> American Association of Variable Star Observers, 49 Bay State Rd., Cambridge, MA 02138, USA
- <sup>30</sup> Center for Backyard Astrophysics Concord, 1730 Helix Ct. Concord, California 94518, USA
- <sup>31</sup> Departamento de Ciencias Integradas, Facultad de Ciencias Experimentales, Universidad de Huelva, 21071 Huelva, Spain
- <sup>32</sup> Center for Backyard Astrophysics, Observatorio del CIECEM, Parque Dunar, Matalascañas, 21760 Almonte, Huelva, Spain
- <sup>33</sup> Department of Biosphere-Geosphere System Science, Faculty of Informatics, Okayama University of Science, 1-1 Ridai-cho, Okayama, Okayama 700-0005, Japan
- <sup>34</sup> 13508 Monitor Ln., Sutter Creek, California 95685, USA
- <sup>35</sup> 9 rue Vasco de GAMA, 59553 Lauwin Planque, France
- <sup>36</sup> Department of Physics, University of Notre Dame, 225 Nieuwland Science Hall, Notre Dame, Indiana 46556, USA
- <sup>37</sup> Camberwarra Drive, Craigie, Western Australia 6025, Australia
- <sup>38</sup> Public observatory Astrolab Iris, Verbrandemolenstraat 5, B 8901 Zillebeke, Belgium
- <sup>39</sup> Flarestar Observatory, San Gwann SGN 3160, Malta
- <sup>40</sup> Okayama Astrophysical Observatory, National Astronomical Observatory of Japan,

Asakuchi, Okayama 719-0232, Japan

<sup>41</sup> Planetary Plasma and Atmospheric Research Center, Graduate School of Science, Tohoku University, Sendai 980-8578, Japan

<sup>42</sup> Hamburger Sternwarte, Universität Hamburg, Gojenbergsweg 112, D-21029 Hamburg, Germany

<sup>43</sup> Kwasan and Hida Observatories, Kyoto University, Yamashina, Kyoto 607-8471, Japan

<sup>44</sup> Terskol Branch of Institute of Astronomy, Russian Academy of Sciences, 361605, Peak Terskol, Kabardino-Balkaria Republic, Russia

<sup>45</sup> International Center for Astronomical, Medical and Ecological Research of NASU, Ukraine  
27 Akademika Zabolotnoho Str. 03680 Kyiv, Ukraine

<sup>46</sup> 2336 Trailcrest Dr., Bozeman, Montana 59718, USA

<sup>47</sup> Physics Department, Rochester Institute of Technology, Rochester, New York 14623, USA

<sup>48</sup> 1, Rivermede, Ponteland, Newcastle upon Tyne, NE20 9XA, UK

<sup>49</sup> 1105 Hazeldean Rd, Ellinbank 3820, Australia

<sup>50</sup> Center for Backyard Astrophysics San Mateo, 5 invernness Way, Hillsborough, CA 94010, USA

<sup>51</sup> Department of Astronomy, the Ohio State University, Columbia, OH 43210, USA

<sup>52</sup> Carnegie Observatories, 813 Santa Barbara Street, Pasadena, CA 91101, USA

<sup>53</sup> Núcleo de Astronomía de la Facultad de Ingeniería, Universidad Diego Portales, Av. Ejército 441, Santiago, Chile

<sup>54</sup> Department of Astrophysical Sciences, Princeton University, NJ 08544, USA

<sup>55</sup> Itagaki Astronomical Observatory, Teppo-cho, Yamagata 990-2492

<sup>56</sup> Miyaki-Argenteus Observatory, Miyaki, Saga 840-1102, Japan

<sup>57</sup> Tetoora Observatory, 2643 Warragul-Korumburra Road, Tetoora Road, Victoria 3821, Australia

<sup>58</sup> Bischmisheim, Am Probstbaum 10, 66132 Saarbrücken, Germany

<sup>59</sup> Vereniging Voor Sterrenkunde (VVS), Moffelstraat 13 3370 Boutersem, Belgium

<sup>60</sup> 759-10 Tokawa, Hadano-shi, Kanagawa 259-1306, Japan

<sup>61</sup> “Pemberton”, School Lane, Bunbury, Tarporley, Cheshire, CW6 9NR, UK

<sup>62</sup> BAA Variable Star Section, 67 Ellerton Road, Kingstanding, Birmingham B44 0QE, UK

<sup>63</sup> 290-383, Ogata-cho, Sasebo, Nagasaki 858-0926, Japan

\*E-mail: \*tkato@kusastro.kyoto-u.ac.jp

Received 201 0; Accepted 201 0

## Abstract

Continuing the project described by Kato et al. (2009, PASJ, 61, S395), we collected times of superhump maxima for 127 SU UMa-type dwarf novae observed mainly during the 2016–2017 season and characterized these objects. We provide updated statistics of relation between the orbital period and the variation of superhumps, the relation between period variations and the rebrightening type in WZ Sge-type objects. We obtained the period minimum of 0.05290(2) d and confirmed the presence of the period gap above the orbital period  $\sim 0.09$  d. We note that four objects (NY Her, 1RXS J161659.5+620014, CRTS J033349.8–282244 and SDSS J153015.04+094946.3) have supercycles shorter than 100 d but show infrequent normal outbursts. We consider that these objects are similar to V503 Cyg, whose normal outbursts are likely suppressed by a disk tilt. These four objects are excellent candidates to search for negative superhumps. DDE 48 appears to be a member of ER UMa-type dwarf novae. We identified a new eclipsing SU UMa-type object MASTER OT J220559.40–341434.9. We observed 21 WZ Sge-type dwarf novae during this interval and reported 18 out of them in this paper. Among them, ASASSN-16js is a good candidate for a period bouncer. ASASSN-16ia showed a precursor outburst for the first time in a WZ Sge-type superoutburst. ASASSN-16kg,

CRTS J000130.5+050624 and SDSS J113551.09+532246.2 are located in the period gap. We have newly obtained 15 orbital periods, including periods from early superhumps.

**Key words:** accretion, accretion disks — stars: novae, cataclysmic variables — stars: dwarf novae

## 1 Introduction

This is a continuation of series of papers Kato et al. (2009), Kato et al. (2010), Kato et al. (2012a), Kato et al. (2013), Kato et al. (2014b), Kato et al. (2014a), Kato et al. (2015a) and Kato et al. (2016a) reporting new observations of superhumps in SU UMa-type dwarf novae. SU UMa-type dwarf novae are a class of cataclysmic variables (CVs) which are close binary systems transferring matter from a low-mass dwarf secondary to a white dwarf, forming an accretion disk [see e.g. Warner (1995) for CVs in general].

In SU UMa-type dwarf novae, there are two types of outbursts (normal outbursts and superoutbursts). Outbursts and superoutbursts in SU UMa-type dwarf novae are considered to be a result of the combination of thermal and tidal instabilities [thermal-tidal instability (TTI) model by Osaki (1989); Osaki (1996)].

During superoutbursts, semi-periodic variations called superhumps are observed whose period (superhump period,  $P_{SH}$ ) is a few percent longer than the orbital period ( $P_{orb}$ ). Superhumps are considered to originate from a precessing eccentric (or flexing) disk in the gravity field of the rotating binary, and the eccentricity in the disk is believed to be a consequence of the 3:1 resonance in the accretion disk [see e.g. Whitehurst (1988); Hirose and Osaki (1990); Lubow (1991); Wood et al. (2011)].

It has become evident since Kato et al. (2009) that the superhump periods systematically vary in a way common to many objects. Kato et al. (2009) introduced superhump stages (stages A, B and C): initial growing stage with a long period (stage A) and fully developed stage with a systematically varying period (stage B) and later stage C with a shorter, almost constant period (see figure 1).

It has recently been proposed by Osaki and Kato (2013b) that stage A superhumps reflect the dynamical precession rate at the 3:1 resonance radius and that the rapid decrease of the period (stage B) reflects the pressure effect which has an effect of retrograde precession (Lubow 1992; Hirose and Osaki 1993; Murray 1998; Montgomery 2001; Pearson 2006). As proposed by Kato and Osaki (2013) stage A superhumps can be then used to “dynamically” determine the mass ratio ( $q$ ), which had been difficult to measure except for eclipsing systems and systems with bright secondaries to detect radial-velocity variations. It has been confirmed that this stage A method gives  $q$  values as precise as in eclipsing systems. There

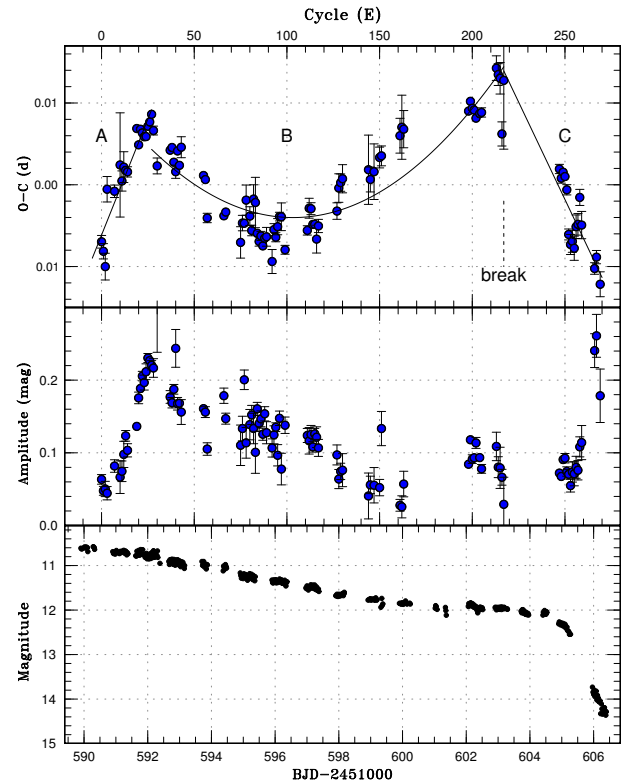


**Fig. 1.** Representative  $O - C$  diagram showing three stages (A–C) of  $O - C$  variation. The data were taken from the 2000 superoutburst of SW UMa. (Upper:  $O - C$  diagram. Three distinct stages (A – evolutionary stage with a longer superhump period, B – middle stage, and C – stage after transition to a shorter period) and the location of the period break between stages B and C are shown. (Middle: Amplitude of superhumps. During stage A, the amplitude of the superhumps grew. (Lower: Light curve. (Reproduction of figure 1 in Kato and Osaki 2013)

have been more than 50 objects whose  $q$  values are determined by this method and it has been proven to be an especially valuable tool in depicting the terminal stage of CV evolution (cf. Kato et al. 2015a; Kato 2015).

In this paper, we present new observations of SU UMa-type dwarf novae mainly obtained in 2016–2017. We present basic observational materials and discussions in relation to individual objects. Starting from Kato et al. (2014a), we have been intending these series of papers to be also a source of compiled information, including historical, of individual dwarf novae.

The material and methods of analysis are given in section 2, observations and analysis of individual objects are given in section 3, including discussions particular to the

objects. General discussions are given in section 4 and the summary is given in section 5. Some tables and figures are available online only.

## 2 Observation and Analysis

### 2.1 Data Source

The data were obtained under campaigns led by the VSNET Collaboration (Kato et al. 2004). We also used the public data from the AAVSO International Database<sup>1</sup>. Outburst detections of many new and known objects relied on the ASAS-SN CV patrol (Davis et al. 2015)<sup>2</sup>, the MASTER network (Gorbovskoy et al. 2013), and Catalina Real-time Transient Survey (CRTS; Drake et al. 2009)<sup>3</sup> in addition to outburst detections reported to VSNET, AAVSO<sup>4</sup>, BAAVSS alert<sup>5</sup> and cvnet-outburst.<sup>6</sup>

For objects detected in CRTS, we preferably used the names provided in Drake et al. (2014) and Coppejans et al. (2016). If these names are not yet available, we used the International Astronomical Union (IAU)-format names provided by the CRTS team in the public data release<sup>7</sup> Since Kato et al. (2009), we have used coordinate-based optical transient (OT) designations for some objects, such as apparent dwarf nova candidates reported in the Transient Objects Confirmation Page of the Central Bureau for Astronomical Telegrams<sup>8</sup> and CRTS objects without registered designations in Drake et al. (2014) or in the CRTS public data release and listed the original identifiers in table 1.

We provided coordinates from astrometric catalogs for ASAS-SN (Shappee et al. 2014) CVs and two objects without precise coordinate-based names other than listed in the General Catalog of Variable Stars (Kholopov et al. 1985) in table 2. We mainly used Gaia DR1 (Gaia Collaboration 2016), Sloan Digital Sky Survey (SDSS, Ahn et al. 2012), the Initial Gaia Source List (IGSL, Smart 2013) and Guide Star Catalog 2.3.2 (GSC 2.3.2, Lasker et al. 2007). Some objects were detected as transients by Gaia<sup>9</sup> and CRTS and we used their coordinates. The coordinates used in this paper are J2000.0. We also supplied SDSS  $g$ , Gaia  $G$  and GALEX NUV magnitudes when counterparts are present.

<sup>1</sup> <<http://www.aavso.org/data-download>>.

<sup>2</sup> <<http://cv.asassn.astronomy.ohio-state.edu/>>.

<sup>3</sup> <<http://nesssi.cacr.caltech.edu/catalina/>>. For the information of the individual Catalina CVs, see <<http://nesssi.cacr.caltech.edu/catalina/AIICV.html>>.

<sup>4</sup> <<https://www.aavso.org/>>.

<sup>5</sup> <<https://groups.yahoo.com/neo/groups/baavss-alert/>>.

<sup>6</sup> <<https://groups.yahoo.com/neo/groups/cvnet-outburst/>>.

<sup>7</sup> <<http://nesssi.cacr.caltech.edu/DataRelease/>>.

<sup>8</sup> <<http://www.cbat.eps.harvard.edu/unconf/tocp.html>>.

<sup>9</sup> <<http://gsaweb.ast.cam.ac.uk/alerts/alertsindex>> and Gaia identifications supplied by the AAVSO VSX.

### 2.2 Observations and Basic Reduction

The majority of the data were acquired by time-resolved CCD photometry by using 20–60cm telescopes located world-wide. The list of outbursts and observers is summarized in table 1. The data analysis was performed in the same way described in Kato et al. (2009) and Kato et al. (2014a) and we mainly used R software<sup>10</sup> for data analysis.

In de-trending the data, we mainly used locally-weighted polynomial regression (LOWESS: Cleveland 1979) and sometimes lower (1–3rd order) polynomial fitting when the observation baseline was short. The times of superhumps maxima were determined by the template fitting method as described in Kato et al. (2009). The times of all observations are expressed in barycentric Julian days (BJD).

In figures, the points are accompanied by  $1\sigma$  error bars whenever available, which are omitted when the error is smaller than the plot mark or the errors were not available (as in some raw light curves of superhumps).

### 2.3 Abbreviations and Terminology

The abbreviations used in this paper are the same as in Kato et al. (2014a): we used  $\epsilon \equiv P_{\text{SH}}/P_{\text{orb}} - 1$  for the fractional superhump excess. We have used since Osaki and Kato (2013a) the alternative fractional superhump excess in the frequency unit  $\epsilon^* \equiv 1 - P_{\text{orb}}/P_{\text{SH}} = \epsilon/(1 + \epsilon)$  because this fractional superhump excess is a direct measure of the precession rate. We therefore used  $\epsilon^*$  in discussing the precession rate.

The  $P_{\text{SH}}$ ,  $P_{\text{dot}}$  and other parameters are listed in table 3 in same format as in Kato et al. (2009). The definitions of parameters  $P_1$ ,  $P_2$ ,  $E_1$ ,  $E_2$  and  $P_{\text{dot}}$  are the same as in Kato et al. (2009):  $P_1$  and  $P_2$  represent periods in stage B and C, respectively ( $P_1$  is averaged during the entire course of the observed segment of stage B), and  $E_1$  and  $E_2$  represent intervals (in cycle numbers) to determine  $P_1$  and  $P_2$ , respectively.<sup>11</sup> Some superoutbursts are not listed in table 3 due to the lack of observations (e.g. single-night observations with less than two superhump maxima or poor observations for the object with already well measured  $P_{\text{SH}}$ ).

We used the same terminology of superhumps summarized in Kato et al. (2012a). We especially call attention to the term “late superhumps”. We only used the concept of “traditional” late superhumps when there is

<sup>10</sup>The R Foundation for Statistical Computing:

<<http://cran.r-project.org/>>.

<sup>11</sup>The intervals ( $E_1$  and  $E_2$ ) for the stages B and C given in the table sometimes overlap because there is sometimes observational ambiguity (usually due to the lack of observations and errors in determining the times of maxima) in determining the stages.

an  $\sim 0.5$  phase shift [Vogt (1983); see also table 1 in Kato et al. (2012a) for various types of superhumps], since we suspect that many of the past claims of detections of “late superhumps” were likely stage C superhumps before it became evident that there are complex structures in the  $O - C$  diagrams of superhumps (see discussion in Kato et al. 2009).

## 2.4 Period Analysis

We used phase dispersion minimization (PDM; Stellingwerf 1978) for period analysis and  $1\sigma$  errors for the PDM analysis was estimated by the methods of Fernie (1989) and Kato et al. (2010). We have used a variety of bootstrapping in estimating the robustness of the result of the PDM analysis since Kato et al. (2012a). We analyzed 100 samples which randomly contain 50% of observations, and performed PDM analysis for these samples. The bootstrap result is shown as a form of 90% confidence intervals in the resultant PDM  $\theta$  statistics. If this paper provides the first solid presentation of a new SU UMa-type classification, we provide the result of PDM period analysis and averaged superhump profile.

## 2.5 $O - C$ Diagrams

Comparisons of  $O - C$  diagrams between different superoutbursts are also presented whenever available. This figure not only provides information about the difference of  $O - C$  diagrams between different superoutbursts but also helps identifying superhump stages especially when observations were insufficient or the start of the outburst was missed. In drawing combined  $O - C$  diagrams, we usually used  $E = 0$  for the start of the superoutburst, which usually refers to the first positive detection of the outburst. This epoch usually has an accuracy of  $\sim 1$  d for well-observed objects, and if the outburst was not sufficiently observed, we mentioned in the figure caption how to estimate  $E$  in such an outburst. In some cases, this  $E = 0$  is defined as the appearance of superhumps. This treatment is necessary since some objects have a long waiting time before appearance of superhumps. We also note that there is sometimes an ambiguity in selecting the true period among aliases. In some cases, this can be resolved by the help of the  $O - C$  analysis. The procedure and example are shown in subsection 2.2 in Kato et al. (2015a).

## 3 Individual Objects

### 3.1 V1047 Aquilae

V1047 Aql was discovered as a dwarf nova (S 8191) by Hoffmeister (1964). Hoffmeister (1964) reported a blue color in contrast to the nearby stars. Mason and Howell (2003) obtained a spectrum typical for a quiescent dwarf nova. According to R. Stubbings, the observation by Greg Bolt during the 2005 August outburst detected superhumps, and the superhump period was about 0.074 d (see Kato et al. 2012b). The object shows rather frequent outbursts (approximately once in 50 d), and a number of outbursts have been detected mainly by R. Stubbings visually since 2004.

The 2016 superoutburst was detected by R. Stubbings at a visual magnitude of 15.0 on July 8. Subsequent observations detected superhumps (vsnet-alert 19974; figure 2). Using the 2005 period, we could identify two maxima on two nights:  $E=0$ , BJD 2457581.3853(7) ( $N=74$ ) and  $E=14$ , BJD 2457582.4190(11) ( $N=72$ ). The period given in table 3 is determined by the PDM method.

Although observations are not sufficient, visual observations by R. Stubbings suggest a supercycle of  $\sim 90$  d, which would make V1047 Aql one of ordinary SU UMa-type dwarf novae with shortest supercycles.

### 3.2 BB Arietis

This object was discovered as a variable star (Ross 182, NSV 907) on a plate on 1926 November 26 (Ross 1927). The dwarf nova-type nature was suspected by the association with an ROSAT source (Kato, vsnet-chat 3317). The SU UMa-type nature was confirmed during the 2004 superoutburst. For more information, see Kato et al. (2014a).

The 2016 superoutburst was detected by P. Schmeer at a visual magnitude of 13.2 on October 30 (vsnet-alert 20273). Thanks to the early detection (this visual detection was 1 d earlier than the ASAS-SN detection), stage A growing superhumps were detected (vsnet-alert 20292). At the time of the initial observation, the object was fading from a precursor outburst. Further observations recorded development of superhumps clearly (vsnet-alert 20312, 20321). The times of superhump maxima are listed in table 4. There were clear stages A–C (figure 3). The 2013 superoutburst had a separate precursor outburst and a comparison of the  $O - C$  diagrams suggests a difference of 44 cycle count from that used in Kato et al. (2014a). The value suggests that superhumps during the 2013 superoutburst evolved 3 d after the precursor outburst.

**Table 1.** List of Superoutbursts.

Subsection	Object	Year	Observers or references*	ID <sup>†</sup>
3.1	V1047 Aql	2016	Trt	
3.2	BB Ari	2016	Kis, AAVSO, SRI, RPc, Ioh, Shu, RAE	
3.3	V391 Cam	2017	Trt, DPV	
3.4	OY Car	2016	SPE, HaC, MGW	
–	HT Cas	2016	Y. Wakamatsu et al. in preparation	
3.5	GS Cet	2016	Kis, OKU, HaC, Shu, CRI, KU, Ioh, Trt	
3.6	GZ Cet	2016	OKU	
3.7	AK Cnc	2016	Aka	
3.8	GZ Cnc	2017	KU, Mdy, HaC	
3.9	GP CVn	2016	RPc, Kai, Trt, IMi, Kis, CRI, deM, AAVSO	
3.10	V337 Cyg	2016	Kai	
3.11	V1113 Cyg	2016	OKU, Ioh, Kis	
3.12	IX Dra	2016	Kis, SGE, COO	

\*Key to observers: Aka (H. Akazawa, OUS), BSM<sup>†</sup>(S. Brincat), COO (L. Cook), CRI (Crimean Astrophys. Obs.), DDe (D. Denisenko), deM (E. de Miguel), DPV (P. Dubovsky), Dub (F. Dubois team), GBo (G. Bolt), GFB<sup>‡</sup>(W. Goff), HaC (F.-J. Hambusch, remote obs. in Chile), IMi<sup>†</sup>(I. Miller), Ioh (H. Itoh), KU (Kyoto U., campus obs.), Kai (K. Kasai), Kis (S. Kiyota), LCO (C. Littlefield), MEV<sup>†</sup>(E. Morelle), NGW (G. Myers), MLF (B. Monard), MNI (N. Mishevskiy), Mdy (Y. Maeda), Mhh (H. Maehara), NKa (N. Katysheva and S. Shugarov), Naz (S. Nazarov), Nel (P. Nelson), OKU (Osaya Kyoiku U.), RAE (T. Rodda), RIT (M. Richmond), RPc<sup>‡</sup>(R. Pickard), Rui (J. Ruiz), SGE<sup>‡</sup>(G. Stone), SPE<sup>‡</sup>(P. Starr), SRI<sup>‡</sup>(R. Sabo), Shu (S. Shugarov team), T60 (Haleakala Obs. T60 telescope), Trt (T. Tordai), Van (T. Vanmunster), Vol (I. Voloshina), AAVSO (AAVSO database)

<sup>†</sup>Original identifications, discoverers or data source.

<sup>‡</sup>Inclusive of observations from the AAVSO database.

### 3.3 V391 Camelopardalis

This object (=1RXS J053234.9+624755) was discovered as a dwarf nova by Bernhard et al. (2005). Kapusta and Thorstensen (2006) provided a radial-velocity study and yielded an orbital period of 0.05620(4) d. The SU UMa-type nature was established during the 2005 superoutburst (Imada et al. 2009). See Kato et al. (2009) for more history. The 2009 superoutburst was also studied in Kato et al. (2010).

The 2017 superoutburst was detected by P. Schmeer at a visual magnitude of 11.4 and also by the ASAS-SN team at  $V=11.82$  on March 15. Single superhump was recorded at BJD 2457829.3171(2) ( $N=236$ ). Although there were observations on three nights immediately after the superoutburst, we could neither detect superhump nor orbital periods.

### 3.4 OY Carinae

See Kato et al. (2015a) for the history of this well-known eclipsing SU UMa-type dwarf nova. The 2016 superoutburst was detected by R. Stubbings at a visual magnitude of 11.6 on April 2 (vsnet-alert 19676). Due to an accidental delay in the start of observations, the earliest time-resolved CCD observations were obtained on April 3 (vsnet-alert 19706). On that night, superhumps (likely in the growing phase) unfortunately overlapped with eclipses (figure 4, upper panel). Distinct superhumps were recorded on April 4 (vsnet-alert 19692; figure 4, middle panel). A further analysis suggested that stage A superhumps escaped detection before April 4 (due to the lack of observations and overlapping eclipses). At the time of April 4, the superhumps were already likely stage B (table 5, maxima outside eclipses). We could, however, confirm a positive  $P_{\text{dot}}$  for stage B superhumps (cf. figure 5), whose confirmation had been still awaited (cf. Kato et al. 2015a).

The combined data used in Kato et al. (2015a) and new

**Table 1.** List of Superoutbursts (continued).

Subsection	Object	Year	Observers or references*	ID <sup>†</sup>
3.13	IR Gem	2016	Kai, Aka, CRI, BSM, AAVSO, Trt	
		2017	Kai, Trt	
3.14	NY Her	2016	GFB, Ioh, DPV, Trt, COO, IMi, SGE	
3.15	MN Lac	2016	Van	
3.16	V699 Oph	2016	Kis, Ioh	
3.17	V344 Pav	2016	HaC	
3.18	V368 Peg	2016	Trt	
3.19	V893 Sco	2016	GBo, HaC, Kis, Aka	
3.20	V493 Ser	2016	Shu	
3.21	AW Sge	2016	DPV	
3.22	V1389 Tau	2016	HaC, KU, Ioh	
3.23	SU UMa	2017	Trt	
3.24	HV Vir	2016	HaC, DPV, AAVSO, deM, Mdy, KU, RPe, GBo, Aka, IMi, BSM, Kis	
3.25	NSV 2026	2016b	Trt, Dub	
3.26	NSV 14681	2016	Van	
3.27	1RXS J161659	2016 2016b	deM, MEV, IMi, Van, Trt MEV, DPV, IMi	1RXS J161659.5+620014
3.28	ASASSN-13ak	2016	Trt, Kis	
3.29	ASASSN-13al	2016	Van	
3.30	ASASSN-13bc	2015 2016	LCO, Rui, Trt SGE, Shu, NKa, Ioh, Rui	
3.31	ASASSN-13bj	2016	Kai, OKU, Trt, SGE, DPV, IMi, KU	
3.32	ASASSN-13bo	2016	IMi, Shu	
3.33	ASASSN-13cs	2016	SGE, KU, COO	
3.34	ASASSN-13cz	2016	Kai, Trt, Rui, DPV	
3.35	ASASSN-14gg	2016	Van, GFB	

observations, we have obtained the eclipse ephemeris for the use of defining the orbital phases in this paper using the MCMC analysis (Kato et al. 2013):

$$\text{Min(BJD)} = 2457120.49413(2) + 0.0631209131(5)E. \quad (1)$$

The epoch corresponds to the center of the entire observation. The mean period, however, did not show a secular decrease (e.g. Han et al. 2015; Kato et al. 2015a). It may be that period changes in this system are sporadic and do not reflect the secular CV evolution.

### 3.5 GS Ceti

This object (SDSS J005050.88+000912.6) was selected as a CV during the course of the SDSS (Szkody et al. 2005). The spectrum was that of a quiescent dwarf nova. Southworth

et al. (2007) obtained 8 hr of photometry giving a suspected orbital period of  $\sim 76$  min.

Although there were no secure outburst record in the past, the object was detected in bright outburst on 2016 November 9 at  $V=13.0$  by the ASAS-SN team (vsnet-alert 20328). Subsequent observations detected early superhumps (vsnet-alert 20334, 20342). Although the profile was not doubly peaked as in many WZ Sge-type dwarf novae (cf. Kato 2015), we consider the signal to be that of early superhumps since it was seen before the appearance of ordinary superhumps and the period was close to the suggested orbital period by quiescent photometry (figure 6). The object started to show ordinary superhumps on November 17 (vsnet-alert 20368, 20381, 20395, 20404; figure 7). The times of superhump maxima are listed in table 6. There were clear stages A and B.



**Table 1.** List of Superoutbursts (continued).

Subsection	Object	Year	Observers or references*	ID <sup>†</sup>
3.36	ASASSN-15cr	2017	DPV, Ioh, Shu, CRI	
3.37	ASASSN-16da	2016	deM, Van, GFB, SGE, Kai	
3.38	ASASSN-16dk	2016	HaC	
3.39	ASASSN-16ds	2016	MLF, HaC, SPE	
–	ASASSN-16dt	2016	Kimura et al. (2017)	
3.40	ASASSN-16dz	2016	Van	
–	ASASSN-16eg	2016	Wakamatsu et al. (2017)	
3.41	ASASSN-16ez	2016	DPV, Ioh, Kis, MEV, IMi, Van, KU	
3.42	ASASSN-16fr	2016	KU, Ioh, HaC	
3.43	ASASSN-16fu	2016	HaC, MLF	
–	ASASSN-16fy	2016	K. Isogai et al. in preparation	
3.44	ASASSN-16gh	2016	MLF	
3.45	ASASSN-16gj	2016	MLF, HaC	
3.46	ASASSN-16gl	2016	MLF, HaC, DDe	
–	ASASSN-16hg	2016	Kimura et al. (2017)	
3.47	ASASSN-16hi	2016	HaC	
3.48	ASASSN-16hj	2016	HaC, KU	
3.49	ASASSN-16ia	2016	GFB, Ioh, Ter, Van, SGE, CRI, COO, Trt	
3.50	ASASSN-16ib	2016	MLF, HaC	
3.51	ASASSN-16ik	2016	MLF, HaC	
3.52	ASASSN-16is	2016	Shu, IMi, Van, Ioh, Rui	
3.53	ASASSN-16iu	2016	HaC, MLF	
3.54	ASASSN-16iw	2016	HaC, SPE, NKa, Kis, Van, Ioh	
3.55	ASASSN-16jb	2016	MLF, HaC, SPE	
3.56	ASASSN-16jd	2016	HaC, Ioh	
3.57	ASASSN-16jk	2016	CRI, Van	
3.58	ASASSN-16js	2016	HaC, MLF, SPE	
3.59	ASASSN-16jz	2016	Van	

The best period of early superhumps by the PDM method was 0.05597(3) d. Combined with the period of stage A superhumps, the  $\epsilon^*$  of 0.0288(8) corresponds to  $q=0.078(2)$ . Although the object is a WZ Sge-type dwarf nova, it is not a very extreme one as judged from the relatively large  $P_{\text{dot}}$  of stage B superhumps and the lack of the feature of an underlying white dwarf in the optical spectra in quiescence (Szkody et al. 2005; Southworth et al. 2007). Although there were some post-superoutburst observations, the quality of the data was not sufficient to detect superhumps.

### 3.6 GZ Ceti

This object was originally selected as a CV (SDSS J013701.06–091234.9) during the course of the SDSS

(Szkody et al. 2003). Szkody et al. (2003) obtained spectra showing broad absorption surrounding the emission lines of H $\beta$  and higher members of the Balmer series. The object showed the TiO bandheads of an M dwarf secondary. A radial-velocity study by Szkody et al. (2003) suggested an orbital period of 80–86 min. There was a superoutburst in 2003 December and Pretorius et al. (2004) reported the orbital and superhump periods of 79.71(1) min and 81.702(7) min, respectively. Pretorius et al. (2004) reported the period variation of superhumps, which can be now interpreted as stages B and C. Pretorius et al. (2004) suggested that this object has a low mass-transfer rate. The same superoutburst was studied by Imada et al. (2006), who reported the superhump period of 0.056686(12) d. Imada et al. (2006) noticed the unusual presence of the TiO bands for this short- $P_{\text{SH}}$  object and discussed that the

**Table 1.** List of Superoutbursts (continued).

Subsection	Object	Year	Observers or references*	ID <sup>†</sup>
3.60	ASASSN-16kg	2016	MLF, HaC	
3.61	ASASSN-16kx	2016	HaC, MLF	
3.62	ASASSN-16le	2016	KU, Ioh	
3.63	ASASSN-16lj	2016	Van	
3.64	ASASSN-16lo	2016	KU, IMi, OKU, Ioh	
3.65	ASASSN-16mo	2016	OKU, KU, Trt, Dub, Van	
3.66	ASASSN-16my	2016	HaC, Ioh	
3.67	ASASSN-16ni	2016	KU, Ioh, Trt	
3.68	ASASSN-16nq	2016	Kis, Ioh, RPc, Van, Trt	
3.69	ASASSN-16nr	2016	MLF, HaC	
3.70	ASASSN-16nw	2016	Kai	
3.71	ASASSN-16ob	2016	MLF, HaC, SPE	
3.72	ASASSN-16oi	2016	MLF, HaC, SPE	
3.73	ASASSN-16os	2016	MLF, HaC, SPE	
3.74	ASASSN-16ow	2016	Ioh, Van, NKa, Mdy, MEV, Kis, Kai	
3.75	ASASSN-17aa	2017	MLF, SPE, HaC	
3.76	ASASSN-17ab	2017	HaC	
3.77	ASASSN-17az	2017	MLF	
3.78	ASASSN-17bl	2017	HaC, SPE	
3.79	ASASSN-17bm	2017	MLF, HaC	
3.80	ASASSN-17bv	2017	MLF, SPE, HaC	
3.81	ASASSN-17ce	2017	SPE, MLF, HaC	
3.82	ASASSN-17ck	2017	HaC	
3.83	ASASSN-17cn	2017	MLF, SPE, HaC, Ioh	
3.84	ASASSN-17cx	2017	Mdy	
3.85	ASASSN-17dg	2017	HaC, MLF, SPE	
3.86	ASASSN-17dq	2017	HaC, MLF	
3.87	CRTS J000130	2016	Van, Shu	CRTS J000130.5+050624
3.88	CRTS J015321	2016	Kai	CRTS J015321.5+340857
3.90	CRTS J033349	2016	MLF, HaC, KU	CRTS J033349.8–282244

secondary should be luminous. Ishioka et al. (2007) obtained an infrared spectrum dominated by the secondary component. Ishioka et al. (2007) suggested that the evolutionary path of GZ Cet is different from that of ordinary CVs, and that it is a candidate of a member of EI Psc-like systems. EI Psc-like systems are CVs below the period minimum showing hydrogen (likely somewhat reduced in abundance) in their spectra (cf. Thorstensen et al. 2002; Uemura et al. 2002; Littlefield et al. 2013) and are considered to be evolving towards AM CVn-type objects. Superhump observations during the superoutbursts in 2009 and 2011 were also reported in Kato et al. (2009) and Kato et al. (2013), respectively.

The 2016 superoutburst was detected by R. Stubbings at a visual magnitude of 12.6 on December 18 (vsnet-alert 20493). The ASAS-SN team also recorded the out-

burst at  $V=12.66$  on December 17. This superoutburst was observed in its relatively late phase to the post-superoutburst phase (vsnet-alert 20594). There was also a post-superoutburst rebrightening on 2017 January 15 (vsnet-alert 20569). The times of superhump maxima are listed in table 7. The times after  $E=266$  represent post-superoutburst superhumps. The maxima for  $E \leq 54$  were stage B superhumps and “textbook” stage C superhumps continued even during the post-superoutburst phase without a phase jump as in traditional late superhumps (figure 8).

### 3.7 AK Cnc

AK Cnc was discovered as a short-period variable star (AN 77.1933) with a photographic range of 14 to fainter

**Table 1.** List of Superoutbursts (continued).

Subsection	Object	Year	Observers or references*	ID <sup>†</sup>
3.89	CRTS J023638	2016	CRI, Trt, Shu, Rui	CRTS J023638.0+111157
3.91	CRTS J044637	2017	Ioh, KU	CRTS J044636.9+083033
3.92	CRTS J082603	2017	Van	CRTS J082603.7+113821
3.93	CRTS J085113	2008	Mhh	CRTS J085113.4+344449
		2016	KU, Trt	
3.94	CRTS J085603	2016	Van, Ioh	CRTS J085603.8+322109
3.95	CRTS J164950	2015	RIT, Van	CRTS J164950.4+035835
		2016	CRI, Rui	
3.96	CSS J062450	2017	Trt, Van	CSS131223:062450+503111
3.97	DDE 26	2016	Ioh, IMi, Shu, RPc	
3.98	DDE 48	2016	MNI, IMi	
3.99	MASTER J021315	2016	Van	MASTER OT J021315.37+533822.7
3.100	MASTER J030205	2016	OKU, deM, Van, COO, Ioh, Mdy, T60, NKa, RPc, Trt, Naz	MASTER OT J030205.67+254834.3
3.101	MASTER J042609	2016	Kis, Ioh, Kai, Shu, Trt	MASTER OT J042609.34+354144.8
3.102	MASTER J043220	2017	Van	MASTER OT J043220.15+784913.8
3.103	MASTER J043915	2016	Ioh, CRI	MASTER OT J043915.60+424232.3
3.104	MASTER J054746	2016	Van	MASTER OT J054746.81+762018.9
3.105	MASTER J055348	2017	Van, Mdy	MASTER OT J055348.98+482209.0
3.106	MASTER J055845	2016	Shu	MASTER OT J055845.55+391533.4
3.107	MASTER J064725	2016	Ioh, RPc, CRI	MASTER OT J064725.70+491543.9
3.108	MASTER J065330	2017	Van, Ioh	MASTER OT J065330.46+251150.9
3.109	MASTER J075450	2017	Van	MASTER OT J075450.18+091020.2
3.110	MASTER J150518	2017	HaC	MASTER OT J150518.03–143933.6
3.111	MASTER J151126	2016	HaC, MLF	MASTER OT J151126.74–400751.9
3.112	MASTER J162323	2015	Van	MASTER OT J162323.48+782603.3
		2016	COO, Trt, IMi	
3.113	MASTER J165153	2017	Van	MASTER OT J165153.86+702525.7
3.114	MASTER J174816	2016	Van, Mdy	MASTER OT J174816.22+501723.3
–	MASTER J191841	2016	K. Isogai et al. in preparation	MASTER OT J191841.98+444914.5

than 15.5 (Morgenroth 1933). Morgenroth (1933) detected two maxima on 48 plates between JD 2425323 and 2426763. Tsesevich (1967) classified this object to be a U Gem-type variable without a particular remark. Williams (1983) reported a G-type spectrum unlike for a CV. The identification was later found to be incorrect (Howell et al. 1990; Wenzel 1993b). The identification chart by Vogt and Bateson (1982) was correct. Amateur observers, particularly AAVSO and VSOLJ observers, made regular monitoring since 1986 and detected several outbursts. Time-resolved CCD observation by Howell et al. (1990) recorded a declining part of an outburst. Szkody and Howell (1992) obtained a spectrum in quiescence, which was characteristic to a dwarf nova. Wenzel (1993b) and Wenzel (1993a) reported observations using photographic archival materials and discussed outburst prop-

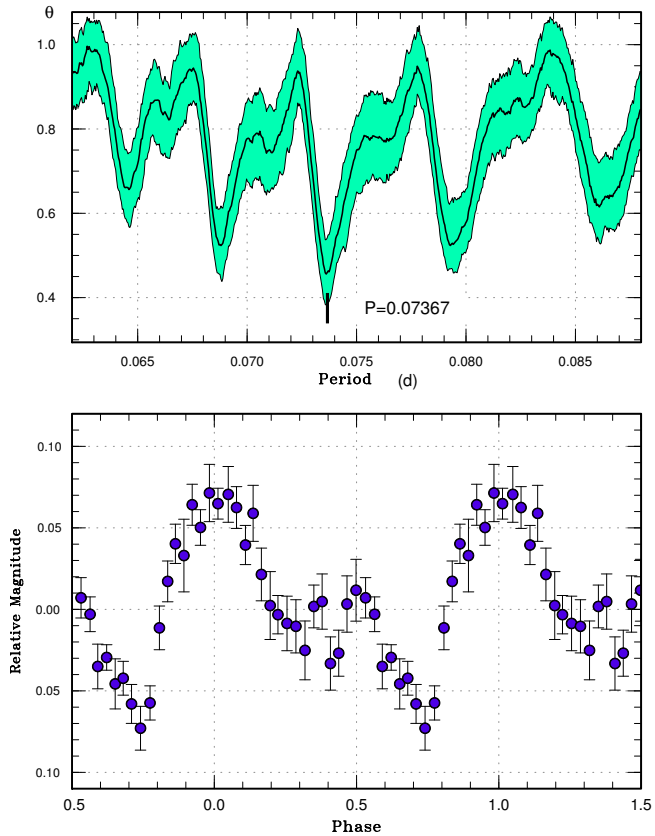
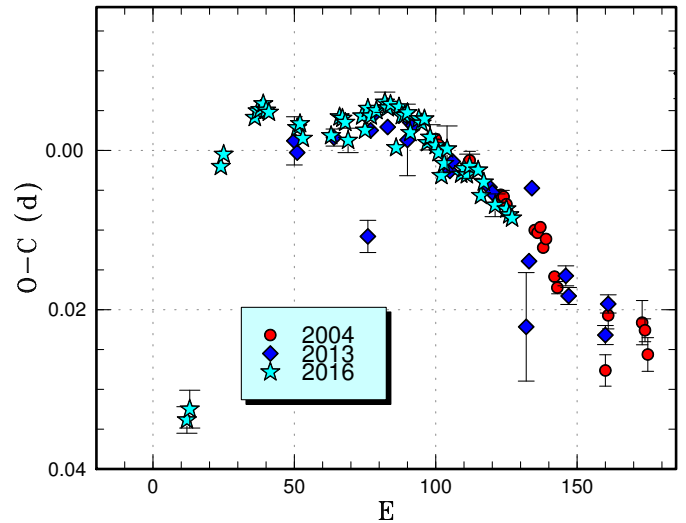
erties. Wenzel (1993b) also gave a summary of confusing history of the identification of this object.

Kato (1994) was the first to identify this object to be an SU UMa-type dwarf nova by observing the 1992 superoutburst. Mennickent et al. (1996) reported another superoutburst in 1995. The orbital period was spectroscopically measured to be 0.0651(2) d (Arenas and Mennickent 1998). Kato et al. (2009) provided analyses of the 1999 and 2003 superoutbursts. Kato et al. (2013) further reported observations of the 2012 superoutburst.

The 2016 superoutburst was detected at a visual magnitude of 13.5 by G. Poyner on April 5. The times of superhump maxima are listed in table 8. Due to the rather poor coverage, we could not determine  $P_{\text{dot}}$  for stage B although the distinction between stages B and C was clear. Although positive  $P_{\text{dot}}$  for stage B is expected for this  $P_{\text{orb}}$ ,

**Table 1.** List of Superoutbursts (continued).

Subsection	Object	Year	Observers or references*	ID <sup>†</sup>
3.115	MASTER J211322	2016	Van	MASTER OT J211322.92+260647.4
3.116	MASTER J220559	2016	MLF, HaC	MASTER OT J220559.40−341434.9
–	OT J002656	2016	Kato et al. (2017)	CSS101212:002657+284933
3.117	SBS 1108	2016	Ioh, COO, Vol, Kai, KU	SBS 1108+574
3.118	SDSS J032015	2016	Van, IMi	SDSS J032015.29+441059.3
3.119	SDSS J032015	2016	Van	SDSS J091001.63+164820.0
3.120	SDSS J113551	2017	Van, Mdy	SDSS J113551.09+532246.2
3.121	SDSS J115207	2009	Kato et al. (2010)	SDSS J115207.00+404947.8
		2017	Mdy, KU, LCO, Ioh, DPV, Kis	
3.122	SDSS J131432	2017	Mdy, Van	SDSS J131432.10+444138.7
3.123	SDSS J153015	2017	Van	SDSS J153015.04+094946.3
3.124	SDSS J155720	2016	HaC, Kis	SDSS J155720.75+180720.2
–	SDSS J173047	2016	K. Isogai et al. in preparation	SDSS J173047.59+554518.5
3.125	SSS J134850	2016	MLF, HaC	SSS J134850.1−310835
3.126	TCP J013758	2016	Kis, IMi, Ioh, RPc, Shu, CRI, Rui, Trt	TCP J01375892+4951055
3.127	TCP J180018	2016	HaC, Nel, SPE	TCP J18001854−3533149

**Fig. 2.** Superhumps in V1047 Aql (2016). (Upper): PDM analysis. (Lower): Phase-averaged profile.**Fig. 3.** Comparison of  $O - C$  diagrams of BB Ari between different superoutbursts. A period of 0.07249 d was used to draw this figure. Approximate cycle counts ( $E$ ) after the starts of outbursts were used. The definition is different from the corresponding figure in Kato et al. (2014a). The 2013 superoutburst had a separate precursor outburst and the cycle count is different by 44 from that used in Kato et al. (2014a). The value suggests that superhumps during the 2013 superoutburst evolved 3 d after the precursor outburst. Since the start of the 2004 superoutburst was not well constrained, we shifted the  $O - C$  diagram to best fit the 2016 one.

**Table 2.** Coordinates of objects without coordinate-based names.

Object	Right Ascension	Declination	Source*	SDSS <i>g</i>	Gaia <i>G</i>	GALEX NUV
ASASSN-13ak	17 <sup>h</sup> 48 <sup>m</sup> 27 <sup>s</sup> .87	+50°50′39″.8	Gaia	19.89(2)	19.06	–
ASASSN-13al	19 <sup>h</sup> 32 <sup>m</sup> 06 <sup>s</sup> .39	+67°27′40″.4	GSC2.3.2	–	–	21.5(4)
ASASSN-13bc	18 <sup>h</sup> 02 <sup>m</sup> 22 <sup>s</sup> .44	+45°52′44″.6	Gaia	19.53(2)	18.40	19.4(1)
ASASSN-13bj	16 <sup>h</sup> 00 <sup>m</sup> 20 <sup>s</sup> .52	+70°50′07″.2	Gaia	–	18.43	–
ASASSN-13bo	01 <sup>h</sup> 43 <sup>m</sup> 54 <sup>s</sup> .23	+29°01′03″.8	SDSS	20.94(4)	–	21.8(2)
ASASSN-13cs	17 <sup>h</sup> 11 <sup>m</sup> 38 <sup>s</sup> .40	+05°39′51″.0	Gaia	–	19.80	20.9(2)
ASASSN-13cz	15 <sup>h</sup> 27 <sup>m</sup> 55 <sup>s</sup> .11	+63°27′54″.2	Gaia	18.94(1)	18.74	–
ASASSN-14gg	18 <sup>h</sup> 21 <sup>m</sup> 38 <sup>s</sup> .61	+61°59′04″.0	Gaia	–	19.74	19.4(1)
ASASSN-15cr	07 <sup>h</sup> 34 <sup>m</sup> 42 <sup>s</sup> .71	+50°42′29″.0	Gaia	–	19.33	20.2(1)
ASASSN-16da	12 <sup>h</sup> 56 <sup>m</sup> 09 <sup>s</sup> .83	+62°37′04″.4	SDSS	21.55(5)	–	21.6(4)
ASASSN-16dk	10 <sup>h</sup> 20 <sup>m</sup> 53 <sup>s</sup> .48	–86°17′29″.77	Gaia	–	20.41	19.31(7)
ASASSN-16ds	18 <sup>h</sup> 25 <sup>m</sup> 09 <sup>s</sup> .96	–46°20′17″.9	ASAS-SN	–	–	–
ASASSN-16dz	06 <sup>h</sup> 42 <sup>m</sup> 25 <sup>s</sup> .58	+08°25′46″.6	Gaia	–	19.10	–
ASASSN-16ez	15 <sup>h</sup> 31 <sup>m</sup> 29 <sup>s</sup> .87	+21°38′30″.2	SDSS	21.28(4)	–	–
ASASSN-16fr	16 <sup>h</sup> 42 <sup>m</sup> 51 <sup>s</sup> .80	–08°52′41″.0	SDSS	20.97(4)	–	–
ASASSN-16fu	22 <sup>h</sup> 14 <sup>m</sup> 05 <sup>s</sup> .03	–09°04′19″.4	SDSS	21.64(7)	–	–
ASASSN-16gh	18 <sup>h</sup> 15 <sup>m</sup> 57 <sup>s</sup> .62	–72°40′38″.1	ASAS-SN	–	–	–
ASASSN-16gj	09 <sup>h</sup> 59 <sup>m</sup> 58 <sup>s</sup> .97	–19°01′00″.0	GSC2.3.2	–	–	21.3(3)
ASASSN-16gl	18 <sup>h</sup> 27 <sup>m</sup> 16 <sup>s</sup> .25	–52°47′44″.1	ASAS-SN	–	–	–
ASASSN-16hi	21 <sup>h</sup> 38 <sup>m</sup> 58 <sup>s</sup> .01	–73°19′17″.5	Gaia	–	18.86	20.9(2)
ASASSN-16ia	20 <sup>h</sup> 51 <sup>m</sup> 59 <sup>s</sup> .24	+34°49′46″.1	Gaia	–	–	–
ASASSN-16ib	14 <sup>h</sup> 32 <sup>m</sup> 03 <sup>s</sup> .74	–33°08′13″.9	IGSL	–	–	21.5(4)
ASASSN-16ik	19 <sup>h</sup> 27 <sup>m</sup> 45 <sup>s</sup> .88	–67°15′16″.7	IGSL	–	–	21.8(5)
ASASSN-16is	18 <sup>h</sup> 31 <sup>m</sup> 03 <sup>s</sup> .63	+11°32′02″.9	Gaia	–	20.36	–
ASASSN-16iu	01 <sup>h</sup> 43 <sup>m</sup> 47 <sup>s</sup> .87	–70°17′01″.1	Gaia	–	19.99	20.39(9)
ASASSN-16iw	00 <sup>h</sup> 58 <sup>m</sup> 11 <sup>s</sup> .10	–01°07′50″.9	SDSS	21.9(1)	–	–

\*source of the coordinates: 2MASS (2MASS All-Sky Catalog of Point Sources; Cutri et al. 2003), ASAS-SN (ASAS-SN measurements), CRTS (CRTS measurements), Gaia (Gaia DR1, Gaia Collaboration 2016 and outburst detections), GSC2.3.2 (The Guide Star Catalog, Version 2.3.2, Lasker et al. 2007), IGSL (The Initial Gaia Source List 3, Smart 2013), IPHAS DR2 (INT/WFC Photometric H $\alpha$  Survey, Witham et al. 2008), SDSS (The SDSS Photometric Catalog, Release 9, Ahn et al. 2012).

it still awaits better observations (figure 9).

### 3.8 GZ Cancri

GZ Cnc was discovered by K. Takamizawa as a variable star (=TmzV34). The object was confirmed as a dwarf nova (Kato et al. 2001b; Kato et al. 2002a). Tappert and Bianchini (2003) obtained the orbital period of 0.08825(28) d by radial-velocity observations. The SU UMa-type nature was established during the 2010 (Kato et al. 2010). See Kato et al. (2014a) for more information.

The 2017 superoutburst was detected by R. Stubbings at a visual magnitude of 13.0 on February 2 and on the same night at 12.5 mag by T. Horie. Subsequent observations detected growing superhumps on February 3 and 4. Superhumps grew further on February 6 (vsnet-alert

20642). The times of superhump maxima are listed in table 9. Thanks to the early detection of the outburst, stage A superhumps were clearly detected (figure 10). The  $\epsilon^*$  for stage A superhumps [0.081(3)] corresponds to  $q=0.27(2)$ .

### 3.9 GP Canum Venaticorum

This object was originally selected as a CV (SDSS J122740.83+513925.0) during the course of the SDSS (Szkody et al. 2006). Szkody et al. (2006) obtained a spectrum showing an underlying white dwarf. Littlefair et al. (2008) clarified that this object is an eclipsing dwarf nova with a short orbital period. The object underwent the first-recorded superoutburst in 2007 June. This 2007 superoutburst was analyzed by Shears et al. (2008) and Kato

**Table 2.** Coordinates of objects without coordinate-based names (continued).

Object	Right Ascension	Declination	Source*	SDSS <i>g</i>	Gaia G	GALEX NUV
ASASSN-16jb	17 <sup>h</sup> 50 <sup>m</sup> 44 <sup>s</sup> .99	−25°58′37″.1	ASAS-SN	–	–	–
ASASSN-16jd	18 <sup>h</sup> 50 <sup>m</sup> 33 <sup>s</sup> .33	−26°50′40″.8	ASAS-SN	–	–	–
ASASSN-16jk	15 <sup>h</sup> 40 <sup>m</sup> 24 <sup>s</sup> .84	+23°07′50″.8	Gaia	20.73(3)	20.68	21.7(3)
ASASSN-16js	00 <sup>h</sup> 51 <sup>m</sup> 19 <sup>s</sup> .17	−65°57′17″.0	Gaia	–	20.08	22.1(2)
ASASSN-16jz	19 <sup>h</sup> 18 <sup>m</sup> 53 <sup>s</sup> .39	+79°32′16″.0	IGSL	–	–	–
ASASSN-16kg	21 <sup>h</sup> 36 <sup>m</sup> 29 <sup>s</sup> .86	−25°13′48″.3	CRTS	–	–	–
ASASSN-16kx	06 <sup>h</sup> 17 <sup>m</sup> 18 <sup>s</sup> .72	−49°38′57″.3	ASAS-SN	–	–	–
ASASSN-16le	23 <sup>h</sup> 34 <sup>m</sup> 35 <sup>s</sup> .56	+54°33′25″.5	Gaia	–	18.83	–
ASASSN-16lj	20 <sup>h</sup> 15 <sup>m</sup> 46 <sup>s</sup> .04	+75°47′41″.7	Gaia	20.99(5)	20.17	21.5(2)
ASASSN-16lo	18 <sup>h</sup> 08 <sup>m</sup> 41 <sup>s</sup> .02	+46°19′34″.9	IGSL	–	–	–
ASASSN-16mo	02 <sup>h</sup> 56 <sup>m</sup> 56 <sup>s</sup> .67	+49°27′47″.1	Gaia	–	20.19	–
ASASSN-16my	07 <sup>h</sup> 41 <sup>m</sup> 08 <sup>s</sup> .46	−30°03′17″.9	Gaia	–	18.52	–
ASASSN-16ni	05 <sup>h</sup> 05 <sup>m</sup> 00 <sup>s</sup> .32	+60°45′53″.7	ASAS-SN	–	–	–
ASASSN-16nq	23 <sup>h</sup> 22 <sup>m</sup> 09 <sup>s</sup> .25	+39°50′07″.8	Gaia	–	19.10	21.1(3)
ASASSN-16nr	07 <sup>h</sup> 09 <sup>m</sup> 49 <sup>s</sup> .33	−49°09′03″.6	GSC2.3.2	–	–	–
ASASSN-16nw	01 <sup>h</sup> 53 <sup>m</sup> 49 <sup>s</sup> .09	+52°52′05″.1	IGSL	–	–	–
ASASSN-16ob	06 <sup>h</sup> 47 <sup>m</sup> 18 <sup>s</sup> .89	−64°37′07″.3	Gaia	–	–	–
ASASSN-16oi	06 <sup>h</sup> 21 <sup>m</sup> 32 <sup>s</sup> .38	−62°58′15″.6	GSC2.3.2	–	–	22.0(5)
ASASSN-16os	08 <sup>h</sup> 43 <sup>m</sup> 05 <sup>s</sup> .59	−84°53′45″.6	GSC2.3.2	–	–	–
ASASSN-16ow	06 <sup>h</sup> 30 <sup>m</sup> 47 <sup>s</sup> .05	+02°39′31″.4	IPHAS	–	–	–
ASASSN-17aa	04 <sup>h</sup> 23 <sup>m</sup> 56 <sup>s</sup> .40	−74°05′27″.5	ASAS-SN	–	–	–
ASASSN-17ab	10 <sup>h</sup> 40 <sup>m</sup> 51 <sup>s</sup> .25	−37°03′30″.2	Gaia	–	–	–
ASASSN-17az	00 <sup>h</sup> 15 <sup>m</sup> 09 <sup>s</sup> .31	−69°45′49″.2	ASAS-SN	–	–	–
ASASSN-17bl	12 <sup>h</sup> 31 <sup>m</sup> 50 <sup>s</sup> .86	−50°25′07″.4	ASAS-SN	–	–	–
ASASSN-17bm	10 <sup>h</sup> 55 <sup>m</sup> 27 <sup>s</sup> .84	−48°04′27″.4	GSC2.3.2	–	–	–
ASASSN-17bv	09 <sup>h</sup> 08 <sup>m</sup> 45 <sup>s</sup> .65	−62°37′11″.0	IGSL	–	–	–
ASASSN-17ce	13 <sup>h</sup> 24 <sup>m</sup> 24 <sup>s</sup> .46	−54°09′21″.7	Gaia	–	18.52	–
ASASSN-17ck	08 <sup>h</sup> 30 <sup>m</sup> 46 <sup>s</sup> .29	−28°58′13″.5	GSC2.3.2	–	–	–
ASASSN-17cn	09 <sup>h</sup> 31 <sup>m</sup> 22 <sup>s</sup> .60	−35°20′54″.3	Gaia	–	–	–
ASASSN-17cx	10 <sup>h</sup> 59 <sup>m</sup> 57 <sup>s</sup> .97	−11°57′56″.8	GSC2.3.2	–	–	20.8(2)
ASASSN-17dg	16 <sup>h</sup> 02 <sup>m</sup> 33 <sup>s</sup> .49	−60°32′50″.3	2MASS	–	–	–
ASASSN-17dq	09 <sup>h</sup> 01 <sup>m</sup> 25 <sup>s</sup> .26	−59°31′40″.1	ASAS-SN	–	–	–
DDE 26	22 <sup>h</sup> 03 <sup>m</sup> 28 <sup>s</sup> .21	+30°56′36″.5	Gaia	19.61(1)	19.32	–
SBS 1108+574	11 <sup>h</sup> 11 <sup>m</sup> 26 <sup>s</sup> .83	+57°12′38″.6	Gaia	19.22(1)	19.26	19.5(1)

**Table 3.** Superhump Periods and Period Derivatives

Object	Year	$P_1$ (d)	err	$E_1^*$	$P_{\dot{\text{d}}}$ <sup>†</sup>	err <sup>†</sup>	$P_2$ (d)	err	$E_2^*$	$P_{\text{orb}}$ (d) <sup>‡</sup>	Q <sup>§</sup>	
V1047 Aql	2016	0.073666	0.000054	0	14	–	–	–	–	–	C	
BB Ari	2016	0.072491	0.000026	27	70	19.7	4.2	0.072179	0.000019	70 115	A	
OY Car	2016	0.064653	0.000028	0	104	9.9	1.7	0.064440	0.000049	103 159	B	
HT Cas	2016	0.076333	0.000005	19	62	–	–	0.075886	0.000005	72 145	A	
GS Cet	2016	0.056645	0.000014	14	156	6.3	0.6	–	–	–	0.05597	AE
GZ Cet	2016	0.056702	0.000028	0	54	11.4	2.8	0.056409	0.000006	141 425	0.055343	B
AK Cnc	2016	0.067454	0.000030	0	76	–	–	–	–	–	0.0651	C
GZ Cnc	2017	0.092881	0.000022	32	91	–0.9	4.9	0.092216	0.000291	91 113	0.08825	C
GP CVn	2016	0.064796	0.000027	17	96	9.5	2.5	–	–	–	0.062950	B
V1113 Cyg	2016	0.078848	0.000028	52	141	–2.4	2.9	–	–	–	–	B
IX Dra	2016	0.066895	0.000045	0	92	4.7	4.6	–	–	–	–	C
IR Gem	2016	0.071090	0.000047	0	33	–	–	0.070633	0.000047	56 104	0.0684	C
IR Gem	2017	0.071098	0.000020	25	56	–	–	–	–	–	0.0684	C
NY Her	2016	0.075832	0.000043	0	42	–	–	0.075525	0.000051	49 114	–	B
V699 Oph	2016	0.070212	0.000096	0	28	–	–	–	–	–	–	C
V344 Pav	2016	0.079878	0.000031	0	76	–8.8	2.7	–	–	–	–	CG
V893 Sco	2016	0.074666	0.000326	0	26	–	–	–	–	–	0.075961	C2
V493 Ser	2016	–	–	–	–	–	–	0.082730	0.000129	0 13	0.08001	C
V1389 Tau	2016	0.080456	0.000081	0	35	–	–	0.079992	0.000025	34 121	–	C

\*Interval used for calculating the period (corresponding to  $E$  in section 3).

<sup>†</sup>Unit  $10^{-5}$ .

<sup>‡</sup>References:

GZ Cet (Pretorius et al. 2004), AK Cnc (Arenas and Mennickent 1998), GZ Cnc (Tappert and Bianchini 2003), IR Gem (Feinswog et al. 1988), V493 Ser (Thorstensen et al. 2015), HV Vir (Patterson et al. 2003), SBS 1108 (Kato et al. 2013), OY Car, GS Cet, GP CVn, V893 Sco, ASASSN-16da, ASASSN-16fu, ASASSN-16ia, ASASSN-16is, ASASSN-16jb, ASASSN-16js, ASASSN-16lo, ASASSN-16oi, ASASSN-16os, ASASSN-17bl, ASASSN-17cn, MASTER J042609, MASTER J220559, SDSS J115207 (this work)

<sup>§</sup>Data quality and comments. A: excellent, B: partial coverage or slightly low quality, C: insufficient coverage or observations with large scatter, G:  $P_{\dot{\text{d}}}$  denotes global  $P_{\dot{\text{d}}}$ , M: observational gap in middle stage, U: uncertainty in alias selection, 2: late-stage coverage, the listed period may refer to  $P_2$ , a: early-stage coverage, the listed period may be contaminated by stage A superhumps, E:  $P_{\text{orb}}$  refers to the period of early superhumps, P:  $P_{\text{orb}}$  refers to a shorter stable periodicity recorded in outburst.

et al. (2009). Kato et al. (2012a) reported on the 2011 superoutburst and provided a corrected eclipse ephemeris. Savoury et al. (2011) reported the orbital parameters (including  $q$ ) by modeling the eclipse profile. Although Zengin Çamurdan et al. (2010) suspected cyclic  $O - C$  variation of eclipses, their result was doubtful due to the very low time-resolution of observations and very few points on the  $O - C$  diagram.

The 2016 superoutburst was detected by the ASAS-SN team at  $V=15.29$  on April 25. Both superhumps and eclipses were recorded (vsnet-alert 19778). Using the combined data of 2007, 2011 and 2016 observations, we have refined the eclipse ephemeris by the MCMC modeling (Kato et al. 2013):

$$\text{Min}(\text{BJD}) = 2455395.37115(4) + 0.0629503676(9)E. \quad (2)$$

The epoch in Littlefair et al. (2008) corresponds to an  $O - C$  value of 0.00168 d against this ephemeris. The ephemeris in Littlefair et al. (2008) predicts eclipses to occur 0.0096 d later than our actual observations in 2016.

The times of superhump maxima during the 2016 superoutburst are listed in table 10. Stage B with a positive  $P_{\dot{\text{d}}}$  and a transition to stage C superhumps were recorded (see also figure 11).

### 3.10 V337 Cygni

V337 Cyg was discovered as a long-period variable (AN 101.1928). The dwarf nova-type nature was confirmed in 1996. The SU UMA-type nature was established during the 2006 superoutburst (cf. Boyd et al. 2007). See Kato

**Table 3.** Superhump Periods and Period Derivatives (continued)

Object	Year	$P_1$	err	$E_1$	$P_{\text{dot}}$	err	$P_2$	err	$E_2$	$P_{\text{orb}}$	Q		
HV Vir	2016	0.058244	0.000009	31	227	3.1	0.4	–	–	–	–	0.057069	A
NSV 2026	2016b	0.069906	0.000022	0	13	–	–	–	–	–	–	–	C
NSV 14681	2016	0.090063	0.000008	0	77	–0.5	0.8	–	–	–	–	–	C
1RXS J161659	2016	0.071370	0.000063	0	43	–	–	0.071063	0.000054	56	74	–	C
1RXS J161659	2016b	0.071229	0.000056	0	58	–	–	–	–	–	–	–	C
ASASSN-13al	2016	0.0783	0.0002	0	3	–	–	–	–	–	–	–	C
ASASSN-13bc	2015	0.070393	0.000118	0	16	–	–	–	–	–	–	–	C
ASASSN-13bc	2016	0.070624	0.000100	0	39	–	–	0.070101	0.000046	39	85	–	C
ASASSN-13bj	2016	0.072553	0.000047	0	21	–	–	0.071918	0.000053	23	44	–	C
ASASSN-13bo	2016	0.071860	0.000025	0	41	–	–	–	–	–	–	–	CU
ASASSN-13cs	2016	0.077105	0.000098	0	20	–	–	–	–	–	–	–	C
ASASSN-13cz	2016	0.080135	0.000044	0	13	–	–	0.079496	0.000368	62	76	–	C
ASASSN-14gg	2016	0.059311	0.000035	0	89	13.1	2.9	–	–	–	–	–	B
ASASSN-15cr	2017	0.061554	0.000021	16	149	7.8	1.5	0.061260	0.000005	146	217	–	B
ASASSN-16da	2016	0.057344	0.000024	10	175	7.5	0.9	0.056994	0.000062	203	239	0.05610	BE
ASASSN-16dk	2016	–	–	–	–	–	–	0.075923	0.000047	0	67	–	C
ASASSN-16ds	2016	0.067791	0.000027	33	195	7.1	0.6	0.067228	0.000051	–	–	–	B
ASASSN-16dt	2016	0.064507	0.000005	62	214	–1.6	0.5	–	–	–	–	0.064197	AE
ASASSN-16dz	2016	0.066260	0.000170	0	16	–	–	–	–	–	–	–	CU
ASASSN-16eg	2016	0.077880	0.000003	15	106	10.4	0.8	0.077589	0.000007	120	181	0.075478	AE
ASASSN-16ez	2016	0.057621	0.000017	0	77	2.1	2.9	–	–	–	–	–	C
ASASSN-16fr	2016	0.071394	0.000144	0	35	–	–	–	–	–	–	–	C
ASASSN-16fu	2016	0.056936	0.000013	35	195	4.6	0.6	–	–	–	–	0.05623	BE
ASASSN-16gh	2016	0.061844	0.000017	16	100	6.7	2.7	–	–	–	–	–	B
ASASSN-16gj	2016	0.057997	0.000022	74	208	7.0	1.0	–	–	–	–	–	B
ASASSN-16gl	2016	0.055834	0.000010	0	118	1.6	1.2	–	–	–	–	–	B
ASASSN-16hg	2016	0.062371	0.000014	15	115	0.6	1.7	–	–	–	–	–	B
ASASSN-16hi	2016	0.059040	0.000024	0	121	8.6	1.5	0.058674	0.000023	118	188	–	B
ASASSN-16hj	2016	0.055644	0.000041	20	145	11.3	1.3	0.055465	0.000036	144	324	0.05499	BE

et al. (2015a) for more history.

The 2016 superoutburst was detected by M. Moriyama at an unfiltered CCD magnitude of 15.5 on November 17. Observations on a single night yielded three superhumps (table 11). The maximum  $E=2$  suffered from large atmospheric extinction and the quality of this measurement was poor. The  $P_{\text{SH}}$  is omitted from table 3 since there were observations with much more accurate values in the past.

### 3.11 V1113 Cygni

V1113 Cyg was discovered as a dwarf nova by Hoffmeister (1966). The SU UMa-type nature was identified by Kato et al. (1996b). See Kato et al. (2016a) for more history.

The 2016 superoutburst was detected by H. Maehara at a visual magnitude of 14.3 on July 27 (vsnet-alert 20003). A visual observation by P. Dubovsky on the same night

and ASAS-SN detection on the next night indicated further brightening (vsnet-alert 20011, 20015). Thanks to the early detection and notification, growing superhumps were detected (vsnet-alert 20022). The times of superhump maxima are listed in table 12, which clearly indicate the presence of stage A superhumps (figure 12). It may be noteworthy that stage A lasted nearly 40 cycles (figure 12), which may be analogous to long- $P_{\text{orb}}$  SU UMa-type dwarf novae with slowly evolving superhumps (such as V1006 Cyg: Kato et al. 2016b; V452 Cas: Kato et al. 2016a). Since stage A superhumps were observed, a spectroscopic radial-velocity study is desired to determine  $q$  using the stage A superhump method.

### 3.12 IX Draconis

IX Dra is one of ER UMa-type dwarf novae (Ishioaka et al. 2001). See Kato et al. (2014a) and Olech et al. (2004) for the



**Table 3.** Superhump Periods and Period Derivatives (continued)

Object	Year	$P_1$	err	$E_1$	$P_{\text{dot}}$	err	$P_2$	err	$E_2$	$P_{\text{orb}}$	Q		
ASASSN-16ib	2016	0.058855	0.000015	47	144	2.2	2.0	–	–	–	C		
ASASSN-16ik	2016	0.064150	0.000018	33	126	1.0	2.1	–	–	–	B		
ASASSN-16is	2016	0.058484	0.000015	0	105	4.2	1.7	–	–	0.05762	CE		
ASASSN-16iu	2016	0.058720	0.000062	0	104	26.7	3.3	0.058661	0.000300	34	53	–	C
ASASSN-16iw	2016	0.065462	0.000039	42	153	10.0	3.2	–	–	–	–	0.06495	BE
ASASSN-16jb	2016	0.064397	0.000021	30	193	5.9	0.7	0.064170	0.000075	193	232	0.06305	AE
ASASSN-16jd	2016	0.058163	0.000039	34	223	7.9	0.6	0.057743	0.000159	223	258	–	B
ASASSN-16jk	2016	0.061391	0.000028	16	146	8.6	1.3	–	–	–	–	–	C
ASASSN-16js	2016	0.060934	0.000015	48	173	4.9	1.0	–	–	–	–	0.06034	AE
ASASSN-16jz	2016	0.060936	0.000014	0	51	–	–	–	–	–	–	–	C
ASASSN-16kg	2016	0.100324	0.000189	0	30	–	–	–	–	–	–	–	CU
ASASSN-16kx	2016	0.080760	0.000036	0	54	–6.4	6.5	0.080536	0.000041	79	153	–	C
ASASSN-16le	2016	0.0808	0.0013	0	2	–	–	–	–	–	–	–	C
ASASSN-16lj	2016	0.0857	0.0004	0	2	–	–	–	–	–	–	–	C
ASASSN-16lo	2016	0.054608	0.000036	38	86	–	–	–	–	–	–	0.05416	CE
ASASSN-16mo	2016	0.066477	0.000016	0	84	3.9	2.3	–	–	–	–	–	C
ASASSN-16my	2016	0.087683	0.000049	23	92	3.0	5.7	–	–	–	–	–	C
ASASSN-16ni	2016	0.115242	0.000442	0	11	–	–	–	–	–	–	–	CU
ASASSN-16nq	2016	0.079557	0.000045	0	39	0.0	9.3	0.079069	0.000035	59	161	–	B
ASASSN-16nr	2016	0.082709	0.000080	0	59	–19.8	10.1	–	–	–	–	–	CG
ASASSN-16nw	2016	0.072813	0.000045	0	43	–	–	–	–	–	–	–	C
ASASSN-16ob	2016	0.057087	0.000014	52	249	1.8	0.5	–	–	–	–	–	B
ASASSN-16oi	2016	0.056241	0.000017	12	122	5.0	1.7	–	–	–	–	0.05548	BE
ASASSN-16os	2016	0.054992	0.000013	39	168	0.3	1.4	–	–	–	–	0.05494	BE
ASASSN-16ow	2016	0.089311	0.000052	0	40	–	–	0.088866	0.000022	55	102	–	B
ASASSN-17aa	2017	0.054591	0.000013	0	182	2.8	0.3	–	–	–	–	0.05393	BE
ASASSN-17ab	2017	0.070393	0.000016	15	88	3.6	2.5	–	–	–	–	–	C
ASASSN-17az	2017	0.056492	0.000038	0	36	–	–	–	–	–	–	–	CU
ASASSN-17bl	2017	0.055367	0.000010	53	237	3.6	0.6	–	–	–	–	0.05467	CE

history.

The 2016 May superoutburst was detected by P. Dubovsky at a visual magnitude of 15.2 on May 29. Subsequent observations detected superhumps (vsnet-alert 19868). The times of superhump maxima are listed in table 13. A combined  $O - C$  diagram (figure 13) did not show a strong sign of a stage transition.

In order to determine the change in the supercycle (cf. Otulakowska-Hypka et al. 2013), we have extracted nine maxima of superoutbursts since 2015 April, when the ASAS-SN team started a good coverage of this field. The mean supercycle between JD 2457142 and 2457305 (2015 April to October) was 54.4(3) d, while it increased to 58.9(3) d between JD 2457420 and 2457657 (2016 February to September). These values are much shorter than what is predicted (should be longer than 62 d by 2015) by a claimed secular trend in Otulakowska-Hypka et al. (2013). The rapid variation suggests that snapshot values as in

Otulakowska-Hypka et al. (2013) probably did not reflect the long-term trend well.

### 3.13 IR Geminorum

IR Gem was discovered as a U Gem-type variable star (AN S5423) by Popowa (1961). Although little was known other than outbursts with an interval of  $\sim 75$  d and amplitudes of  $\sim 2.5$  mag (Popova 1960; Meinunger 1976),<sup>12</sup> this object has been well monitored by AAVSO observers since its discovery. Several outbursts were already recorded in the 1960s (Mayall 1968). Bond (1978) obtained a spectrum typical for an outbursting dwarf nova. Burenkov and Voikhanskaia (1979) reported a dwarf nova-type spectrum in quiescence. Shafter et al. (1984) identified this object to be an SU UMa-type dwarf

<sup>12</sup>There is a close companion star and old literature often referred to combined magnitudes.

**Table 3.** Superhump Periods and Period Derivatives (continued)

Object	Year	$P_1$	err	$E_1$	$P_{\dot{}}$	err	$P_2$	err	$E_2$	$P_{\text{orb}}$	Q
ASASSN-17bm	2017	0.082943	0.000056	0	53	–	–	–	–	–	C
ASASSN-17bv	2017	0.082690	0.000021	12	52	–6.3	3.9	0.082489	0.000048	58 103	B
ASASSN-17ce	2017	0.081293	0.000111	0	22	–	–	0.080796	0.000042	21 139	C
ASASSN-17ck	2017	0.083	0.001	0	1	–	–	–	–	–	C
ASASSN-17cn	2017	0.053991	0.000014	0	137	5.6	0.8	–	–	–	0.05303 BE
ASASSN-17cx	2017	0.0761	0.0007	0	2	–	–	–	–	–	C
ASASSN-17dg	2017	–	–	–	–	–	–	0.066482	0.000046	0 36	C
ASASSN-17dq	2017	0.058052	0.000034	0	93	9.3	3.5	0.057660	0.000076	90 142	C
CRTS J000130	2016	0.094749	0.000066	0	63	–	–	–	–	–	C
CRTS J023638	2016	0.073703	0.000057	0	42	–	–	0.073504	0.000053	40 80	C
CRTS J033349	2016	–	–	–	–	–	–	0.076159	0.000049	0 60	C
CRTS J082603	2017	0.0719	0.0004	0	1	–	–	–	–	–	C
CRTS J085113	2016	0.08750	0.00009	0	1	–	–	–	–	–	C
CRTS J085603	2016	0.060043	0.000193	0	18	–	–	–	–	–	C
CRTS J164950	2016	0.064905	0.000091	0	61	–	–	–	–	–	C
CSS J044637	2017	0.093	0.001	0	1	–	–	–	–	–	C
CSS J062450	2017	0.077577	0.000094	0	14	–	–	–	–	–	C
DDE 26	2016	0.088804	0.000067	0	44	–	–	–	–	–	C
MASTER J021315	2016	0.105124	0.000252	10	21	–	–	–	–	–	C
MASTER J030205	2016	0.061553	0.000022	1	96	8.4	2.5	–	–	–	B
MASTER J042609	2016	0.067624	0.000016	0	64	6.4	2.7	0.067221	0.000051	64 122	0.065502 B
MASTER J043220	2017	0.0640	0.0006	0	1	–	–	–	–	–	C
MASTER J043915	2016	0.062428	0.000045	0	112	–	–	–	–	–	C
MASTER J054746	2016	0.0555	0.0004	0	3	–	–	–	–	–	C
MASTER J055348	2017	0.0750	0.0001	0	24	–	–	–	–	–	CU
MASTER J064725	2016	0.067584	0.000020	0	108	1.2	3.5	–	–	–	CG
MASTER J065330	2017	0.064012	0.000167	0	13	–	–	–	–	–	C
MASTER J075450	2017	0.0664	0.0050	0	1	–	–	–	–	–	C
MASTER J150518	2017	0.071145	0.000125	0	56	–29.5	1.0	–	–	–	CGU

nova by detecting superhumps. Shafter et al. (1984) suggested a small mass ratio (either a massive white dwarf or an undermassive secondary) based on a radial-velocity study. Although Feinswog et al. (1988), Lázaro et al. (1990) and Lazaro et al. (1991) reported more detailed spectroscopic studies, the orbital period was not well measured. Observations of superhumps during the 1991 superoutburst were reported in Kato (2001). Kato et al. (2009) reanalyzed this superoutburst and reported another one in 2009. Another superoutburst in 2010 was reported in Kato et al. (2010).

The 2016 superoutburst was detected by the ASAS-SN team at  $V=12.95$  on March 22 and  $V=12.00$  on March 24. Subsequent observations detected superhumps (vsnet-alert 19645). The times of superhump maxima are listed in table 14. The observation started two days later than the announcement and stage A superhumps were not recorded.

The 2017 superoutburst was detected by K. Kasai on March 12 (vsnet-alert 20763) while observing KaiV36, an ellipsoidal variable star in the field of IR Gem. The outburst was detected early enough and stage A superhumps were observed (figure 14). The object was still in quiescence on March 10. The times of superhump maxima are listed in table 15. The observations were not long enough and  $P_{\dot{}}$  was not determined. The  $\epsilon^*$  for stage A superhumps is 0.068(11), whose errors mainly comes from the uncertainty in the orbital period [0.0684(6) d] (Feinswog et al. 1988). This  $\epsilon^*$  corresponds to  $q=0.22(4)$ . Accurate determination of the orbital period is desired since the object is bright enough and its behavior during superoutbursts has been well documented.

**Table 3.** Superhump Periods and Period Derivatives (continued)

Object	Year	$P_1$	err	$E_1$	$P_{\text{dot}}$	err	$P_2$	err	$E_2$	$P_{\text{orb}}$	Q		
MASTER J151126	2016	0.058182	0.000016	16	171	4.5	0.6	–	–	–	C		
MASTER J055845	2016	0.058070	0.000081	0	19	–	–	–	–	–	C2		
MASTER J162323	2016	0.09013	0.00007	0	4	–	–	–	–	–	Ca		
MASTER J165153	2017	0.071951	0.000079	0	31	–	–	–	–	–	C		
MASTER J174816	2016	0.083328	0.000120	0	21	–	–	–	–	–	CU		
MASTER J191841	2016	0.022076	0.000007	0	51	–	–	–	–	–	B		
MASTER J220559	2016	0.061999	0.000067	0	83	28.4	6.5	0.061434	0.000078	81	116	0.061286	C
OT J002656	2016	0.132240	0.000054	30	112	16.4	1.6	–	–	–	–	–	B
SBS 1108	2016	0.039051	0.000008	0	72	–	–	–	–	–	0.038449	–	CP
SDSS J032015	2016	0.073757	0.000028	0	137	2.5	4.2	–	–	–	–	–	CG
SDSS J091001	2017	0.0734	0.0002	0	2	–	–	–	–	–	–	–	C
SDSS J113551	2017	0.0966	0.0001	0	18	–	–	–	–	–	–	–	CU
SDSS J115207	2009	0.070028	0.000088	0	68	–	–	–	–	–	–	0.067750	CG
SDSS J115207	2017	0.070362	0.000044	0	52	–	–	0.069914	0.000019	52	131	0.067750	B
SDSS J131432	2017	0.065620	0.000034	0	55	18.3	8.6	–	–	–	–	–	C
SDSS J153015	2017	0.075241	0.000039	0	41	–	–	–	–	–	–	–	C
SDSS J155720	2016	0.085565	0.000131	0	29	–	–	–	–	–	–	–	C
SDSS J173047	2016	0.024597	0.000007	0	329	0.8	0.3	–	–	–	–	–	B
SSS J134850	2016	0.084534	0.000017	0	80	–3.0	1.6	–	–	–	–	–	CG
TCP J013758	2016	0.061692	0.000024	31	142	12.6	0.8	0.061408	0.000032	140	208	–	B
TCP J180018	2016	0.058449	0.000024	26	233	5.7	0.7	–	–	–	–	–	B

### 3.14 NY Herculis

NY Her was originally discovered by Hoffmeister (1949) as a Mira-type variable. Based on photographic observations by Pastukhova (1988) and the CRTS detection on 2011 June 10, the object was identified as an SU UMa-type dwarf nova with a short supercycle (Kato et al. 2013). For more history, see Kato et al. (2013).

The 2016 June superoutburst was detected by the ASAS-SN team at  $V=16.19$  on June 28. Subsequent observations detected superhumps (vsnet-alert 19938, 19939, 19948). The times of superhump maxima are listed in table 16. There was a rather smooth transition from stage B to C. Since the 2016 observations was much better than the 2011 one, we provide an updated superhump profile in figure 15. It is noteworthy that the mean superhump amplitude (0.10 mag) is much smaller than most of SU UMa-type dwarf novae with similar  $P_{\text{SH}}$  (or  $P_{\text{orb}}$ ) (see figure 16). Such an unusual low superhump amplitude is commonly seen in period bouncers and it may be a signature that NY Her is in a different evolutionary location from the standard one with this  $P_{\text{orb}}$ .

ASAS-SN light curve suggest that bright outbursts (likely superoutbursts) tend to occur in every  $\sim 60$ –70 d (figure 17). We selected long outbursts (presumable superoutbursts) from the ASAS-SN and Poyner’s observa-

tions and listed in table 17. Note that we selected the brightest points of outbursts and they do not necessarily reflect the starts of the outbursts. These maxima can be well expressed by a period of 63.5(2) d with residuals less than 5 d. We consider that this period is the supercycle of this system. The entire durations of superoutbursts were less than 10 d, which are much shorter than those in ER UMa-type dwarf nova (cf. Kato and Kunjaya 1995; Robertson et al. 1995) but are similar to that of V503 Cyg with a supercycle of 89 d (Harvey et al. 1995). Although the supercycle is between ER UMa-type dwarf novae and ordinary SU UMa-type dwarf novae, it is not clear whether NY Her fills a gap between them since NY Her does not have intermediate properties between them. NY Her may be classified as an unique object with a short supercycle and a small superhump amplitude despite the relatively long  $P_{\text{SH}}$ .

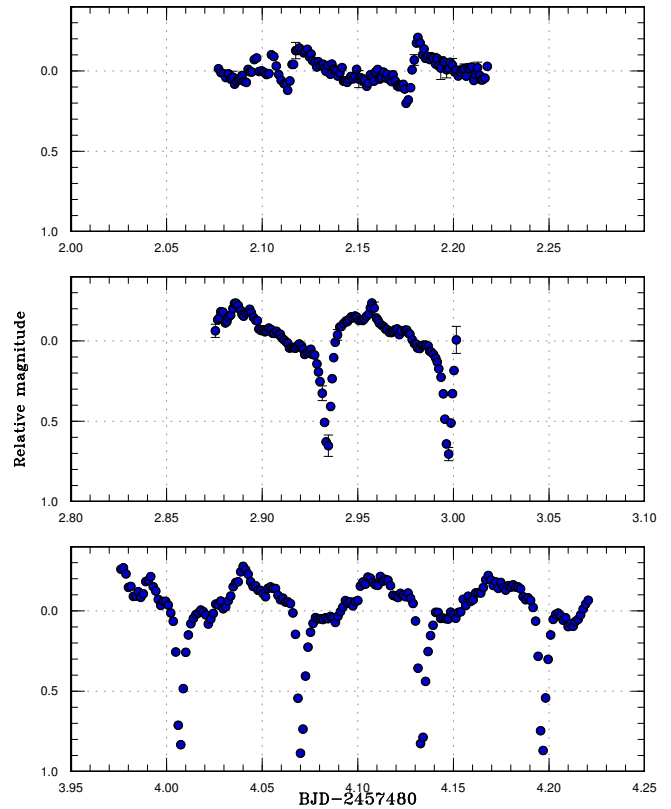
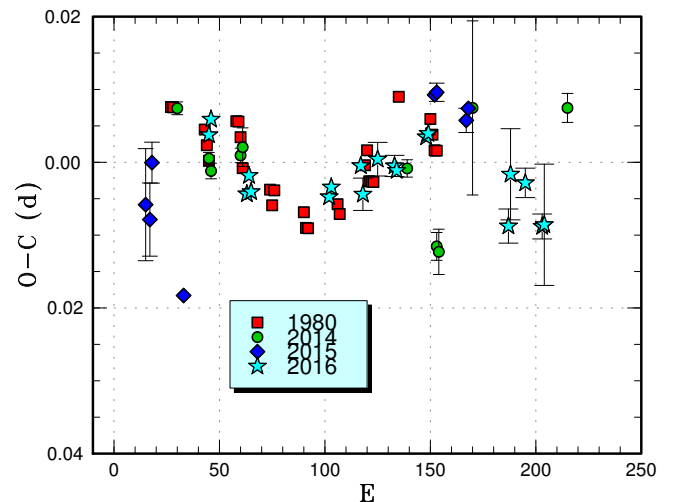
### 3.15 MN Lacertae

This object (=VV 381) was discovered by Miller (1971). Relatively frequent outbursts were recorded in Miller (1971) and the object was originally considered to be a Z Cam-type dwarf nova. T. Kato, however, noted a very faint quiescence during a systematic survey of  $I$ -band photometry of dwarf novae (1990, unpublished) and he

**Table 4.** Superhump maxima of BB Ari (2016)

$E$	max*	error	$O - C^\dagger$	$N^\ddagger$
0	57692.5399	0.0017	-0.0323	194
1	57692.6138	0.0024	-0.0310	72
12	57693.4416	0.0003	-0.0008	129
13	57693.5156	0.0003	0.0008	125
24	57694.3177	0.0003	0.0051	188
25	57694.3910	0.0002	0.0059	162
26	57694.4636	0.0002	0.0061	182
27	57694.5368	0.0002	0.0068	194
28	57694.6085	0.0002	0.0059	80
29	57694.6808	0.0002	0.0057	153
39	57695.4037	0.0004	0.0035	80
40	57695.4767	0.0004	0.0040	81
41	57695.5474	0.0005	0.0021	69
51	57696.2726	0.0003	0.0022	82
54	57696.4924	0.0006	0.0045	42
55	57696.5648	0.0005	0.0043	115
56	57696.6367	0.0007	0.0038	128
57	57696.7070	0.0015	0.0015	100
62	57697.0725	0.0006	0.0044	69
63	57697.1432	0.0005	0.0026	48
64	57697.2184	0.0011	0.0054	20
65	57697.2899	0.0012	0.0044	41
67	57697.4356	0.0006	0.0050	47
70	57697.6541	0.0013	0.0060	75
71	57697.7259	0.0012	0.0053	93
72	57697.7988	0.0011	0.0057	113
74	57697.9384	0.0005	0.0002	134
75	57698.0160	0.0004	0.0053	153
76	57698.0874	0.0009	0.0042	216
77	57698.1599	0.0004	0.0042	242
78	57698.2327	0.0003	0.0045	241
79	57698.3027	0.0006	0.0020	133
82	57698.5219	0.0008	0.0037	23
83	57698.5939	0.0004	0.0031	86
84	57698.6669	0.0003	0.0036	77
85	57698.7364	0.0011	0.0006	124
86	57698.8096	0.0016	0.0012	71
88	57698.9535	0.0007	0.0001	135
89	57699.0251	0.0005	-0.0008	135
90	57699.0947	0.0005	-0.0037	127
91	57699.1687	0.0005	-0.0022	135
92	57699.2430	0.0029	-0.0004	49
97	57699.6023	0.0007	-0.0036	33
98	57699.6755	0.0003	-0.0030	74
99	57699.7472	0.0011	-0.0038	111
100	57699.8208	0.0015	-0.0027	83
103	57700.0378	0.0004	-0.0033	129
104	57700.1071	0.0006	-0.0065	127
105	57700.1812	0.0005	-0.0048	134
109	57700.4683	0.0014	-0.0078	40
113	57700.7578	0.0011	-0.0084	144
114	57700.8295	0.0011	-0.0091	90
115	57700.9016	0.0004	-0.0096	67

\*BJD-2400000.

**Fig. 4.** Eclipses and superhumps in OY Car in the earliest phase (2016). The data were binned to 0.001 d. During the first run (upper panel), eclipses were very shallow since they overlapped with superhumps.**Fig. 5.** Comparison of  $O - C$  diagrams of OY Car between different superoutbursts. A period of 0.06465 d was used to draw this figure. Approximate cycle counts ( $E$ ) after the starts of outbursts were used. The 2015 superoutburst with a separate precursor outburst was shifted by 15 cycles to best match the others. Since the start of the 2016 superoutburst was not well constrained, the values were shifted by 45 cycles to best match the others. This shift suggests that the actual start of the 2016 superoutburst occurred 2 d before the initial detection.

**Table 5.** Superhump maxima of OY Car (2016)

$E$	max*	error	$O - C^\dagger$	phase‡	$N^\S$
0	57482.8885	0.0006	0.0027	0.27	47
1	57482.9553	0.0006	0.0049	0.33	49
18	57484.0441	0.0007	-0.0047	0.58	36
19	57484.1113	0.0006	-0.0022	0.65	33
20	57484.1737	0.0006	-0.0044	0.63	33
57	57486.5651	0.0009	-0.0037	0.52	25
58	57486.6311	0.0012	-0.0023	0.56	24
72	57487.5391	0.0009	0.0012	0.95	15
73	57487.5998	0.0022	-0.0027	0.91	19
80	57488.0572	0.0023	0.0024	0.16	29
88	57488.5735	0.0015	0.0018	0.34	21
89	57488.6375	0.0009	0.0012	0.35	15
103	57489.5472	0.0010	0.0063	0.76	21
104	57489.6123	0.0010	0.0068	0.80	20
142	57492.0563	0.0023	-0.0044	0.51	39
143	57492.1281	0.0063	0.0027	0.65	33
150	57492.5795	0.0020	0.0018	0.80	17
158	57493.0907	0.0017	-0.0039	0.90	28
159	57493.1556	0.0083	-0.0036	0.93	14

\*BJD-2400000.

†Against max = 2457482.8858 + 0.064612E.

‡Orbital phase.

§Number of points used to determine the maximum.

suggested that the outburst amplitude should be comparable to those of SU UMa-type dwarf novae.

Since this object was initially cataloged as a Z Cam-type dwarf nova, Simonsen (2011) included it as a target for “Z CamPaign” project. As a result, the outburst behavior was relatively well recorded in the AAVSO database, particularly in 2010–2012. The possibility of an SU UMa-type dwarf nova was particularly noted after a long outburst in 2011 June (vsnet-alert 13420, 13424). During this outburst, accurate astrometry was obtained confirming that the true quiescent magnitude is indeed faint (22nd mag or even fainter). There was another outburst in 2012 October, during which a call for observations of superhumps was issued (vsnet-alert 15063). Following this outburst, the object was withdrawn from the Z CamPaign project and it has not been observed as frequently as before.

The 2016 bright outburst was detected by the ASAS-SN team at  $V=15.32$  on October 30. Single-night observations on October 31 indeed detected superhumps (vsnet-alert 20283; figure 18). The times of superhump maxima were BJD 2457693.2873(15) ( $N=37$ ) and 2457693.3684(8) ( $N=53$ ). The best superhump period by the PDM method

**Table 6.** Superhump maxima of GS Cet (2016)

$E$	max*	error	$O - C^\dagger$	$N^\ddagger$
0	57709.1297	0.0005	-0.0088	62
7	57709.5380	0.0008	0.0029	12
8	57709.5897	0.0008	-0.0021	19
9	57709.6481	0.0020	-0.0004	15
14	57709.9371	0.0005	0.0054	138
15	57709.9942	0.0004	0.0059	191
16	57710.0499	0.0002	0.0049	158
17	57710.1048	0.0002	0.0032	222
18	57710.1611	0.0003	0.0027	143
25	57710.5575	0.0006	0.0026	21
26	57710.6147	0.0007	0.0032	21
27	57710.6706	0.0009	0.0024	23
39	57711.3486	0.0010	0.0005	100
40	57711.4036	0.0002	-0.0011	322
43	57711.5759	0.0007	0.0012	22
44	57711.6342	0.0014	0.0029	14
52	57712.0830	0.0010	-0.0016	59
73	57713.2710	0.0006	-0.0033	28
74	57713.3268	0.0008	-0.0041	24
78	57713.5523	0.0015	-0.0052	21
79	57713.6095	0.0013	-0.0047	20
80	57713.6660	0.0005	-0.0049	23
89	57714.1783	0.0031	-0.0025	18
90	57714.2345	0.0007	-0.0030	93
91	57714.2918	0.0006	-0.0023	70
92	57714.3491	0.0005	-0.0016	31
102	57714.9150	0.0010	-0.0023	150
103	57714.9737	0.0004	-0.0002	179
107	57715.1981	0.0005	-0.0024	32
108	57715.2538	0.0004	-0.0034	33
109	57715.3118	0.0005	-0.0020	57
110	57715.3695	0.0006	-0.0010	60
113	57715.5381	0.0039	-0.0023	13
114	57715.5945	0.0011	-0.0026	21
115	57715.6503	0.0018	-0.0035	20
131	57716.5634	0.0011	0.0032	22
132	57716.6198	0.0031	0.0029	13
133	57716.6754	0.0038	0.0019	14
140	57717.0650	0.0019	-0.0052	97
149	57717.5867	0.0053	0.0066	22
150	57717.6428	0.0063	0.0061	12
155	57717.9271	0.0017	0.0072	50
156	57717.9815	0.0021	0.0049	81

\*BJD-2400000.

†Against max = 2457709.1385 + 0.056654E.

‡Number of points used to determine the maximum.

**Table 7.** Superhump maxima of GZ Cet (2016)

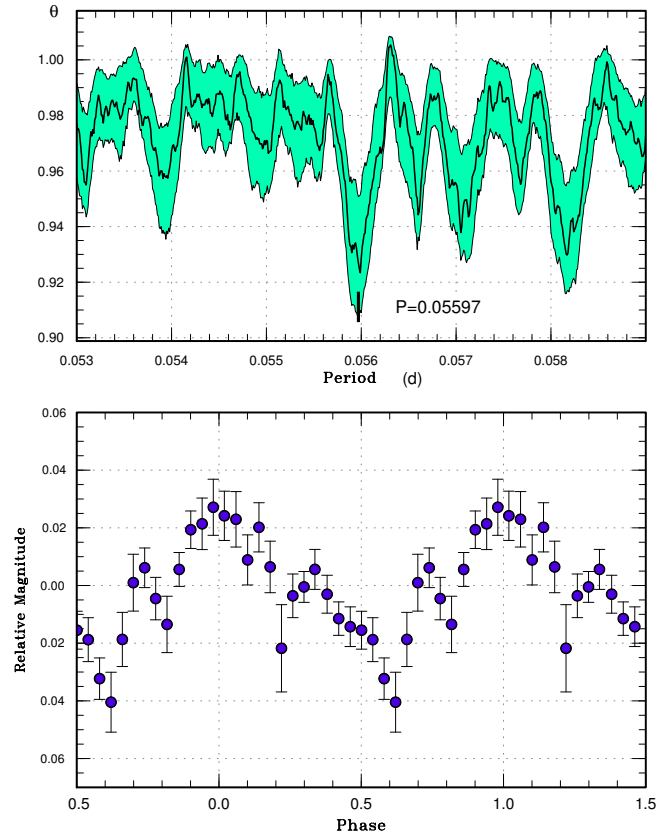
$E$	max*	error	$O - C^\dagger$	$N^\ddagger$
0	57743.0047	0.0001	-0.0090	108
1	57743.0605	0.0001	-0.0097	121
2	57743.1185	0.0013	-0.0082	27
17	57743.9670	0.0001	-0.0070	121
18	57744.0226	0.0002	-0.0079	117
19	57744.0801	0.0003	-0.0069	80
54	57746.0667	0.0005	0.0027	86
141	57750.9873	0.0003	0.0088	72
159	57752.0029	0.0002	0.0077	121
160	57752.0582	0.0005	0.0064	67
177	57753.0200	0.0003	0.0079	120
193	57753.9237	0.0002	0.0079	98
194	57753.9799	0.0002	0.0076	120
195	57754.0336	0.0002	0.0047	116
212	57754.9954	0.0004	0.0062	78
213	57755.0499	0.0006	0.0043	103
229	57755.9562	0.0003	0.0068	120
230	57756.0114	0.0004	0.0055	118
247	57756.9729	0.0003	0.0067	121
248	57757.0278	0.0004	0.0051	120
266	57758.0403	0.0004	0.0008	49
299	57759.9016	0.0018	-0.0020	21
300	57759.9609	0.0008	0.0009	43
301	57760.0189	0.0006	0.0023	42
371	57763.9655	0.0008	-0.0052	27
372	57764.0213	0.0010	-0.0058	38
424	57766.9494	0.0014	-0.0152	42
425	57767.0057	0.0015	-0.0153	21

\*BJD-2400000.

 $^\dagger$ Against max = 2457743.0137 + 0.056488E. $^\ddagger$ Number of points used to determine the maximum.**Table 8.** Superhump maxima of AK Cnc (2016)

$E$	max*	error	$O - C^\dagger$	$N^\ddagger$
0	57485.9732	0.0025	-0.0043	17
1	57486.0453	0.0003	0.0004	38
2	57486.1121	0.0010	-0.0002	24
15	57486.9901	0.0005	0.0014	28
16	57487.0571	0.0006	0.0010	38
60	57490.0249	0.0007	0.0025	38
75	57491.0388	0.0009	0.0053	21
76	57491.0993	0.0033	-0.0017	22
104	57492.9853	0.0018	-0.0033	26
105	57493.0550	0.0031	-0.0011	26

\*BJD-2400000.

 $^\dagger$ Against max = 2457485.9775 + 0.067415E. $^\ddagger$ Number of points used to determine the maximum.**Fig. 6.** Early superhumps in GS Cet (2016). (Upper): PDM analysis. (Lower): Phase-averaged profile.**Table 9.** Superhump maxima of GZ Cnc (2017)

$E$	max*	error	$O - C^\dagger$	$N^\ddagger$
0	57788.0546	0.0015	-0.0381	208
11	57789.1105	0.0007	-0.0062	120
32	57791.0878	0.0002	0.0162	156
33	57791.1809	0.0003	0.0162	185
34	57791.2760	0.0007	0.0182	88
48	57792.5748	0.0008	0.0138	19
91	57796.5686	0.0028	0.0047	33
102	57797.5774	0.0024	-0.0104	23
113	57798.5974	0.0030	-0.0145	34

\*BJD-2400000.

 $^\dagger$ Against max = 2457788.0927 + 0.093090E. $^\ddagger$ Number of points used to determine the maximum.

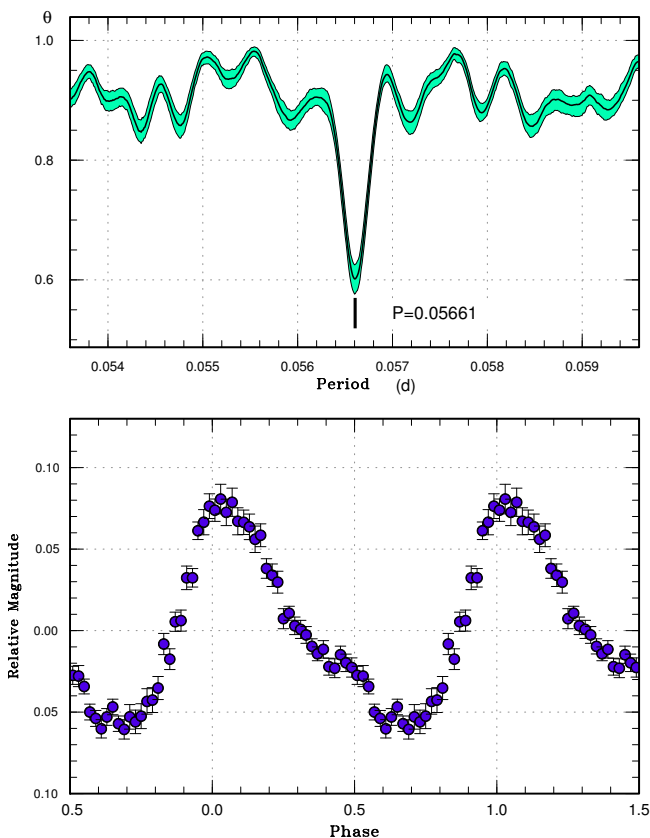


Fig. 7. Ordinary superhumps in GS Cet (2016). (Upper): PDM analysis. (Lower): Phase-averaged profile.

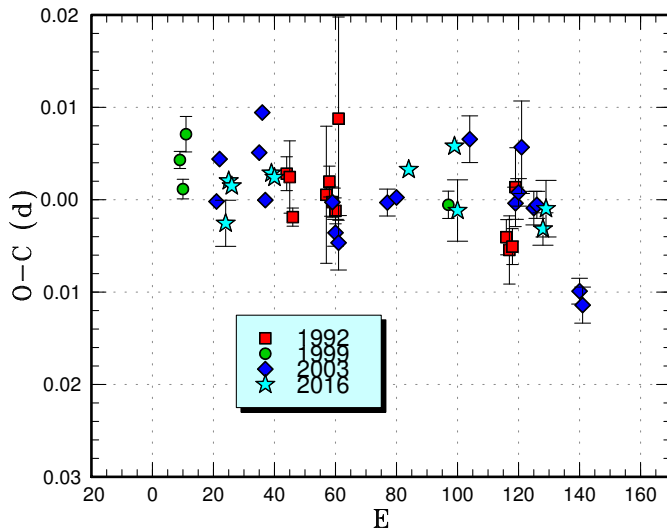


Fig. 9. Comparison of  $O - C$  diagrams of AK Cnc between different superoutbursts. A period of 0.06743 d was used to draw this figure. Approximate cycle counts ( $E$ ) after the start of the superoutburst were used.

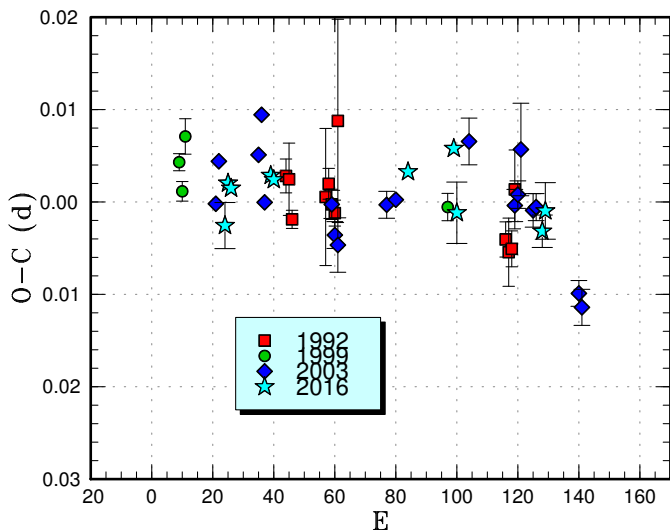


Fig. 8. Comparison of  $O - C$  diagrams of GZ Cet between different superoutbursts. A period of 0.05672 d was used to draw this figure. Approximate cycle counts ( $E$ ) after the start of the superoutburst were used.

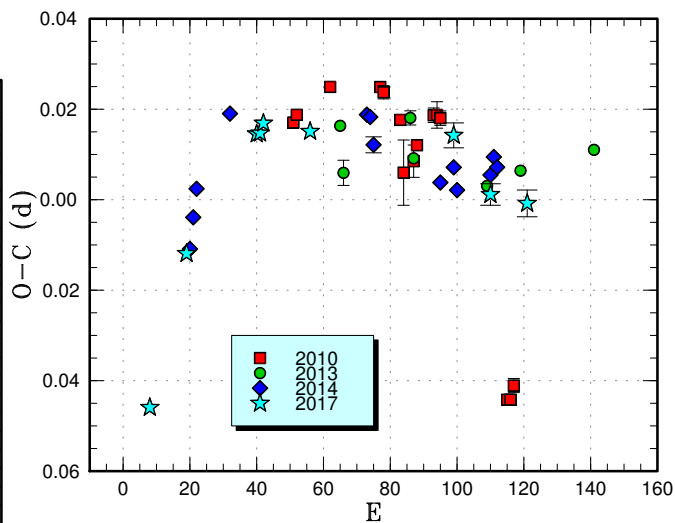
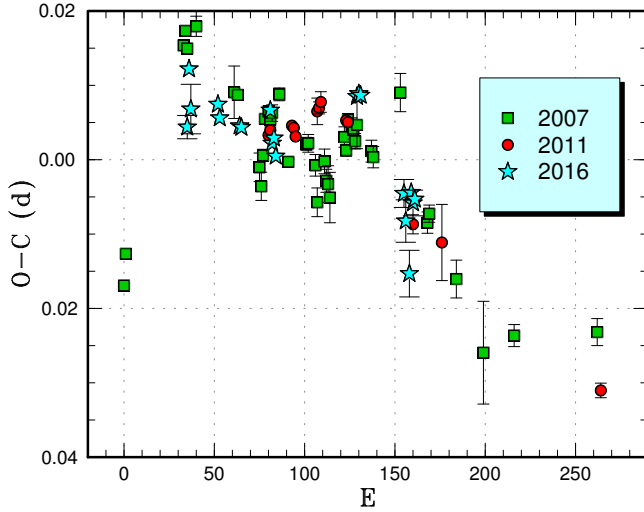
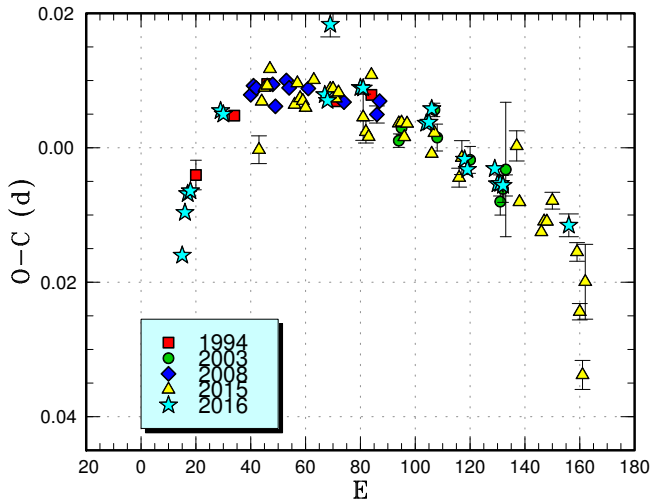


Fig. 10. Comparison of  $O - C$  diagrams of GZ Cnc between different superoutbursts. A period of 0.09290 d was used to draw this figure. Approximate cycle counts ( $E$ ) after the start of the superoutburst were used.



**Fig. 11.** Comparison of  $O - C$  diagrams of GP CVn between different superoutbursts. A period of 0.05828 d was used to draw this figure. Approximate cycle counts ( $E$ ) after the appearance of superhumps were used. Note that this treatment is different from the corresponding figure in Kato et al. (2012a). Since the 2007 observation apparently caught the early part of stage A, we set the initial superhump of 2007 to be  $E=0$  in this figure. Other superoutbursts have been shifted to best match the 2007 one. The shift value suggests that the ASAS-SN detection of the 2016 superoutburst occurred  $\sim 13$  cycles after the appearance of superhumps.



**Fig. 12.** Comparison of  $O - C$  diagrams of V1113 Cyg between different superoutbursts. A period of 0.07911 d was used to draw this figure. Approximate cycle counts ( $E$ ) after the peak of the superoutburst were used. Since the start of the 2016 superoutburst was very well defined, we used the peak of the superoutburst and redefined the cycle counts. The other outbursts were shifted to best match the 2016 one.

**Table 10.** Superhump maxima of GP CVn (2016)

$E$	max*	error	$O - C^\dagger$	phase $^\ddagger$	$N^\S$
0	57505.4014	0.0016	-0.0043	0.95	20
1	57505.4740	0.0004	0.0036	0.10	41
2	57505.5333	0.0033	-0.0016	0.05	21
17	57506.5052	0.0002	0.0005	0.49	140
18	57506.5681	0.0002	-0.0012	0.48	143
29	57507.2793	0.0003	-0.0012	0.78	43
30	57507.3439	0.0005	-0.0013	0.81	47
46	57508.3822	0.0007	0.0027	0.30	63
47	57508.4425	0.0004	-0.0017	0.26	135
48	57508.5079	0.0003	-0.0009	0.30	117
49	57508.5702	0.0003	-0.0032	0.29	103
94	57511.4920	0.0006	0.0094	0.70	59
95	57511.5571	0.0004	0.0099	0.74	57
96	57511.6217	0.0010	0.0098	0.76	39
120	57513.1625	0.0019	-0.0010	0.24	54
121	57513.2235	0.0029	-0.0046	0.21	41
123	57513.3460	0.0031	-0.0115	0.15	24
124	57513.4216	0.0005	-0.0005	0.36	54
125	57513.4850	0.0017	-0.0018	0.36	61
126	57513.5502	0.0008	-0.0012	0.40	63

\*BJD-2400000.

$^\dagger$ Against max = 2457505.4057 + 0.064648E.

$^\ddagger$ Orbital phase.

$^\S$ Number of points used to determine the maximum.

**Table 11.** Superhump maxima of V337 Cyg (2016)

$E$	max*	error	$O - C^\dagger$	$N^\ddagger$
0	57722.2200	0.0011	0.0015	68
1	57722.2925	0.0021	-0.0030	76
2	57722.3739	0.0022	0.0015	65

\*BJD-2400000.

$^\dagger$ Against max = 2457722.2185 + 0.076935E.

$^\ddagger$ Number of points used to determine the maximum.



**Table 12.** Superhump maxima of V1113 Cyg (2016)

$E$	max*	error	$O - C^\dagger$	$N^\ddagger$
0	57599.0116	0.0013	-0.0162	63
1	57599.0971	0.0005	-0.0099	64
2	57599.1790	0.0003	-0.0071	201
3	57599.2586	0.0004	-0.0066	148
14	57600.1407	0.0002	0.0053	238
15	57600.2193	0.0003	0.0048	158
52	57603.1492	0.0003	0.0078	144
53	57603.2275	0.0006	0.0070	157
54	57603.3179	0.0019	0.0183	55
65	57604.1787	0.0006	0.0089	158
66	57604.2578	0.0006	0.0089	157
89	57606.0721	0.0006	0.0037	87
90	57606.1513	0.0005	0.0039	96
91	57606.2324	0.0011	0.0059	92
103	57607.1743	0.0008	-0.0016	452
104	57607.2518	0.0013	-0.0031	104
114	57608.0431	0.0006	-0.0030	96
115	57608.1199	0.0007	-0.0052	92
116	57608.1991	0.0005	-0.0052	97
117	57608.2779	0.0016	-0.0054	60
141	57610.1706	0.0017	-0.0113	98

\*BJD-2400000.

$^\dagger$ Against max = 2457599.0279 + 0.079107E.

$^\ddagger$ Number of points used to determine the maximum.

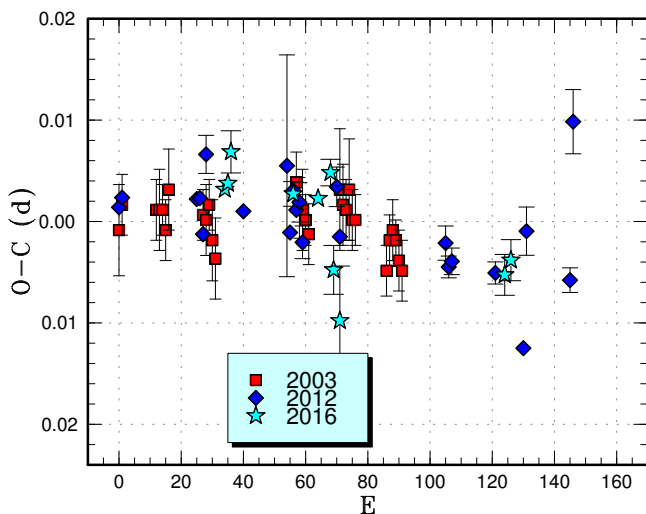


**Fig. 13.** Comparison of  $O - C$  diagrams of IX Dra between different superoutbursts. A period of 0.06700 d was used to draw this figure. Approximate cycle counts ( $E$ ) after the start of the superoutburst were used.

**Table 13.** Superhump maxima of IX Dra (2016)

$E$	max*	error	$O - C^\dagger$	$N^\ddagger$
0	57540.7847	0.0005	-0.0004	56
1	57540.8523	0.0008	0.0003	62
2	57540.9224	0.0021	0.0035	26
22	57542.2582	0.0012	0.0014	95
30	57542.7938	0.0006	0.0018	71
34	57543.0643	0.0013	0.0048	123
35	57543.1217	0.0024	-0.0047	123
37	57543.2507	0.0054	-0.0095	117
90	57546.8062	0.0020	0.0006	64
92	57546.9417	0.0020	0.0022	58

\*BJD-2400000.

$^\dagger$ Against max = 2457540.7852 + 0.066895E.

$^\ddagger$ Number of points used to determine the maximum.

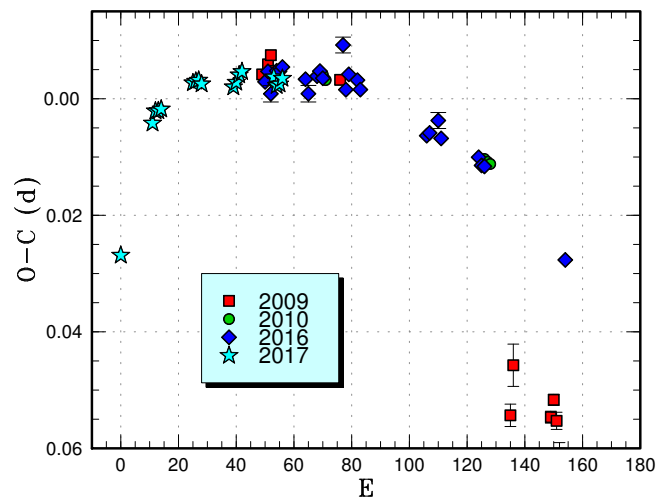


**Fig. 14.** Comparison of  $O - C$  diagrams of IR Gem between different superoutbursts. A period of 0.07109 d was used to draw this figure. Approximate cycle counts ( $E$ ) after the start of the superoutburst were used. The 2010 superoutburst was preceded by a separate precursor. We shifted the  $O - C$  values to best fit the 2016 ones. The result suggests that superhumps started to evolve 20 cycles after the peak of the precursor outburst. The final points in the 2009 superoutbursts probably correspond to traditional late superhumps.

**Table 14.** Superhump maxima of IR Gem (2016)

$E$	max*	error	$O - C^\dagger$	$N^\ddagger$
0	57474.0108	0.0006	-0.0046	79
1	57474.0837	0.0007	-0.0026	78
2	57474.1509	0.0014	-0.0062	57
4	57474.2971	0.0003	-0.0017	176
5	57474.3681	0.0003	-0.0015	192
6	57474.4399	0.0003	-0.0006	164
14	57475.0065	0.0012	-0.0007	50
15	57475.0751	0.0014	-0.0029	33
18	57475.2914	0.0003	0.0009	142
19	57475.3633	0.0003	0.0020	176
20	57475.4332	0.0004	0.0010	145
27	57475.9366	0.0014	0.0085	35
28	57476.0000	0.0007	0.0011	53
29	57476.0737	0.0011	0.0039	52
32	57476.2860	0.0005	0.0037	60
33	57476.3554	0.0005	0.0023	42
56	57477.9826	0.0009	0.0002	101
57	57478.0542	0.0010	0.0009	89
60	57478.2696	0.0014	0.0038	34
61	57478.3376	0.0004	0.0010	63
74	57479.2585	0.0004	0.0010	103
75	57479.3282	0.0004	-0.0002	127
76	57479.3991	0.0004	-0.0001	152
104	57481.3736	0.0007	-0.0091	67

\*BJD-2400000.

 $^\dagger$ Against max = 2457474.0154 + 0.070840E. $^\ddagger$ Number of points used to determine the maximum.

is 0.080(1) d. Although the SU UMa-type nature was confirmed, more observations are needed to establish a more accurate superhump period.

Thanks to the excellent coverage in 2010–2012, we could determine the supercycle. The maxima of superoutbursts (table 18) can be expressed by a supercycle of 180(8) d with the maximum  $|O - C|$  of 14 d. The result is consistent with the high outburst frequency reported in Miller (1971).

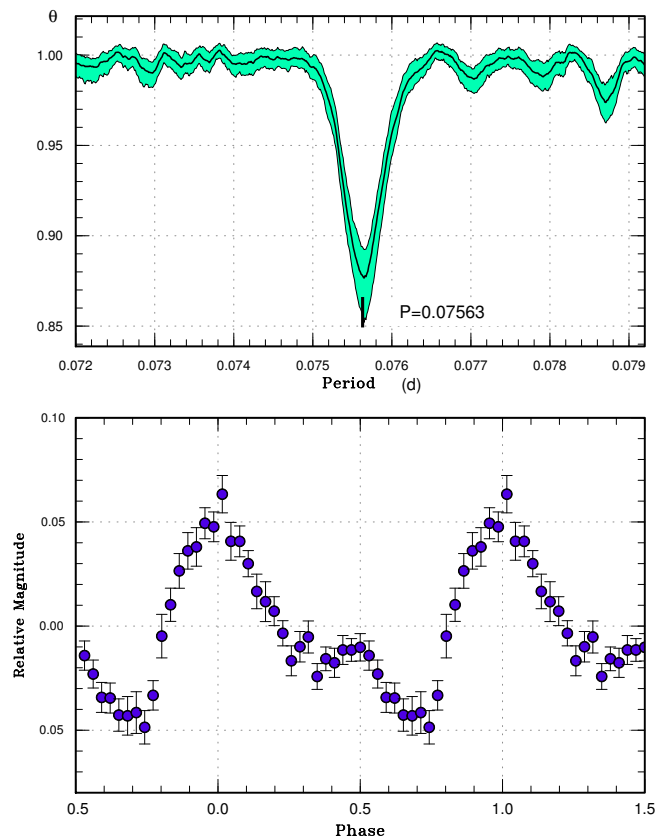
### 3.16 V699 Ophiuchi

This object was discovered as a dwarf nova (HV 10577) with a photographic range of 13.8 to fainter than 16.0 (Boyce 1942). Boyce (1942) recorded five outbursts between 1937 June 5 and 1940 July 5. The intervals of the first four outbursts were in the range of 320–390 d. Although Walker and Olmsted (1958) presented a finding chart, later spectroscopic studies have shown that the marked object is a normal star (Zwitter and Munari 1996;

**Table 15.** Superhump maxima of IR Gem (2017)

$E$	max*	error	$O - C^\dagger$	$N^\ddagger$
0	57825.4884	0.0014	-0.0181	72
11	57826.2930	0.0001	0.0015	314
12	57826.3662	0.0002	0.0033	78
13	57826.4373	0.0003	0.0031	78
14	57826.5087	0.0005	0.0031	60
25	57827.2952	0.0001	0.0045	232
26	57827.3666	0.0002	0.0045	218
27	57827.4378	0.0002	0.0044	116
28	57827.5083	0.0004	0.0035	68
39	57828.2898	0.0005	-0.0000	78
40	57828.3617	0.0009	0.0005	56
41	57828.4340	0.0004	0.0014	78
42	57828.5057	0.0005	0.0017	67
53	57829.2867	0.0003	-0.0022	65
54	57829.3563	0.0004	-0.0040	78
55	57829.4277	0.0005	-0.0040	79
56	57829.4998	0.0005	-0.0033	72

\*BJD-2400000.

 $^\dagger$ Against max = 2457825.5065 + 0.071368E. $^\ddagger$ Number of points used to determine the maximum.**Fig. 15.** Superhumps in NY Her during the superoutburst plateau (2016). (Upper): PDM analysis. (Lower): Phase-averaged profile.

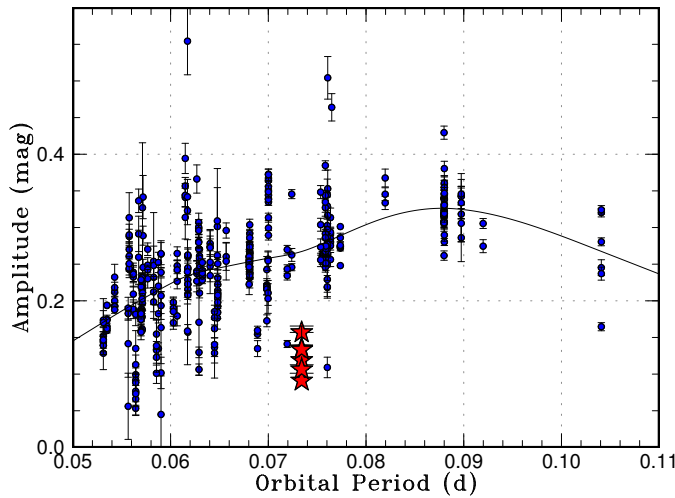


Fig. 16. Dependence of superhump amplitudes on orbital period. The superoutburst samples are described in subsection 4.7.1 in Kato et al. (2012a). We selected the range of  $-5 < E < 10$  respect to the peak superhump amplitude to illustrate the maximum superhump amplitudes. The curve indicates a spline-smoothed interpolation of the sample in Kato et al. (2012a). The location of NY Her (reflecting the first night of observation; we consider that these observations were early enough to make a comparison in this figure) is shown by stars. The single point right to NY Her is a superhump of QY Per in 1999. The other superhumps of the same superoutburst had amplitudes larger than 0.2 mag and this measurement does not reflect the characteristic amplitude of superhumps in QY Per.

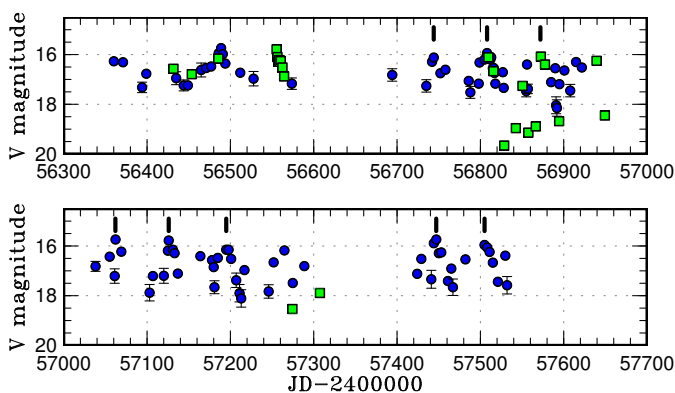


Fig. 17. ASAS-SN and unfiltered CCD light curve of NY Her. Filled circles and squares represent ASAS-SN and Poyner's measurements, respectively. Although details of each outburst are not very clear, bright outbursts (likely superoutbursts) tend to occur in every  $\sim 60\text{--}70$  d. The maxima of bright outbursts listed in table 17 and covered by observations in this figure are shown by ticks.

Table 16. Superhump maxima of NY Her (2016)

$E$	max*	error	$O - C^\dagger$	$N^\ddagger$
0	57568.7208	0.0015	-0.0081	85
1	57568.8020	0.0010	-0.0026	141
2	57568.8771	0.0009	-0.0032	106
3	57568.9548	0.0039	-0.0011	40
9	57569.4083	0.0010	-0.0016	39
10	57569.4829	0.0009	-0.0026	33
13	57569.7107	0.0050	-0.0018	38
14	57569.7885	0.0017	0.0004	74
15	57569.8671	0.0028	0.0033	75
16	57569.9368	0.0015	-0.0027	67
27	57570.7743	0.0011	0.0025	74
29	57570.9240	0.0023	0.0010	75
36	57571.4560	0.0013	0.0033	54
37	57571.5267	0.0015	-0.0017	52
40	57571.7561	0.0013	0.0007	73
41	57571.8337	0.0014	0.0027	66
42	57571.9149	0.0016	0.0082	74
49	57572.4354	0.0010	-0.0009	38
50	57572.5121	0.0012	0.0001	36
53	57572.7474	0.0027	0.0084	72
54	57572.8150	0.0018	0.0004	66
55	57572.8892	0.0017	-0.0011	74
56	57572.9733	0.0048	0.0074	29
58	57573.1254	0.0084	0.0081	73
59	57573.1964	0.0032	0.0035	74
63	57573.4910	0.0012	-0.0046	103
64	57573.5729	0.0019	0.0016	48
66	57573.7205	0.0019	-0.0020	56
67	57573.8032	0.0024	0.0050	66
68	57573.8722	0.0015	-0.0017	72
69	57573.9475	0.0030	-0.0020	50
75	57574.3993	0.0028	-0.0042	19
76	57574.4757	0.0012	-0.0035	38
80	57574.7808	0.0012	-0.0010	68
81	57574.8619	0.0014	0.0044	74
82	57574.9277	0.0016	-0.0054	52
106	57576.7464	0.0051	-0.0026	24
114	57577.3474	0.0036	-0.0069	30

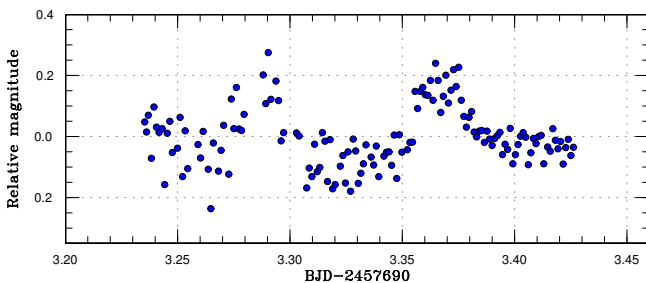
\*BJD-2400000.

$^\dagger$ Against max =  $2457568.7289 + 0.075661E$ .

$^\ddagger$ Number of points used to determine the maximum.

**Table 17.** List of recent superoutbursts of NY Her

Cycle	JD–2400000	magnitude
0	56744	16.12
1	56808	15.94
2	56872	16.08
5	57062	15.74
6	57126	15.78
7	57195	16.15
8	57258	15.94
11	57447	15.74
12	57505	15.96
13	57568	16.19

**Fig. 18.** Superhumps in MN Lac (2016).

Liu et al. 1999).

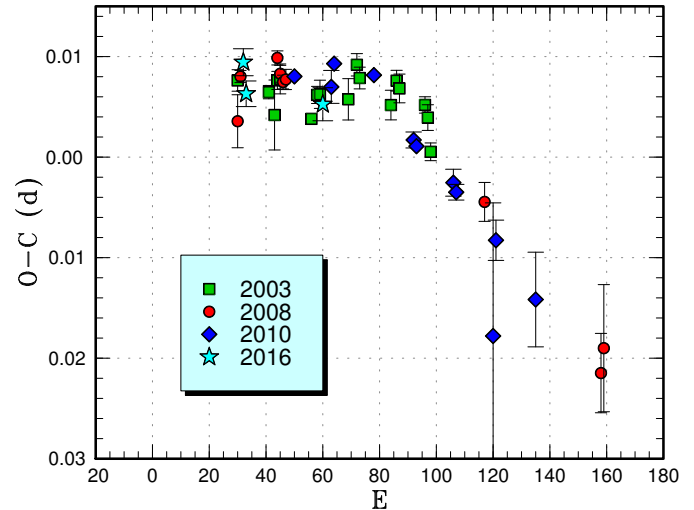
On 1999 April 16, A. Pearce detected an outburst (vsnet-alert 2877). Accurate astrometry and photometry of the outbursting object indicated that the true V699 Oph is an unresolved companion to a 16-th magnitude star (vsnet-alert 2878, vsnet-chat 1810, 1868). The first confirmed superoutburst was recorded in 2003. This outburst was preceded by a separate precursor and followed by a rebrightening, forming a “triple outburst”. (Kato et al. 2009). The 2008 and 2010 superoutbursts were also reported in Kato et al. (2009) and Kato et al. (2010), respectively.

The 2016 superoutburst was detected by the ASAS-SN team at  $V=14.56$  on May 15 and by R. Stubbings at a visual magnitude of 14.4 on the same night. Time-resolved photometric observations were obtained on two nights and

**Table 18.** List of likely superoutbursts of MN Lac in 2010–2012

Year	Month	Day	max*	V-mag
2010	11	6	55506	15.93
2011	5	31	55713	15.74
2011	11	24	55890	16.12
2012	4	30	56048	15.94

\*JD–2400000.

**Fig. 19.** Comparison of  $O - C$  diagrams of V699 Oph between different superoutbursts. A period of 0.07031 d was used to draw this figure. Approximate cycle counts ( $E$ ) after the start of the superoutburst were used.**Table 19.** Superhump maxima of V699 Oph (2016)

$E$	max*	error	$O - C^\dagger$	$N^\ddagger$
0	57527.1699	0.0013	0.0015	122
1	57527.2371	0.0013	–0.0015	128
28	57529.1344	0.0016	0.0001	77

\*BJD–2400000.

$^\dagger$ Against max = 2457527.1684 + 0.070212E.

$^\ddagger$ Number of points used to determine the maximum.

the times of superhump maxima are listed in table 19. The 2016 observation probably recorded the early part of stage B superhumps (figure 19).

### 3.17 V344 Pavonis

This dwarf nova was discovered in outburst on 1990 July 21. The object was spectroscopically confirmed as a dwarf nova. There were two outbursts recorded in archival plates between 1979 May and 1984 September (Maza et al. 1990). Mason and Howell (2003) obtained a typical spectrum of a dwarf nova in quiescence. Uemura et al. (2004) studied the 2004 outburst and identified the SU UMA-type nature. The analysis was refined in Kato et al. (2009).

The 2016 superoutburst was detected by R. Stubbings at a visual magnitude of 14.4 on April 25. Subsequent observations detected superhumps (vsnet-alert 19796). The times of superhump maxima are listed in table 20. Time-resolved photometry was obtained only in the later phase of the superoutbursts both in 2004 and 2016. The superhump stage has been therefore unclear (figure 20). We

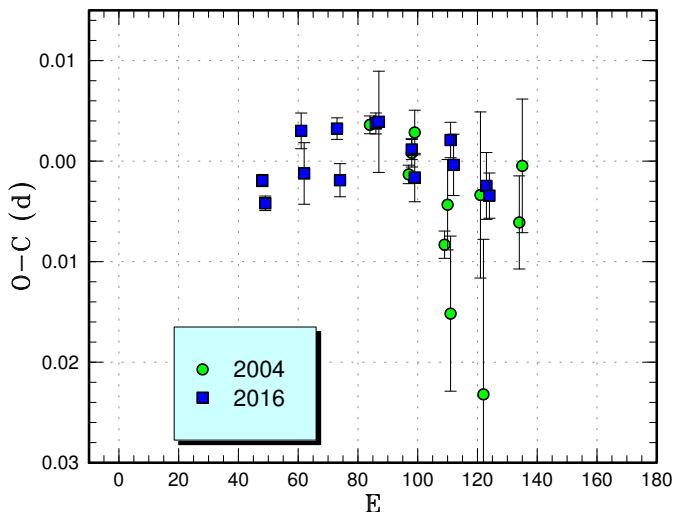


**Fig. 20.** Comparison of  $O - C$  diagrams of V344 Pav between different superoutbursts. A period of 0.07988 d was used to draw this figure. Approximate cycle counts ( $E$ ) after the start of the superoutburst were used. Since the start of the 2004 outburst was not well constrained, we shifted the  $O - C$  diagram so that the rapid fading of the two superoutbursts match each other.

**Table 20.** Superhump maxima of V344 Pav (2016)

$E$	max*	error	$O - C^\dagger$	$N^\ddagger$
0	57507.7957	0.0006	-0.0020	20
1	57507.8734	0.0007	-0.0043	22
13	57508.8391	0.0018	0.0030	22
14	57508.9148	0.0031	-0.0013	6
25	57509.7979	0.0011	0.0032	23
26	57509.8726	0.0016	-0.0019	21
38	57510.8369	0.0010	0.0037	22
39	57510.9169	0.0050	0.0039	8
50	57511.7928	0.0010	0.0012	22
51	57511.8699	0.0024	-0.0016	21
63	57512.8322	0.0018	0.0022	23
64	57512.9096	0.0031	-0.0003	10
75	57513.7862	0.0033	-0.0024	20
76	57513.8651	0.0022	-0.0034	21

\*BJD-2400000.

$^\dagger$ Against max = 2457507.7977 + 0.079878E.

$^\ddagger$ Number of points used to determine the maximum.

listed a global  $P_{\text{dot}}$  in table 3. Observations in the earlier phase of the superoutburst are needed to characterize superhumps of this object better.

### 3.18 V368 Pegasi

V368 Peg is a dwarf nova (Antipin Var 63) discovered by Antipin (1999). See Kato et al. (2016a) for the summary

**Table 21.** Superhump maxima of V893 Sco (2016)

$E$	max*	error	$O - C^\dagger$	phase $^\ddagger$	$N^\S$
0	57476.1964	0.0017	-0.0062	0.10	92
1	57476.2774	0.0007	0.0002	0.05	118
2	57476.3528	0.0007	0.0009	0.06	117
13	57477.1799	0.0011	0.0067	0.09	115
14	57477.2601	0.0049	0.0122	0.11	111
15	57477.3120	0.0015	-0.0105	0.07	112
16	57477.3987	0.0016	0.0015	0.11	69
26	57478.1390	0.0013	-0.0049	0.17	42

\*BJD-2400000.

$^\dagger$ Against max = 2457476.2025 + 0.074666E.

$^\ddagger$ Orbital phase.

$^\S$ Number of points used to determine the maximum.

of the history. The 2016 superoutburst was detected by P. Schmeer at a visual magnitude of 13.0 on September 28. Time-resolved photometry was performed only on a single night. The resultant superhump maxima were BJD 2457661.4175(5) ( $N=66$ ) and 2457661.4883(4) ( $N=76$ ).

### 3.19 V893 Sco

V893 Sco was discovered as a variable star by Satyvoldiev (1972). The variable had been lost for a long time, and was rediscovered by K. Haseda (Kato et al. 1998). For more historical information, see Kato et al. (2014a). This object is an eclipsing SU UMa-type dwarf nova (cf. Bruch et al. 2000; Matsumoto et al. 2000).

The 2016 superoutburst was detected by R. Stubbings at a visual magnitude of 12.8 on March 21. It once faded to  $V=13.64$  on the same night and brightened to  $V=12.37$  on March 25 (vsnet-alert 19652). The outburst on March 21 should have been a precursor. Our time-resolved photometry started on March 28 and detected superhumps (vsnet-alert 19661; figure 21). Since our observation started relatively late, we could record only the final part of the superoutburst. Later observations were dominated by the orbital humps and we could only extract a small number of superhump maxima outside the eclipses (table 21). We obtained the eclipse ephemeris for the use of defining the orbital phases in this paper

$$\text{Min(BJD)} = 2454173.3030(3) + 0.0759614600(16)E \quad (3)$$

using the MCMC modeling (Kato et al. 2013) using the data up to Kato et al. (2014a) and current set of observation.

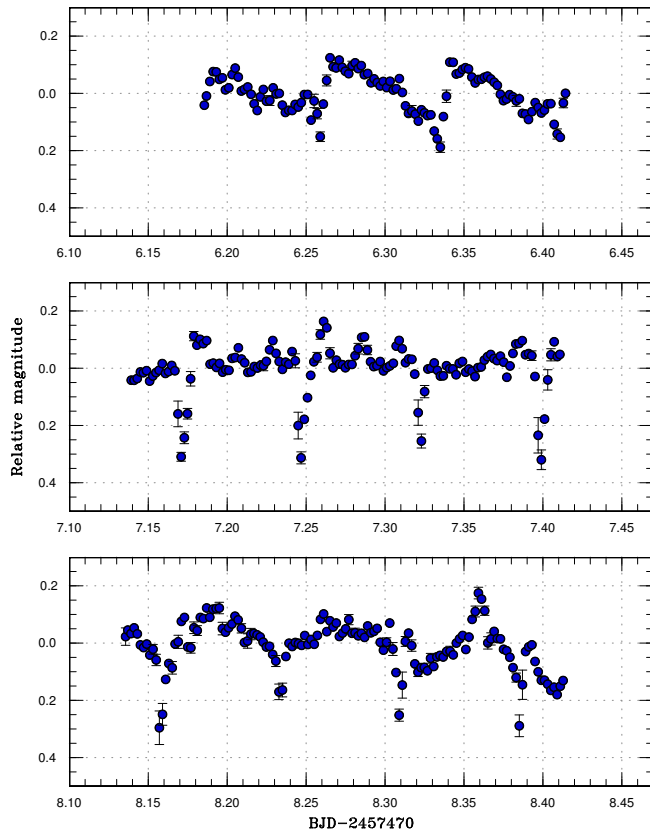


Fig. 21. Eclipses and superhumps in V893 Sco (2016). The data were binned to 0.002 d.

### 3.20 V493 Serpents

This object (=SDSS J155644.24–000950.2) was selected as a dwarf nova by SDSS (Szkody et al. 2002). The SU UMa-type nature was identified by observations of the 2006 and 2007 superoutbursts (Kato et al. 2009). See Kato et al. (2014b) for more history.

The 2016 superoutburst was detected by T. Horie at a visual magnitude of 12.5 on June 5. It was pointed out by H. Maehara the outburst already started on June 1 (vsnet-alert 19872). Time-resolved photometry was carried out on two nights, yielding superhump maxima in table 22. A comparison of  $O - C$  diagrams (figure 22) suggest that these observations recorded the early phase of stage C.

### 3.21 AW Sagittae

AW Sge was discovered as a dwarf nova by Wolf and Wolf (1906). The object was identified as an SU UMa-type dwarf nova during the 2000 outburst (Kato et al. 2009). See Kato et al. (2014a) for more history.

The 2016 superoutburst was detected by R. Stubbings at a visual magnitude of 14.6 on June 14. Time-resolved

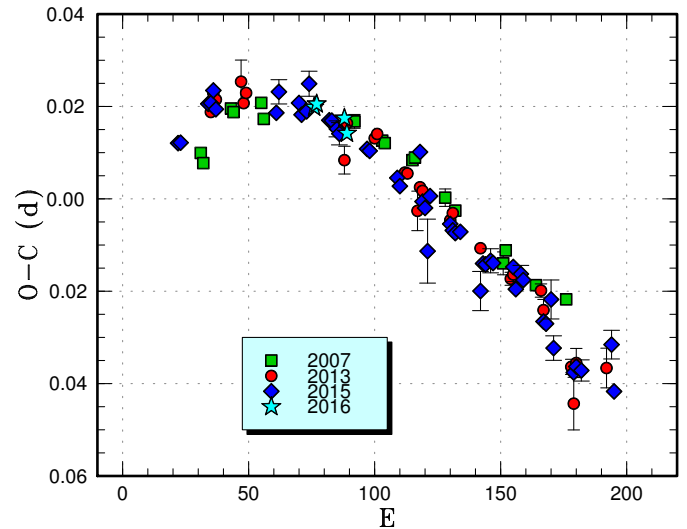


Fig. 22. Comparison of  $O - C$  diagrams of V493 Ser between different superoutbursts. A period of 0.08310 d was used to draw this figure. Approximate cycle counts ( $E$ ) after the start of the superoutburst were used.

Table 22. Superhump maxima of V493 Ser (2016)

$E$	max*	error	$O - C^\dagger$	$N^\ddagger$
0	57547.3780	0.0013	-0.0006	26
1	57547.4618	0.0008	0.0005	25
12	57548.3728	0.0012	0.0015	22
13	57548.4526	0.0008	-0.0014	25

\*BJD-2400000.

$^\dagger$ Against max = 2457547.3786 + 0.082730E.

$^\ddagger$ Number of points used to determine the maximum.

photometric observations were carried out on a single night and yielded the superhumps maxima: BJD 2457558.3859(5) ( $N=75$ ) and 2457558.4606(9) ( $N=50$ ).

### 3.22 V1389 Tauri

This object was discovered by K. Itagaki at an unfiltered CCD magnitude of 14.1 on 2008 August 7 (Yamaoka et al. 2008). There was an X-ray counterpart (1RXS J040700.2+005247) and the dwarf nova-type classification was readily suggested. The object was recorded already in outburst at  $V=13.5$  on August 4 in the ASAS-3 (Pojmański 2002) data (vsnet-alert 10419). There were two past outbursts (2004 October 20 and 2006 March 16) recorded in the ASAS-3 data (vsnet-alert 10419). Subsequent observations detected superhumps (vsnet-alert 10422, 10423). This outburst was studied in Kato et al. (2009). Another superoutburst in 2010 was studied in Kato et al. (2010).

The 2016 superoutburst was detected by the ASAS-SN

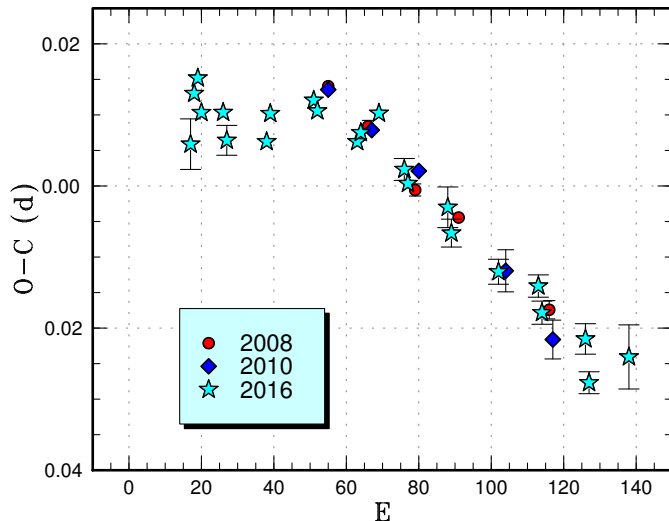


**Fig. 23.** Comparison of  $O - C$  diagrams of V1389 Tau between different superoutbursts. A period of 0.08046 d was used to draw this figure. Approximate cycle counts ( $E$ ) after the start of the superoutburst were used. Since the start of the 2010 superoutburst was not known, we have shifted the  $O - C$  diagram to best fit the others.

team at  $V=13.52$  on October 23. Subsequent observations detected superhumps (vsnet-alert 20267). The times of superhump maxima are listed in table 23. As in other typical long- $P_{\text{SH}}$  systems (cf. figure 4 in Kato et al. 2009), stage B was relatively short. A comparison of the  $O - C$  diagrams has confirmed that the superhumps recorded in 2008 were indeed stage C ones (figure 23). Although individual superhump maxima were not measured, a PDM analysis of the post-superoutburst data (4.5 d segment after BJD 2457697) detected a period of 0.08000(11) d. This value suggests that stage C superhump lasted even after the termination of the superoutburst.

### 3.23 SU Ursae Majoris

This object is the prototype of SU UMa-type dwarf novae. See Kato et al. (2015a) for the history. The 2017 superoutburst was detected by E. Muylaert at a visual magnitude of 11.3 on February 23. Only single superhump at BJD 2457810.5647(3) ( $N=89$ ) was observed.

### 3.24 HV Virginis

HV Vir was originally discovered by Schneller (1931) in outburst on 1929 February 11. The object was also given a designation of NSV 6201 as a suspected variable. Duerbeck (1984) and Duerbeck (1987) classified it as a classical nova and provided a light curve of the 1929 outburst based on his examination of archival

**Table 23.** Superhump maxima of V1389 Tau (2016)

$E$	max*	error	$O - C^\dagger$	$N^\ddagger$
0	57686.0276	0.0036	-0.0098	97
1	57686.1152	0.0006	-0.0023	176
2	57686.1979	0.0004	0.0002	178
3	57686.2735	0.0008	-0.0044	104
9	57686.7562	0.0009	-0.0025	25
10	57686.8328	0.0021	-0.0061	21
21	57687.7177	0.0013	-0.0029	17
22	57687.8021	0.0010	0.0014	21
34	57688.7695	0.0009	0.0069	23
35	57688.8484	0.0006	0.0058	17
46	57689.7291	0.0010	0.0048	15
47	57689.8109	0.0008	0.0064	16
52	57690.2159	0.0009	0.0107	98
59	57690.7712	0.0015	0.0050	20
60	57690.8497	0.0007	0.0033	16
71	57691.7314	0.0029	0.0033	22
72	57691.8082	0.0020	0.0000	20
85	57692.8488	0.0018	-0.0014	16
96	57693.7318	0.0016	0.0000	22
97	57693.8085	0.0016	-0.0034	20
109	57694.7704	0.0021	-0.0034	20
110	57694.8447	0.0015	-0.0093	16
121	57695.7334	0.0045	-0.0022	22

\*BJD-2400000.

$^\dagger$ Against max = 2457686.0374 + 0.080150E.

$^\ddagger$ Number of points used to determine the maximum.

plates. Amateur observers, particularly by the Variable Star Observers' League in Japan (VSOLJ), suspected it to be a dwarf nova and started monitoring since 1987 [i.e. following the publication of Duerbeck (1987)]. The object was caught in outburst by P. Schmeer on 1992 April 20 at a visual magnitude of 12.0 (Schmeer et al. 1992). The 1992 outburst was extensively studied (Barwig et al. 1992; Leibowitz et al. 1994; Kato et al. 2001). It might be worth noting that Barwig et al. (1992) recorded low-amplitude variations with a period corresponding to the orbital period, their interpretation (originating from the hot spot as in quiescence) was strongly affected by Patterson et al. (1981). Although Szkody et al. (1992) reported the detection of superhumps, the detailed result has not been published. Leibowitz et al. (1994) reported the detection of historical outbursts in 1939, 1970 and 1981 in archival plates. Although Leibowitz et al. (1994) noted chaotic "early superhump variability", its period was not precisely determined. Leibowitz et al. (1994) recorded superhumps and reported a negative  $P_{\text{dot}}$ , which was incorrect due to an error in cycle counts probably misguided by the

received wisdom at that time that SU UMa-type dwarf novae universally show negative  $P_{\text{dot}}$  (cf. Warner 1985; Patterson et al. 1993). Using additional observations and all available data, Kato et al. (2001) clarified that this object showed two types of superhumps (early superhumps and ordinary superhumps) and the  $P_{\text{dot}}$  for ordinary superhumps was positive. Kato et al. (2001) proposed the close similarity to AL Com (cf. Kato et al. 1996a) and WZ Sge, giving a basis of the modern concept of WZ Sge-type dwarf novae (Kato 2015).

The object underwent another superoutburst in 2002. This outburst was also extensively studied by Ishioka et al. (2003), who established the positive  $P_{\text{dot}}$  using a much more complete set of observations than in 1992. Patterson et al. (2003) also reported the superhump period of the same outburst and the orbital period of 0.057069(6) d from quiescent photometry. There was another superoutburst in 2008, which was reported in Kato et al. (2009).

The 2016 superoutburst was detected by the ASAS-SN team at  $V=12.0$  on March 10 (cf. vsnet-alert 19571). Initial observations already detected early superhumps (vsnet-alert 19573, 19576, 19589; figure 25). The object then developed ordinary superhumps (vsnet-alert 19581, 19599, 19633). The times of superhump maxima are listed in table 24. The data very clearly demonstrate the presence of stages A and B, although there was an observational gap in the middle of stage B. The superhump period of stage A was very ideally determined to be 0.05907(6) d (cf. figure 24). This period gives the fractional superhump excess of  $\epsilon^*=0.034(1)$ , which corresponds to  $q=0.093(3)$ . This value supersedes the earlier determination by the same method to be  $q=0.072(1)$  using the less extensive 2002 data. The period was determined for the 2002 data from single-night observations assuming that stage A continued up to the first observation of stage B while the present observation obtained an almost complete coverage of stage A (see figure 24). It was likely that the error was underestimated in the 2002 superoutburst. The outburst started rapid fading on March 29–30 and the entire duration of the superoutburst was at least 20 d. Despite dense observations, no post-outburst rebrightening was recorded.

A PDM analysis of the post-superoutburst observations yielded a period of 0.05799(2) d (figure 26). This period corresponds to a disk radius of  $0.33a$  assuming that the precession rate is not affected by the pressure effect. The value is in the range of  $0.30\text{--}0.38a$  determined for well-observed WZ Sge-type dwarf novae (Kato and Osaki 2013).

The period of early superhumps [0.057000(8) d] is in agreement with 0.056996(9) d determined from the 2008

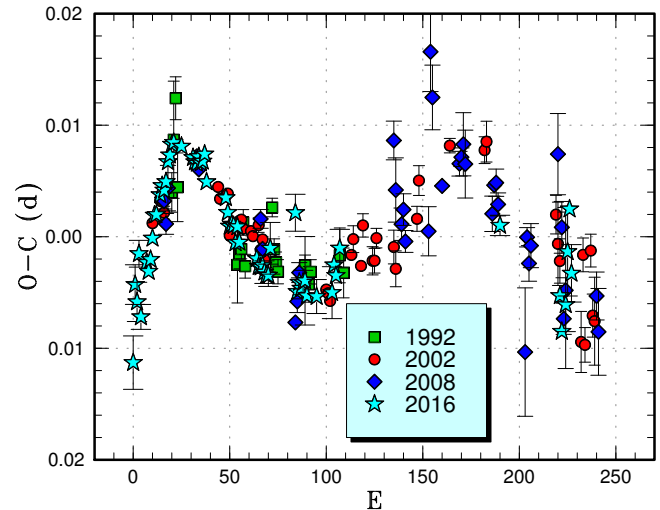


**Fig. 24.** Comparison of  $O - C$  diagrams of HV Vir between different superoutbursts. A period of 0.05828 d was used to draw this figure. Approximate cycle counts ( $E$ ) after the emergence of ordinary superhumps were used. After the high-quality observations in 2016, it became apparent that the emergence of ordinary superhumps was not well recorded in the past superoutbursts. The cycle counts were shifted by 20, 10 and 15 for the 1992, 2002 and 2008 superoutbursts, respectively, to match the 2016 observations.

observation (from the observations reported in Kato et al. 2009). The quality of past observations were lower: 0.057085 d (without error estimate) for the 1992 outburst (Kato et al. 2001), which was based only on published times of maxima, and 0.0569(1) d for the 2002 outburst (Ishioka et al. 2003). The current observations, combined with the 2008 data, established the period of early superhumps of this object to a precision directly comparable to the orbital period for the first time. The 2016 and 2008 periods were 0.13(2)% and 0.13(3)% shorter than the orbital period, respectively.

### 3.25 NSV 2026

This object was discovered as a variable star (=HV 6907) by Hoffleit (1935). The SU UMa-type nature was confirmed during the 2015 superoutburst. For more history, see Kato et al. (2016a).

There was a superoutburst in 2016 February (Kato et al. 2016a). Another superoutburst occurred in 2016 November, which was detected by J. Shears at an unfiltered CCD magnitude of 14.19 and by E. Muylaert at a visual magnitude of 14.0 on November 25. The object was further observed to brighten to a visual magnitude of 13.2 on November 26. The times of superhump maxima are listed in table 25. These superhumps were likely stage B ones (figure 27). As judged from the interval of two superoutbursts in 2016 and the supercycle of  $\sim 95$  d (Kato et al.



**Table 24.** Superhump maxima of HV Vir (2016)

$E$	max*	error	$O - C^\dagger$	$N^\ddagger$	$E$	max*	error	$O - C^\dagger$	$N^\ddagger$
0	57463.6347	0.0024	-0.0131	24	52	57466.6775	0.0004	0.0006	28
1	57463.6999	0.0018	-0.0061	29	53	57466.7342	0.0005	-0.0009	23
2	57463.7567	0.0018	-0.0076	24	54	57466.7940	0.0005	0.0006	19
3	57463.8193	0.0012	-0.0033	20	55	57466.8508	0.0004	-0.0008	21
4	57463.8719	0.0011	-0.0089	23	64	57467.3739	0.0002	-0.0020	108
7	57464.0516	0.0006	-0.0039	52	65	57467.4315	0.0003	-0.0027	118
8	57464.1091	0.0005	-0.0047	48	66	57467.4897	0.0003	-0.0027	152
9	57464.1684	0.0008	-0.0036	33	67	57467.5481	0.0004	-0.0025	59
10	57464.2286	0.0005	-0.0017	58	68	57467.6058	0.0010	-0.0031	48
11	57464.2889	0.0005	0.0004	60	69	57467.6638	0.0005	-0.0033	73
12	57464.3473	0.0003	0.0005	47	70	57467.7221	0.0010	-0.0033	23
14	57464.4656	0.0003	0.0023	137	71	57467.7828	0.0023	-0.0009	14
15	57464.5247	0.0002	0.0032	172	84	57468.5436	0.0017	0.0027	41
16	57464.5826	0.0002	0.0028	172	85	57468.5948	0.0006	-0.0044	65
17	57464.6416	0.0002	0.0036	150	86	57468.6539	0.0008	-0.0035	27
18	57464.7017	0.0003	0.0054	40	87	57468.7117	0.0009	-0.0040	24
19	57464.7606	0.0004	0.0060	32	88	57468.7705	0.0011	-0.0035	20
20	57464.8198	0.0005	0.0070	19	89	57468.8289	0.0040	-0.0033	20
21	57464.8783	0.0005	0.0072	25	90	57468.8858	0.0005	-0.0046	26
25	57465.1110	0.0006	0.0070	50	95	57469.1772	0.0015	-0.0045	30
31	57465.4597	0.0002	0.0061	166	103	57469.6438	0.0023	-0.0040	28
32	57465.5176	0.0003	0.0058	81	104	57469.7045	0.0008	-0.0015	25
33	57465.5758	0.0003	0.0057	119	105	57469.7619	0.0008	-0.0024	21
34	57465.6346	0.0002	0.0063	134	107	57469.8809	0.0017	0.0001	26
35	57465.6924	0.0004	0.0058	46	190	57474.7202	0.0009	0.0045	25
36	57465.7508	0.0003	0.0060	38	221	57476.5205	0.0007	-0.0010	52
37	57465.8097	0.0007	0.0066	15	222	57476.5756	0.0009	-0.0041	50
38	57465.8655	0.0007	0.0042	23	224	57476.6946	0.0024	-0.0017	14
48	57466.4469	0.0005	0.0030	56	225	57476.7576	0.0040	0.0031	15
49	57466.5038	0.0004	0.0017	57	226	57476.8197	0.0008	0.0069	33
50	57466.5609	0.0004	0.0005	58	227	57476.8722	0.0026	0.0012	39
51	57466.6193	0.0003	0.0007	79	-	-	-	-	-

\*BJD-2400000.

 $^\dagger$ Against max = 2457463.6478 + 0.058252E. $^\ddagger$ Number of points used to determine the maximum.

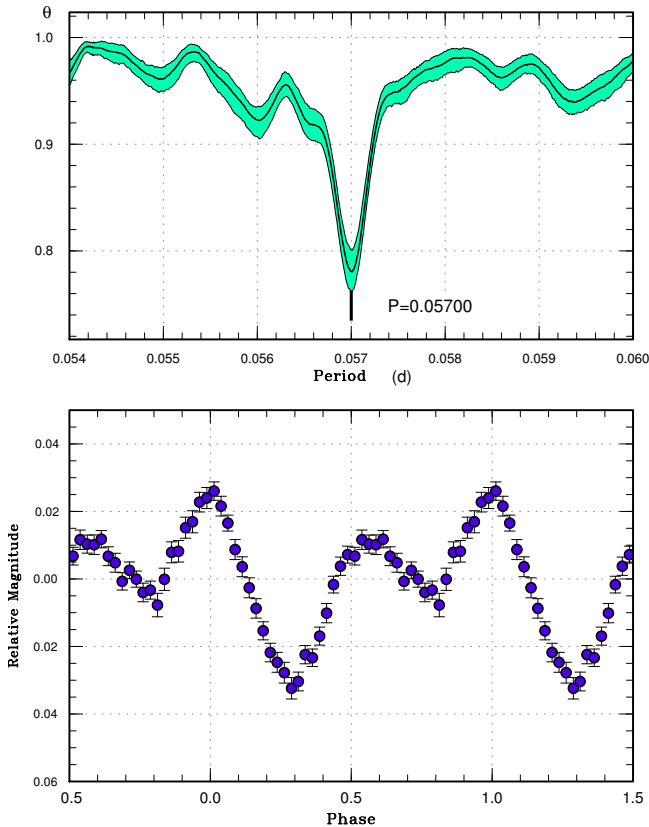


Fig. 25. Early superhumps in HV Vir (2016). (Upper): PDM analysis. (Lower): Phase-averaged profile.

Table 25. Superhump maxima of NSV 2026 (2016b)

$E$	max*	error	$O - C^\dagger$	$N^\ddagger$
0	57722.4877	0.0005	-0.0002	78
1	57722.5579	0.0006	0.0002	64
13	57723.3966	0.0005	-0.0000	59

\*BJD-2400000.

†Against max = 2457722.4878 + 0.069906E.

‡Number of points used to determine the maximum.

2016a), two superoutbursts were likely missed between the two superoutbursts in 2016.

### 3.26 NSV 14681

NSV 14681 was discovered as a variable star (SVS 749) of unknown type with a photographic range of 14 to fainter than 14.5 (Belyavskii 1936). The CRTS team detected an outburst at an unfiltered CCD magnitude of 15.6 on 2007 June 13 and it was readily identified with NSV 14681 (Drake et al. 2014). The CV is a fainter component of a close pair (Kato et al. 2012b). The CRTS team detected another outburst at 16.4 mag on 2009 September 14.

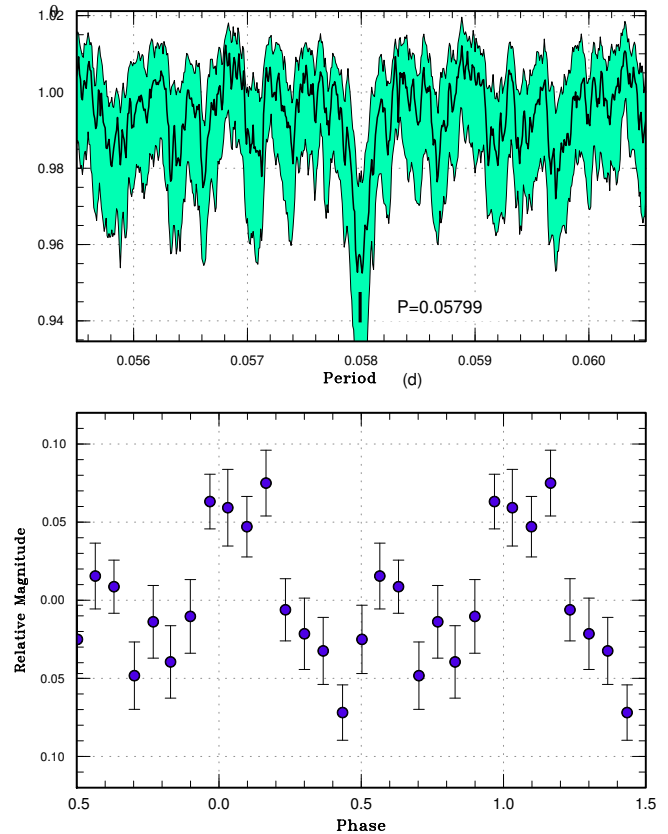


Fig. 26. Post-superoutburst superhumps in HV Vir (2016). (Upper): PDM analysis. The data for BJD 2457478–2457494 were used. (Lower): Phase-averaged profile.

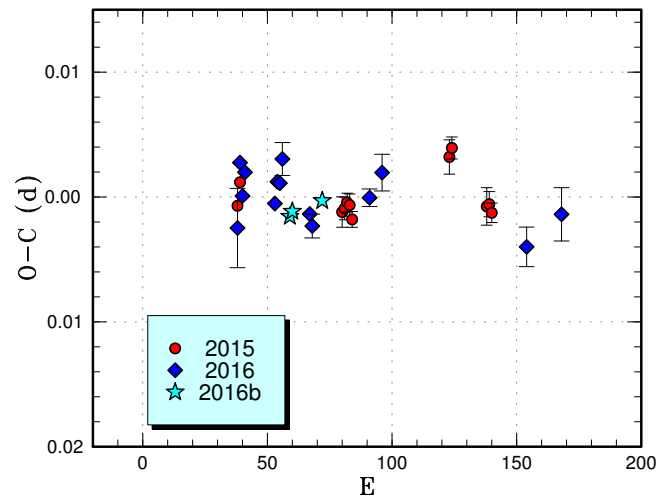


Fig. 27. Comparison of  $O - C$  diagrams of NSV 2026 between different superoutbursts. A period of 0.06982 d was used to draw this figure. Approximate cycle counts ( $E$ ) after the starts of the outbursts were used. The start of the 2016 outburst refers to the precursor outburst. Since the start of the 2015 outburst was not well constrained, the  $O - C$  curve was shifted as in the 2016 one.

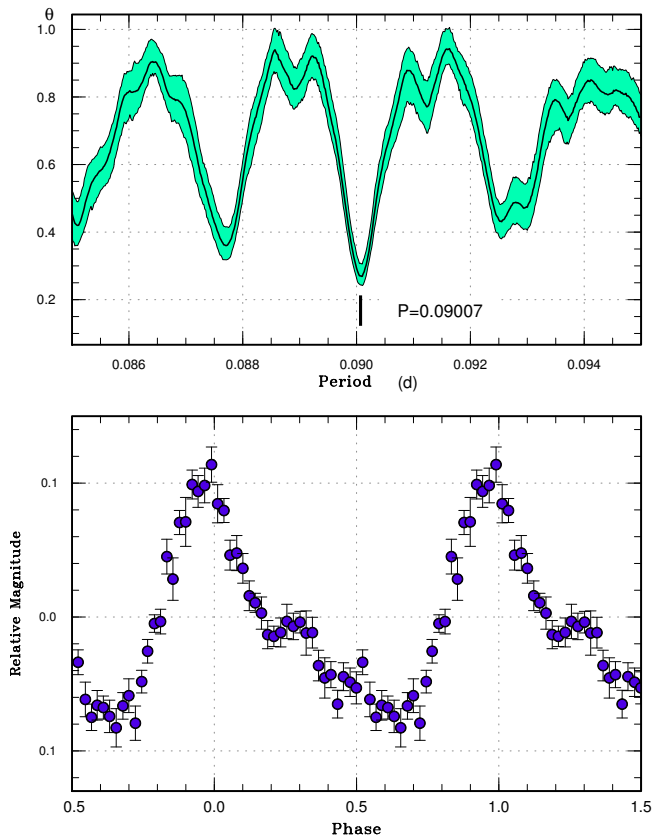


Fig. 28. Superhumps in NSV 14681 (2016). (Upper): PDM analysis. (Lower): Phase-averaged profile.

Table 26. Superhump maxima of NSV 14681 (2016)

$E$	max*	error	$O - C^\dagger$	$N^\ddagger$
0	57684.5223	0.0004	-0.0002	90
34	57687.5852	0.0005	0.0005	90
35	57687.6745	0.0013	-0.0002	59
77	57691.4572	0.0010	-0.0001	76

\*BJD-2400000.

$^\dagger$ Against max = 2457684.5225 + 0.090063E.

$^\ddagger$ Number of points used to determine the maximum.

The 2016 outburst was detected by the ASAS-SN team at  $V=14.35$  on October 19. Subsequent observations detected superhumps (vsnet-alert 20245, 20256; figure 28). The times of superhump maxima are listed in table 26. The superhump stage is unknown. The object is on the lower edge of the period gap.

### 3.27 1RXS J161659.5+620014

This object (hereafter 1RXS J161659) was initially identified as an X-ray selected variable (also given a name as MASTER OT J161700.81+620024.9), which was first de-

tected in bright state on 2012 September 11 at an unfiltered CCD magnitude of 14.4 (Balanutsa et al. 2013). The dwarf nova-type variability was confirmed by analysis of the CRTS data (Balanutsa et al. 2013; see also vsnet-alert 16079, 16720).

The 2016 April outburst was detected by the ASAS-SN team at  $V=14.74$  on April 22. Subsequent observations detected superhumps (vsnet-alert 19763, 19765, 19772; figure 29). The times of superhump maxima are listed in table 27. The nature of the humps for  $E \geq 155$  (post-superoutburst) is unclear due to the gap in the observation. These humps may be either traditional late superhumps or the extension of stage C superhumps (if it is the case, the cycle count should be increased by one). We consider the latter possibility less likely, since this interpretation requires the period of stage C superhumps to be 0.07065(2) d, which appears to be too short (by  $\sim 1\%$ ) shorter than that of stage B superhumps. We do not use these maxima in obtaining the periods in table 3.

The 2016 July outburst was detected by the CRTS team at an unfiltered CCD magnitude of 14.63 on July 10 (cf. vsnet-alert 19970). Although it was considered to be too early for a next superoutburst, subsequent observations detected superhumps (vsnet-alert 19996). The times of superhump maxima are listed in table 28. As in the superoutburst in 2016 April, the nature of maxima for  $E \geq 112$  (post-superoutburst) was unclear. A comparison of  $O - C$  diagrams between two superoutbursts is given in figure 30.

These observations indicate that the supercycle is only  $\sim 80$  d. We studied past ASAS-SN observations and detected outbursts (table 29). The outburst pattern became more regular since the 2015 July (it may have been due to the change in the variability in this system or the improvement of observations in ASAS-SN) and we obtained a mean supercycle of 89(1) d from five most recent superoutbursts (with  $|O - C|$  values less than 8 d). Despite the shortness of the supercycle, normal outbursts are not as frequent as in ER UMa-type dwarf novae (Kato and Kunjaya 1995; Robertson et al. 1995) or active SU UMa-type dwarf novae, such as SS UMi (Kato et al. 2000; Olech et al. 2006) and BF Ara (Kato et al. 2001a). The object resembles V503 Cyg with a supercycle of 89 d with a few normal outbursts between superoutbursts (Harvey et al. 1995). V503 Cyg is known to show different states (Kato et al. 2002b), which is now considered to be a result of the disk tilt suppressing normal outbursts (Ohshima et al. 2012; Osaki and Kato 2013a; Osaki and Kato 2013b). A search for negative superhumps in 1RXS J161659 would be fruitful.

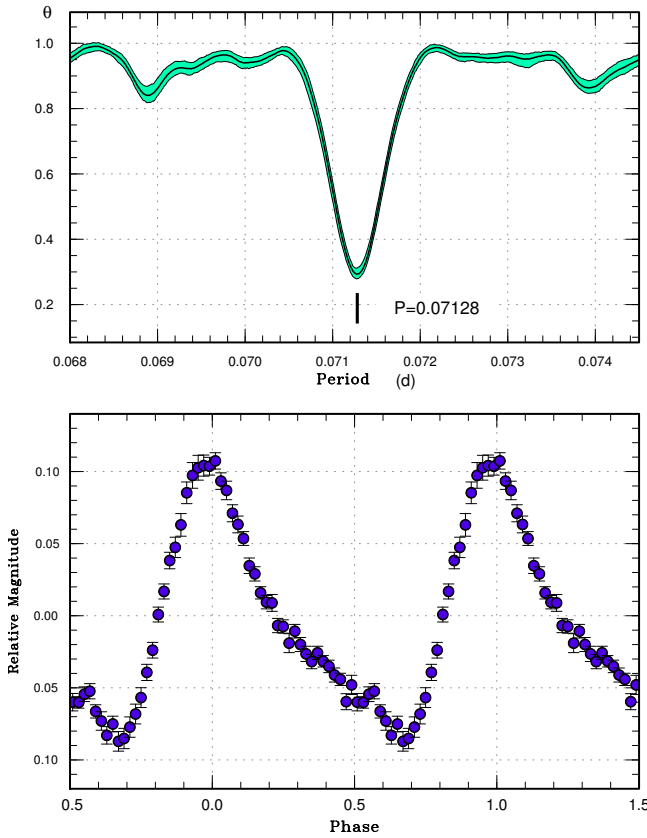


Fig. 29. Superhumps in 1RXS J161659 during the superoutburst plateau (2016). (Upper): PDM analysis. (Lower): Phase-averaged profile.

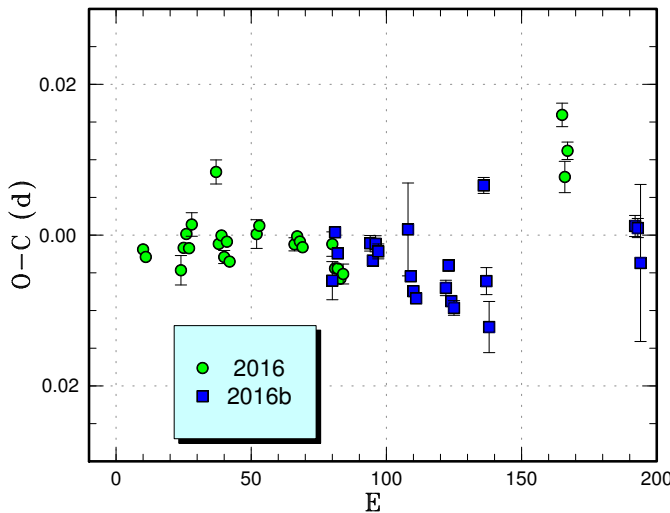


Fig. 30. Comparison of  $O - C$  diagrams of 1RXS J161659 between different superoutbursts. A period of 0.07130 d was used to draw this figure. Approximate cycle counts ( $E$ ) after the start of the superoutburst were used.

Table 27. Superhump maxima of 1RXS J161659 (2016)

$E$	max*	error	$O - C^\dagger$	$N^\ddagger$
0	57502.3747	0.0003	0.0019	72
1	57502.4450	0.0004	0.0008	72
14	57503.3701	0.0020	-0.0019	26
15	57503.4444	0.0004	0.0010	64
16	57503.5175	0.0007	0.0028	65
17	57503.5870	0.0007	0.0008	70
18	57503.6614	0.0016	0.0039	41
27	57504.3101	0.0016	0.0102	47
28	57504.3718	0.0005	0.0006	127
29	57504.4442	0.0005	0.0016	149
30	57504.5127	0.0009	-0.0013	68
31	57504.5860	0.0007	0.0007	70
32	57504.6547	0.0006	-0.0021	50
42	57505.3713	0.0019	0.0009	37
43	57505.4437	0.0006	0.0019	76
56	57506.3682	0.0009	-0.0015	74
57	57506.4405	0.0004	-0.0005	149
58	57506.5111	0.0004	-0.0013	92
59	57506.5817	0.0005	-0.0021	68
70	57507.3664	0.0016	-0.0025	50
71	57507.4345	0.0005	-0.0058	90
72	57507.5058	0.0005	-0.0059	83
73	57507.5757	0.0005	-0.0073	79
74	57507.6476	0.0013	-0.0068	47
155	57513.4440	0.0016	0.0084	27
156	57513.5071	0.0021	0.0001	32
157	57513.5819	0.0012	0.0035	36

\*BJD-2400000.

$^\dagger$ Against max = 2457502.3728 + 0.071373E.

$^\ddagger$ Number of points used to determine the maximum.

### 3.28 ASASSN-13ak

This object was detected as a transient at  $V=15.4$  on 2013 May 23 by the ASAS-SN team (Stanek et al. 2013). There was an independent detection by the MASTER network (Shurpakov et al. 2013b). The SU UMA-type nature was identified during the 2015 superoutburst (Kato et al. 2016a).

The 2016 superoutburst was detected by the ASAS-SN team at  $V=14.43$  on August 2. We obtained time-resolved observations on two nights, yielding superhump maxima in table 30. The resultant period is longer than that in 2015 (Kato et al. 2016a) and these superhumps may have been stage A ones, despite that the amplitudes were already large since the 2016 observations were obtained in the earlier phase than in 2015.

**Table 28.** Superhump maxima of 1RXS J161659 (2016b)

$E$	max*	error	$O - C^\dagger$	$N^\ddagger$
0	57585.3665	0.0025	0.0033	31
1	57585.4442	0.0005	0.0095	69
2	57585.5127	0.0007	0.0065	67
14	57586.3697	0.0010	0.0059	47
15	57586.4387	0.0006	0.0035	68
16	57586.5122	0.0011	0.0055	67
17	57586.5825	0.0010	0.0044	46
28	57587.3697	0.0062	0.0055	25
29	57587.4348	0.0005	-0.0009	66
30	57587.5041	0.0006	-0.0031	71
31	57587.5745	0.0007	-0.0042	46
42	57588.3602	0.0010	-0.0046	48
43	57588.4344	0.0008	-0.0018	130
44	57588.5010	0.0007	-0.0067	138
45	57588.5714	0.0010	-0.0077	79
56	57589.3720	0.0011	0.0067	30
57	57589.4306	0.0018	-0.0062	35
58	57589.4958	0.0034	-0.0124	34
112	57593.3594	0.0014	-0.0079	34
113	57593.4304	0.0013	-0.0083	38
114	57593.4971	0.0104	-0.0131	37
126	57594.3679	0.0008	0.0001	38
127	57594.4345	0.0012	-0.0048	38
128	57594.5075	0.0023	-0.0031	19
168	57597.4031	0.0040	0.0339	39

\*BJD-2400000.

 $^\dagger$ Against max = 2457585.3633 + 0.071464E. $^\ddagger$ Number of points used to determine the maximum.

### 3.29 ASASSN-13al

This object was detected as a transient at  $V=15.2$  on 2013 June 1 by the ASAS-SN team (Prieto et al. 2013) (The ASAS-SN Transients page gave a magnitude of 16.03 with a “BADCAL” flag). The CV-type nature was confirmed by spectroscopy.<sup>13</sup>

The 2016 outburst was detected by the ASAS-SN team at  $V=14.77$  on October 9. There was a previous detection in the ASAS-SN data at  $V=14.75$  on 2012 June 7. Subsequent observations detected superhumps (vsnet-alert 20220; figure 31). The time of superhump maxima are listed in table 31. The period was not very well determined since the observations were undertaken only on a single night. The best superhump period by the PDM method is 0.0783(2) d.

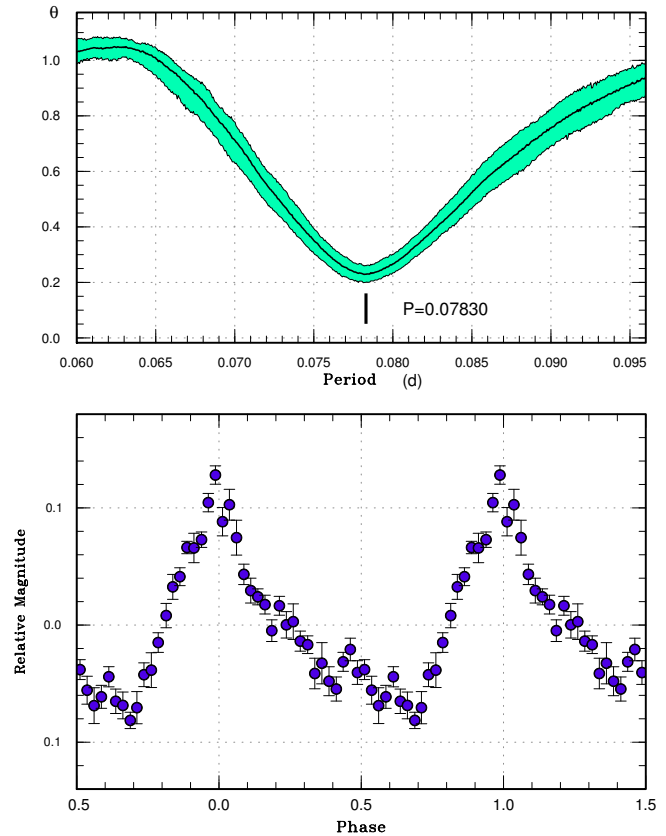


**Fig. 31.** Superhumps in ASASSN-13al (2016). (Upper): PDM analysis. (Lower): Phase-averaged profile.

### 3.30 ASASSN-13bc

This object was detected as a transient at  $V=16.9$  on 2013 July 4 by the ASAS-SN team. A number of past outbursts were recorded in the CRTS data.

The 2015 outburst was detected by the ASAS-SN team at  $V=14.83$  on July 30. Subsequent observations detected superhumps (vsnet-alert 18921, 18930). The times of superhump maxima are listed in table 32.

The 2016 outburst was detected by the ASAS-SN team at  $V=15.19$  on May 24. Superhumps were also observed (vsnet-alert 19843, 19867). The object underwent a post-superoutburst rebrightening at  $V=16.13$  on June 9 (cf. vsnet-alert 19883). The times of superhump maxima are listed in table 33. The superhump profile is given for the better observed 2016 one (figure 32). A combined  $O - C$  diagram (figure 33) suggests that the 2015 observations covered the early phase of stage B and the 2016 ones recorded both stages B and C, although the later part of stage B was not well recorded due to the lack of observa-

<sup>13</sup>[http://www.astronomy.ohio-state.edu/~assassin/followup/spec\\_asassn13al.png](http://www.astronomy.ohio-state.edu/~assassin/followup/spec_asassn13al.png)

**Table 29.** List of outbursts of 1RXS J161659

Year	Month	Day	max*	V-mag	type
2013	4	25	56408	15.02	super
2013	7	12	56486	15.26	?
2013	8	21	56526	15.20	super
2014	6	17	56826	15.44	normal?
2014	8	4	56874	15.01	super
2014	9	16	56917	15.62	?
2015	3	18	57100	15.41	normal
2015	4	7	57120	15.14	super
2015	5	6	57149	15.89	normal?
2015	6	27	57201	15.56	normal
2015	7	18	57222	15.27	normal
2015	7	31	57235	14.64	super
2016	1	7	57395	15.58	normal
2016	1	24	57412	14.61	super
2016	2	9	57428	15.84	normal
2016	2	23	57442	15.58	normal
2016	3	2	57450	15.66	normal
2016	4	21	57500	14.66	super
2016	6	26	57566	16.16	normal
2016	7	11	57581	14.86	super
2016	7	26	57596	15.75	normal
2017	1	17	57771	14.84	super

\*JD–2400000.

**Table 30.** Superhump maxima of ASASSN-13ak (2016)

<i>E</i>	max*	error	$O - C^\dagger$	$N^\ddagger$
0	57604.4248	0.0004	–0.0019	97
1	57604.5177	0.0004	0.0021	35
8	57605.1371	0.0010	–0.0003	88

\*BJD–2400000.

 $^\dagger$ Against max = 2457604.4267 + 0.088838*E*. $^\ddagger$ Number of points used to determine the maximum.**Table 31.** Superhump maxima of ASASSN-13al (2016)

<i>E</i>	max*	error	$O - C^\dagger$	$N^\ddagger$
0	57672.4399	0.0007	0.0004	79
1	57672.5178	0.0006	–0.0001	80
2	57672.5954	0.0007	–0.0009	78
3	57672.6755	0.0008	0.0007	56

\*BJD–2400000.

 $^\dagger$ Against max = 2457672.4395 + 0.078452*E*. $^\ddagger$ Number of points used to determine the maximum.**Table 32.** Superhump maxima of ASASSN-13bc (2015)

<i>E</i>	max*	error	$O - C^\dagger$	$N^\ddagger$
0	57235.4745	0.0011	0.0013	79
2	57235.6146	0.0007	0.0006	47
4	57235.7551	0.0006	0.0004	407
5	57235.8219	0.0007	–0.0032	226
15	57236.5294	0.0004	0.0004	138
16	57236.5999	0.0008	0.0005	94

\*BJD–2400000.

 $^\dagger$ Against max = 2457235.4732 + 0.070393*E*. $^\ddagger$ Number of points used to determine the maximum.

### 3.31 ASASSN-13bj

This object was detected as a transient at  $V=16.2$  on 2013 July 10 by the ASAS-SN team. Two superhump maxima were obtained during the 2013 superoutburst (Kato et al. 2014b).

The 2016 superoutburst was detected by the ASAS-SN team at  $V=14.98$  on July 3. Subsequent observations detected superhumps (vsnet-alert 19957, 19965, 19975; figure 34). The times of superhump maxima are listed in table 34. There was a marked decrease in the superhump

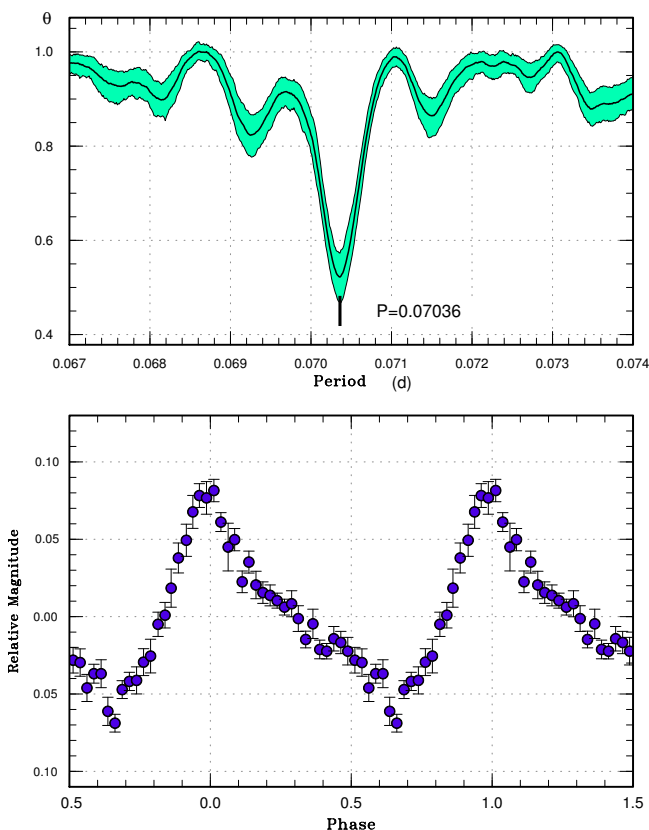


Fig. 32. Superhumps in ASASSN-13bc during the superoutburst plateau (2016). (Upper): PDM analysis. (Lower): Phase-averaged profile.

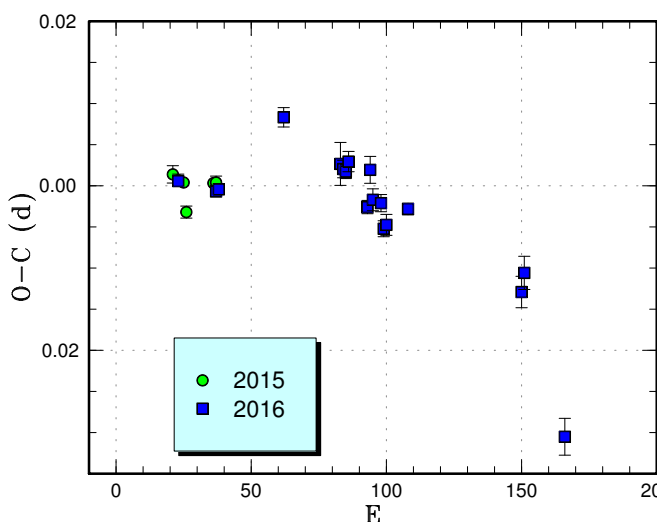


Fig. 33. Comparison of  $O - C$  diagrams of ASASSN-13bc between different superoutbursts. A period of 0.07040 d was used to draw this figure. Approximate cycle counts ( $E$ ) after the start of the superoutburst were used.

Table 33. Superhump maxima of ASASSN-13bc (2016)

$E$	max*	error	$O - C^\dagger$	$N^\ddagger$
0	57534.4878	0.0006	-0.0109	21
14	57535.4722	0.0004	-0.0090	80
15	57535.5428	0.0005	-0.0085	90
39	57537.2412	0.0012	0.0057	77
60	57538.7139	0.0026	0.0048	59
61	57538.7837	0.0011	0.0044	54
62	57538.8538	0.0008	0.0043	54
63	57538.9254	0.0012	0.0058	40
70	57539.4127	0.0008	0.0018	35
71	57539.4876	0.0016	0.0066	28
72	57539.5544	0.0013	0.0032	17
75	57539.7652	0.0010	0.0034	56
76	57539.8324	0.0010	0.0005	53
77	57539.9033	0.0013	0.0012	39
85	57540.4684	0.0007	0.0050	63
127	57543.4152	0.0019	0.0044	41
128	57543.4879	0.0020	0.0069	17
142	57544.4432	0.0011	-0.0202	28
143	57544.5240	0.0022	-0.0096	21

\*BJD-2400000.

$^\dagger$ Against max = 2457534.4987 + 0.070174E.

$^\ddagger$ Number of points used to determine the maximum.

period and we tentatively identified a stage B-C transition around  $E = 22$ . The accuracy of the resultant periods was not sufficiently high since they were determined by only short baselines.

### 3.32 ASASSN-13bo

This object was detected as a transient at  $V=15.96$  on 2013 July 13 by the ASAS-SN team. The 2016 outburst was detected by the ASAS-SN team at  $V=15.19$  on August 1. The 2016 outburst was the brightest recorded one and a superoutburst was suspected. Subsequent observations detected superhumps (vsnet-alert 20053, 20068). There was a 3-d gap in the observations and alias periods are possible (figure 35). The period in table 3 refers to the one giving smallest residuals and it was determined by the PDM method. The object faded to  $\sim 20$  mag on August 13.

### 3.33 ASASSN-13cs

This object was detected as a transient at  $V=14.9$  on 2013 September 2 by the ASAS-SN team. The object was spectroscopically identified as a dwarf nova in outburst.<sup>14</sup>

The 2016 outburst was detected by the ASAS-SN team

<sup>14</sup><[http://www.astronomy.ohio-state.edu/~assassin/followup/spec\\_asassn13cs.png](http://www.astronomy.ohio-state.edu/~assassin/followup/spec_asassn13cs.png)>.

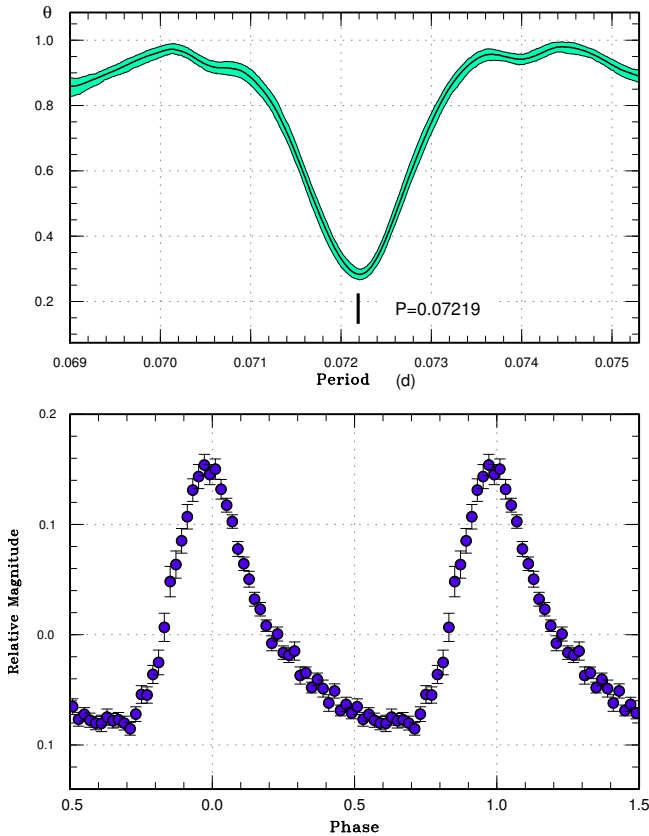


Fig. 34. Superhumps in ASASSN-13bj (2016). (Upper): PDM analysis. (Lower): Phase-averaged profile.

at  $V=15.03$  on June 21. The light curves of past outbursts suggested an SU UMa-type dwarf nova. Subsequent observations detected superhumps (vsnet-alert 19920, 19923; figure 36). The times of superhump maxima are listed in table 36.

### 3.34 ASASSN-13cz

This object was detected as a transient at  $V=14.9$  on 2013 September 14 by the ASAS-SN team. The 2013 outburst turned out to be a superoutburst by the detection of superhumps (Kato et al. 2014a).

The 2016 superoutburst was detected by the ASAS-SN team at  $V=14.47$  on July 27. Subsequent observations detected superhumps (vsnet-alert 20023, 20042). The times of superhump maxima are listed in table 37. We suspect that stages B and C were partially observed (cf. figure 37). We provide a superhump profile (figure 38), which was determined much better than in 2013.

Table 34. Superhump maxima of ASASSN-13bj (2016)

$E$	max*	error	$O - C^\dagger$	$N^\ddagger$
0	57574.3923	0.0003	-0.0048	41
1	57574.4669	0.0004	-0.0024	50
2	57574.5373	0.0007	-0.0043	49
15	57575.4823	0.0003	0.0017	71
16	57575.5555	0.0004	0.0026	68
19	57575.7716	0.0005	0.0021	44
20	57575.8436	0.0006	0.0018	45
21	57575.9157	0.0006	0.0016	46
23	57576.0605	0.0005	0.0020	77
24	57576.1313	0.0006	0.0006	77
25	57576.2077	0.0017	0.0047	35
27	57576.3482	0.0003	0.0007	117
28	57576.4226	0.0003	0.0030	170
29	57576.4943	0.0006	0.0023	112
30	57576.5656	0.0008	0.0015	72
41	57577.3560	0.0007	-0.0028	45
42	57577.4288	0.0005	-0.0022	117
43	57577.4992	0.0004	-0.0040	119
44	57577.5715	0.0007	-0.0039	71

\*BJD-2400000.

$^\dagger$ Against max = 2457574.3971 + 0.072236E.

$^\ddagger$ Number of points used to determine the maximum.

Table 35. Superhump maxima of ASASSN-13bo (2016)

$E$	max*	error	$O - C^\dagger$	$N^\ddagger$
0	57606.6548	0.0017	0.0000	28
40	57609.5212	0.0009	-0.0006	68
41	57609.5941	0.0009	0.0006	70

\*BJD-2400000.

$^\dagger$ Against max = 2457606.6548 + 0.071675E.

$^\ddagger$ Number of points used to determine the maximum.

### 3.35 ASASSN-14gg

This object was detected as a transient at  $V=14.8$  on 2014 August 23 by the ASAS-SN team. The 2016 outburst was detected by the ASAS-SN team at  $V=13.95$  on August 11. Subsequent observations detected superhumps (vsnet-alert 20079; figure 39). The times of superhump maxima are listed in table 38. The positive  $P_{\text{dot}}$  for stage B superhumps is a common feature in many short- $P_{\text{SH}}$  systems.

### 3.36 ASASSN-15cr

This object was detected as a transient at  $V=14.9$  on 2015 February 7 by the ASAS-SN team. The 2017 outburst was detected by the ASAS-SN team at  $V=14.73$  on January 9. Subsequent observations detected superhumps (vsnet-



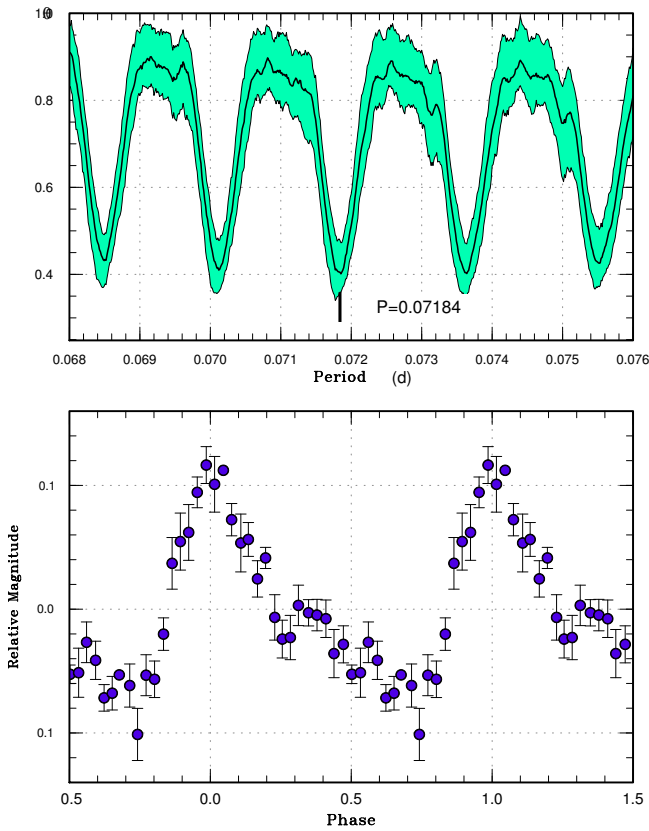


Fig. 35. Superhumps in ASASSN-13bo (2016). (Upper): PDM analysis. (Lower): Phase-averaged profile.

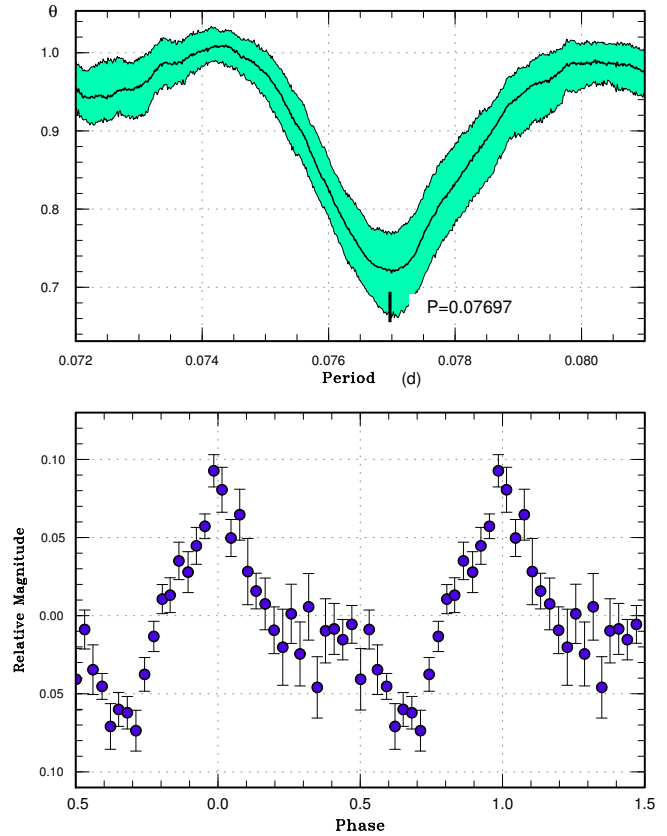


Fig. 36. Superhumps in ASASSN-13cs (2016). (Upper): PDM analysis. (Lower): Phase-averaged profile.

Table 36. Superhump maxima of ASASSN-13cs (2016)

$E$	max*	error	$O - C^\dagger$	$N^\ddagger$
0	57562.4140	0.0027	-0.0035	17
1	57562.4950	0.0015	0.0003	36
2	57562.5705	0.0017	-0.0012	26
4	57562.7279	0.0015	0.0020	35
5	57562.8043	0.0039	0.0013	23
8	57563.0344	0.0015	0.0000	167
13	57563.4238	0.0017	0.0039	17
14	57563.4957	0.0030	-0.0013	22
15	57563.5781	0.0042	0.0040	10
17	57563.7267	0.0011	-0.0016	45
18	57563.8052	0.0015	-0.0002	39
19	57563.8825	0.0016	0.0000	45
20	57563.9559	0.0031	-0.0037	32

\*BJD-2400000.

$^\dagger$ Against max = 2457562.4175 + 0.077105E.

$^\ddagger$ Number of points used to determine the maximum.

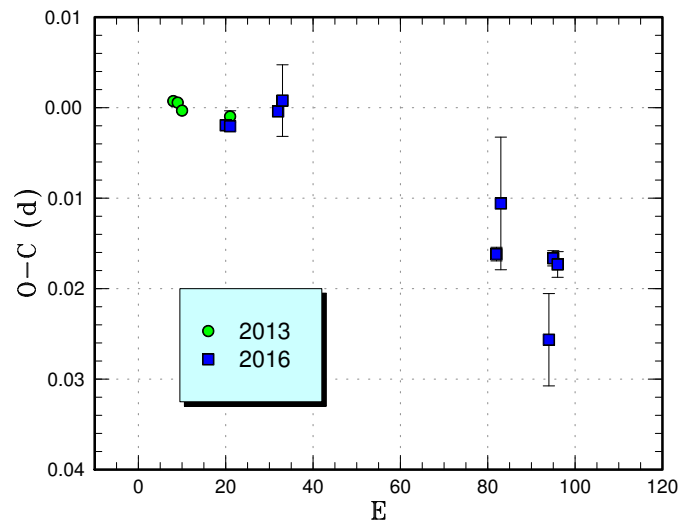


Fig. 37. Comparison of  $O - C$  diagrams of ASASSN-13cz between different superoutbursts. A period of 0.07995 d was used to draw this figure. Approximate cycle counts ( $E$ ) after the start of the superoutburst were used.

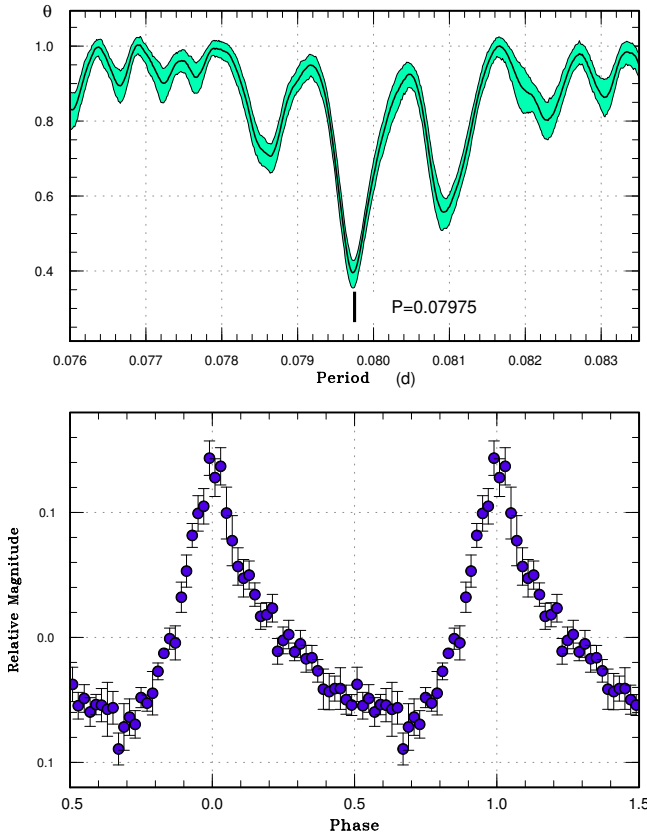


Fig. 38. Superhumps in ASASSN-13cz (2016). (Upper): PDM analysis. (Lower): Phase-averaged profile.

Table 37. Superhump maxima of ASASSN-13cz (2016)

$E$	max*	error	$O - C^\dagger$	$N^\ddagger$
0	57598.4226	0.0003	-0.0026	59
1	57598.5024	0.0004	-0.0024	73
12	57599.3835	0.0004	0.0020	90
13	57599.4647	0.0040	0.0034	15
62	57603.3653	0.0008	-0.0010	90
63	57603.4508	0.0073	0.0048	28
74	57604.3152	0.0051	-0.0074	20
75	57604.4041	0.0008	0.0018	131
76	57604.4834	0.0014	0.0014	112

\*BJD-2400000.

$^\dagger$ Against max = 2457598.4252 + 0.079695E.

$^\ddagger$ Number of points used to determine the maximum.

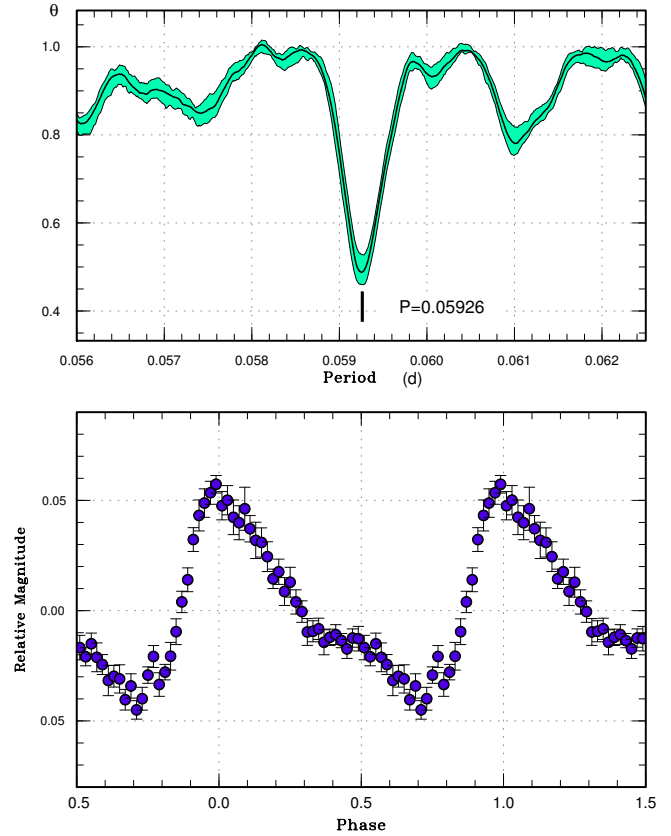


Fig. 39. Superhumps in ASASSN-14gg (2016). (Upper): PDM analysis. (Lower): Phase-averaged profile.

alert 20558, 20590; figure 40). The times of superhump maxima are listed in table 39. Despite that observational coverage was not sufficient, all stages of A-C were recorded thanks to the early detection by the ASAS-SN team.

### 3.37 ASASSN-16da

This object was detected as a transient at  $V=16.1$  on 2016 March 8 by the ASAS-SN team. The outburst was confirmed and announced on March 12, when the object was at  $V=15.5$ . The brightness peak was on March 10 at  $V=15.1$ . The object was identified with an  $g=21.5$  mag SDSS object. The large outburst amplitude received attention.

The object showed double-wave early superhumps on March 13 and 14 (vsnet-alert 19579, 19592; figure 41). On March 15 (5 d after the brightness peak), the object started to show ordinary superhumps (vsnet-alert 19598, 19617, 19653; figure 42). The times of superhump maxima are listed in table 40. The epochs for  $E \leq 2$  and  $E \geq 203$  were apparently those of stage A and C superhumps, respectively. If we consider that stage A just ended at  $E=10$

**Table 38.** Superhump maxima of ASASSN-14gg (2016)

$E$	max*	error	$O - C^\dagger$	$N^\ddagger$
0	57614.5584	0.0003	0.0054	59
1	57614.6181	0.0004	0.0057	43
31	57616.3897	0.0003	-0.0020	56
32	57616.4486	0.0003	-0.0024	61
33	57616.5077	0.0004	-0.0026	61
34	57616.5667	0.0005	-0.0030	59
35	57616.6274	0.0010	-0.0015	34
54	57617.7523	0.0006	-0.0036	57
55	57617.8131	0.0006	-0.0021	59
56	57617.8714	0.0010	-0.0031	38
66	57618.4646	0.0007	-0.0030	61
67	57618.5282	0.0011	0.0012	59
68	57618.5824	0.0007	-0.0039	60
70	57618.7119	0.0070	0.0070	31
71	57618.7615	0.0012	-0.0027	58
72	57618.8234	0.0014	-0.0001	59
87	57619.7210	0.0023	0.0078	47
88	57619.7722	0.0013	-0.0003	57
89	57619.8351	0.0022	0.0033	59

\*BJD-2400000.

 $^\dagger$ Against max = 2457614.5531 + 0.059311E. $^\ddagger$ Number of points used to determine the maximum.

(which may not be a bad assumption as compared with  $O - C$  diagrams of well-observed objects), the period of stage A superhumps was 0.05858(10) d. The resultant  $\epsilon^*$  of 0.042(2) corresponds to  $q=0.12(1)$ . This relatively large  $q$  for a WZ Sge-type dwarf nova is consistent with the appearance of stage C superhumps, short duration of stage A, relatively large  $P_{\text{dot}}$  in stage B [ $+7.5(0.9) \times 10^{-5}$ ], and relatively early appearance of ordinary superhumps. This object is probably close to the borderline of WZ Sge-type dwarf novae and ordinary SU UMa-type dwarf novae.

### 3.38 ASASSN-16dk

This object was detected as a transient at  $V=16.4$  on 2016 March 21 by the ASAS-SN team. The outburst was confirmed and announced on March 24, when the object was at  $V=15.1$ . Subsequent observations detected superhumps. The times of superhump maxima are listed in table 41. Since the observations were apparently obtained during the late phase of the superoutburst, the superhump stage was probably C. The lack of period variation is consistent with this interpretation.

**Table 39.** Superhump maxima of ASASSN-15cr (2017)

$E$	max*	error	$O - C^\dagger$	$N^\ddagger$
0	57764.2386	0.0018	-0.0035	107
1	57764.2945	0.0013	-0.0091	130
2	57764.3613	0.0010	-0.0039	129
3	57764.4223	0.0011	-0.0044	95
4	57764.4852	0.0012	-0.0030	120
15	57765.1730	0.0008	0.0079	35
16	57765.2378	0.0004	0.0113	60
46	57767.0734	0.0006	0.0010	53
47	57767.1359	0.0010	0.0020	36
50	57767.3198	0.0014	0.0013	60
51	57767.3771	0.0068	-0.0029	33
65	57768.2382	0.0005	-0.0032	62
66	57768.2986	0.0020	-0.0043	35
80	57769.1604	0.0009	-0.0040	64
81	57769.2209	0.0010	-0.0049	65
82	57769.2877	0.0022	0.0003	18
114	57771.2557	0.0007	-0.0006	98
130	57772.2419	0.0017	0.0012	64
131	57772.3037	0.0011	0.0014	69
132	57772.3703	0.0009	0.0066	63
133	57772.4353	0.0013	0.0100	49
134	57772.4886	0.0011	0.0018	59
135	57772.5505	0.0013	0.0021	63
136	57772.6142	0.0009	0.0043	63
137	57772.6745	0.0014	0.0031	63
146	57773.2292	0.0006	0.0040	33
147	57773.2901	0.0008	0.0034	31
148	57773.3523	0.0007	0.0041	31
149	57773.4131	0.0006	0.0033	28
200	57776.5375	0.0013	-0.0102	22
217	57777.5786	0.0020	-0.0151	24

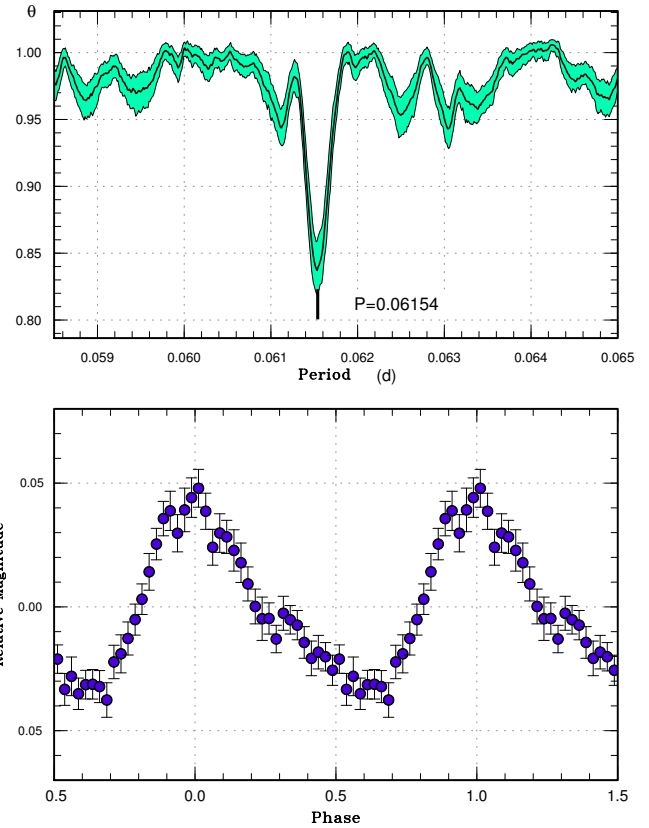
\*BJD-2400000.

 $^\dagger$ Against max = 2457764.2421 + 0.061528E. $^\ddagger$ Number of points used to determine the maximum.

**Table 40.** Superhump maxima of ASASSN-16da (2016)

$E$	max*	error	$O - C^\dagger$	$N^\ddagger$
0	57463.7303	0.0006	-0.0037	56
1	57463.7898	0.0005	-0.0016	56
2	57463.8468	0.0006	-0.0019	56
10	57464.3162	0.0005	0.0087	41
11	57464.3725	0.0004	0.0076	83
12	57464.4302	0.0003	0.0079	88
13	57464.4869	0.0003	0.0072	88
14	57464.5434	0.0005	0.0064	56
15	57464.6012	0.0007	0.0069	39
21	57464.9407	0.0013	0.0023	27
28	57465.3407	0.0005	0.0007	38
29	57465.3973	0.0005	-0.0000	38
30	57465.4511	0.0008	-0.0035	39
31	57465.5124	0.0006	0.0004	34
35	57465.7381	0.0007	-0.0033	27
36	57465.7975	0.0006	-0.0013	25
37	57465.8534	0.0007	-0.0028	27
52	57466.7106	0.0029	-0.0058	27
53	57466.7723	0.0054	-0.0015	26
54	57466.8299	0.0013	-0.0012	22
63	57467.3402	0.0062	-0.0072	18
64	57467.3988	0.0006	-0.0059	39
65	57467.4560	0.0010	-0.0061	43
66	57467.5136	0.0010	-0.0058	41
67	57467.5808	0.0028	0.0041	10
70	57467.7395	0.0033	-0.0093	17
117	57470.4310	0.0093	-0.0135	28
118	57470.4957	0.0020	-0.0062	54
119	57470.5599	0.0029	0.0007	54
171	57473.5506	0.0039	0.0089	31
174	57473.7204	0.0017	0.0067	54
175	57473.7768	0.0029	0.0057	56
203	57475.3872	0.0023	0.0103	31
204	57475.4405	0.0012	0.0062	32
205	57475.4939	0.0010	0.0023	32
206	57475.5518	0.0013	0.0028	32
207	57475.6112	0.0011	0.0048	32
221	57476.4068	0.0028	-0.0025	32
222	57476.4643	0.0022	-0.0024	31
223	57476.5205	0.0056	-0.0036	32
238	57477.3807	0.0033	-0.0036	23
239	57477.4338	0.0020	-0.0080	26

\*BJD-2400000.

 $^\dagger$ Against max = 2457463.7340 + 0.057355E. $^\ddagger$ Number of points used to determine the maximum.**Fig. 40.** Superhumps in ASASSN-15cr (2017). (Upper): PDM analysis. (Lower): Phase-averaged profile.**Table 41.** Superhump maxima of ASASSN-16dk (2016)

$E$	max*	error	$O - C^\dagger$	$N^\ddagger$
0	57476.5381	0.0012	-0.0047	37
1	57476.6159	0.0008	-0.0029	48
2	57476.7012	0.0023	0.0065	12
13	57477.5314	0.0017	0.0016	30
14	57477.6037	0.0007	-0.0020	49
15	57477.6839	0.0035	0.0022	19
26	57478.5228	0.0157	0.0059	25
27	57478.5874	0.0013	-0.0054	50
28	57478.6703	0.0070	0.0016	28
40	57479.5760	0.0025	-0.0037	51
41	57479.6536	0.0049	-0.0021	38
53	57480.5667	0.0029	0.0000	45
54	57480.6472	0.0025	0.0046	37
66	57481.5497	0.0031	-0.0040	43
67	57481.6321	0.0040	0.0024	40

\*BJD-2400000.

 $^\dagger$ Against max = 2457476.5428 + 0.075923E. $^\ddagger$ Number of points used to determine the maximum.

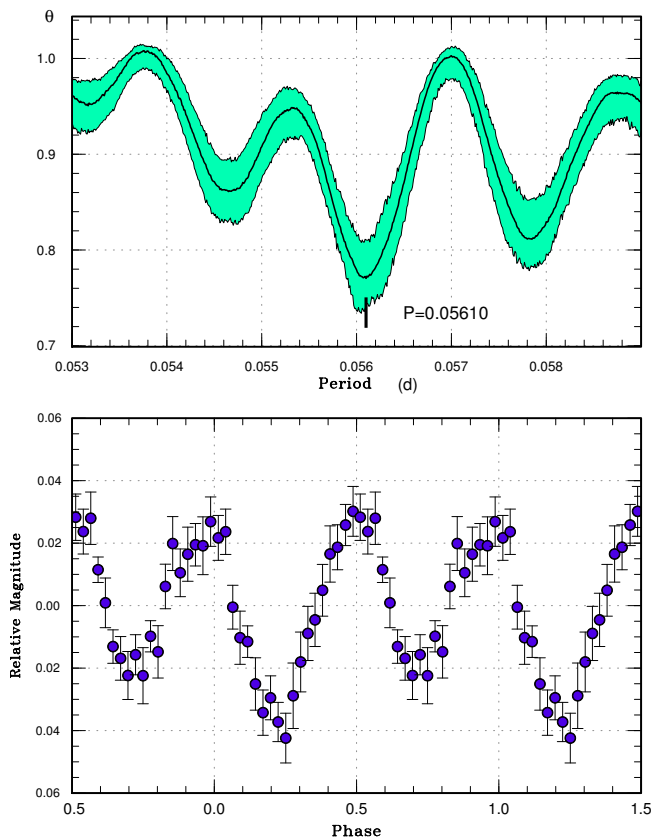


Fig. 41. Early superhumps in ASASSN-16da (2016). (Upper): PDM analysis. (Lower): Phase-averaged profile.

### 3.39 ASASSN-16ds

This object was detected as a transient at  $V=14.7$  on 2016 April 1 by the ASAS-SN team. Subsequent observations detected growing superhumps (vsnet-alert 19680), which later became fully developed ones. The times of superhump maxima are listed in table 42. The  $O - C$  values indicates typical stages A and B (vsnet-alert 19704). Although individual times of superhump maxima could not be measured after BJD 2457495, a PDM analysis of the corresponding segment yielded a signal of 0.06723(5) d, which is included in table 3.

### 3.40 ASASSN-16dz

This object was detected as a transient at  $V=15.0$  on 2016 April 2 by the ASAS-SN team. The outburst was announced after the observation on April 3 at  $V=14.2$ . The object had been listed as an emission-line object IPHAS2 J064225.58+082546.7 (Witham et al. 2008). Although superhumps were detected, the period was not well determined due to short runs and the limited coverage only on two nights (figure 45). The times of superhump maxima

Table 42. Superhump maxima of ASASSN-16ds (2016)

$E$	max*	error	$O - C^\dagger$	$N^\ddagger$
0	57481.5700	0.0006	-0.0031	156
1	57481.6348	0.0017	-0.0060	76
3	57481.7760	0.0007	-0.0003	17
4	57481.8496	0.0009	0.0055	14
5	57481.9135	0.0008	0.0017	11
10	57482.2567	0.0009	0.0062	33
13	57482.4617	0.0003	0.0080	156
14	57482.5290	0.0004	0.0076	132
15	57482.5977	0.0004	0.0085	121
33	57483.8143	0.0006	0.0058	32
34	57483.8810	0.0005	0.0047	40
47	57484.7613	0.0017	0.0044	21
48	57484.8259	0.0004	0.0013	35
58	57485.5005	0.0008	-0.0015	131
59	57485.5678	0.0006	-0.0020	156
60	57485.6361	0.0004	-0.0014	156
62	57485.7657	0.0009	-0.0073	13
63	57485.8377	0.0004	-0.0031	41
64	57485.9058	0.0005	-0.0027	25
73	57486.5121	0.0006	-0.0060	117
74	57486.5817	0.0006	-0.0042	156
75	57486.6507	0.0013	-0.0029	70
87	57487.4620	0.0008	-0.0046	121
88	57487.5275	0.0007	-0.0068	156
89	57487.5961	0.0005	-0.0060	156
90	57487.6611	0.0010	-0.0086	108
107	57488.8155	0.0007	-0.0059	34
108	57488.8843	0.0008	-0.0048	30
136	57490.7870	0.0020	0.0011	20
137	57490.8520	0.0032	-0.0016	12
181	57493.8452	0.0023	0.0110	19
195	57494.7958	0.0021	0.0132	19

\*BJD-2400000.

$^\dagger$ Against max = 2457481.5731 + 0.067741E.

$^\ddagger$ Number of points used to determine the maximum.

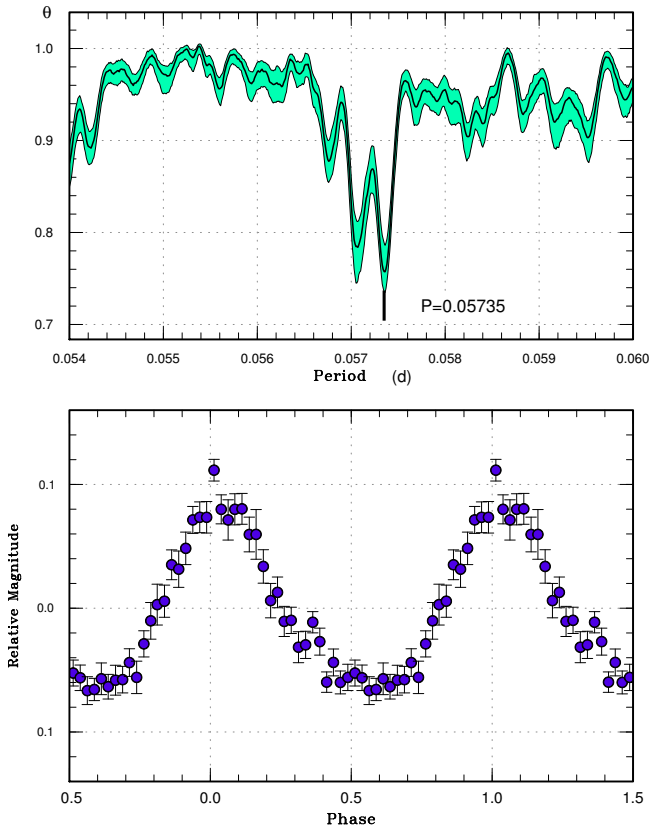


Fig. 42. Ordinary superhumps in ASASSN-16da (2016). (Upper): PDM analysis. (Lower): Phase-averaged profile.

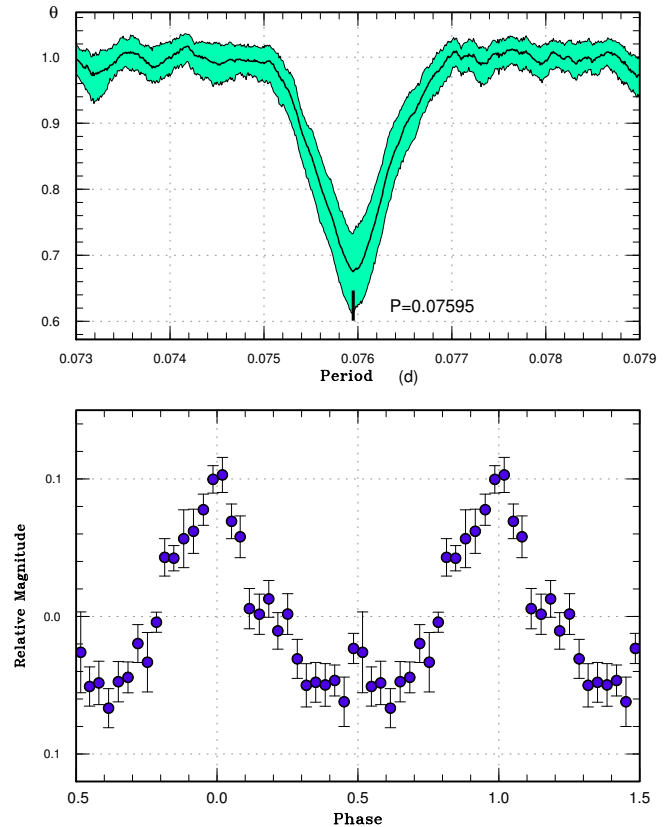


Fig. 43. Superhumps in ASASSN-16dk (2016). (Upper): PDM analysis. (Lower): Phase-averaged profile.

Table 43. Superhump maxima of ASASSN-16dz (2016)

$E$	max*	error	$O - C^\dagger$	$N^\ddagger$
0	57484.3064	0.0052	0.0011	22
1	57484.3703	0.0012	-0.0012	63
16	57485.3655	0.0019	0.0001	47

\*BJD-2400000.

$^\dagger$ Against max = 2457484.3053 + 0.066259E.

$^\ddagger$ Number of points used to determine the maximum.

are listed in table 43, which is based on one of the aliases giving the smallest  $O - C$  scatter.

### 3.41 ASASSN-16ez

This object was detected as a transient at  $V=14.3$  on 2016 May 6 by the ASAS-SN team. The large outburst amplitude suggested an SU UMa-type superoutburst (cf. vsnet-alert 19804).

On May 12, this object started to show large-amplitude superhumps (vsnet-alert 19823, 19829). The times of superhump maxima are listed in table 44. These superhumps were stage B ones and there was little period varia-

tion. The object was still in outburst on May 23 (17 d after the outburst detection and 11 d after the first detection of superhumps). Although there were some variations before May 12, we could not confidently detect stage A superhumps (probably due to a 1.5-d gap in the observation). Although the small  $P_{\text{dot}}$  might suggest a small  $q$  (cf. Kato 2015), the relatively large amplitude of superhumps (figure 46) and the lack of long duration of stage A do not support this interpretation. The seemingly small  $P_{\text{dot}}$  may be a result of a relatively short observational coverage of 4 d.

### 3.42 ASASSN-16fr

This object was detected as a transient at  $V=16.6$  on 2016 May 30 by the ASAS-SN team. Subsequent observations detected superhumps (vsnet-alert 19863; figure 47). The times of superhump maxima are listed in table 45. Due to the faintness of the object (17 mag around the observations), the statistics was not good.

**Table 44.** Superhump maxima of ASASSN-16ez (2016)

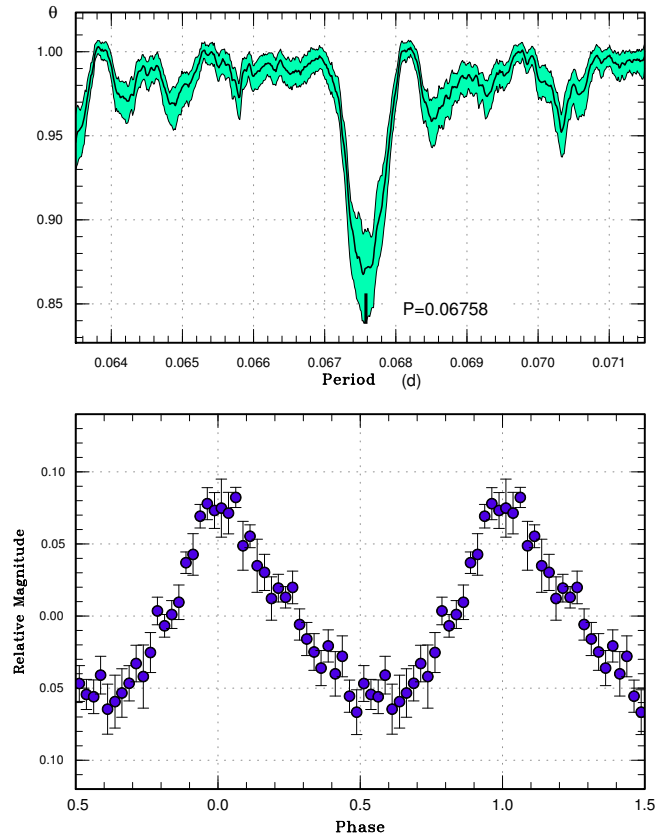
$E$	max*	error	$O - C^\dagger$	$N^\ddagger$
0	57521.1188	0.0010	-0.0002	117
1	57521.1731	0.0005	-0.0035	170
2	57521.2352	0.0011	0.0009	153
7	57521.5236	0.0024	0.0012	30
8	57521.5837	0.0003	0.0037	61
18	57522.1562	0.0050	-0.0001	14
20	57522.2717	0.0016	0.0002	37
22	57522.3882	0.0014	0.0015	32
23	57522.4453	0.0004	0.0010	58
24	57522.4995	0.0025	-0.0024	19
40	57523.4212	0.0004	-0.0027	94
41	57523.4799	0.0005	-0.0017	85
42	57523.5410	0.0006	0.0018	59
59	57524.5158	0.0005	-0.0028	59
60	57524.5759	0.0005	-0.0004	56
61	57524.6349	0.0016	0.0010	22
74	57525.3826	0.0007	-0.0004	28
75	57525.4416	0.0007	0.0009	30
76	57525.4972	0.0006	-0.0010	33
77	57525.5589	0.0007	0.0030	32

\*BJD-2400000.

 $^\dagger$ Against max = 2457521.1190 + 0.057621E. $^\ddagger$ Number of points used to determine the maximum.**Table 45.** Superhump maxima of ASASSN-16fr (2016)

$E$	max*	error	$O - C^\dagger$	$N^\ddagger$
0	57541.1447	0.0015	-0.0026	60
1	57541.2179	0.0032	-0.0008	70
14	57542.1502	0.0014	0.0034	141
15	57542.2167	0.0018	-0.0016	129
21	57542.6523	0.0036	0.0057	16
35	57543.6420	0.0028	-0.0041	17

\*BJD-2400000.

 $^\dagger$ Against max = 2457541.1473 + 0.071394E. $^\ddagger$ Number of points used to determine the maximum.**Fig. 44.** Superhumps in ASASSN-16ds (2016). (Upper): PDM analysis. (Lower): Phase-averaged profile.

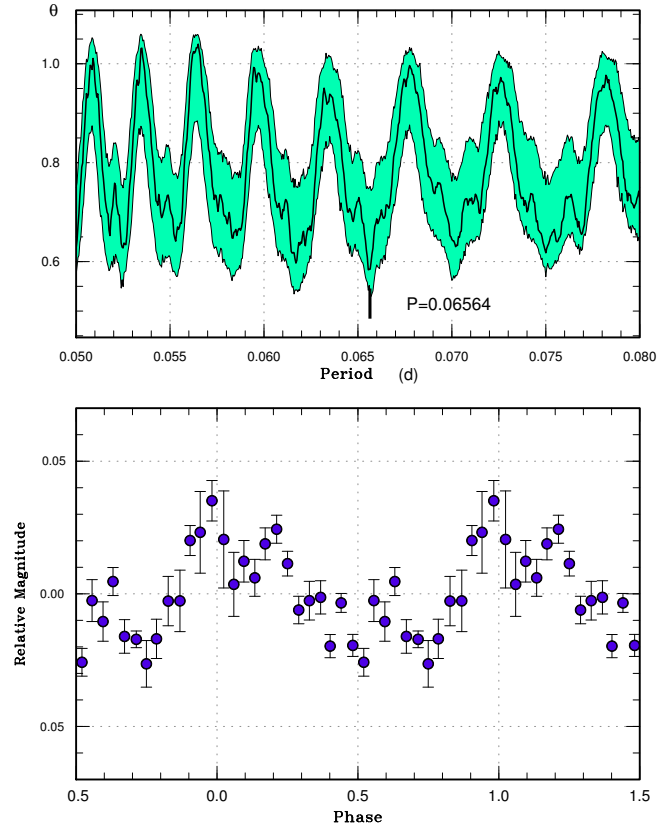
### 3.43 ASASSN-16fu

This object was detected as a transient at  $V=13.9$  on 2016 June 5 by the ASAS-SN team. The large outburst amplitude received attention (cf. vsnet-alert 19864). On June 14 (9 d after the outburst detection), this object showed fully developed superhumps (vsnet-alert 19899, 19901; figure 48). The times of superhump maxima are listed in table 46. Although the maxima for  $E \leq 1$  were stage A superhumps, the period of stage A superhumps was not determined due to the unfortunate 2 d gap before the full growth of the superhumps. The relatively small  $P_{\text{dot}}$  in stage B [ $+4.6(0.6) \times 10^{-5}$ ] suggests a relatively small  $q$  [ $q \sim 0.08(1)$  according to equation (6) in Kato (2015)]. This expectation is consistent with the small amplitude of the superhumps (figure 48). A retrospective analysis of the data before ordinary superhumps appeared (BJD before 2457553) detected possible early superhumps with a period of 0.05623(3) d (figure 49). We consider that this object is a WZ Sge-type dwarf nova, which appears consistent with the small  $q$  as inferred from the small  $P_{\text{dot}}$ .

**Table 46.** Superhump maxima of ASASSN-16fu (2016)

$E$	max*	error	$O - C^\dagger$	$N^\ddagger$
0	57551.7331	0.0018	-0.0139	17
1	57551.7932	0.0017	-0.0108	16
35	57553.7478	0.0006	0.0070	17
36	57553.8032	0.0008	0.0054	16
37	57553.8641	0.0009	0.0093	16
38	57553.9174	0.0009	0.0056	16
53	57554.7719	0.0021	0.0056	16
54	57554.8269	0.0005	0.0036	16
55	57554.8843	0.0009	0.0040	17
70	57555.7347	0.0008	-0.0001	14
71	57555.7901	0.0019	-0.0017	16
72	57555.8531	0.0025	0.0044	16
73	57555.9081	0.0011	0.0024	16
89	57556.8175	0.0021	0.0003	16
90	57556.8733	0.0012	-0.0008	16
106	57557.7815	0.0012	-0.0041	16
108	57557.8972	0.0007	-0.0024	17
123	57558.7476	0.0013	-0.0065	16
124	57558.8044	0.0033	-0.0067	16
125	57558.8685	0.0020	0.0005	17
140	57559.7208	0.0015	-0.0017	13
141	57559.7797	0.0023	0.0002	16
143	57559.8915	0.0010	-0.0020	17
159	57560.7995	0.0052	-0.0054	16
160	57560.8631	0.0017	0.0011	17
161	57560.9148	0.0014	-0.0041	14
175	57561.7171	0.0017	0.0006	13
176	57561.7713	0.0059	-0.0021	16
178	57561.8893	0.0020	0.0019	17
193	57562.7473	0.0031	0.0053	16
194	57562.8003	0.0055	0.0014	16
195	57562.8596	0.0025	0.0037	17

\*BJD-2400000.

 $^\dagger$ Against max = 2457551.7470 + 0.056969E. $^\ddagger$ Number of points used to determine the maximum.**Fig. 45.** Superhumps in ASASSN-16dz (2016). (Upper): PDM analysis. (Lower): Phase-averaged profile.

### 3.44 ASASSN-16gh

This object was detected as a transient at  $V=15.5$  on 2016 June 16 by the ASAS-SN team. The outburst was announced on June 18, when the object further brightened to  $V=14.3$ . No strong superhumps were detected up to observations on June 24. Growing superhumps were recorded on June 28 (12 d after the outburst detection; vsnet-alert 19935). Further development of superhumps were observed (vsnet-alert 19943, 19952; figure 50). Although we could not detect early superhumps, the object may be a WZ Sge-type dwarf nova since the waiting time (12 d) of the growth of the superhumps was long. If this identification is true, the object appears to be a candidate for a period bouncer. The relatively small amplitude of the superhumps (figure 50) and the large outburst amplitude (there was no known quiescent counterpart) would favor this possibility.

### 3.45 ASASSN-16gj

This object was detected as a transient at  $V=13.3$  on 2016 June 18 by the ASAS-SN team (cf. vsnet-alert 19905). The



**Table 47.** Superhump maxima of ASASSN-16gh (2016)

$E$	max*	error	$O - C^\dagger$	$N^\ddagger$
0	57568.3036	0.0012	-0.0060	78
1	57568.3688	0.0007	-0.0026	136
2	57568.4292	0.0007	-0.0041	141
3	57568.4950	0.0009	-0.0002	143
16	57569.3045	0.0006	0.0050	109
17	57569.3628	0.0005	0.0015	141
18	57569.4252	0.0006	0.0019	142
19	57569.4851	0.0008	0.0000	136
20	57569.5482	0.0008	0.0012	127
21	57569.6117	0.0007	0.0028	132
22	57569.6678	0.0014	-0.0029	102
31	57570.2316	0.0008	0.0040	137
32	57570.2933	0.0011	0.0039	137
33	57570.3534	0.0014	0.0021	139
34	57570.4134	0.0012	0.0002	141
35	57570.4785	0.0014	0.0034	136
36	57570.5365	0.0014	-0.0005	137
65	57572.3319	0.0009	0.0007	142
66	57572.3929	0.0010	-0.0002	141
67	57572.4564	0.0008	0.0015	143
68	57572.5139	0.0016	-0.0030	141
69	57572.5744	0.0069	-0.0043	49
81	57573.3185	0.0009	-0.0026	142
82	57573.3832	0.0014	0.0002	143
83	57573.4425	0.0016	-0.0024	141
84	57573.5055	0.0015	-0.0013	143
85	57573.5644	0.0020	-0.0043	142
86	57573.6275	0.0018	-0.0030	133
87	57573.6893	0.0026	-0.0031	42
97	57574.3115	0.0029	0.0004	142
98	57574.3753	0.0019	0.0023	143
99	57574.4372	0.0012	0.0023	143
100	57574.5036	0.0033	0.0069	106

\*BJD-2400000.

†Against max = 2457568.3096 + 0.061872E.

‡Number of points used to determine the maximum.

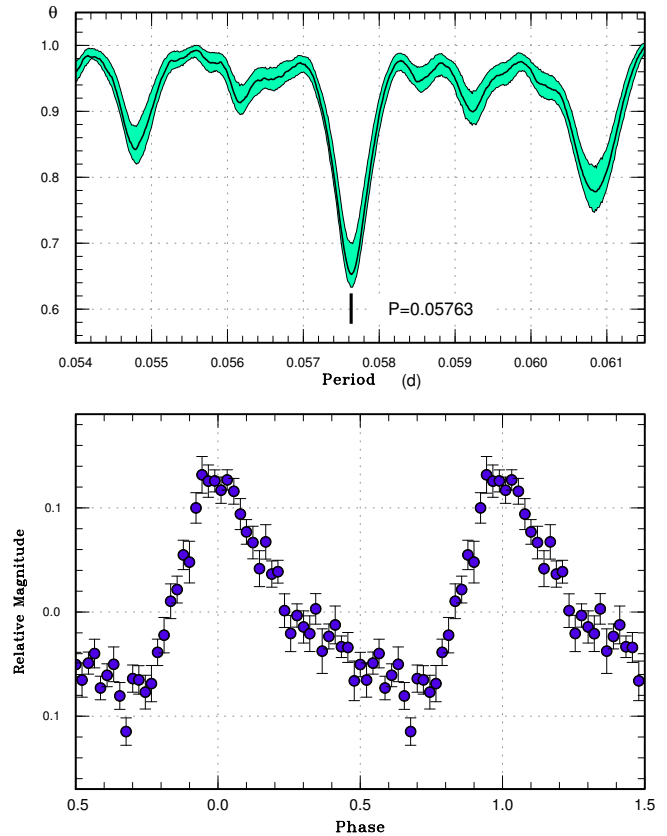


**Fig. 46.** Superhumps in ASASSN-16ez (2016). (Upper): PDM analysis. (Lower): Phase-averaged profile.

object was also detected on June 17 by the MASTER network (independent detection, Balanutsa et al. 2016a). The object was undetected on June 12 (Balanutsa et al. 2016a) and June 11 (ASAS-SN data). Observations on June 21 already recorded superhumps (vsnet-alert 19927). The superhumps grew further (vsnet-alert 19934, 19936, 19953; figure 51, figure 52). It took, however, some time to establish the superhump period since nightly observations were short. The times of superhump maxima are listed in table 48. The maxima for  $E \leq 23$  were most likely stage A superhumps as judged from the growing amplitudes and  $O - C$  values (figure 52). The period of stage A superhumps, however, was not convincingly determined due to the shortness of nightly observations.

The object showed a likely plateau-type rebrightening (figure 52; the plateau-type rebrightening was favored by the lack of rising/fading trends in the nightly light curves in the rebrightening phase). Although we could not observe early superhumps, we consider that this object is a WZ Sge-type dwarf nova as judged from the long rebrightening (cf. Kato 2015). The duration of the phase of early superhumps, if it was present, must have been

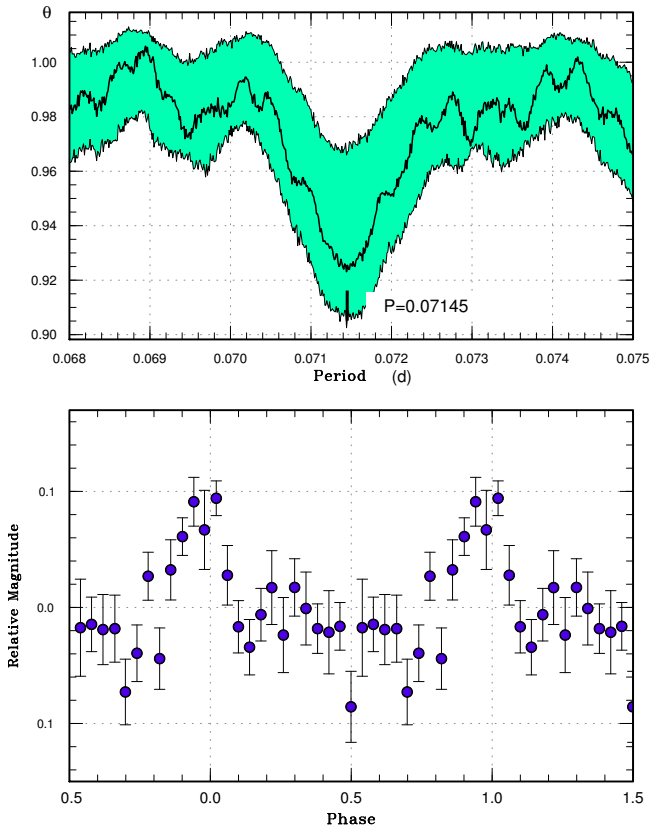


Fig. 47. Superhumps in ASASSN-16fr (2016). (Upper): PDM analysis. (Lower): Phase-averaged profile.

shorter than 9 d. This shortness suggests that this object may not be an extreme WZ Sge-type dwarf nova. There was, however, the case of the 2015 superoutburst of AL Com (Kimura et al. 2016), in which no early superhumps were observed despite that the same object showed long phases of early superhumps in previous superoutbursts. It may be premature to draw any conclusion about the evolutionary state of ASASSN-16gj only from the present observation.

### 3.46 ASASSN-16gl

This object was detected as a transient at  $V=14.8$  on 2016 June 19 by the ASAS-SN team. The outburst was announced on June 22, when the object faded to  $V=15.4$ . Subsequent observations detected superhumps (vsnet-alert 19940, 19942, 19949; figure 53). The times of superhump maxima are listed in table 49. The object was still in outburst on July 11, and the entire duration of the superoutburst exceeded 22 d. Although our initial observation was already 8 d after the outburst detection, the possibility that we observed stage C superhumps may be rather small considering the long duration of the superoutburst

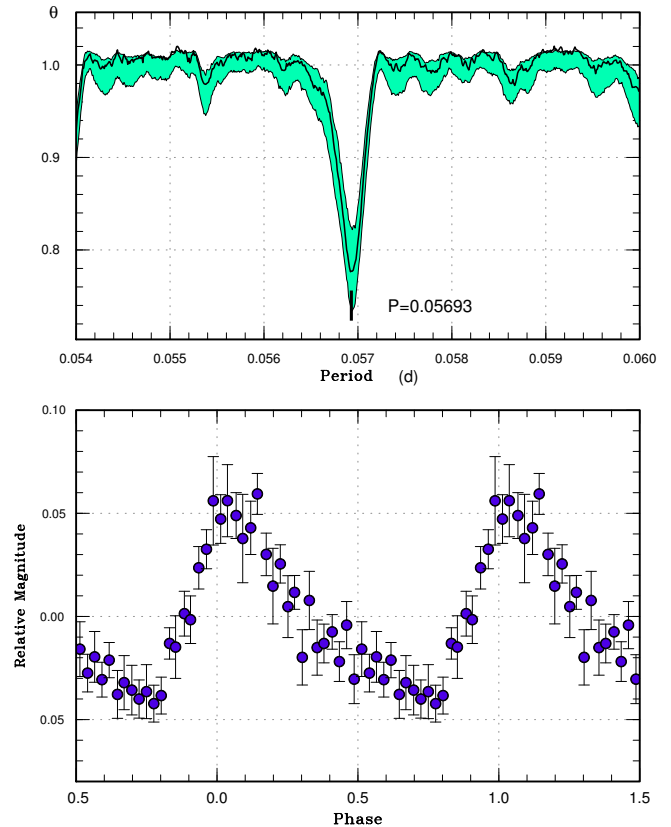


Fig. 48. Ordinary superhumps in ASASSN-16fu during stage B (2016). (Upper): PDM analysis. (Lower): Phase-averaged profile.

(stage B-C transitions usually occur very late in such systems, e.g. SW UMa in figure 1).

### 3.47 ASASSN-16hi

This object was detected as a transient at  $V=15.5$  on 2016 July 15 by the ASAS-SN team. Subsequent observations detected superhumps (vsnet-alert 20002, 20018; figure 54). The times of superhump maxima are listed in table 50. The observed maxima well illustrate typical stages B and C. Although the outburst was rather well recorded, the faintness (around 16 mag) made the quality of the averaged superhump profile rather poor.

### 3.48 ASASSN-16hj

This object was detected as a transient at  $V=14.2$  on 2016 July 18 by the ASAS-SN team. Subsequent observations detected likely early superhumps and ordinary superhumps (vsnet-alert 20006, 20029; figure 55). On August 2–3, the object faded rapidly to a temporary dip (around 18.5 mag, figure 57). The object then entered a plateau-type rebrightening (vsnet-alert 20049), during which ordinary

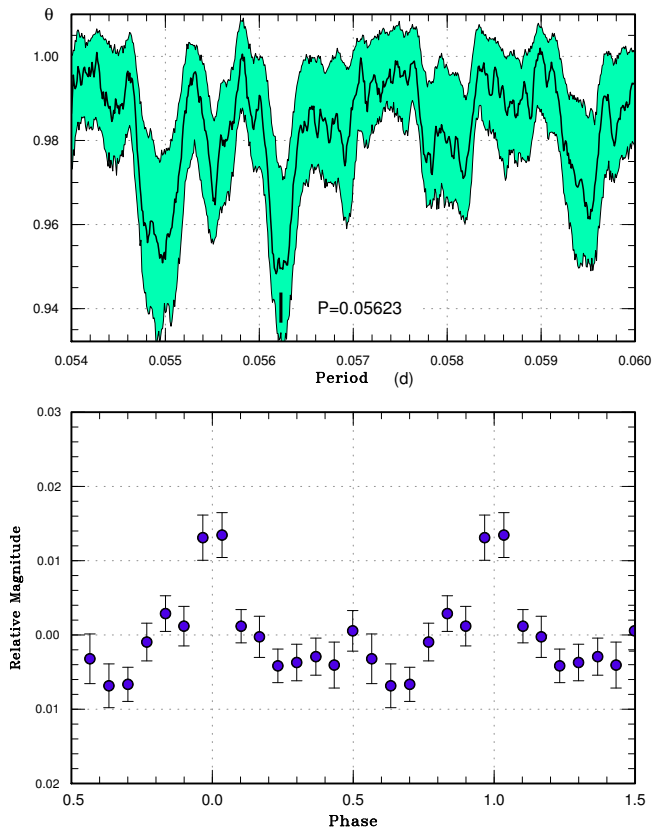


Fig. 49. Possible early superhumps in ASASSN-16fu (2016). (Upper): PDM analysis. (Lower): Phase-averaged profile.

superhumps were present (figure 56). The object showed another separate rebrightening on August 18 (vsnet-alert 20089). Although later observations suggested another rebrightening on September 11–13, the reality of this rebrightening needs to be confirmed since it was long after the previous rebrightening and the observations were at the end of the observing season (figure 57).

The times of superhump maxima are listed in table 51. This table includes superhump maxima after a short dip. There were apparent stages A–C, although observations of stage C were rather poor (figure 57).

We give the possible signal of early superhumps in figure 58. Although the signal was close to the detection limit, the period appears to be consistent with the superhump period and the profile is also consistent with that of early superhumps. The period with the PDM method was 0.05499(6) d. The  $\epsilon^*$  for stage A superhumps was 0.034(7), which corresponds to  $q=0.09(2)$ .

### 3.49 ASASSN-16ia

This object was detected as a transient at  $V=14.6$  on 2016 August 1 by the ASAS-SN team. The object was also de-

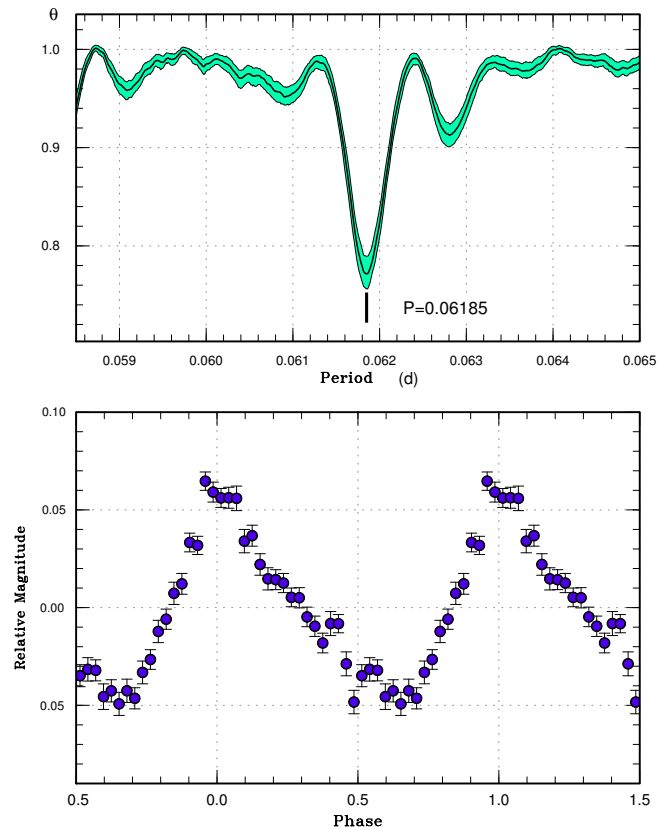
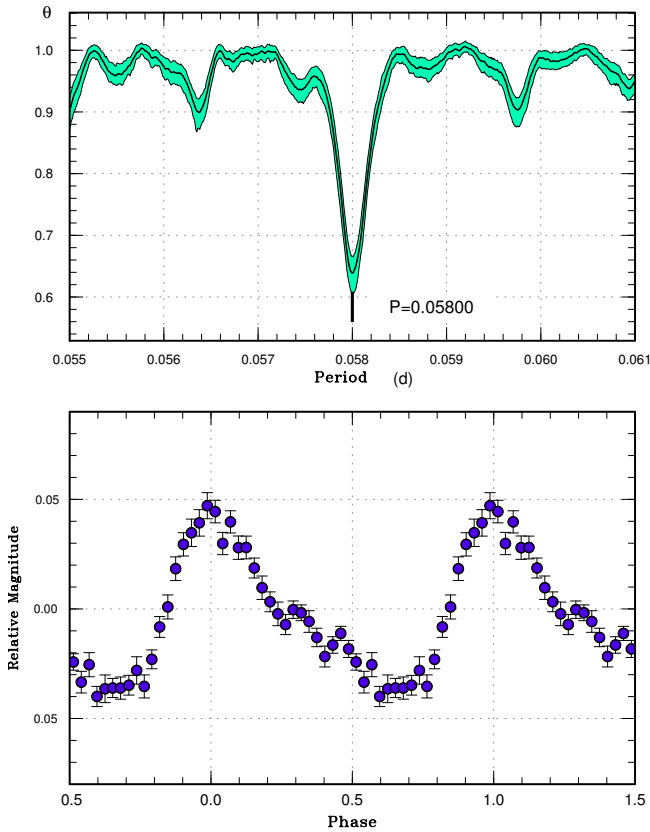


Fig. 50. Ordinary superhumps in ASASSN-16gh during stage B (2016). (Upper): PDM analysis. (Lower): Phase-averaged profile.

tected by Gaia (Gaia16azd) at a magnitude of 16.71 on August 7.<sup>15</sup> The coordinates of the object were taken from this Gaia detection. The object once faded to  $V=17.1$  on August 5. It was observed bright (16.0 mag) again on August 7 and showed strong early superhumps (vsnet-alert 20055, 20069, 20076). The object was followed until August 15, when early superhumps were still present. A transition to ordinary superhumps was not observed since the object became too faint.

The mean profile of early superhumps is shown in figure 59. The large (0.42 mag) full amplitude is exceptional and is largest among the known WZ Sge-type dwarf novae (cf. figure 15 in Kato 2015). The deeper minimum around phase 0.3 in figure 59 is somewhat flat-bottomed, which may be suggestive of an eclipsing component (see numerical model for MASTER OT J005740.99+443101.5 in Kato et al. 2014a). Nightly variation of early superhumps is shown in figure 60. It is noteworthy that the amplitudes of early superhump remained sufficiently large even 8 d after our initial observation. The systematic shift of the phase of the deeper minimum may reflect the varying de-

<sup>15</sup><http://gsaweb.ast.cam.ac.uk/alerts/alert/Gaia16azd/>.



**Fig. 51.** Ordinary superhumps in ASASSN-16gj during stage B (2016). (Upper): PDM analysis. (Lower): Phase-averaged profile.

gree of the contribution of the eclipsing component. Since the object is expected to have a very high inclination, detailed observations in quiescence are desired to determine the system parameters.

It is noteworthy that a precursor outburst was apparently present before the phase of the early superhumps. This is probably the first case in WZ Sge-type dwarf novae and the reason why the cooling wave started during the initial peak needs to be clarified.

### 3.50 ASASSN-16ib

This object was detected as a transient at  $V=14.2$  on 2016 August 5 by the ASAS-SN team. Subsequent observations detected growing superhumps (vsnet-alert 20066, 20083). The times of superhump maxima are listed in table 52. During the epochs for  $E \leq 14$ , the amplitudes of superhumps grew, and these superhumps can be safely identified as stage A superhumps. The distinction of stages B and C was unclear. We listed a value for  $47 \leq E \leq 133$  as stage B in table 3. The mean profile of the superhumps is shown in figure 61.

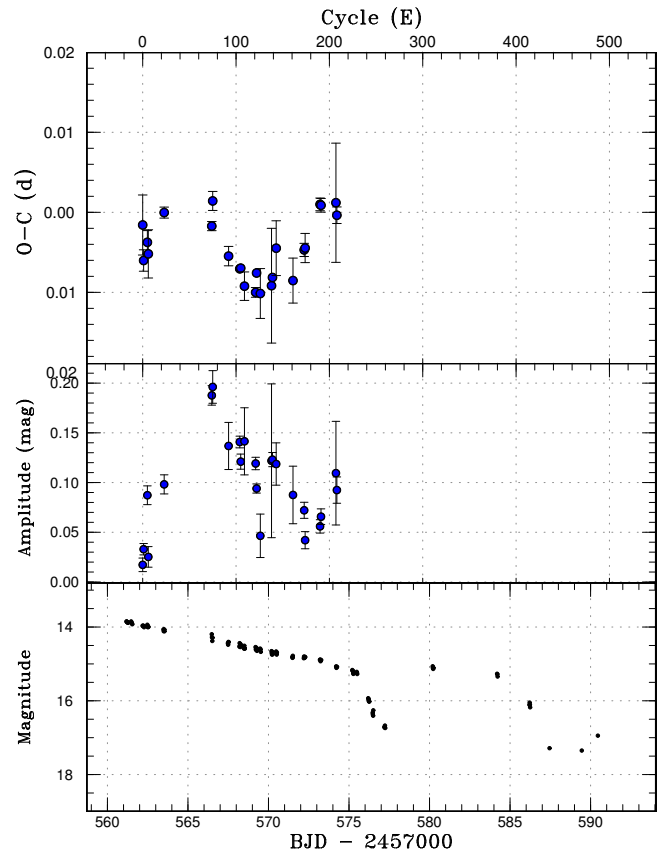


**Fig. 52.**  $O - C$  diagram of superhumps in ASASSN-16gj (2016). (Upper:)  $O - C$  diagram. We used a period of 0.05796 d for calculating the  $O - C$  residuals. (Middle:) Amplitudes of superhumps. (Lower:) Light curve. The data were binned to 0.019 d.

### 3.51 ASASSN-16ik

This object was detected as a transient at  $V=15.26$  on 2016 August 6 by the ASAS-SN team. The object further brightened to  $V=13.9$  on August 8. The object started to show superhumps on August 11–12 (vsnet-alert 20082; figure 62). The times of superhump maxima are listed in table 53. The data very clearly show stages A (growing superhumps) and B. The object showed a rebrightening on August 25 (vsnet-alert 20109), which faded rapidly. During this rebrightening phase, a weak superhump signal was detected with a period of 0.0649(3) d.

### 3.52 ASASSN-16is

This object was detected as a transient at  $V=14.9$  on 2016 August 9 by the ASAS-SN team. Initial observations detected double-wave modulations attributable to early superhumps (vsnet-alert 20078, 20084; figure 63). The period of early superhumps was 0.05762(2) d. The object started to show ordinary superhumps at least on August

**Table 48.** Superhump maxima of ASASSN-16gj (2016)

$E$	max*	error	$O - C^\dagger$	$N^\ddagger$
0	57562.1891	0.0038	0.0034	88
1	57562.2427	0.0013	-0.0010	126
5	57562.4768	0.0015	0.0013	15
6	57562.5333	0.0030	-0.0002	21
23	57563.5238	0.0007	0.0049	24
74	57566.4780	0.0006	0.0030	16
75	57566.5391	0.0012	0.0062	12
92	57567.5176	0.0012	-0.0008	21
104	57568.2115	0.0003	-0.0024	134
105	57568.2695	0.0004	-0.0024	114
109	57568.4991	0.0018	-0.0046	26
121	57569.1939	0.0006	-0.0054	80
122	57569.2543	0.0004	-0.0030	133
126	57569.4835	0.0031	-0.0056	18
138	57570.1800	0.0072	-0.0047	42
139	57570.2390	0.0004	-0.0037	130
143	57570.4745	0.0034	-0.0000	14
161	57571.5138	0.0028	-0.0041	18
173	57572.2131	0.0008	-0.0003	133
174	57572.2713	0.0018	-0.0001	87
190	57573.2041	0.0008	0.0053	125
191	57573.2620	0.0009	0.0052	109
207	57574.1896	0.0074	0.0054	56
208	57574.2460	0.0010	0.0039	122

\*BJD-2400000.

 $^\dagger$ Against max = 2457562.1857 + 0.057964E. $^\ddagger$ Number of points used to determine the maximum.

20 (vsnet-alert 20101, 20106; figure 64). The times of superhump maxima are listed in table 54. The superoutburst plateau was terminated by rapid fading on August 28. The object is confirmed to be a WZ Sge-type dwarf nova.

### 3.53 ASASSN-16iu

This object was detected as a transient at  $V=15.3$  on 2016 August 4 by the ASAS-SN team. The object once faded to fainter than  $V=17.6$  on August 6 and brightened again to  $V=15.2$  on August 9. The detection of the outburst was announced after this brightening. Superhumps were soon detected on August 11 (vsnet-alert 20075). The amplitudes of superhumps decreased and they became less prominent on subsequent nights. They became detectable again on August 15 (figure 65). The times of superhump maxima are listed in table 55. Due to the long period of undetectable superhumps, the  $P_{\text{dot}}$  for stage B superhumps is very uncertain. The period for stage C given in

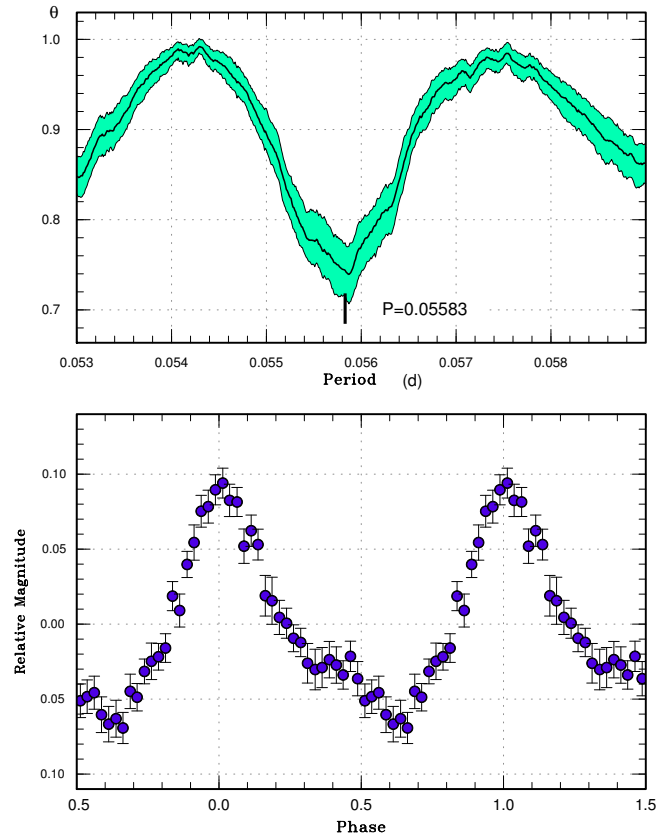
**Fig. 53.** Ordinary superhumps in ASASSN-16gj (2016). (Upper): PDM analysis. (Lower): Phase-averaged profile.

table 3 is very approximate due to the short baseline.

### 3.54 ASASSN-16iw

This object was detected as a transient at  $V=13.9$  on 2016 August 10 by the ASAS-SN team. There was a faint ( $g=21.9$ ) SDSS counterpart (there were 17 measurements in the SDSS data with a range of 21.8–22.2 in  $g$ ) and the large outburst amplitude suggested a WZ Sge-type dwarf nova.

The object started to show superhumps on August 17 (vsnet-alert 20086, 20091, 20100; figure 66). The times of superhump maxima are listed in table 56. The superhumps grew slowly and it took at least 47 cycles to reach the full superhump amplitude. Based on  $O - C$  variations, we have identified  $E \leq 32$  to be stage A superhumps (figure 67).

The object showed at least five post-superoutburst rebrightenings (vsnet-alert 20129, 20147, 20164, 20167; figure 68).

An analysis of the early part of the light curve detected a possible signal of early superhumps (figure 69). Although the signal was weak (the amplitude was smaller

**Table 49.** Superhump maxima of ASASSN-16gl (2016)

$E$	max*	error	$O - C^\dagger$	$N^\ddagger$
0	57569.2036	0.0009	-0.0003	15
2	57569.3180	0.0006	0.0024	128
3	57569.3714	0.0005	-0.0001	127
4	57569.4287	0.0006	0.0013	128
5	57569.4846	0.0008	0.0015	122
6	57569.5388	0.0008	-0.0002	116
7	57569.5933	0.0016	-0.0015	74
8	57569.6507	0.0015	0.0000	88
9	57569.7068	0.0010	0.0003	17
10	57569.7630	0.0011	0.0007	17
11	57569.8171	0.0011	-0.0011	14
20	57570.3185	0.0008	-0.0021	128
21	57570.3732	0.0010	-0.0033	115
22	57570.4315	0.0008	-0.0008	124
23	57570.4890	0.0015	0.0009	86
24	57570.5436	0.0010	-0.0004	98
25	57570.6036	0.0028	0.0038	30
27	57570.7118	0.0011	0.0003	17
28	57570.7663	0.0023	-0.0011	17
45	57571.7162	0.0013	-0.0003	17
100	57574.7851	0.0026	-0.0022	14
117	57575.7377	0.0033	0.0011	13
118	57575.7936	0.0042	0.0013	12

\*BJD-2400000.

 $^\dagger$ Against max = 2457569.2040 + 0.055834E. $^\ddagger$ Number of points used to determine the maximum.

than 0.01 mag) and the profile was not doubly humped as expected for early superhumps, we suspect that this is a candidate period of early superhumps since the period excess was close to what is expected for a WZ Sge-type dwarf nova. The period was 0.06495(5) d. The  $\epsilon^*$  of 0.029(1) for stage A superhumps corresponds to  $q=0.079(2)$ . This  $q$  value is not as small as expected for a period bouncer at this orbital period. The relatively large  $P_{\text{dot}}$  for stage B superhump may also be suggestive for a relatively large  $q$ . The object may be similar to WZ Sge-type dwarf novae with multiple rebrightenings with relatively large  $q$ , such as MASTER OT J211258.65+242145.4 and MASTER OT J203749.39+552210.3 (Nakata et al. 2013).

### 3.55 ASASSN-16jb

This object was detected as a transient at  $V=13.3$  on 2016 August 18 by the ASAS-SN team. The object was caught on the rise to the maximum. The object was initially suspected to be a Galactic nova (cf. vsnet-alert 20092). The

**Table 50.** Superhump maxima of ASASSN-16hi (2016)

$E$	max*	error	$O - C^\dagger$	$N^\ddagger$
0	57589.8022	0.0018	0.0037	15
1	57589.8600	0.0019	0.0025	16
2	57589.9157	0.0011	-0.0007	12
17	57590.7958	0.0033	-0.0049	15
18	57590.8560	0.0018	-0.0037	16
19	57590.9144	0.0034	-0.0043	13
34	57591.7973	0.0015	-0.0056	19
51	57592.8014	0.0024	-0.0036	19
52	57592.8569	0.0027	-0.0071	20
53	57592.9204	0.0048	-0.0025	14
68	57593.8115	0.0043	0.0043	19
69	57593.8664	0.0035	0.0003	19
85	57594.8077	0.0027	-0.0017	16
86	57594.8664	0.0080	-0.0019	16
102	57595.8167	0.0033	0.0052	15
103	57595.8718	0.0041	0.0013	15
118	57596.7673	0.0024	0.0126	20
119	57596.8236	0.0024	0.0099	27
120	57596.8825	0.0019	0.0099	27
121	57596.9419	0.0014	0.0102	11
135	57597.7583	0.0052	0.0014	17
136	57597.8210	0.0016	0.0052	27
137	57597.8786	0.0019	0.0038	26
138	57597.9378	0.0063	0.0041	8
152	57598.7549	0.0028	-0.0042	16
153	57598.8157	0.0035	-0.0024	26
154	57598.8743	0.0031	-0.0027	26
169	57599.7574	0.0047	-0.0038	19
170	57599.8143	0.0054	-0.0059	26
171	57599.8754	0.0018	-0.0038	26
187	57600.8147	0.0044	-0.0076	27
188	57600.8734	0.0080	-0.0079	27

\*BJD-2400000.

 $^\dagger$ Against max = 2457589.7986 + 0.058951E. $^\ddagger$ Number of points used to determine the maximum.

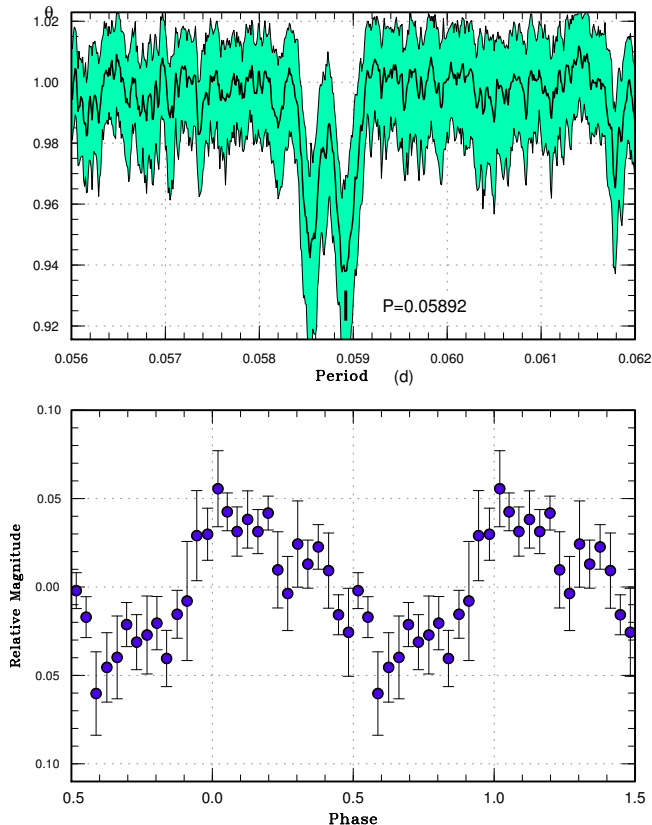


**Fig. 54.** Superhumps in ASASSN-16hi (2016). (Upper): PDM analysis. (Lower): Phase-averaged profile.

object was confirmed to be blue, confirming the dwarf nova-type nature (vsnet-alert 20094). Subsequent observations detected early superhumps (vsnet-alert 20098, 20095; figure 70). The object started to show ordinary superhumps (figure 71) on August 25 and showed behavior similar to a short-period SU UMa-type dwarf nova rather than an extreme WZ Sge-type dwarf nova (vsnet-alert 20112, 20125, 20154).

The times of superhump maxima are listed in table 57. All stages (A–C) are clearly seen. The period of stage A superhumps listed in table 3 was determined by the PDM method.

The period of early superhumps was 0.06305(2) d (figure 70). The fractional superhump excess of stage A superhumps  $\epsilon^*$  was 0.0321(5), which corresponds to  $q=0.088(1)$ . This value is larger than what is expected for a period bouncer having this orbital period. The  $O - C$  behavior (positive  $P_{\text{dot}}$  for stage B and the appearance of stage C) is also consistent with an object having an intermediately low  $q$ .

The object was also detected in outburst by ASAS-3 on 2006 March 10 ( $V=13.66$ , superoutburst), and possibly on 2009 November 3 ( $V=13.63$ , single observation at the end

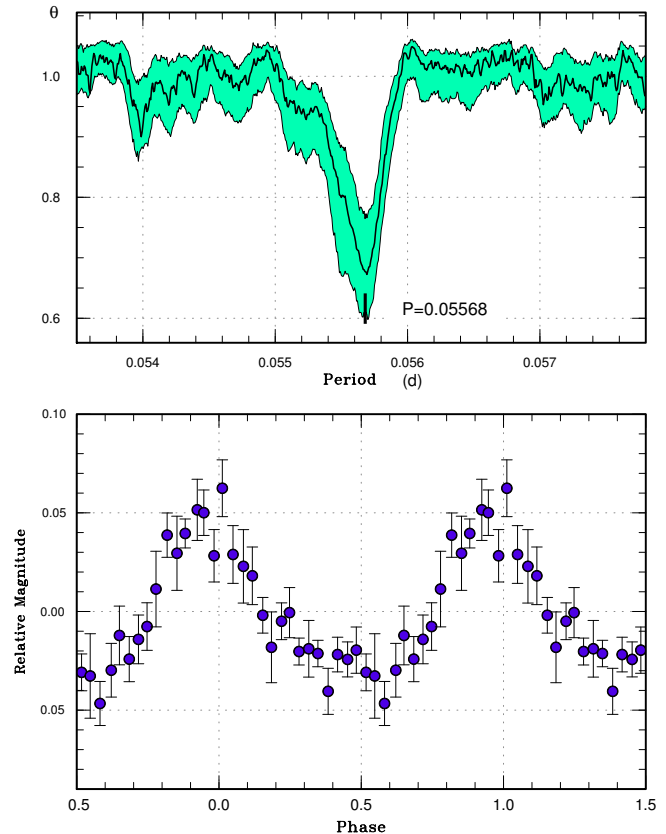


**Fig. 55.** Ordinary superhumps in ASASSN-16hj before the dip (2016). The data segment BJD 2457593–2457604 was used. (Upper): PDM analysis. (Lower): Phase-averaged profile.

of the observing season). The presence of earlier outbursts also seems to exclude the possibility of a period bouncer.

The identification in AAVSO VSX with UGPS J175044.95–255837.2 appears to be doubtful considering its red color ( $J - K=2.7$ ). This supposed identification likely came from the initial proposed classification as a classical nova. We adopted coordinates by the ASAS-SN team.

### 3.56 ASASSN-16jd

This object was detected as a transient at  $V=13.6$  on 2016 August 20 by the ASAS-SN team. Superhumps started to appear on August 25 (vsnet-alert 20108, 20113; figure 72). The times of superhump maxima are listed in table 58. The period reported in vsnet-alert 20113 was a one-day alias of the true period. The period in this paper has been confirmed by the PDM analysis (figure 72) and the much smoother  $O - C$  diagram than obtained using the former period [the case is the same as presented in subsection 2.2 in Kato et al. (2015a)].

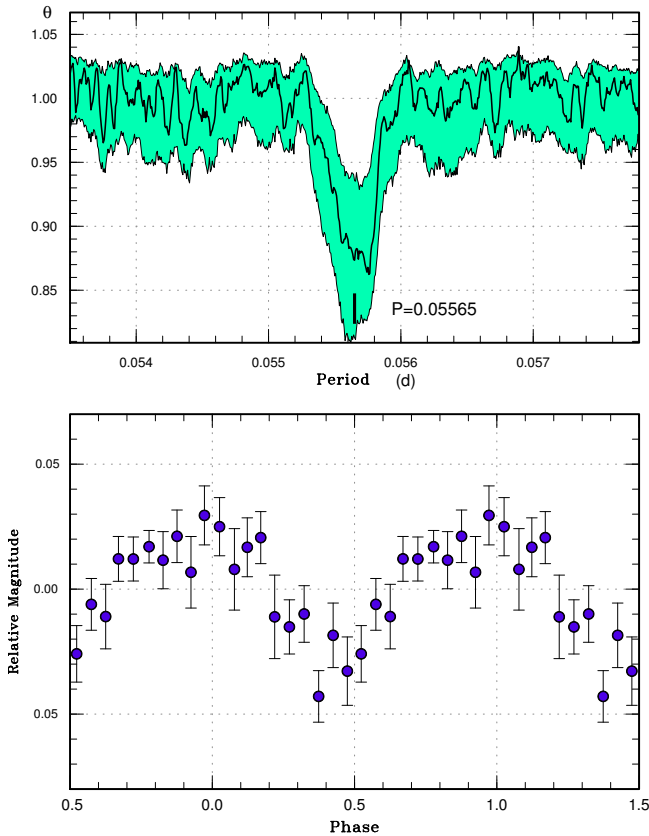


**Fig. 56.** Ordinary superhumps in ASASSN-16hj during the long rebrightening phase (2016). The data segment BJD 2457605–2457612 was used. (Upper): PDM analysis. (Lower): Phase-averaged profile.

### 3.57 ASASSN-16jk

This object was detected as a transient at  $V=13.9$  on 2016 August 27 by the ASAS-SN team. The object has a blue  $g=20.72$  SDSS counterpart. A neural network analysis of SDSS colors (Kato et al. 2012b) yielded an expected orbital period shorter than 0.06 d. One long outburst reaching 14.36 mag (unfiltered CCD) was recorded by the CRTS team on 2007 May 7. This outburst lasted at least until May 21. There was another detection at  $r=13.87$  by the Carlsberg Meridian telescope (Niels Bohr Institute et al. 2014).

Subsequent observations of the 2016 outburst detected superhumps (vsnet-alert 20119, 20124; figure 73). The times of superhump maxima are listed in table 59. Although the maxima for  $E < 16$  are clearly stage A superhumps, the period was not determined due to the shortness of the segment. Although there was apparent stage B-C transition around  $E=146$ , the period of stage C superhumps was not well determined.

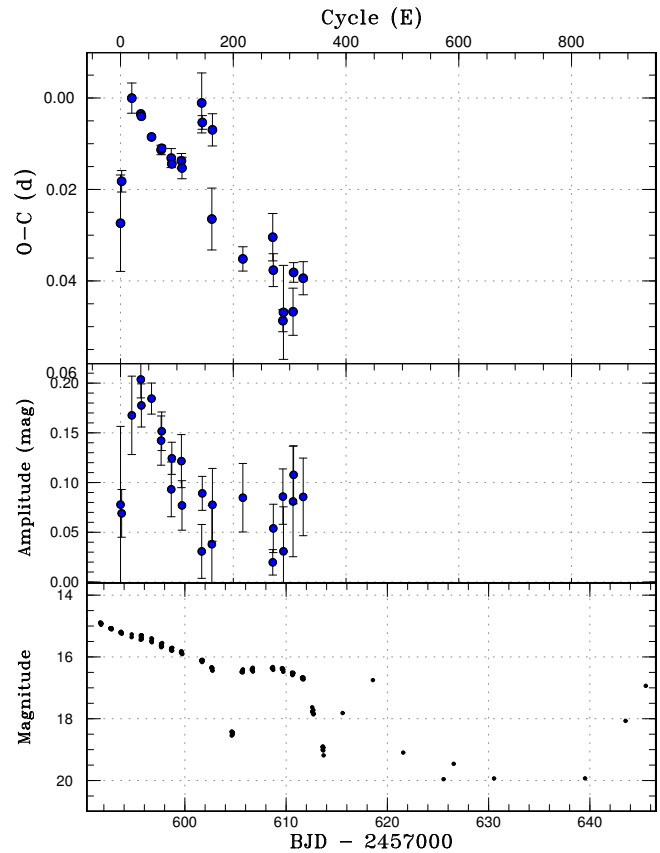


**Fig. 57.**  $O - C$  diagram of superhumps in ASASSN-16hj (2016). (Upper:)  $O - C$  diagram. We used a period of 0.05568 d for calculating the  $O - C$  residuals. (Middle:) Amplitudes of superhumps. (Lower:) Light curve. The data were binned to 0.018 d.

### 3.58 ASASSN-16js

This object was detected as a transient at  $V=13.0$  on 2016 August 30 by the ASAS-SN team. Early superhumps were immediately detected (vsnet-alert 20122, 20126, 20155; figure 74). Ordinary superhump emerged on September 9 (vsnet-alert 20165, 20187). The period of early superhumps was 0.060337(5) d. The times of superhump maxima are listed in table 60. The  $O - C$  somewhat flattened after  $E=32$  and there was a rather smooth transition to stage B, which started at around  $E=48$ . The mean profile of ordinary superhumps is given in figure 75.

The fractional superhump excess  $\epsilon^*$  for stage A superhumps was 0.0213(16), which corresponds to  $q=0.056(5)$ . The small  $q$  and an orbital period significantly longer than the period minimum suggest that this object is a period bouncer. Although the mean superhump amplitude is larger than those of period bouncer candidates, this may have been due to the high orbital inclination as suggested by the strong early superhumps.



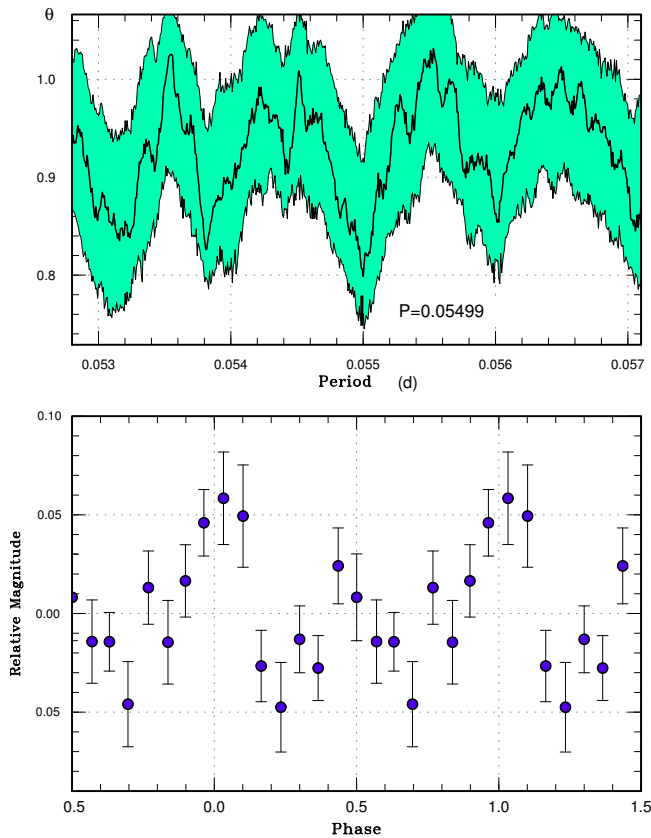


Fig. 58. Possible early superhumps in ASASSN-16hj (2016). (Upper): PDM analysis. (Lower): Phase-averaged profile.

### 3.59 ASASSN-16jz

This object was detected as a transient at  $V=15.7$  on 2016 September 5 by the ASAS-SN team. Observations immediately detected superhumps (vsnet-alert 20142; figure 76). The time of superhump maxima are listed in table 61. There was some hint of decrease in the  $O - C$  values, which may reflect a stage transition. The exact identification of the superhump stage was impossible due to the short baseline.

### 3.60 ASASSN-16kg

This object was detected as a transient at  $V=16.1$  on 2016 September 7 by the ASAS-SN team. The object brightened to  $V=15.2$  on September 8 and the outburst was announced. There was no quiescent counterpart recorded in previous plates, and the large outburst amplitude received attention. Subsequent observations detected superhumps (vsnet-alert 20182; figure 77). The superhump period was around 0.10 d, which was not expected from the large outburst amplitude. Since there was a 3-d gap in the observation and individual runs were compara-

Table 51. Superhump maxima of ASASSN-16hj (2016)

$E$	max*	error	$O - C^\dagger$	$N^\ddagger$
0	57593.6178	0.0105	-0.0239	6
2	57593.7383	0.0023	-0.0145	16
20	57594.7588	0.0033	0.0058	7
36	57595.6462	0.0005	0.0042	12
37	57595.7014	0.0008	0.0038	13
55	57596.6991	0.0005	0.0014	12
72	57597.6428	0.0010	0.0006	12
73	57597.6988	0.0009	0.0010	13
90	57598.6433	0.0021	0.0009	14
91	57598.6977	0.0009	-0.0002	14
108	57599.6449	0.0016	0.0024	14
109	57599.6990	0.0024	0.0010	14
144	57601.6620	0.0066	0.0193	15
145	57601.7135	0.0015	0.0151	15
162	57602.6389	0.0068	-0.0040	15
163	57602.7141	0.0035	0.0156	16
217	57605.6926	0.0027	-0.0062	22
270	57608.6484	0.0052	0.0047	20
271	57608.6968	0.0036	-0.0024	21
288	57609.6323	0.0024	-0.0114	18
289	57609.6898	0.0103	-0.0095	22
306	57610.6365	0.0052	-0.0073	15
307	57610.7008	0.0021	0.0014	15
324	57611.6461	0.0036	0.0021	15

\*BJD-2400000.

$^\dagger$ Against max = 2457593.6417 + 0.055563E.

$^\ddagger$ Number of points used to determine the maximum.

ble to one superhump cycle, it was impossible to select the alias uniquely. The candidate periods by the PDM methods (figure 78) are 0.09676(4) d, 0.10013(4) d, 0.10373(5) d, 0.107610(5) d and 0.11178(5) d. Other aliases can be likely rejected because they give large  $O - C$  scatters. Among them, we have selected 0.10013(4) d which gives the smallest  $\theta$  in the PDM analysis to make cycle counts in table 62. One should note that there remains cycle count ambiguities due to the ambiguity in the alias selection. The object, however, is certainly located in the period gap. It might be worth noting that such a large-amplitude dwarf nova exists in the period gap.

The object was detected in outburst at an unfiltered CCD magnitude of 17.27 on September 26 by the CRTS team (=CSS160926:213630-251348). Since the object had already faded to 18.0 mag on September 20, this CRTS observation appears to have detected a post-superoutburst rebrightening.

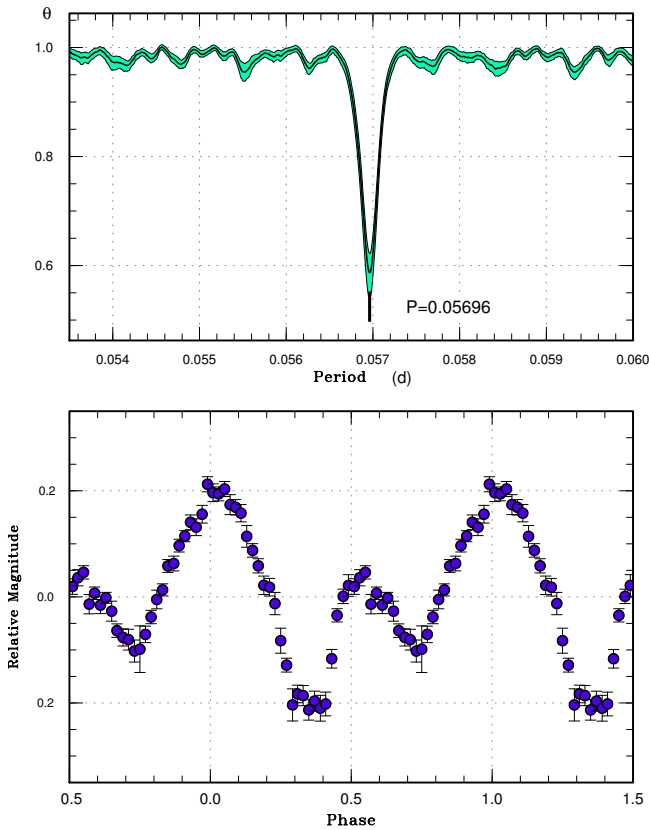


Fig. 59. Early superhumps in ASASSN-16ia (2016). (Upper): PDM analysis. (Lower): Phase-averaged profile.

Table 52. Superhump maxima of ASASSN-16ib (2016)

$E$	max*	error	$O - C^\dagger$	$N^\ddagger$
0	57608.4691	0.0119	-0.0160	14
13	57609.2543	0.0007	0.0032	133
14	57609.3136	0.0006	0.0036	134
47	57611.2595	0.0005	0.0051	136
48	57611.3181	0.0006	0.0047	135
64	57612.2579	0.0008	0.0017	136
65	57612.3166	0.0011	0.0015	120
68	57612.4919	0.0017	0.0001	18
97	57614.2021	0.0120	0.0015	60
98	57614.2605	0.0010	0.0010	131
99	57614.3172	0.0013	-0.0012	133
119	57615.4961	0.0042	-0.0009	21
133	57616.3198	0.0054	-0.0021	79
187	57619.5039	0.0020	0.0003	26
204	57620.5057	0.0058	0.0004	26
221	57621.5042	0.0053	-0.0029	39

\*BJD-2400000.

$^\dagger$ Against max = 2457608.4851 + 0.058923E.

$^\ddagger$ Number of points used to determine the maximum.

Table 53. Superhump maxima of ASASSN-16ik (2016)

$E$	max*	error	$O - C^\dagger$	$N^\ddagger$
0	57611.4511	0.0031	-0.0274	147
1	57611.5177	0.0020	-0.0253	148
2	57611.5843	0.0017	-0.0231	163
14	57612.3862	0.0011	0.0056	146
15	57612.4513	0.0018	0.0064	88
17	57612.5819	0.0008	0.0081	13
18	57612.6469	0.0010	0.0087	17
33	57613.6169	0.0005	0.0122	16
34	57613.6832	0.0008	0.0141	17
45	57614.3886	0.0004	0.0108	146
46	57614.4517	0.0004	0.0094	147
47	57614.5158	0.0004	0.0092	144
48	57614.5835	0.0006	0.0124	74
49	57614.6439	0.0006	0.0084	23
64	57615.6038	0.0010	0.0018	22
65	57615.6699	0.0008	0.0036	22
76	57616.3758	0.0005	0.0008	148
77	57616.4376	0.0006	-0.0018	147
78	57616.5021	0.0021	-0.0018	60
80	57616.6340	0.0009	0.0013	22
81	57616.7004	0.0041	0.0032	10
95	57617.5932	0.0014	-0.0060	21
96	57617.6612	0.0014	-0.0024	22
111	57618.6254	0.0018	-0.0046	22
112	57618.6849	0.0015	-0.0095	13
126	57619.5827	0.0022	-0.0138	19

\*BJD-2400000.

$^\dagger$ Against max = 2457611.4786 + 0.064428E.

$^\ddagger$ Number of points used to determine the maximum.

Table 54. Superhump maxima of ASASSN-16is (2016)

$E$	max*	error	$O - C^\dagger$	$N^\ddagger$
0	57621.3260	0.0007	0.0012	20
1	57621.3835	0.0008	0.0003	26
20	57622.4946	0.0006	0.0002	39
21	57622.5531	0.0005	0.0002	54
69	57625.3568	0.0005	-0.0033	34
70	57625.4167	0.0007	-0.0019	37
87	57626.4111	0.0007	-0.0018	43
88	57626.4727	0.0019	0.0013	22
103	57627.3522	0.0008	0.0036	30
104	57627.4073	0.0009	0.0001	50
105	57627.4658	0.0009	0.0002	39

\*BJD-2400000.

$^\dagger$ Against max = 2457621.3248 + 0.058484E.

$^\ddagger$ Number of points used to determine the maximum.

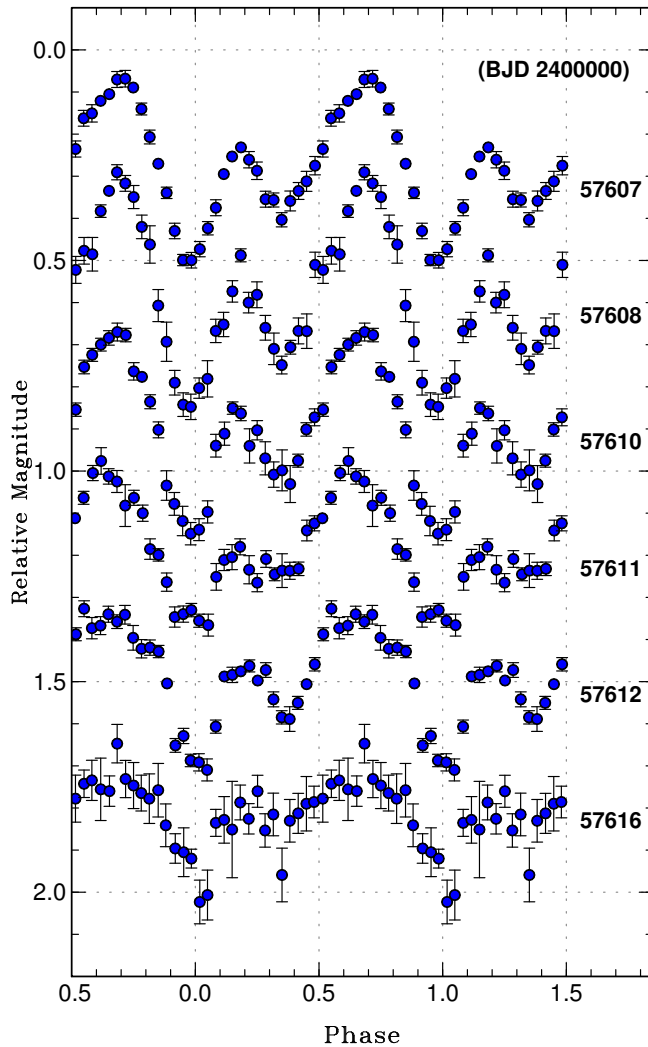


Fig. 60. Evolution of profile of early superhumps in ASASSN-16ia (2016). A period of 0.056962 d was used to draw this figure. The zero phase was defined to be BJD 2457607.428

### 3.61 ASASSN-16kx

This object was detected as a transient at  $V=14.8$  on 2016 September 26 by the ASAS-SN team. Subsequent observations detected superhumps (vsnet-alert 20210; figure 79). The times of superhump maxima are listed in table 63.

### 3.62 ASASSN-16le

This object was detected as a transient at  $V=15.5$  on 2016 October 2 by the ASAS-SN team. Subsequent observations detected superhumps (vsnet-alert 20214). Since the object was observed only on one night, only three superhump maxima were recorded: BJD 2457668.1480(38) ( $N=26$ ), 2457668.2486(13) ( $N=176$ ) and 2457668.3286(20)

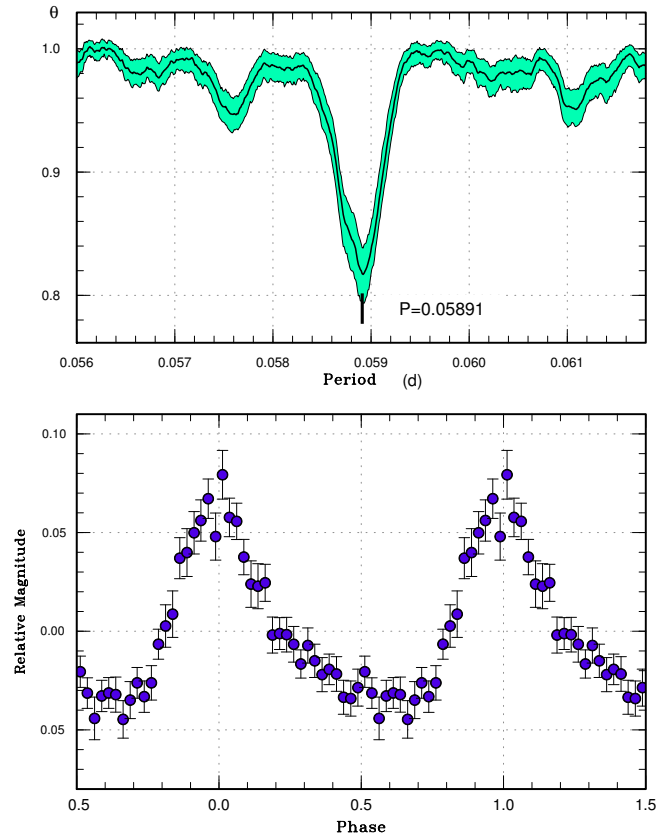


Fig. 61. Superhumps in ASASSN-16ib (2016). (Upper): PDM analysis. (Lower): Phase-averaged profile.

( $N=147$ ). The best period determined by the PDM method was 0.0808(13) d (figure 80). The object faded to fainter than 17.5 mag on October 14.

### 3.63 ASASSN-16lj

This object was detected as a transient at  $V=15.8$  on 2016 October 6 by the ASAS-SN team. Subsequent observations detected superhumps (vsnet-alert 20217). Since the object was observed only on one night, only three superhump maxima were recorded: BJD 2457670.3611(5) ( $N=82$ ), 2457670.4447(5) ( $N=87$ ) and 2457670.5325(22) ( $N=45$ ). The best period determined by the PDM method was 0.0857(4) d (figure 81).

### 3.64 ASASSN-16lo

This object was detected as a transient at  $V=14.3$  on 2016 October 8 by the ASAS-SN team. Subsequent observations detected early superhumps (vsnet-alert 20219, 20222; figure 82) confirming that this object is a WZ Sge-type dwarf nova. The best period of early superhump was 0.05416(1) d. Ordinary superhump developed on October

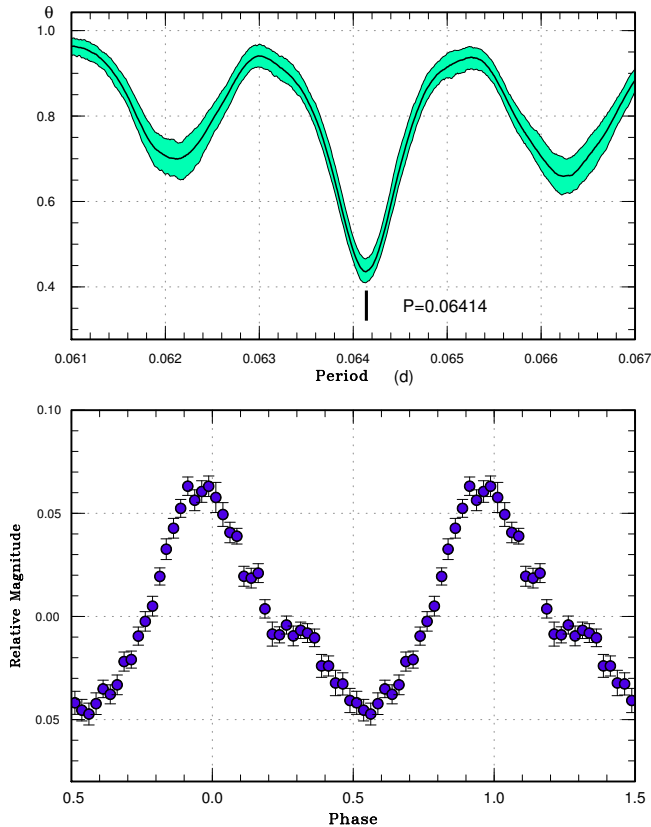


Fig. 62. Superhumps in ASASSN-16ik during stage B (2016). (Upper): PDM analysis. (Lower): Phase-averaged profile.

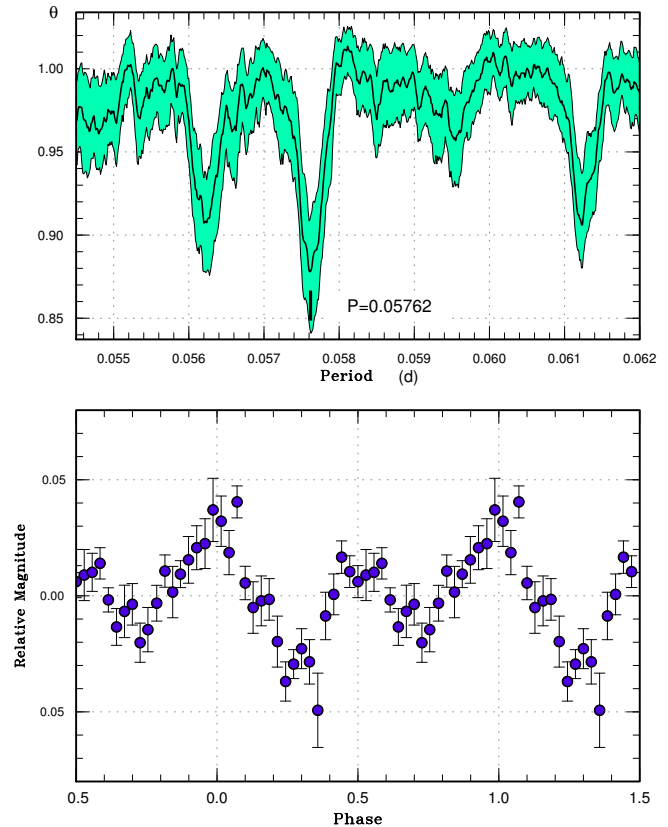


Fig. 63. Early superhumps in ASASSN-16is (2016). (Upper): PDM analysis. (Lower): Phase-averaged profile.

19 (vsnet-alert 20230, 20243; figure 83). The times of superhump maxima are listed in table 64. Although epochs  $E \leq 2$  were stage A superhumps, the period of stage A superhumps could not be determined. Although observations were present after BJD 2457690, superhumps were not clearly detected since the object was very faint (16.5–17.0 mag). The outburst lasted at least until November 7.

### 3.65 ASASSN-16mo

This object was detected as a transient at  $V=15.0$  on 2016 October 28 by the ASAS-SN team. Subsequent observations detected superhumps (vsnet-alert 20280, 20294, 20311; figure 84). The times of superhump maxima are listed in table 65. Although there was likely stage B-C transition after  $E=84$ , later observations could not detect superhumps very clearly and we did not determine the period of stage C superhumps.

### 3.66 ASASSN-16my

This object was detected as a transient at  $V=14.4$  on 2016 November 6 by the ASAS-SN team. Subsequent observations detected superhumps (vsnet-alert 20325, 20357; figure 85). The times of superhump maxima are listed in table 66. Although the  $O - C$  values suggest that  $E \leq 12$  were still stage A superhumps, we did not determine the period of stage A superhumps since superhump amplitudes were already large (0.3–0.4 mag) and it is likely that the period was already affected by the pressure effect (i.e. transition to stage B).

### 3.67 ASASSN-16ni

This object was detected as a transient at  $V=16.5$  on 2016 November 16 by the ASAS-SN team. The large outburst amplitude received attention. Subsequent observations detected long-period superhumps (vsnet-alert 20446; the period reported in vsnet-alert 20398 was probably in error). Such a long period [0.1152(4) d determined in this paper] was unexpected for a large-amplitude dwarf nova. Observations were, however, insufficient to determine the

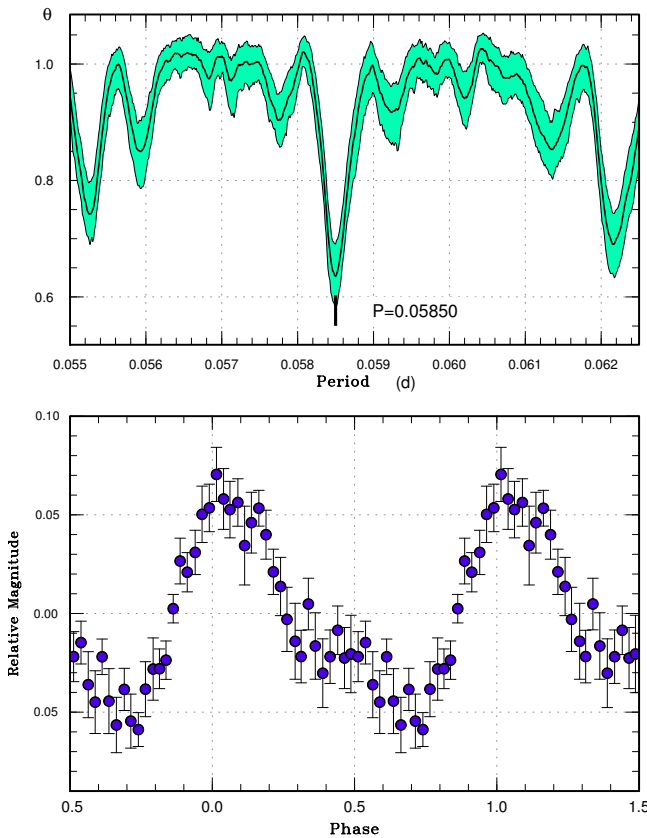


Fig. 64. Ordinary superhumps in ASASSN-16is (2016). (Upper): PDM analysis. (Lower): Phase-averaged profile.

period uniquely due to the faintness. We selected the most likely alias in calculating the  $O - C$  values in table 67. The superhump amplitudes were growing on the first two nights, and the period reported here may refer to that of stage A superhumps. The small amplitudes (figure 86) may also support this stage identification.

The quiescent counterpart was originally proposed to be a very faint ( $g=22.9$ ) object SDSS J050500.40+605455.3. This object, however, has a red color ( $u - g = +2.6$ ) and it is unlikely a CV. The true quiescent counterpart should be fainter than  $g=23$ . We adopted the coordinates by the ASAS-SN team.

### 3.68 ASASSN-16nq

This object was detected as a transient at  $V=15.0$  on 2016 November 26 by the ASAS-SN team. Observations on November 28 detected superhumps (vsnet-alert 20411; figure 87). Although the observations were obtained two nights after the outburst detection, stage A was already over (vsnet-alert 20431, 20472; figure 88). The times of superhump maxima are listed in table 68. Both stages B and C can be recognized. There was one post-superoutburst

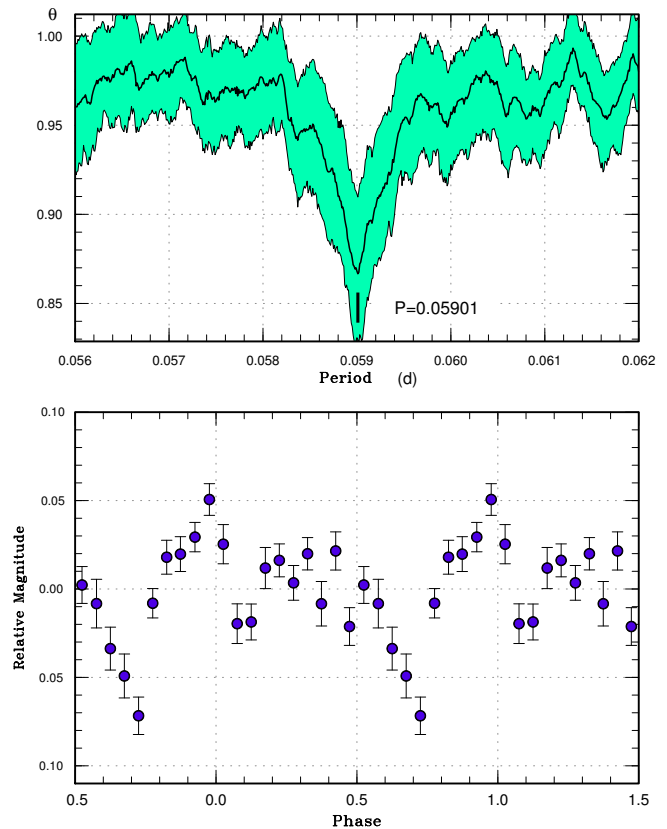


Fig. 65. Superhumps in ASASSN-16iu (2016). The data segment BJD 2457615–2457619 was used when superhumps were continuously detected. (Upper): PDM analysis. (Lower): Phase-averaged profile.

rebrightening on December 23 (figure 88), which is relatively rare for such a long  $P_{SH}$  system.

### 3.69 ASASSN-16nr

This object was detected as a transient at  $V=15.1$  on 2016 November 26 by the ASAS-SN team. The outburst was announced after the observation on November 27 at  $V=15.1$ . The object showed superhumps (vsnet-alert 20420, 20432; figure 89). The times of superhump maxima are listed in table 69. Although a large outburst amplitude ( $\sim 7$  mag) was suggested, the object was not a WZ Sge-type dwarf nova since it showed well-developed ordinary superhumps immediately after the outburst detection.

### 3.70 ASASSN-16nw

This object was detected as a transient at  $V=15.6$  on 2016 November 23 by the ASAS-SN team. The outburst was announced after the observation on November 27 at  $V=16.1$  and November 29 at  $V=16.3$ . Superhumps were

**Table 55.** Superhump maxima of ASASSN-16iu (2016)

$E$	max*	error	$O - C^\dagger$	$N^\ddagger$
0	57611.7578	0.0015	0.0071	37
1	57611.8157	0.0011	0.0062	36
2	57611.8753	0.0009	0.0072	39
68	57615.7425	0.0014	-0.0048	22
69	57615.7942	0.0031	-0.0118	21
70	57615.8549	0.0012	-0.0099	22
71	57615.9147	0.0027	-0.0089	13
82	57616.5640	0.0024	-0.0061	137
83	57616.6224	0.0012	-0.0064	129
85	57616.7401	0.0029	-0.0063	22
86	57616.7998	0.0028	-0.0054	21
87	57616.8573	0.0025	-0.0067	23
102	57617.7467	0.0101	0.0011	21
103	57617.8182	0.0043	0.0139	21
104	57617.8752	0.0041	0.0121	23
119	57618.7466	0.0024	0.0019	20
120	57618.8082	0.0034	0.0047	20
121	57618.8745	0.0108	0.0122	22

\*BJD-2400000.

 $^\dagger$ Against max = 2457611.7506 + 0.058774E. $^\ddagger$ Number of points used to determine the maximum.

detected in observations on two nights (vsnet-alert 20445; figure 90). The alias selection is most likely based on the single long run on the first night giving a period of 0.073(1) d. The times of superhump maxima are listed in table 70.

### 3.71 ASASSN-16ob

This object was detected as a transient at  $V=14.3$  on 2016 November 28 by the ASAS-SN team. The outburst was announced after its further brightening to  $V=13.8$  on November 30. Although the object was initially identified with a  $B=18.4$  mag star in USNO catalog, B. Monard obtained outburst astrometry which indicated that the true counterpart is much fainter (vsnet-alert 20438). The object was also detected by Gaia (Gaia16bzl)<sup>16</sup> at a magnitude of 13.84 on November 30 and was announced (with an identification with ASASSN-16ob) on December 7. The large outburst amplitude suggested a WZ Sge-type dwarf nova. On December 11, low-amplitude superhumps were detected (vsnet-alert 20464, 20465, 20481), which grew to full superhumps (vsnet-alert 20484, 20498). The times of superhump maxima are listed in table 71. The maxima for  $E \leq 36$  correspond to stage A superhumps. Although a PDM analysis of ordinary superhumps gave several can-

<sup>16</sup><<http://gsaweb.ast.cam.ac.uk/alerts/alert/Gaia16bzl/>>.

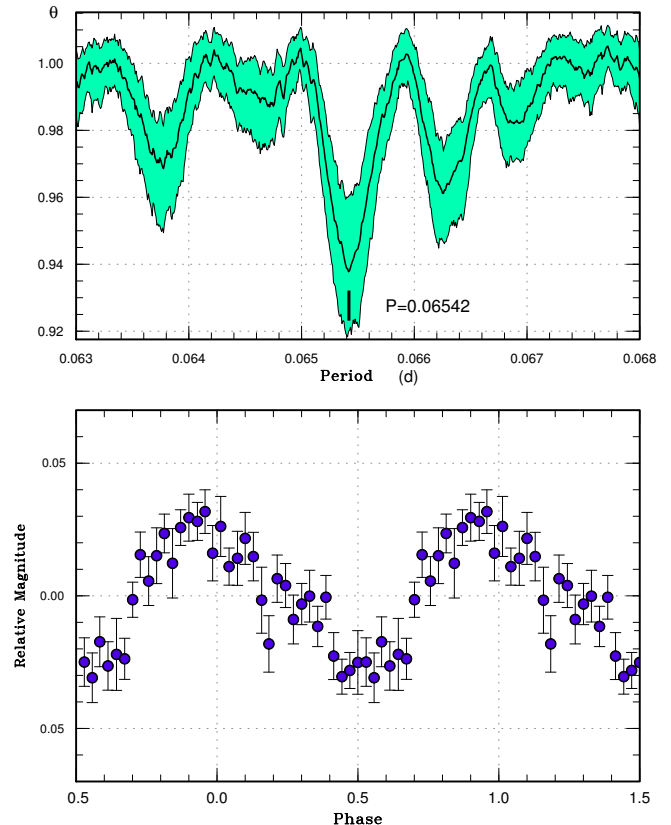


**Fig. 66.** Ordinary superhumps in ASASSN-16iw (2016). The data segment BJD 2457617.5–2457628 was used. (Upper): PDM analysis. (Lower): Phase-averaged profile.

didate periods (figure 91), we consider them false signals due to low signal-to-noise ratio since an analysis restricted to better observation quality gave a single period (figure 92; one-day aliases can be safely ruled out by  $O - C$  analysis).

By using the data before BJD 2457734, we could not detect early superhumps. The upper limit of the amplitude of early superhumps was 0.01 mag. Although we could not detect early superhumps, we consider that this object belongs to WZ Sge-type dwarf novae based on its long waiting time (13 d) for ordinary superhumps to appear and the large outburst amplitude. Using the empirical relation between  $q$  and  $P_{\text{dot}}$  for stage B superhumps [equation (6) in Kato 2015], the expected  $q$  is 0.069(3) (the error reflects the error in  $P_{\text{dot}}$ ).

### 3.72 ASASSN-16oi

This object was detected as a transient at  $V=13.4$  on 2016 December 3 by the ASAS-SN team (vsnet-alert 20443). Low-amplitude early superhumps were detected (vsnet-alert 20466; figure 93). The object subsequently showed

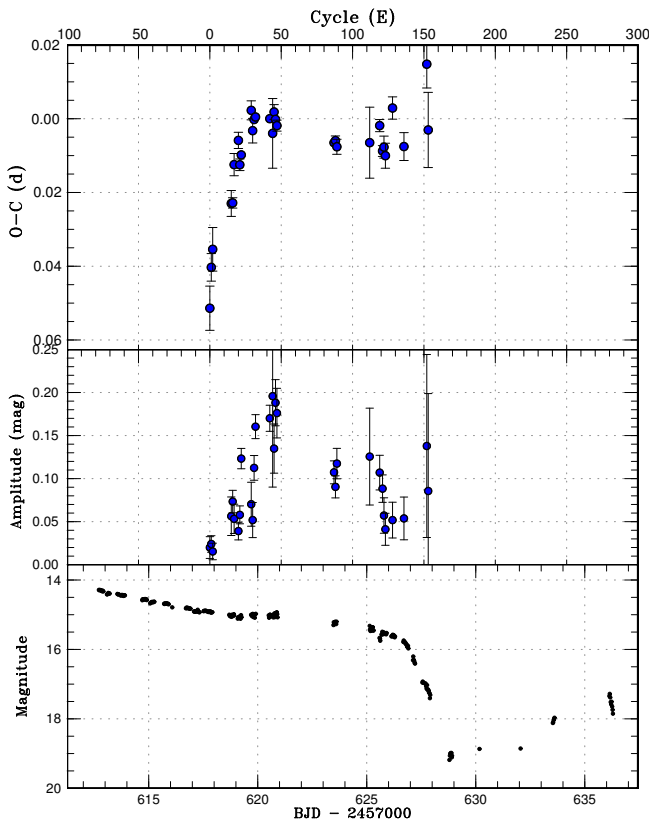


**Fig. 67.**  $O - C$  diagram of superhumps in ASASSN-16iw (2016). (Upper:)  $O - C$  diagram. We used a period of 0.06546 d for calculating the  $O - C$  residuals. (Middle:) Amplitudes of superhumps. (Lower:) Light curve. The data were binned to 0.022 d. The final part of this figure (BJD 2457636) corresponds to the fading part from the first rebrightening.

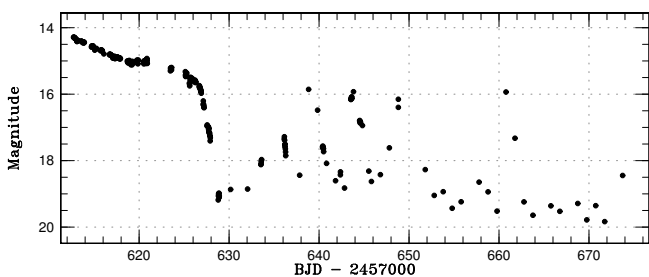


**Fig. 68.** Overall light curve of ASASSN-16iw (2016). The data were binned to 0.022 d. The data on BJD 2457636 represent observations of the fading branch of the first rebrightening. There may have been a rebrightening on BJD 2457674, which was not well sampled.

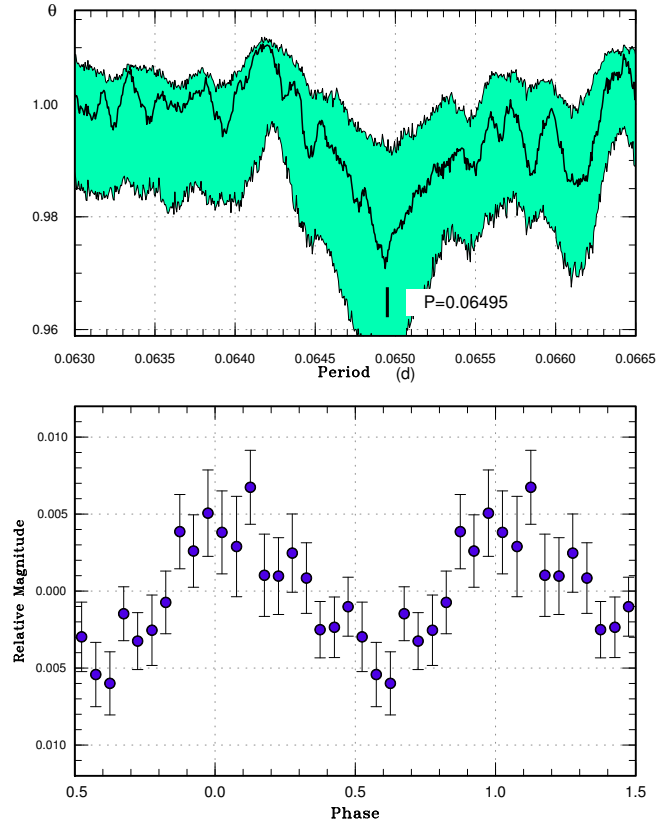


**Fig. 69.** Possible early superhumps in ASASSN-16iw (2016). The data segment before BJD 2457617.5 was used. (Upper): PDM analysis. (Lower): Phase-averaged profile.

ordinary superhumps (vsnet-alert 20466, 20485; figure 94). The object is confirmed to be a WZ Sge-type dwarf nova. The times of superhump maxima are listed in table 72. The best period of early superhumps with the PDM method is 0.05548(7) d. The fractional superhump excess  $\epsilon^*$  for stage A superhumps is 0.033(2), which gives  $q=0.091(7)$ . The relatively large  $q$  is consistent with a relatively large  $P_{\text{dot}}$  for stage B superhumps and the relatively large amplitude of superhumps.

### 3.73 ASASSN-16os

This object was detected as a transient at  $V=13.6$  on 2016 December 10 by the ASAS-SN team. The large outburst amplitude ( $\sim 8$  mag) attracted attention. The object started to show ordinary superhumps on December 18 (vsnet-alert 20501). These superhumps grew further (vsnet-alert 20504, 20508; figure 95). The times of superhump maxima are listed in table 73. Both stages A and B were very clearly recorded (figure 96).

A PDM analysis of the early part of the data yielded a signal which may be early superhumps (figure 97). This

**Table 56.** Superhump maxima of ASASSN-16iw (2016)

$E$	max*	error	$O - C^\dagger$	$N^\ddagger$
0	57617.7525	0.0060	-0.0338	24
1	57617.8290	0.0037	-0.0228	24
2	57617.8994	0.0059	-0.0181	26
15	57618.7628	0.0035	-0.0074	22
16	57618.8284	0.0014	-0.0074	23
17	57618.9043	0.0030	0.0028	20
20	57619.1072	0.0022	0.0090	41
21	57619.1661	0.0016	0.0022	41
22	57619.2342	0.0010	0.0048	35
29	57619.7045	0.0026	0.0159	19
30	57619.7644	0.0033	0.0102	22
31	57619.8329	0.0011	0.0131	24
32	57619.8991	0.0007	0.0137	21
42	57620.5532	0.0008	0.0118	57
44	57620.6801	0.0094	0.0075	20
45	57620.7514	0.0020	0.0132	30
46	57620.8149	0.0010	0.0111	44
47	57620.8786	0.0015	0.0092	45
87	57623.4924	0.0009	-0.0010	59
88	57623.5584	0.0013	-0.0005	53
89	57623.6222	0.0020	-0.0023	29
112	57625.1289	0.0096	-0.0044	35
119	57625.5918	0.0016	-0.0008	40
121	57625.7158	0.0015	-0.0079	20
122	57625.7823	0.0030	-0.0070	20
123	57625.8454	0.0034	-0.0095	21
128	57626.1857	0.0030	0.0027	99
136	57626.6989	0.0038	-0.0088	17
152	57627.7686	0.0065	0.0113	20
153	57627.8162	0.0102	-0.0067	22

\*BJD-2400000.

 $^\dagger$ Against max = 2457617.7863 + 0.065599E. $^\ddagger$ Number of points used to determine the maximum.

period was close to that of ordinary superhumps and we checked a possible contamination of ordinary superhumps by testing different segments. Although the test suggested that the period was not from a contamination of ordinary superhumps, we were not very confident about the reality of the signal since the amplitude was small and mostly only low time-resolution observations were obtained. If the detected period, 0.05494(6) d, is that of early superhumps, the fractional superhump excess for stage A superhumps is  $e^*=0.018(1)$ . Although this value corresponds to  $q=0.047(3)$ , it needs to be treated with caution due to the limitation of the quality of observations. The overall behavior, however, suggests that this object is a rather extreme WZ Sge-type dwarf nova.

**Table 57.** Superhump maxima of ASASSN-16jb (2016)

$E$	max*	error	$O - C^\dagger$	$N^\ddagger$
0	57624.6304	0.0047	-0.0112	35
10	57625.2808	0.0004	-0.0048	148
11	57625.3462	0.0005	-0.0038	149
11	57625.3459	0.0005	-0.0040	148
14	57625.5548	0.0011	0.0116	22
15	57625.6074	0.0013	-0.0002	35
16	57625.6691	0.0010	-0.0029	21
21	57625.9981	0.0007	0.0041	20
22	57626.0629	0.0004	0.0046	33
30	57626.5830	0.0003	0.0094	35
31	57626.6469	0.0003	0.0089	33
46	57627.6099	0.0005	0.0058	35
53	57628.0585	0.0003	0.0036	40
58	57628.3837	0.0029	0.0069	66
68	57629.0183	0.0006	-0.0025	44
69	57629.0824	0.0003	-0.0029	80
76	57629.5392	0.0018	0.0031	20
77	57629.5982	0.0005	-0.0023	32
92	57630.5609	0.0007	-0.0056	35
93	57630.6241	0.0007	-0.0069	35
107	57631.5255	0.0084	-0.0070	18
108	57631.5927	0.0007	-0.0043	35
109	57631.6651	0.0015	0.0038	11
118	57632.2403	0.0089	-0.0006	25
119	57632.2994	0.0006	-0.0060	123
120	57632.3640	0.0005	-0.0058	148
121	57632.4301	0.0013	-0.0041	70
123	57632.5574	0.0012	-0.0056	35
124	57632.6227	0.0013	-0.0046	35
138	57633.5300	0.0026	0.0010	21
139	57633.5928	0.0017	-0.0006	35
140	57633.6577	0.0023	-0.0001	12
154	57634.5602	0.0011	0.0007	36
155	57634.6248	0.0012	0.0010	33
169	57635.5316	0.0011	0.0061	26
170	57635.5929	0.0016	0.0030	35
185	57636.5614	0.0013	0.0055	29
186	57636.6254	0.0010	0.0051	21
193	57637.0777	0.0031	0.0066	7
201	57637.5882	0.0007	0.0019	29
216	57638.5490	0.0017	-0.0033	21
217	57638.6155	0.0014	-0.0013	18
232	57639.5803	0.0029	-0.0025	18

\*BJD-2400000.

 $^\dagger$ Against max = 2457624.6415 + 0.064402E. $^\ddagger$ Number of points used to determine the maximum.



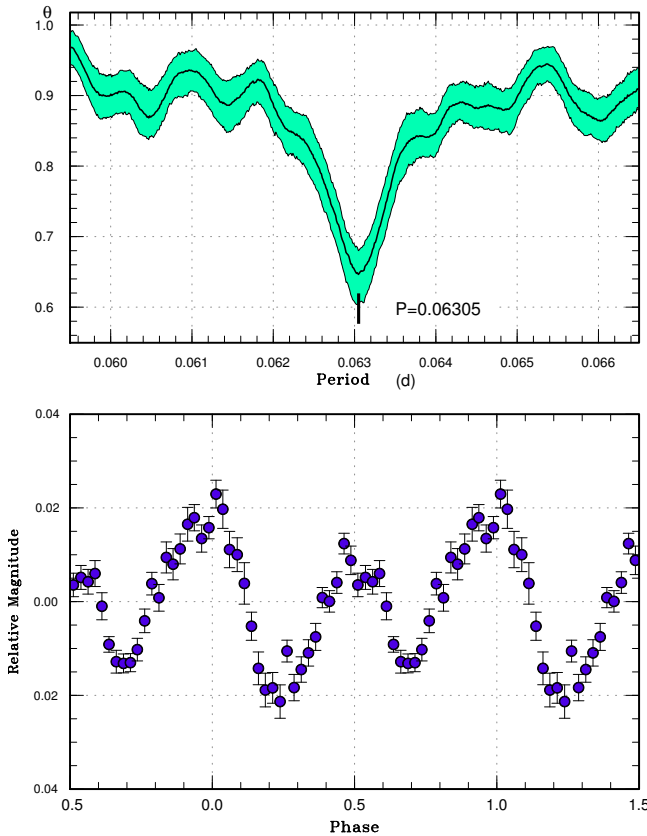


**Fig. 70.** Early superhumps in ASASSN-16jb (2016). (Upper): PDM analysis. (Lower): Phase-averaged profile.

### 3.74 ASASSN-16ow

This object was detected as a transient at  $V=13.9$  on 2016 December 13 by the ASAS-SN team. Since the object was near the Galactic plane, it was also suspected to be a nova. The presence of a GALEX UV counterpart and an  $H\alpha$  emission in IPHAS catalog (IPHAS2 J063047.05+023931.4) suggested a dwarf nova (vsnet-alert 20474, 20476). The dwarf nova-type nature was confirmed by spectroscopy (Siviero and Munari 2016). Subsequent observations detected superhumps (vsnet-alert 20483, 20497, 20503, 20510; figure 98). The times of superhump maxima are listed in table 74. The superoutburst lasted at least up to December 25.

In contrast to many long- $P_{SH}$  SU UMa-type dwarf novae, this object showed a post-superoutburst rebrightening on December 29–31 (vsnet-alert 20571). Although modulations were detected during this rebrightening, we could not detect a secure signal of superhumps.

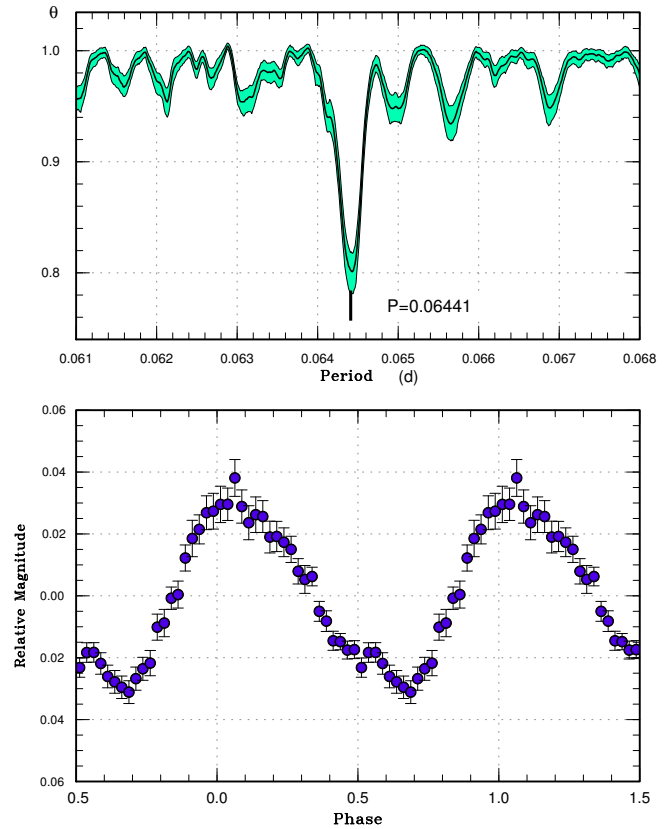


**Fig. 71.** Ordinary superhumps in ASASSN-16jb (2016). (Upper): PDM analysis. (Lower): Phase-averaged profile.

### 3.75 ASASSN-17aa

This object was detected as a transient at  $V=13.9$  on 2017 January 2 by the ASAS-SN team (vsnet-alert 20527). On January 11, superhumps were finally observed (vsnet-alert 20562; figure 99). Although these superhumps were originally suspected to be stage A ones (vsnet-alert 20572, 20573), the large superhump amplitudes suggest that they were already stage B ones. The cycle numbers in table 75 follows this interpretation. There were possibly low-amplitude early superhumps (figure 100) with a period of 0.05393(3) d. These properties suggest the WZ Sge-type classification.

### 3.76 ASASSN-17ab

This object was detected as a transient at  $V=13.4$  on 2017 January 2 by the ASAS-SN team (vsnet-alert 20527). The object was already in outburst at  $V=13.1$  on January 1. Subsequent observations detected superhumps (vsnet-alert 20531; figure 101). The times of superhump maxima are listed in table 76. Although the maxima for  $E \leq 2$  were stage A superhumps, we could not determine the period.

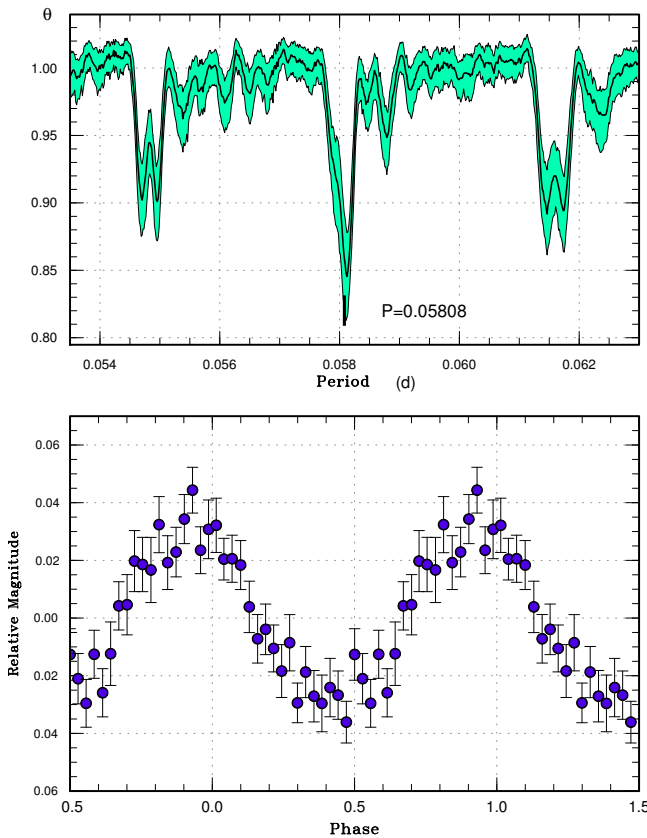


Fig. 72. Ordinary superhumps in ASASSN-16jd (2016). (Upper): PDM analysis. (Lower): Phase-averaged profile.

The object was also detected by Gaia (Gaia17aep)<sup>17</sup> at a magnitude of 17.33 on January 18.

### 3.77 ASASSN-17az

This object was detected as a transient at  $V=14.4$  on 2017 January 19 by the ASAS-SN team. Subsequent observations detected superhumps (vsnet-alert 20626; figure 102). The times of superhump maxima are listed in table 77. Since there was a 2-d gap between observations, there remained viable aliases. Among these aliases, the listed period gave the smallest  $O - C$  values and we selected it as the most likely one.

### 3.78 ASASSN-17bl

This object was detected as a transient at  $V=13.7$  on 2017 January 24 by the ASAS-SN team. On February 4, the object started to show superhumps (vsnet-alert 20641). The long waiting time (11 d) of superhumps strongly suggested a WZ Sge-type object. Further development of su-

Table 58. Superhump maxima of ASASSN-16jd (2016)

$E$	max*	error	$O - C^\dagger$	$N^\ddagger$
0	57625.5891	0.0010	0.0003	32
1	57625.6514	0.0017	0.0044	25
17	57626.5792	0.0007	0.0018	32
18	57626.6391	0.0012	0.0035	31
34	57627.5778	0.0003	0.0117	32
35	57627.6351	0.0005	0.0109	31
69	57629.6035	0.0009	0.0020	28
86	57630.5850	0.0007	-0.0052	32
87	57630.6446	0.0008	-0.0037	26
103	57631.5677	0.0010	-0.0110	33
104	57631.6292	0.0006	-0.0077	32
120	57632.5643	0.0012	-0.0031	32
121	57632.6180	0.0017	-0.0075	32
137	57633.5461	0.0014	-0.0100	29
138	57633.6084	0.0014	-0.0058	27
154	57634.5405	0.0046	-0.0042	24
155	57634.5946	0.0012	-0.0082	31
206	57637.5748	0.0015	0.0060	26
207	57637.6316	0.0028	0.0047	21
223	57638.5721	0.0024	0.0147	19
240	57639.5516	0.0022	0.0056	16
241	57639.6047	0.0015	0.0006	16
258	57640.5933	0.0025	0.0004	16

\*BJD-2400000.

<sup>†</sup>Against max = 2457625.5888 + 0.058155E.

<sup>‡</sup>Number of points used to determine the maximum.

perhumps was recorded (vsnet-alert 20646; figure 103). The times of superhump maxima are listed in table 78. Although individual superhumps were not very well covered (most of them had only 10 observations or even less; the maxima could be reasonably determined since the object was bright), the overall  $O - C$  diagram indicates the clear presence of stage A and stage B with a positive  $P_{\text{dot}}$ . The stage A-B transition was rather uncertain due to the lack of observations in the initial part.

An analysis of the early part of the superoutburst yielded a possible signal of early superhumps (figure 104). Although there was a stronger signal around 0.0563 d, we consider it a false alias since it does not match the period of ordinary superhumps (the period of early superhumps should be shorter than that of ordinary superhumps). The suggested period by the PDM method was 0.05467(5) d. The  $\epsilon^*$  of stage A superhumps determined using this period was 0.0235(9), which corresponds to  $q=0.062(3)$ . This value, however, could have a larger uncertainty since both the orbital period and the period of stage A superhumps were determined from insufficient

<sup>17</sup><<http://gsaweb.ast.cam.ac.uk/alerts/alert/Gaia17aep/>>.

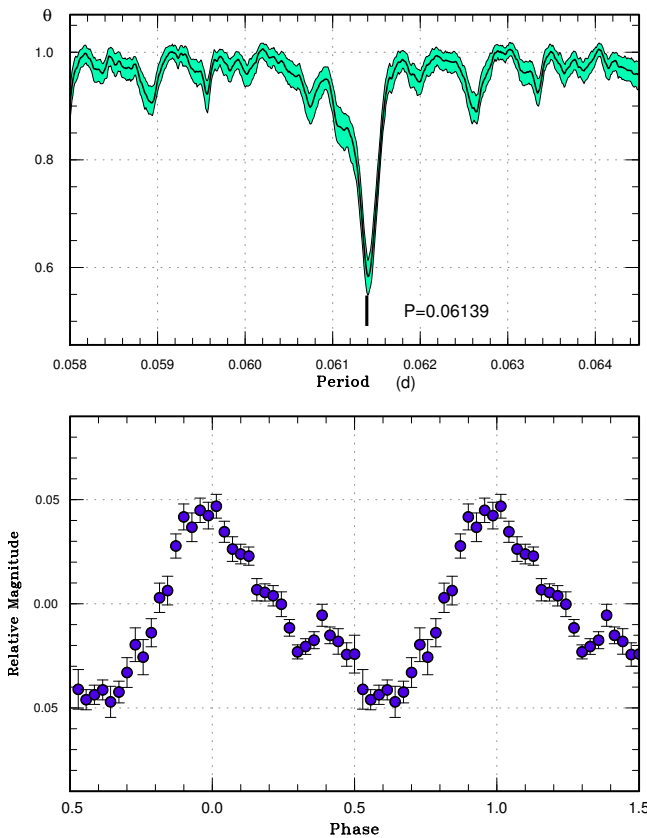


Fig. 73. Superhumps in ASASSN-16jk (2016). (Upper): PDM analysis. (Lower): Phase-averaged profile.

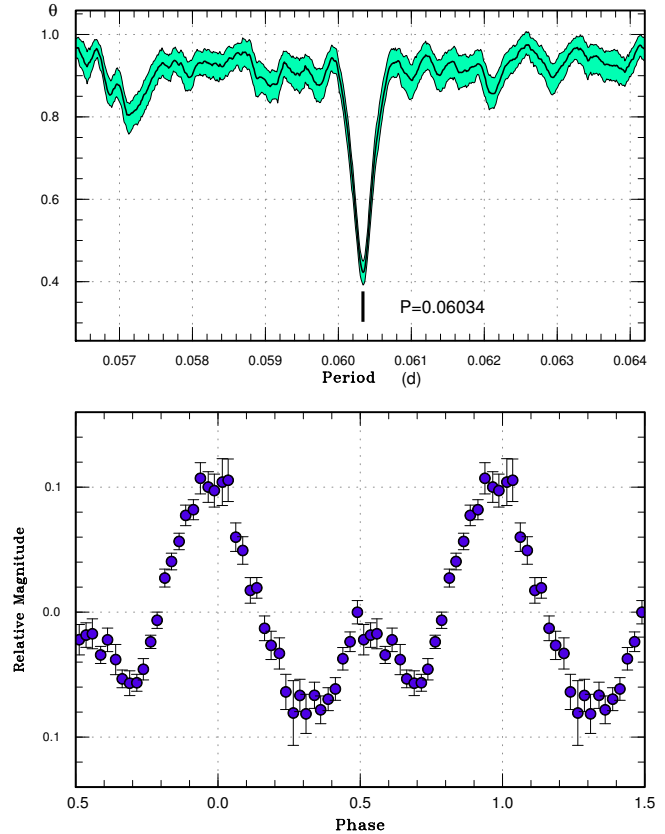


Fig. 74. Early superhumps in ASASSN-16js (2016). (Upper): PDM analysis. (Lower): Phase-averaged profile.

Table 59. Superhump maxima of ASASSN-16jk (2016)

$E$	max*	error	$O - C^\dagger$	$N^\ddagger$
0	57631.2947	0.0004	0.0002	47
1	57631.3572	0.0004	0.0012	62
16	57632.2814	0.0002	0.0045	32
17	57632.3438	0.0011	0.0054	25
32	57633.2605	0.0002	0.0011	55
33	57633.3210	0.0005	0.0001	62
48	57634.2378	0.0007	-0.0041	37
49	57634.2984	0.0004	-0.0048	56
97	57637.2444	0.0005	-0.0061	52
98	57637.3071	0.0006	-0.0048	66
113	57638.2352	0.0010	0.0022	41
114	57638.2917	0.0008	-0.0027	66
130	57639.2770	0.0011	0.0002	65
146	57640.2646	0.0008	0.0054	57
179	57642.2834	0.0016	-0.0020	13
211	57644.2496	0.0011	-0.0008	34
212	57644.3168	0.0022	0.0050	23

\*BJD-2400000.

$^\dagger$ Against max = 2457631.2946 + 0.061402E.

$^\ddagger$ Number of points used to determine the maximum.

observations. The small  $q$  value, however, appears to be consistent with the WZ Sge-type behavior, the small amplitude of ordinary superhumps and the small  $P_{\text{dot}}$  for stage B superhumps.

### 3.79 ASASSN-17bm

This object was detected as a transient at  $V=15.9$  on 2017 January 25 by the ASAS-SN team. The outburst was announced after confirmation on January 27. Subsequent observations detected superhumps (vsnet-alert 20627; figure 105). The times of superhump maxima are listed in table 79. The period in table 3 was determined by the PDM method since individual maxima were not very well determined.

### 3.80 ASASSN-17bv

This object was detected as a transient at  $V=15.0$  on 2017 January 31 by the ASAS-SN team. The outburst was announced after confirmation at  $V=14.9$  on February 1. Subsequent observations starting on February 3 detected superhumps (vsnet-alert 20634; figure 106). The times of

**Table 60.** Superhump maxima of ASASSN-16js (2016)

$E$	max*	error	$O - C^\dagger$	$N^\ddagger$	$E$	max*	error	$O - C^\dagger$	$N^\ddagger$
0	57640.7131	0.0033	-0.0166	13	67	57644.8191	0.0019	0.0017	13
1	57640.7772	0.0023	-0.0135	13	68	57644.8796	0.0014	0.0012	14
2	57640.8339	0.0015	-0.0179	13	81	57645.6749	0.0016	0.0034	13
16	57641.6950	0.0022	-0.0109	13	82	57645.7340	0.0017	0.0015	13
17	57641.7580	0.0015	-0.0089	13	83	57645.7951	0.0032	0.0016	13
18	57641.8198	0.0016	-0.0081	12	84	57645.8553	0.0013	0.0007	16
19	57641.8865	0.0047	-0.0024	13	92	57646.3434	0.0007	0.0008	140
32	57642.6874	0.0011	0.0054	14	93	57646.4027	0.0018	-0.0009	65
33	57642.7478	0.0012	0.0047	13	97	57646.6522	0.0018	0.0045	14
34	57642.8092	0.0012	0.0051	12	98	57646.7101	0.0022	0.0014	13
35	57642.8701	0.0010	0.0051	16	99	57646.7715	0.0024	0.0018	13
39	57643.1152	0.0007	0.0061	38	100	57646.8290	0.0013	-0.0018	14
40	57643.1765	0.0006	0.0064	38	101	57646.8942	0.0024	0.0024	10
41	57643.2370	0.0004	0.0059	37	113	57647.6223	0.0022	-0.0016	14
42	57643.2988	0.0007	0.0067	24	114	57647.6794	0.0028	-0.0054	18
44	57643.4201	0.0005	0.0060	140	115	57647.7406	0.0017	-0.0053	17
45	57643.4815	0.0004	0.0063	139	116	57647.8035	0.0028	-0.0033	14
46	57643.5439	0.0004	0.0078	132	117	57647.8668	0.0047	-0.0011	16
48	57643.6665	0.0012	0.0083	14	120	57648.0456	0.0008	-0.0054	38
49	57643.7251	0.0008	0.0059	13	121	57648.1078	0.0010	-0.0041	38
50	57643.7851	0.0012	0.0048	13	122	57648.1671	0.0009	-0.0059	38
51	57643.8457	0.0013	0.0045	15	123	57648.2278	0.0011	-0.0062	30
55	57644.0893	0.0007	0.0040	26	130	57648.6533	0.0027	-0.0078	19
56	57644.1499	0.0005	0.0036	33	131	57648.7183	0.0044	-0.0037	17
57	57644.2111	0.0005	0.0038	37	133	57648.8389	0.0032	-0.0051	15
58	57644.2718	0.0004	0.0035	37	149	57649.8181	0.0024	-0.0021	13
64	57644.6350	0.0012	0.0007	12	172	57651.2298	0.0035	0.0063	38
65	57644.6988	0.0017	0.0035	13	173	57651.2832	0.0054	-0.0012	15
66	57644.7600	0.0014	0.0036	13	-	-	-	-	-

\*BJD-2400000.

 $^\dagger$ Against max = 2457640.7297 + 0.061010E. $^\ddagger$ Number of points used to determine the maximum.

superhump maxima are listed in table 80. The  $O - C$  values suggest that the maxima for  $E \leq 1$  were stage A superhumps, although the amplitudes were already large. The period of stage C superhumps in table 3 is rather uncertain due to the large scatter in the final part of observations. The object faded to 19 mag on February 13.

### 3.81 ASASSN-17ce

This object was detected as a transient at  $V=14.6$  on 2017 February 13 by the ASAS-SN team. Subsequent observations detected superhumps (vsnet-alert 20668, 20676; figure 107). The times of superhump maxima are listed in table 81. The maxima for  $E \leq 6$  likely correspond to a short stage B usually seen in long- $P_{\text{orb}}$  systems (Kato et al. 2009).

The object faded close to 18 mag on February 26.

### 3.82 ASASSN-17ck

This object was detected as a transient at  $V=16.6$  on 2017 February 15 by the ASAS-SN team. The object was already in outburst at  $V=16.5$  on February 13. Single-night observations on February 17 detected superhumps (vsnet-alert 20680, figure 108). The times of maxima were BJD 2457801.5269(7) ( $N=25$ ) and 2457801.6099(17) ( $N=21$ ). The superhump period by the PDM analysis was 0.083(1) d.

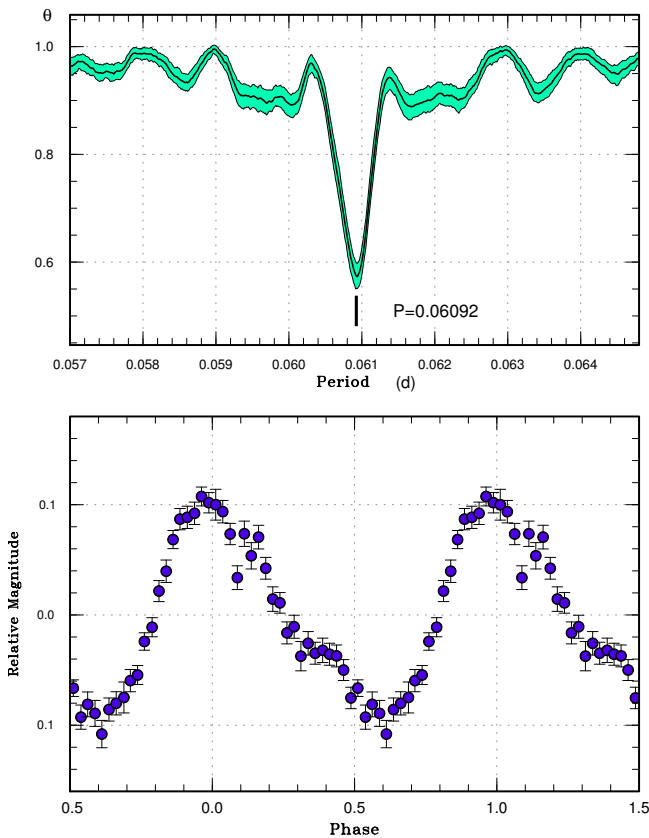


Fig. 75. Ordinary superhumps in ASASSN-16js (2016). (Upper): PDM analysis. (Lower): Phase-averaged profile.

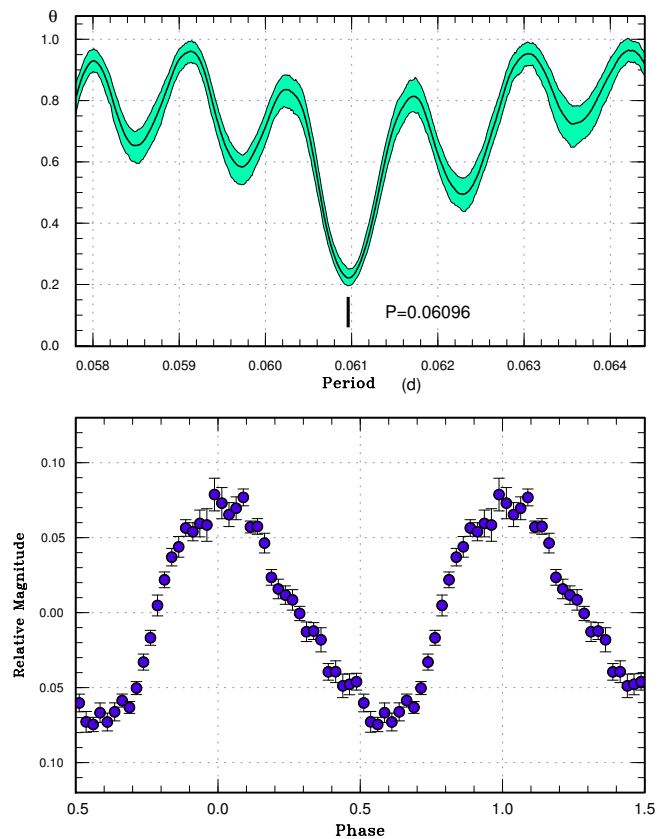


Fig. 76. Ordinary superhumps in ASASSN-16jz (2016). (Upper): PDM analysis. (Lower): Phase-averaged profile.

Table 61. Superhump maxima of ASASSN-16jz (2016)

$E$	max*	error	$O - C^\dagger$	$N^\ddagger$
0	57638.3632	0.0004	0.0001	59
1	57638.4232	0.0004	-0.0008	61
2	57638.4856	0.0005	0.0006	62
3	57638.5458	0.0004	-0.0001	62
4	57638.6062	0.0004	-0.0007	62
16	57639.3390	0.0004	0.0010	60
49	57641.3501	0.0008	0.0012	62
50	57641.4098	0.0012	-0.0001	61
51	57641.4695	0.0011	-0.0013	42

\*BJD-2400000.

$^\dagger$ Against max = 2457638.3631 + 0.060936E.

$^\ddagger$ Number of points used to determine the maximum.

Table 62. Superhump maxima of ASASSN-16kg (2016)

$E$	max*	error	$O - C^\dagger$	$N^\ddagger$
0	57643.3970	0.0026	-0.0050	94
1	57643.5076	0.0004	0.0053	224
29	57646.3094	0.0022	-0.0020	153
30	57646.4135	0.0038	0.0018	108

\*BJD-2400000.

$^\dagger$ Against max = 2457643.4020 + 0.100324E.

$^\ddagger$ Number of points used to determine the maximum.

**Table 63.** Superhump maxima of ASASSN-16kx (2016)

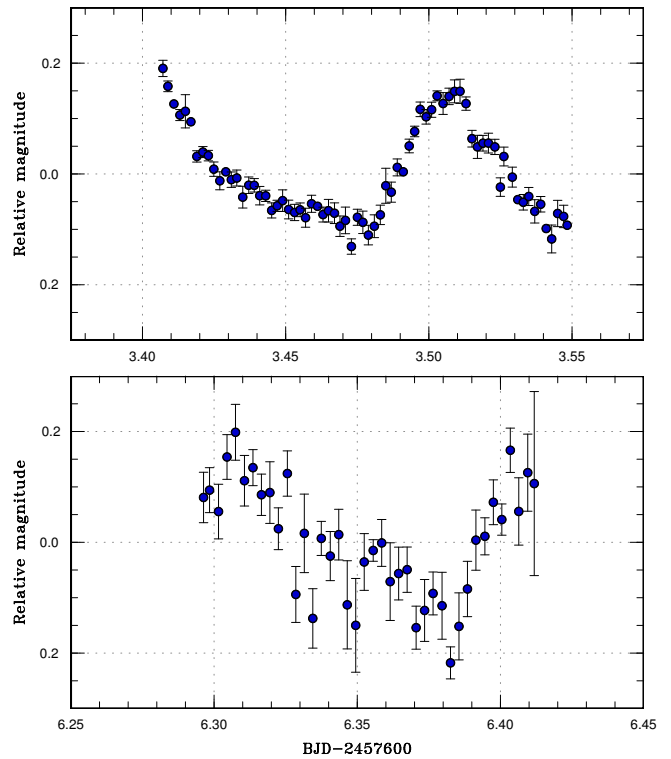
$E$	max*	error	$O - C^\dagger$	$N^\ddagger$
0	57662.4690	0.0074	0.0003	64
1	57662.5451	0.0006	-0.0043	185
2	57662.6234	0.0021	-0.0066	104
4	57662.7892	0.0011	-0.0021	20
5	57662.8715	0.0019	-0.0005	17
17	57663.8416	0.0007	0.0020	27
29	57664.8090	0.0009	0.0017	27
30	57664.8904	0.0035	0.0025	11
41	57665.7775	0.0038	0.0025	19
42	57665.8563	0.0025	0.0007	23
54	57666.8270	0.0011	0.0037	27
79	57668.8412	0.0016	0.0020	18
91	57669.8137	0.0020	0.0067	26
103	57670.7746	0.0019	0.0000	16
104	57670.8574	0.0027	0.0022	13
116	57671.8205	0.0023	-0.0024	24
128	57672.7909	0.0029	0.0003	24
129	57672.8663	0.0040	-0.0049	15
141	57673.8394	0.0028	0.0005	23
153	57674.8022	0.0045	-0.0043	24

\*BJD-2400000.

 $^\dagger$ Against max = 2457662.4687 + 0.080639E. $^\ddagger$ Number of points used to determine the maximum.**Table 64.** Superhump maxima of ASASSN-16lo (2016)

$E$	max*	error	$O - C^\dagger$	$N^\ddagger$
0	57681.3009	0.0007	-0.0064	57
1	57681.3580	0.0009	-0.0041	56
2	57681.4156	0.0021	-0.0014	27
38	57683.3986	0.0005	0.0066	57
39	57683.4529	0.0004	0.0060	54
54	57684.2738	0.0005	0.0040	45
55	57684.3278	0.0005	0.0032	59
56	57684.3832	0.0006	0.0037	58
57	57684.4378	0.0005	0.0034	56
84	57685.9076	0.0041	-0.0080	10
85	57685.9654	0.0007	-0.0051	140
86	57686.0235	0.0020	-0.0019	72

\*BJD-2400000.

 $^\dagger$ Against max = 2457681.3073 + 0.054861E. $^\ddagger$ Number of points used to determine the maximum.**Fig. 77.** Superhumps in ASASSN-16kx (2016). The data were binned to 0.003 d.**Table 65.** Superhump maxima of ASASSN-16mo (2016)

$E$	max*	error	$O - C^\dagger$	$N^\ddagger$
0	57692.5886	0.0005	0.0042	57
13	57693.4488	0.0004	0.0001	60
17	57693.7134	0.0007	-0.0012	46
23	57694.1115	0.0003	-0.0021	147
24	57694.1804	0.0004	0.0004	146
39	57695.1761	0.0004	-0.0013	113
40	57695.2417	0.0005	-0.0022	120
67	57697.0402	0.0004	0.0012	73
68	57697.1059	0.0004	0.0003	73
69	57697.1740	0.0004	0.0020	74
81	57697.9692	0.0007	-0.0007	74
82	57698.0352	0.0004	-0.0011	74
83	57698.1027	0.0005	-0.0002	74
84	57698.1683	0.0006	-0.0011	50
99	57699.1652	0.0030	-0.0015	50
112	57700.0344	0.0048	0.0033	50

\*BJD-2400000.

 $^\dagger$ Against max = 2457692.5844 + 0.066488E. $^\ddagger$ Number of points used to determine the maximum.

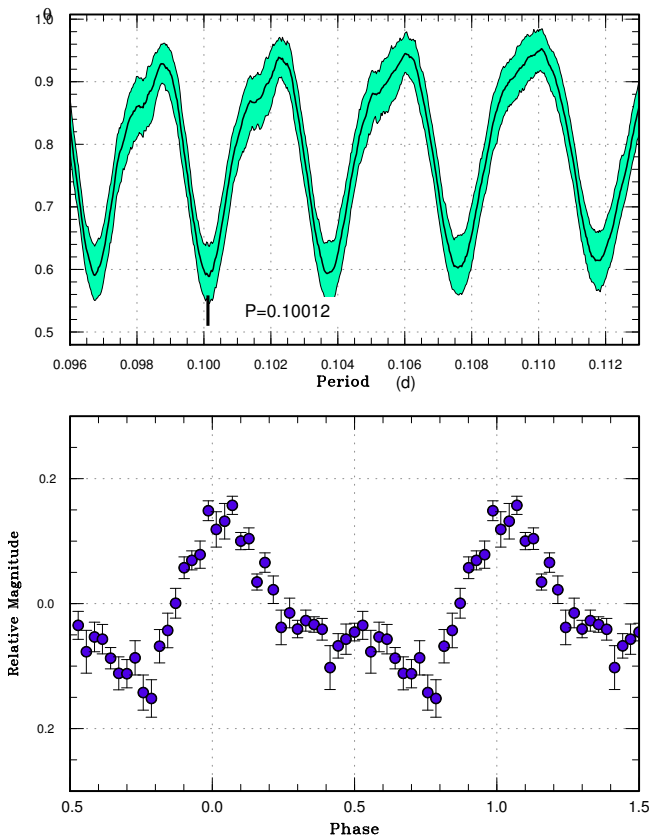


Fig. 78. PDM analysis of superhumps in ASASSN-16kg (2016). (Upper): PDM analysis. The alias selection was one of the possibilities. (Lower): Phase-averaged profile.

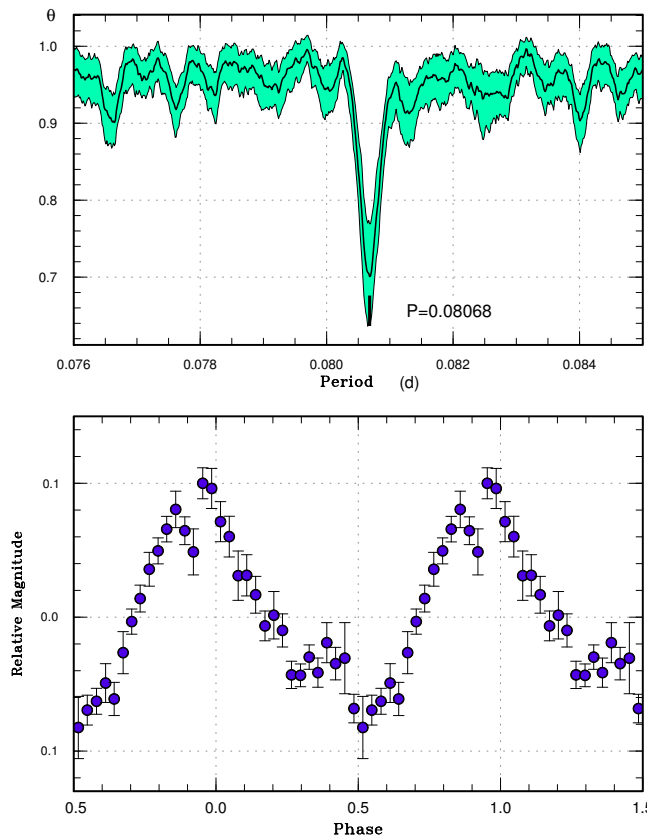


Fig. 79. Superhumps in ASASSN-16kx (2016). (Upper): PDM analysis. (Lower): Phase-averaged profile.

### 3.83 ASASSN-17cn

This object was detected as a transient at  $V=13.7$  on 2017 February 13 by the ASAS-SN team. The outburst announcement was made after an observation of  $V=13.2$  on February 16. The object showed low-amplitude double-wave early superhumps (figure 109) and then ordinary superhumps (vsnet-alert 20750, 20755; figure 110). The behavior was typical for a WZ Sge-type dwarf nova. There was a 7 d gap in the observations, which hindered the detection of stage A superhumps. The times of superhump maxima are listed in table 82. Although the maxima after  $E=137$  were stage C superhumps, we could not determine the period due to the limited quality of the data. The period of early superhumps by the PDM method was 0.05303(2) d. The object was also detected by Gaia (Gaia17arq)<sup>18</sup> at a magnitude of 16.07 on March 14. This detection was made during the superoutburst plateau.

The long waiting time to develop ordinary superhumps ( $\geq 9$  d counted from the outburst peak,  $\geq 12$  d from

Table 66. Superhump maxima of ASASSN-16my (2016)

$E$	max*	error	$O - C^\dagger$	$N^\ddagger$
0	57700.7424	0.0006	-0.0065	17
1	57700.8318	0.0005	-0.0049	17
12	57701.8010	0.0009	-0.0013	19
23	57702.7675	0.0012	-0.0004	24
24	57702.8628	0.0016	0.0071	8
34	57703.7418	0.0029	0.0083	23
35	57703.8262	0.0013	0.0049	20
46	57704.7908	0.0029	0.0039	19
52	57705.3052	0.0025	-0.0084	44
57	57705.7561	0.0019	0.0035	25
58	57705.8428	0.0029	0.0025	14
68	57706.7180	0.0042	-0.0002	18
69	57706.8033	0.0024	-0.0027	23
80	57707.7724	0.0027	0.0009	27
81	57707.8540	0.0061	-0.0054	12
91	57708.7356	0.0029	-0.0015	28
92	57708.8251	0.0032	0.0002	21

\*BJD-2400000.

<sup>†</sup>Against max = 2457700.7489 + 0.087783E.

<sup>‡</sup>Number of points used to determine the maximum.

<sup>18</sup><<http://gsaweb.ast.cam.ac.uk/alerts/alert/Gaia17arq/>>.

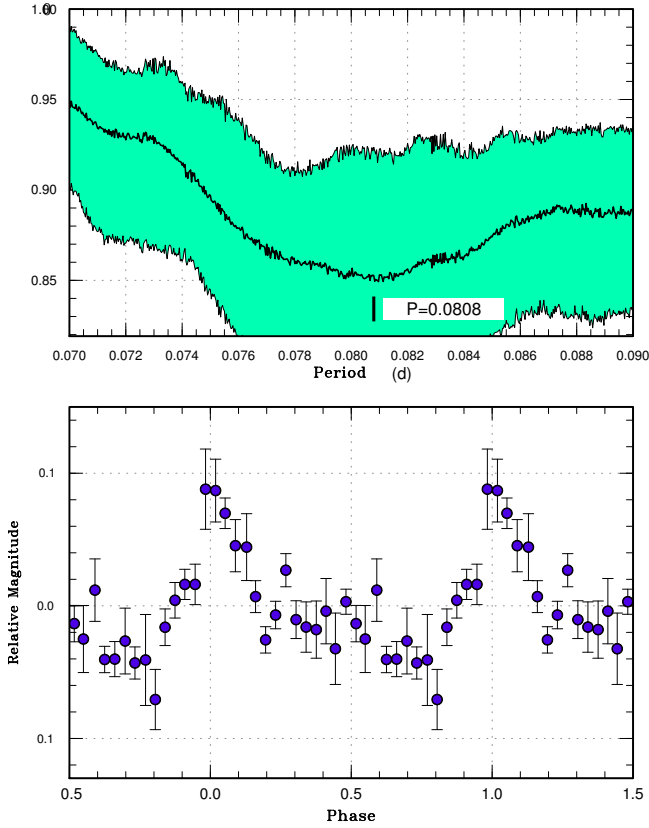


**Fig. 80.** Superhumps in ASASSN-16le (2016). (Upper): PDM analysis. (Lower): Phase-averaged profile.

**Table 67.** Superhump maxima of ASASSN-16ni (2016)

$E$	max*	error	$O - C^\dagger$	$N^\ddagger$
0	57717.0368	0.0025	-0.0037	257
1	57717.1598	0.0026	0.0040	256
2	57717.2712	0.0026	0.0001	256
11	57718.3078	0.0040	-0.0004	337

\*BJD-2400000.

$^\dagger$ Against max = 2457717.0406 + 0.115242E.

$^\ddagger$ Number of points used to determine the maximum.

**Table 68.** Superhump maxima of ASASSN-16nq (2016)

$E$	max*	error	$O - C^\dagger$	$N^\ddagger$
0	57721.2429	0.0005	-0.0061	74
1	57721.3229	0.0002	-0.0053	128
2	57721.4021	0.0002	-0.0054	147
8	57721.8784	0.0006	-0.0044	47
9	57721.9563	0.0005	-0.0058	81
10	57722.0339	0.0011	-0.0074	82
12	57722.1983	0.0045	-0.0014	27
13	57722.2757	0.0005	-0.0032	164
14	57722.3563	0.0004	-0.0018	252
15	57722.4361	0.0005	-0.0013	154
16	57722.5188	0.0025	0.0022	22
27	57723.3906	0.0002	0.0025	87
28	57723.4702	0.0003	0.0029	88
39	57724.3445	0.0004	0.0057	81
59	57725.9337	0.0007	0.0104	83
60	57726.0107	0.0010	0.0082	82
61	57726.0900	0.0019	0.0083	53
65	57726.4091	0.0003	0.0105	87
66	57726.4879	0.0007	0.0101	45
77	57727.3555	0.0039	0.0062	28
78	57727.4377	0.0006	0.0092	86
111	57730.0398	0.0015	-0.0031	77
122	57730.9117	0.0012	-0.0028	80
123	57730.9881	0.0016	-0.0055	79
135	57731.9451	0.0038	0.0008	78
136	57732.0277	0.0056	0.0042	149
137	57732.0859	0.0018	-0.0169	75
147	57732.8879	0.0013	-0.0072	76
148	57732.9830	0.0042	0.0087	158
149	57733.0476	0.0018	-0.0059	56
153	57733.3638	0.0006	-0.0066	64
160	57733.9249	0.0023	-0.0001	82
161	57733.9942	0.0009	-0.0100	81
198	57736.9455	0.0045	0.0100	52

\*BJD-2400000.

$^\dagger$ Against max = 2457721.2490 + 0.079225E.

$^\ddagger$ Number of points used to determine the maximum.



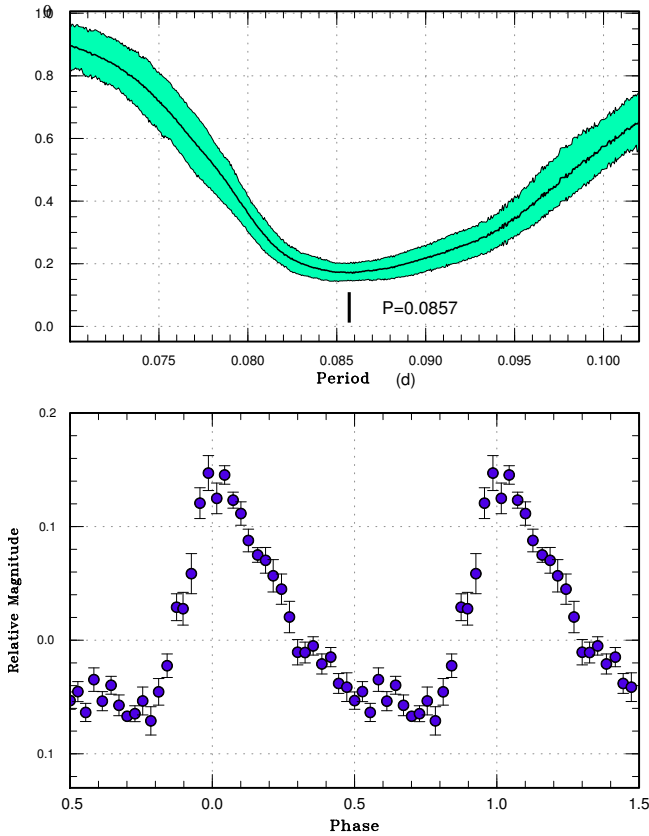


Fig. 81. Superhumps in ASASSN-16lj (2016). (Upper): PDM analysis. (Lower): Phase-averaged profile.

Table 69. Superhump maxima of ASASSN-16nr (2016)

$E$	max*	error	$O - C^\dagger$	$N^\ddagger$
0	57720.6594	0.0047	-0.0044	10
1	57720.7443	0.0010	-0.0022	22
2	57720.8298	0.0026	0.0006	16
12	57721.6464	0.0072	-0.0098	8
13	57721.7419	0.0020	0.0030	21
14	57721.8241	0.0020	0.0024	18
21	57722.4024	0.0005	0.0018	161
22	57722.4874	0.0007	0.0040	165
23	57722.5674	0.0005	0.0013	182
32	57723.3206	0.0078	0.0102	56
33	57723.3915	0.0008	-0.0016	190
34	57723.4754	0.0007	-0.0005	155
49	57724.7288	0.0131	0.0123	29
50	57724.7952	0.0024	-0.0040	30
58	57725.4552	0.0005	-0.0056	163
59	57725.5361	0.0006	-0.0074	189

\*BJD-2400000.

$^\dagger$ Against max = 2457720.6638 + 0.082709E.

$^\ddagger$ Number of points used to determine the maximum.

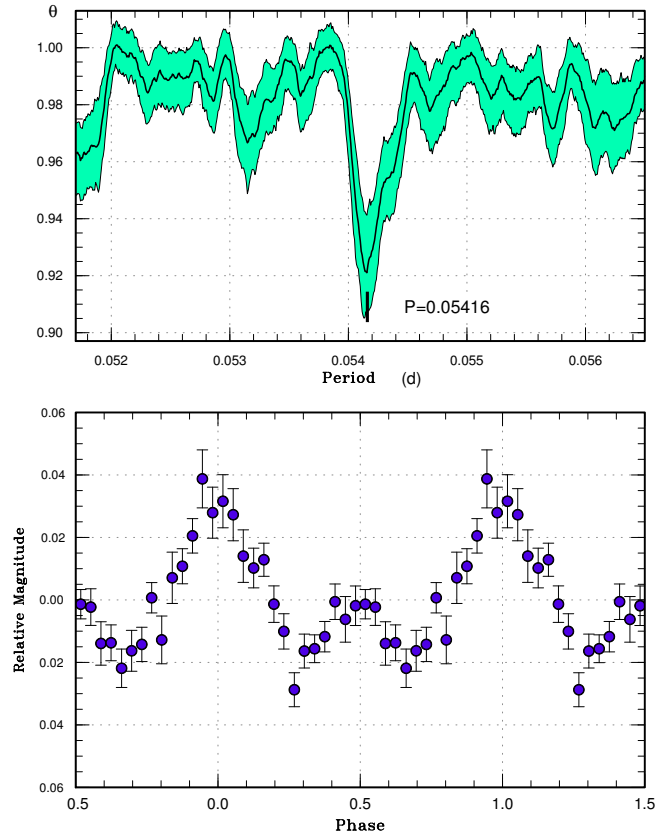


Fig. 82. Early superhumps in ASASSN-16lo (2016). (Upper): PDM analysis. The data before BJD 2457678 were used. (Lower): Phase-averaged profile.

Table 70. Superhump maxima of ASASSN-16nw (2016)

$E$	max*	error	$O - C^\dagger$	$N^\ddagger$
0	57724.3969	0.0011	-0.0028	72
1	57724.4743	0.0015	0.0018	79
2	57724.5471	0.0012	0.0018	80
3	57724.6175	0.0032	-0.0007	35
39	57727.2412	0.0067	0.0018	80
40	57727.3116	0.0023	-0.0006	78
41	57727.3802	0.0060	-0.0048	74
42	57727.4585	0.0029	0.0007	73
43	57727.5334	0.0036	0.0027	36

\*BJD-2400000.

$^\dagger$ Against max = 2457724.3997 + 0.072813E.

$^\ddagger$ Number of points used to determine the maximum.

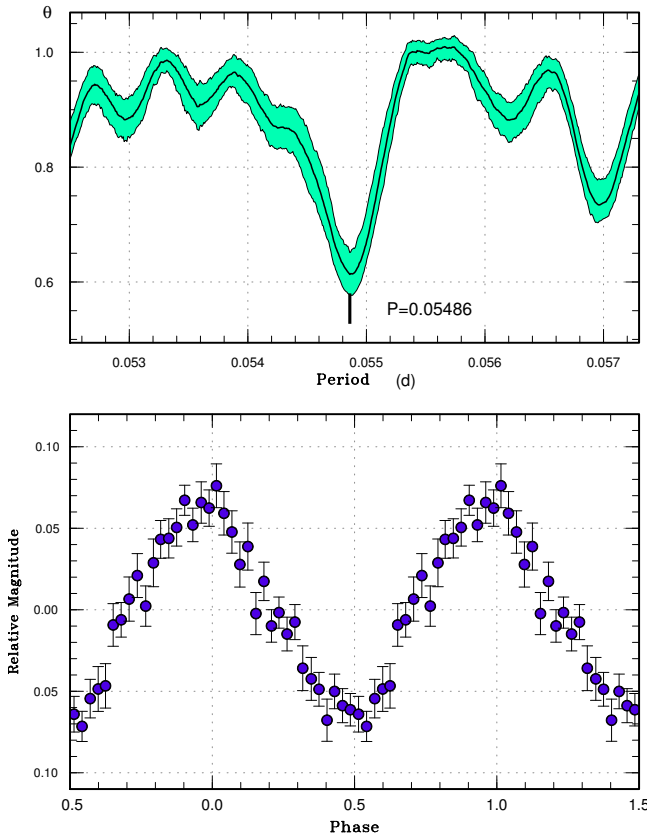


**Fig. 83.** Ordinary superhumps in ASASSN-16lo (2016). (Upper): PDM analysis. The interval of BJD 2457681–2457686 was used. (Lower): Phase-averaged profile.

the outburst detection) and the large outburst amplitude ( $\gtrsim 9$  mag) suggest that the object is a rather extreme WZ Sge-type dwarf nova.

### 3.84 ASASSN-17cx

This object was detected as a transient at  $V=16.4$  on 2017 February 21 by the ASAS-SN team. The object was already in outburst at  $V=16.6$  on February 18 and the outburst was announced after an observation at  $V=16.7$  on February 23. Single-night observations on February 24 detected superhumps. The maxima were BJD 2457809.0621(9) ( $N=52$ ), 2457809.1406(6) ( $N=48$ ) and 2457809.2151(14) ( $N=50$ ). The superhump period by the PDM method was 0.0761(7) d.

### 3.85 ASASSN-17dg

This object was detected as a transient at  $V=13.8$  on 2017 March 7 by the ASAS-SN team. The object was already in outburst at  $V=13.8$  on March 6. The last negative observation was on February 23. There is an ROSAT X-ray

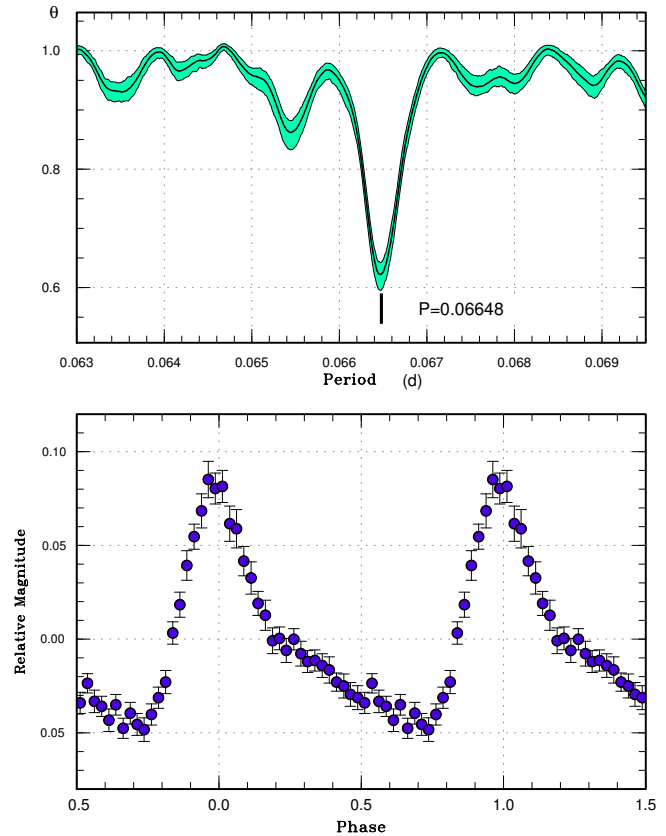


**Fig. 84.** Superhumps in ASASSN-16mo (2016). (Upper): PDM analysis. (Lower): Phase-averaged profile.

counterpart 1RXS J160232.8–603240. There was also an outburst with a maximum of  $V=13.03$  on 2002 September 25, which lasted at least for 6 d in the ASAS-3 data. The actual maximum may have been even brighter since ASAS-3 did not observe this field for 6 d before this detection. The object has a bright ( $J=13.68$ ) and blue ( $J - K = +0.10$ ) 2MASS counterpart, indicating that the object was in outburst during 2MASS scans.

Observations started on March 9 and superhumps were immediately detected (vsnet-alert 20760; figure 112). The object started fading rapidly already on March 11. It was most likely the true maximum was missed by ASAS-SN observations for more than  $\sim 5$  d. The times of superhump maxima are listed in table 83. These superhumps were most likely stage C ones since observations were performed in the final phase of the superoutburst. The low amplitudes of superhumps (vsnet-alert 20760) suggested that superhumps were already decaying.

There was one post-superoutburst rebrightening on March 19 ( $V=14.3$ , vsnet-alert 20809). A PDM analysis of the post-superoutburst data (BJD 2457825.7–2457842.9) yielded a period of 0.06655(5) d, which is likely a contin-

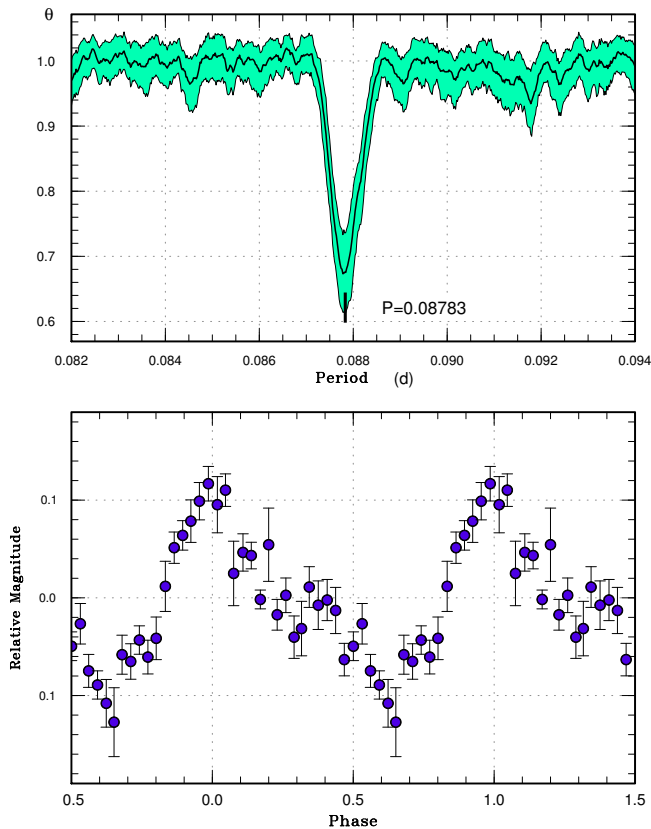


**Fig. 85.** Superhumps in ASASSN-16my (2016). (Upper): PDM analysis. (Lower): Phase-averaged profile.

uation of stage C superhumps.

### 3.86 ASASSN-17dq

This object was detected as a transient at  $V=15.4$  on 2017 March 11 by the ASAS-SN team. The outburst was announced after the observation at  $V=15.2$  on March 14. Observations starting on March 15 recorded superhumps (vsnet-alert 20791, 20810; figure 113). The times of superhump maxima are listed in table 84. The object started fading rapidly on March 24.

### 3.87 CRTS J000130.5+050624

This object (=CSS101127:000130+050624, hereafter CRTS J000130) was detected by the CRTS team at an unfiltered CCD magnitude of 15.68 on 2010 November 27.

The 2016 outburst was detected by the ASAS-SN team at  $V=16.73$  on September 3 while the object was still rising. The detection announcement was made when it reached  $V=15.47$  on September 9. The past outbursts in the ASAS-SN data suggested an SU UMa-type dwarf nova. Subsequent observations detected superhumps

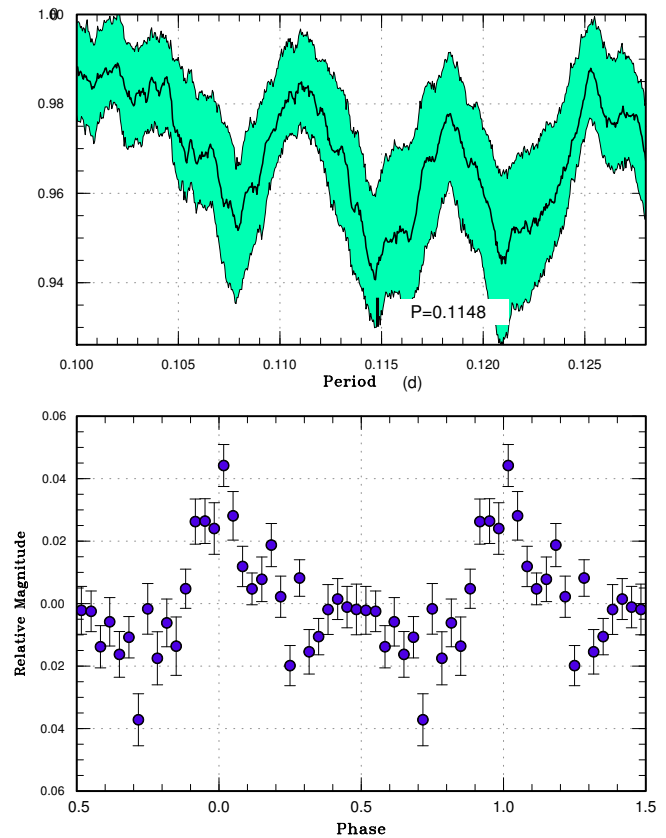


**Fig. 86.** Superhumps in ASASSN-16ni (2016). (Upper): PDM analysis. (Lower): Phase-averaged profile.

(vsnet-alert 20152, 20176). The times of superhump maxima are listed in table 85. The data were insufficient to give a solid value of  $P_{\text{dot}}$ . The superhump period of 0.09477(1) d (by the PDM method) places the object in the period gap.

### 3.88 CRTS J015321.5+340857

This object (=CSS081026:015321+340857, hereafter CRTS J015321) was discovered by the CRTS team on 2008 October 26. The SU UMa-type nature was established during the 2012 superoutburst (see Kato et al. 2014b for more history). The 2016 superoutburst was detected by the ASAS-SN team at  $V=15.95$  on November 16. One superhump maximum at BJD 2457710.3850(10) ( $N=72$ ) was observed.

### 3.89 CRTS J023638.0+111157

This object (=CSS091106:023638+111157, hereafter CRTS J023638) was detected by the CRTS team at an unfiltered CCD magnitude of 16.23 on 2009 November 6. Seven outbursts were detected in the CRTS data and there was a

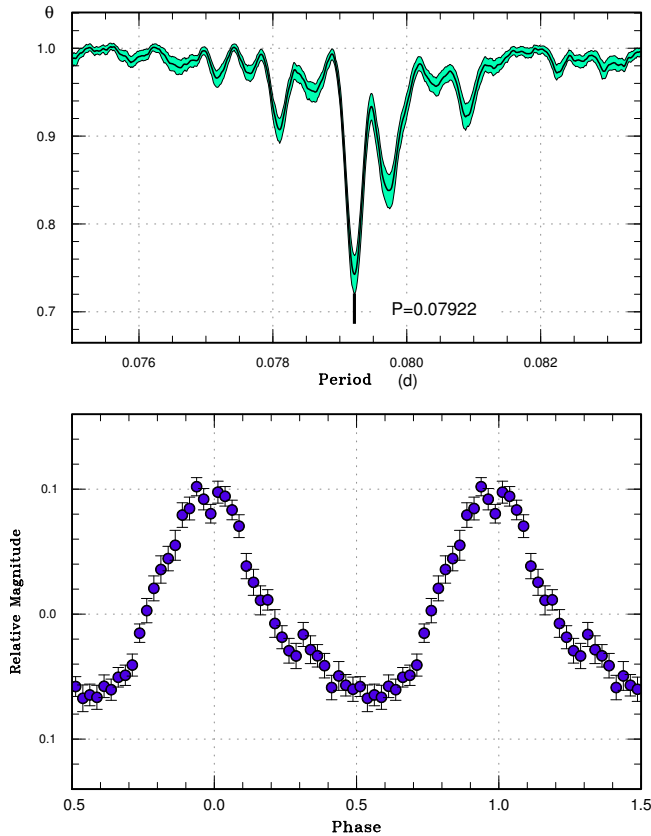


**Fig. 87.** Superhumps in ASASSN-16nq (2016). (Upper): PDM analysis. (Lower): Phase-averaged profile.

brighter ( $V=15.17$ ) outburst in 2013 (vsnet-alert 16477).

The 2016 outburst was detected by the ASAS-SN team at  $V=14.90$  on August 29. Subsequent observations detected superhumps (vsnet-alert 20118, 20128, 20153; figure 115). The times of superhump maxima are listed in table 86. The maxima for  $E \geq 137$  were post-superoutburst ones. There was most likely a phase jump between  $E=80$  and  $E=137$  and the humps for  $E \geq 137$  were likely traditional late superhumps. The transition between stages B and C was rather smooth as in other relatively long  $P_{SH}$  systems.

### 3.90 CRTS J033349.8–282244

This object (=SSS110224:033350–282244, hereafter CRTS J033349) was discovered by the CRTS team at an unfiltered CCD magnitude of 15.06 on 2011 February 24. The bright outburst in 2016 November was detected by the ASAS-SN team at  $V=14.46$  on November 19. Subsequent observations detected superhumps (vsnet-alert 20400, 20403; figure 116). The times of superhump maxima are listed in table 87. The observations were performed during the later course of the superoutburst and the period

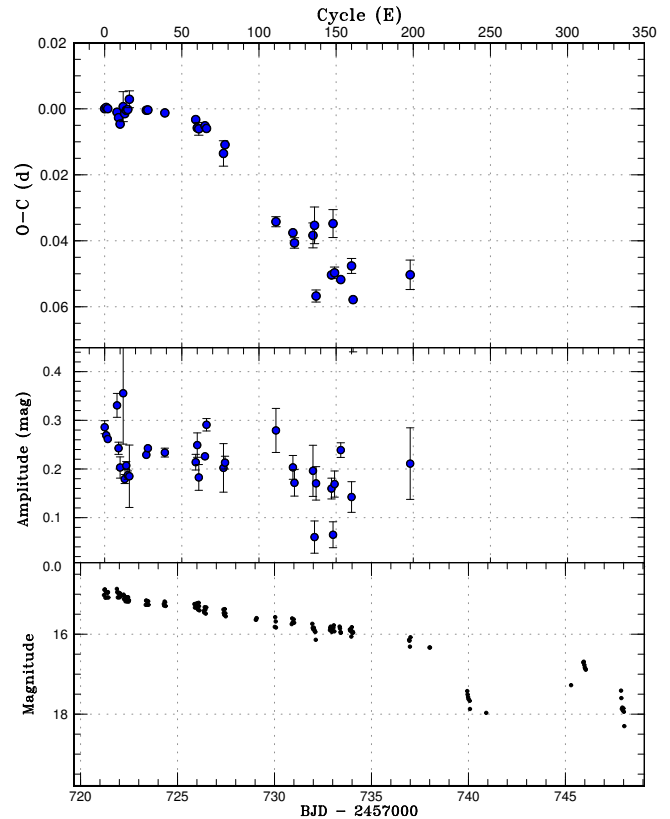


**Fig. 88.**  $O - C$  diagram of superhumps in ASASSN-16nq (2016). (Upper):  $O - C$  diagram. We used a period of 0.05796 d for calculating the  $O - C$  residuals. (Middle): Amplitudes of superhumps. (Lower): Light curve. The data were binned to 0.026 d.

probably refers to stage C one.

We listed well-defined superoutbursts in the ASAS-SN data since 2014 in table 88. These superoutbursts can be well expressed by a supercycle of 108(1) d with maximum  $|O - C|$  values of 10 d. There have been typically two normal outbursts between superoutbursts. These features closely resemble those of V503 Cyg (Harvey et al. 1995) (vsnet-alert 20386). V503 Cyg, however, sometimes showed frequent normal outbursts (e.g. Kato et al. 2002b) and these alternations between phases of different number of normal outbursts have been considered to be a result of a disk tilt, which is considered to suppress normal outbursts (see the subsection of 1RXS J161659, subsection 3.27). Detection of negative superhumps is expected in CRTS J033349.

### 3.91 CRTS J044636.9+083033

This object (=CSS130201:044637+083033, hereafter CRTS J044637) was detected by the CRTS team at an unfiltered CCD magnitude of 17.70 on 2013 February 1. There was a bright outburst at  $V=15.12$  on 2017 January 12 de-

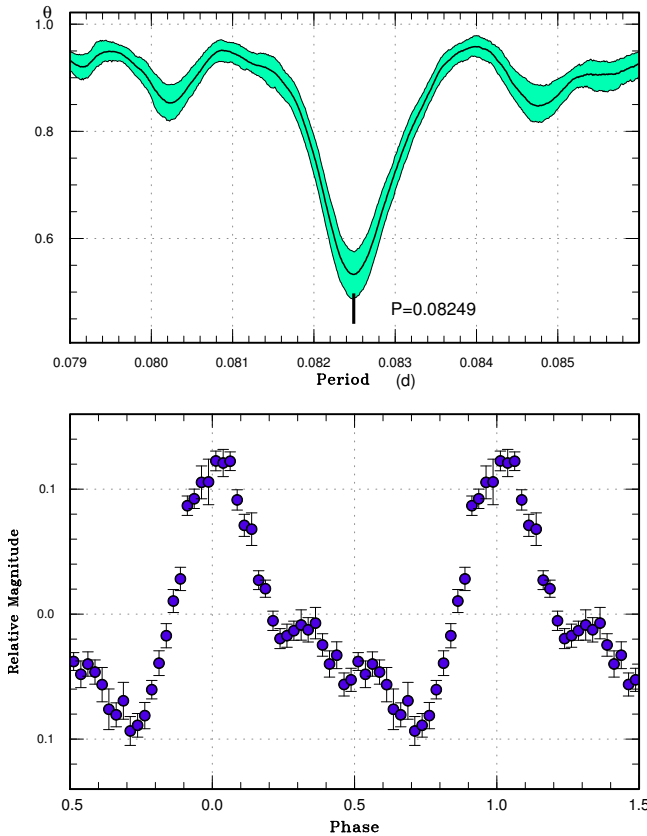


**Fig. 89.** Superhumps in ASASSN-16nr (2016). (Upper): PDM analysis. (Lower): Phase-averaged profile.

tected by the ASAS-SN team. Subsequent observations detected two superhumps on a single night (vsnet-alert 20580). The maxima were BJD 2457768.9773(11) ( $N=97$ ) and 2457769.0716(14) ( $N=98$ ). A PDM analysis yielded a period of 0.093(1) d. Although there were single-night observations 4 d later, the observing condition was not sufficient to detect superhumps.

### 3.92 CRTS J082603.7+113821

This object (=CSS110124:082604+113821, hereafter CRTS J082603) was detected by the CRTS team at an unfiltered CCD magnitude of 15.95 on 2011 January 24 (Drake et al. 2014).

The 2017 outburst was detected by the ASAS-SN team at  $V=14.9$  on January 3. The observation on January 5 detected superhumps (vsnet-alert 20542). The best period with the PDM method was 0.0719(4) d. Two superhump maxima were measured: BJD 2457759.4542(5) ( $N=72$ ) and 2457759.5245(5) ( $N=68$ ).

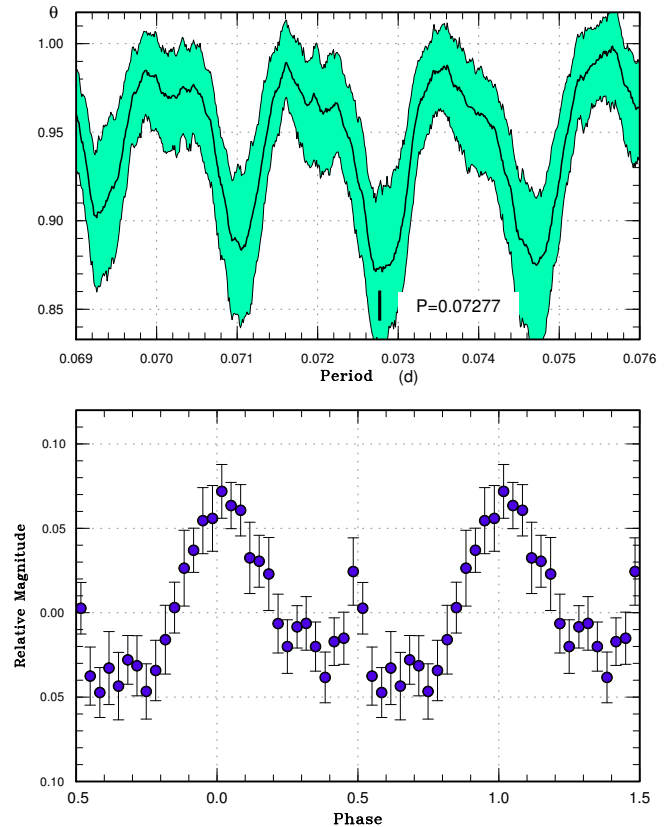


**Fig. 90.** Superhumps in ASASSN-16nw (2016). (Upper): PDM analysis. (Lower): Phase-averaged profile.

### 3.93 CRTS J085113.4+344449

This object (=CSS080401:085113+344449, hereafter CRTS J085113) was detected by the CRTS team at an unfiltered CCD magnitude of 16.4 on 2008 April 1 (Drake et al. 2008). The past data suggested that there was a bright ( $I=14$ ) outburst in the past (vsnet-alert 10009). There was a bright outburst at unfiltered CCD magnitudes of 14.14–14.73 on 2008 November 20, detected by the CRTS team (cf. vsnet-alert 10717). The outburst was suspected to be a superoutburst. Subsequent observations detected a superhump with a period of  $\sim 0.08$  d (vsnet-alert 10723; figure 119). There have been eight outbursts (up to 2016) in the CRTS database. The SDSS colors in quiescence suggested an orbital period of 0.08–0.12 d (Kato et al. 2012b).

The 2016 superoutburst was detected by the ASAS-SN team at  $V=13.85$  on November 1. Subsequent observations detected superhumps (vsnet-alert 20315; figure 120). The times of superhump maxima were BJD 2457697.2246(2) ( $N=181$ ) and 2457697.3114(3) ( $N=176$ ). The best superhump period by the PDM method was 0.08750(9) d.

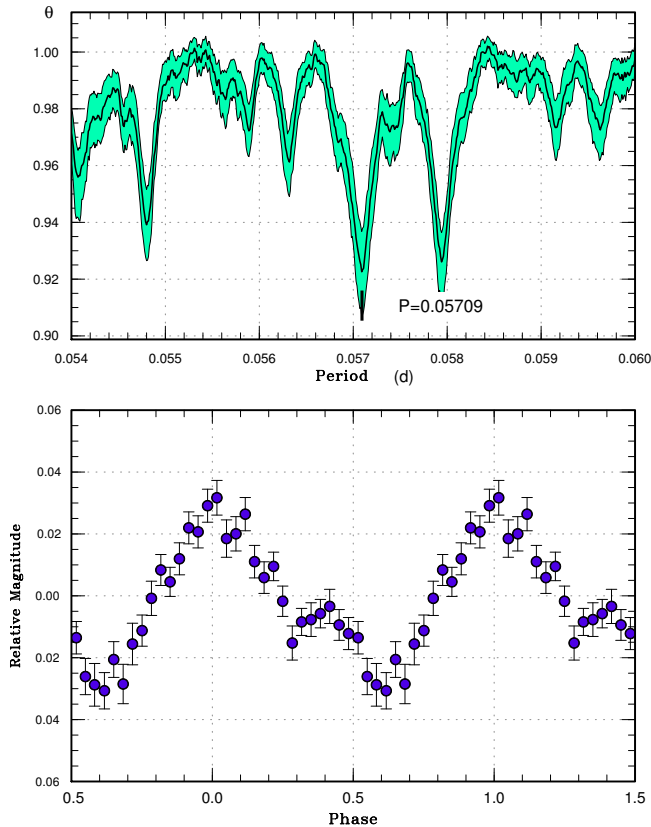


**Fig. 91.** Ordinary superhumps in ASASSN-16ob (2016). The segment of BJD 2457734–2457749 was used. (Upper): PDM analysis. (Lower): Phase-averaged profile.

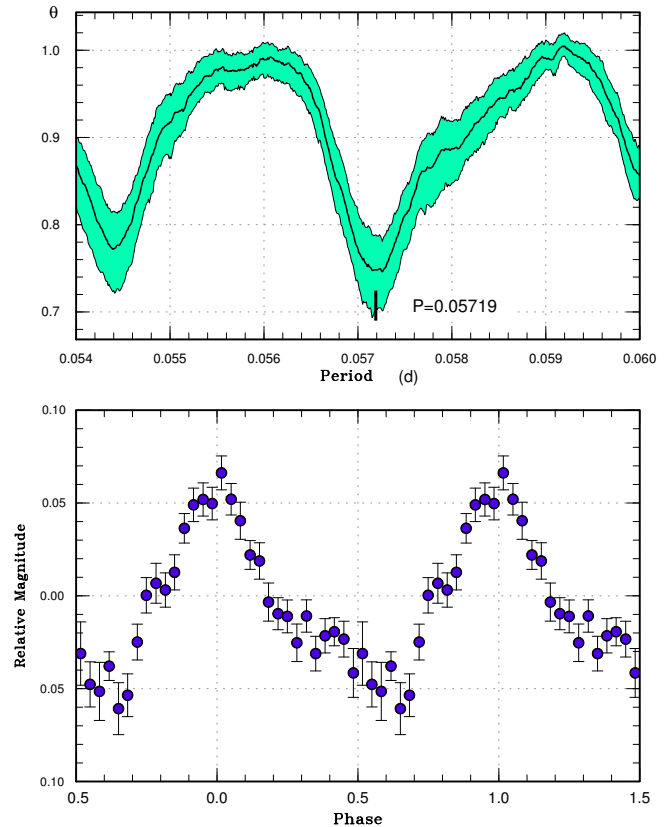


**Fig. 92.** Ordinary superhumps in ASASSN-16ob (2016). The best-observed segment of BJD 2457736–2457740 was used. (Upper): PDM analysis. (Lower): Phase-averaged profile.

### 3.94 CRTS J085603.8+322109

This object (=CSS100508:085604+322109, hereafter CRTS J085603) was detected by the CRTS team at an unfiltered CCD magnitude of 16.20 on 2010 May 8. There is a  $g=19.6$ -mag SDSS counterpart and its colors yielded an expected orbital period of 0.067(1) d (Kato et al. 2012b).

The 2016 outburst was detected by the ASAS-SN team at  $V=16.62$  on November 26. Subsequent observations detected superhumps (vsnet-alert 20428; figure 121). The times of superhump maxima are listed in table 89.

The ASAS-SN data indicate that past outbursts occurred rather regularly. We listed outburst maxima (they are likely superoutburst as judged from the brightness) in table 90. These maxima can be expressed by a super-cycle of 232(10) d, with the maximum  $|O - C|$  of 33 d. It was likely that the peak of the 2016 superoutburst was not covered by ASAS-SN observations.

### 3.95 CRTS J164950.4+035835

This object (=CSS100707:164950+035835, hereafter CRTS J164950) was detected by the CRTS team at an unfiltered

CCD magnitude of 14.1 on 2010 July 7. There were seven outbursts recorded in the CRTS data.

The 2015 superoutburst was detected by the ASAS-SN team at  $V=13.80$  on April 13. Subsequent observations detected superhumps (vsnet-alert 18545). The times of superhump maxima are listed in table 91.

The 2016 superoutburst was detected by the ASAS-SN team at  $V=13.41$  on August 31. Subsequent observations detected superhumps (vsnet-alert 20132). The times of superhump maxima are listed in table 92.

The period for the 2015 observations was much longer than in 2016. The 2015 observations were carried out soon after the outburst detection and they may have recorded stage A superhumps. This interpretation is illustrated in figure 122. A mean superhump profile is given for the better observed 2016 superoutburst (figure 123).

### 3.96 CSS J062450.1+503114

This object (=CSS131223:062450+503111, hereafter CSS J062450) was detected by the CRTS team at an unfiltered CCD magnitude of 14.76 on 2013 December 23. The 2017

**Table 71.** Superhump maxima of ASASSN-16ob (2016)

$E$	max*	error	$O - C^\dagger$	$N^\ddagger$
0	57734.3298	0.0094	-0.0111	131
1	57734.3770	0.0028	-0.0210	132
2	57734.4519	0.0037	-0.0033	132
3	57734.4903	0.0031	-0.0221	131
34	57736.2939	0.0009	0.0087	107
35	57736.3500	0.0011	0.0076	131
36	57736.4074	0.0012	0.0078	131
52	57737.3262	0.0009	0.0117	106
53	57737.3825	0.0007	0.0108	131
54	57737.4414	0.0007	0.0125	131
104	57740.2935	0.0009	0.0054	106
105	57740.3464	0.0010	0.0010	130
106	57740.4061	0.0010	0.0036	131
107	57740.4636	0.0014	0.0039	131
108	57740.5184	0.0065	0.0016	32
109	57740.5774	0.0019	0.0034	30
110	57740.6307	0.0015	-0.0006	16
111	57740.6879	0.0036	-0.0005	10
112	57740.7462	0.0023	0.0006	10
126	57741.5406	0.0046	-0.0056	29
127	57741.6035	0.0013	0.0001	25
128	57741.6570	0.0032	-0.0036	11
129	57741.7198	0.0038	0.0020	10
130	57741.7789	0.0075	0.0040	10
248	57748.5146	0.0021	-0.0082	144
249	57748.5714	0.0020	-0.0086	151

\*BJD-2400000.

 $^\dagger$ Against max = 2457734.3409 + 0.057185E. $^\ddagger$ Number of points used to determine the maximum.

outburst was detected by the ASAS-SN team at  $V=14.59$  on March 11. Subsequent observations detected superhumps (vsnet-alert 20766, 20770; figure 124). The times of superhump maxima are listed in table 93.

According to the ASAS-SN data, this object showed relatively regular superoutbursts (table 94). These superoutburst can be expressed by a supercycle of 128(2) d with maximum  $|O - C|$  of 20 d. The interval between the 2016 September and 2017 March superoutbursts was 166 d, which was rather unusually long for this object.

### 3.97 DDE 26

DDE 26 is a dwarf nova discovered by Denisenko (2012). See Kato et al. (2014b) for more information. The 2016 superoutburst was detected by the ASAS-SN team at  $V=15.95$  on August 1. Superhumps were recorded (vsnet-alert 20067). The times of superhump maxima are listed in

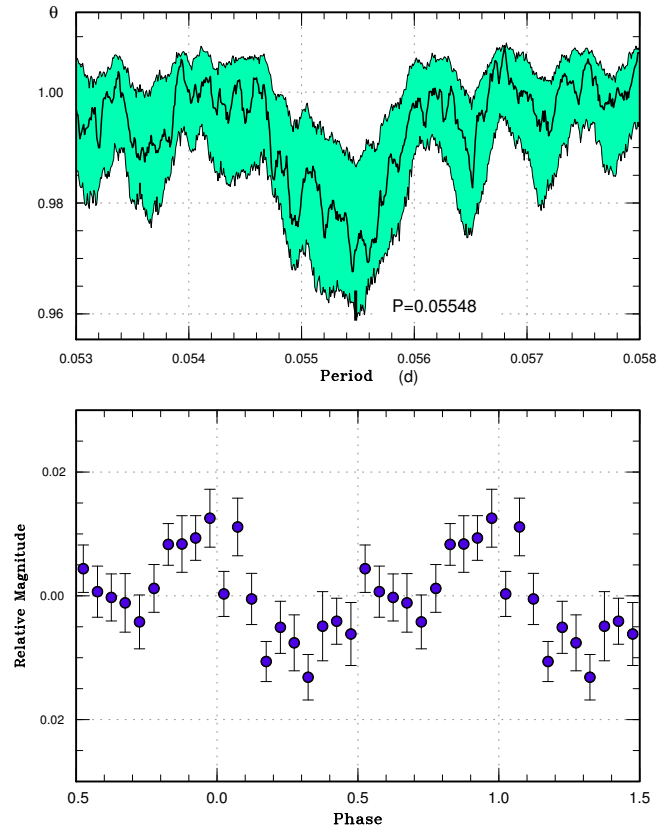
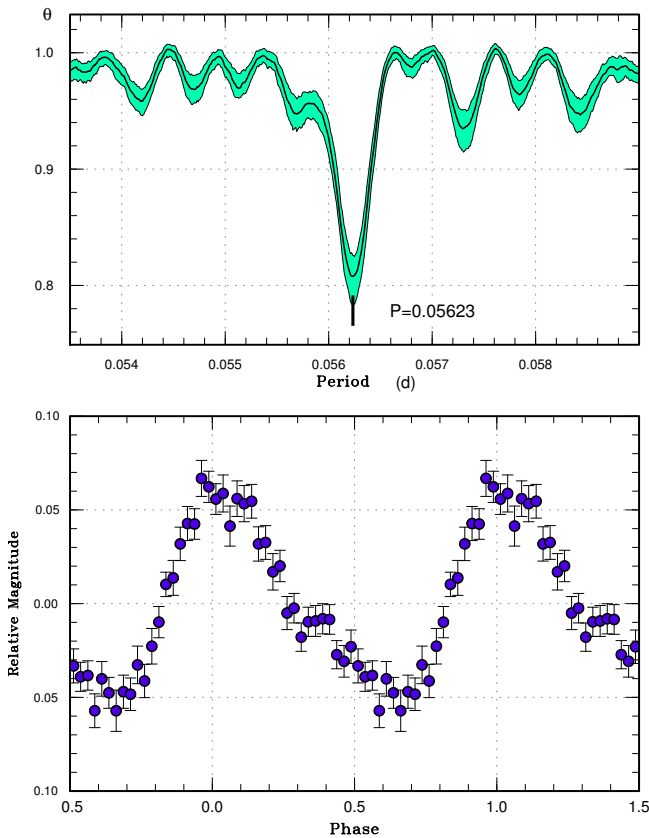
**Fig. 93.** Early superhumps in ASASSN-16oi (2016). (Upper): PDM analysis. (Lower): Phase-averaged profile.

table 95. The observation probably covered stage B (figure 125).

### 3.98 DDE 48

DDE 48 is a dwarf nova discovered by D. Denisenko (vsnet-alert 20146) in the vicinity of the dwarf nova MASTER OT J204627.96+242218.0 (Shumkov et al. 2016a). N. Mishevskiy monitored this object in 2016 and detected a bright outburst at  $V=15.5$  on November 1 (vsnet-alert 20290). Subsequent observations detected a superhump (vsnet-alert 20291). Although this superhump was recorded only on a single night, the profile suggests a genuine superhump (figure 126). The superhump maximum was at BJD 2457694.2662(6) ( $N=43$ ). The superhump became undetectable on two nights during the same superoutburst.

This object shows frequent outbursts (cf. vsnet-alert 20291; figure 127). The shortest interval of outbursts was 3 d. The initial long outburst in figure 127 was also likely a superoutburst recorded in its the final phase. If it is indeed the case, the supercycle is around 62 d. The object may belong to ER UMA-type dwarf novae (Kato and



**Fig. 94.** Ordinary superhumps in ASASSN-16oi (2016). The segment of BJD 2457733–2457741 was used. (Upper): PDM analysis. (Lower): Phase-averaged profile.

Kunjaya 1995; Robertson et al. 1995). (see also vsnet-alert 20291). Future continuous observations to determine the outburst characteristics, duty cycle and superhump period are desired.

### 3.99 MASTER OT J021315.37+533822.7

This object (hereafter MASTER J021315) was discovered as a transient at an unfiltered CCD magnitude of 16.8 mag on 2013 November 1 by the MASTER network (Yecheistov et al. 2013). The 2016 outburst was detected by the ASAS-SN team at  $V=16.39$  on October 2. The ASAS-SN also detected the 2013 outburst and its duration was long (at least 8 d). During the 2016 outburst, long-period superhumps were detected (vsnet-alert 20218; figure 128). The period indicates that the object is in the period gap. The times of superhump maxima are listed in table 96. The period markedly decreased with a global  $P_{\text{dot}}$  of  $-205(35) \times 10^{-5}$ . As recently recognized in many long- $P_{\text{orb}}$  objects, such a large period decrease is most likely a result of stage A-B transition (cf. V1006 Cyg and MN Dra: Kato et al. 2016b; CRTS J214738.4+244554 and OT

**Table 72.** Superhump maxima of ASASSN-16oi (2016)

$E$	max*	error	$O - C^\dagger$	$N^\ddagger$
0	57733.6808	0.0038	-0.0088	25
2	57733.7938	0.0012	-0.0082	23
12	57734.3675	0.0033	0.0027	52
13	57734.4273	0.0003	0.0062	129
14	57734.4830	0.0003	0.0056	129
24	57735.0428	0.0004	0.0027	25
25	57735.0991	0.0003	0.0027	34
26	57735.1548	0.0004	0.0021	35
27	57735.2104	0.0003	0.0014	35
46	57736.2774	0.0038	-0.0007	69
47	57736.3351	0.0009	0.0007	129
48	57736.3894	0.0008	-0.0013	130
64	57737.2917	0.0031	0.0006	71
65	57737.3464	0.0010	-0.0009	130
66	57737.4020	0.0010	-0.0017	130
67	57737.4573	0.0013	-0.0026	74
118	57740.3246	0.0015	-0.0054	129
119	57740.3852	0.0012	-0.0010	130
120	57740.4389	0.0021	-0.0036	130
121	57740.5039	0.0017	0.0051	129
122	57740.5595	0.0013	0.0044	129

\*BJD-2400000.

$^\dagger$ Against max = 2457733.6895 + 0.056275E.

$^\ddagger$ Number of points used to determine the maximum.

J064833.4+065624: Kato et al. 2015a; KK Tel, possibly V452 Cas and ASASSN-15cl: Kato et al. 2016a). The case is also likely since the initial observation of MASTER J021315 started only 1 d after the outburst detection. We gave values in table 3 following this interpretation. The ASAS-SN data suggest that outbursts in this system were relatively rare (only two were known with a separation of  $\sim 3$  yr). The object should have a low mass-transfer rate.

### 3.100 MASTER OT J030205.67+254834.3

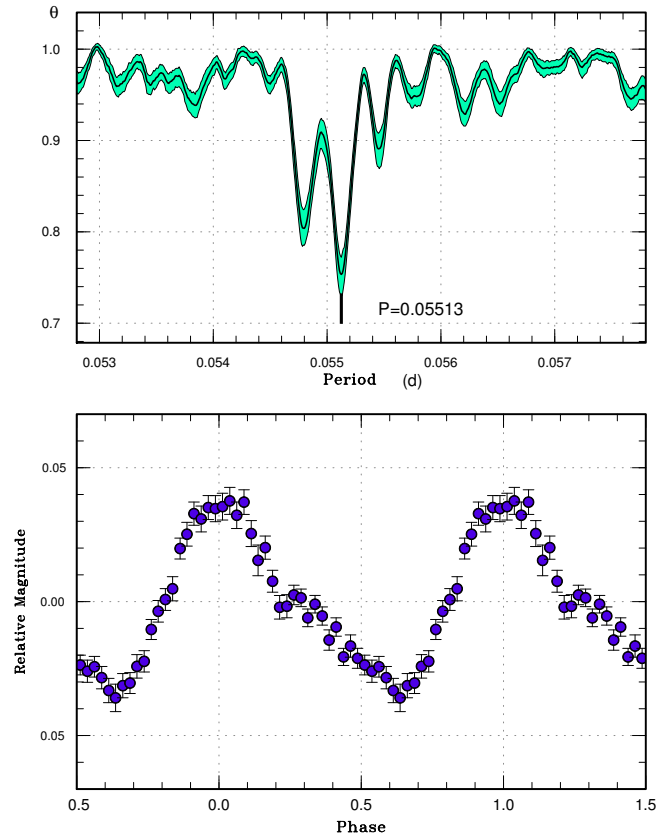
This object (hereafter MASTER J030205) was discovered as a transient at an unfiltered CCD magnitude of 13.7 mag on 2016 December 4 by the MASTER network (Balanutsa et al. 2016b). Although initial observations suggested the presence of early superhumps of the WZ Sge-type dwarf nova (vsnet-alert 20447), they were later identified as developing superhumps (stage A) with double maxima (vsnet-alert 20449, 20451). Further development of superhumps were reported (vsnet-alert 20456, 20471; figure 129). The times of superhump maxima are listed in table 97. Stages A and B can be recognized and the  $P_{\text{dot}}$  of stage B superhumps is positive, which is expected for



**Table 73.** Superhump maxima of ASASSN-16os (2016)

$E$	max*	error	$O - C^\dagger$	$N^\ddagger$
0	57741.4738	0.0012	-0.0195	127
1	57741.5276	0.0016	-0.0209	127
2	57741.5846	0.0014	-0.0190	78
5	57741.7572	0.0043	-0.0118	10
23	57742.7630	0.0008	0.0017	7
24	57742.8160	0.0019	-0.0005	5
30	57743.1526	0.0001	0.0054	34
31	57743.2073	0.0004	0.0049	30
39	57743.6520	0.0007	0.0086	10
40	57743.7066	0.0011	0.0080	10
41	57743.7597	0.0013	0.0061	9
42	57743.8155	0.0020	0.0067	7
54	57744.4783	0.0003	0.0080	88
55	57744.5320	0.0003	0.0065	109
57	57744.6412	0.0018	0.0055	9
58	57744.6993	0.0011	0.0084	8
59	57744.7506	0.0018	0.0046	8
60	57744.8099	0.0014	0.0088	8
71	57745.4138	0.0003	0.0062	126
72	57745.4675	0.0003	0.0048	124
73	57745.5228	0.0005	0.0050	126
74	57745.5771	0.0004	0.0041	112
76	57745.6872	0.0015	0.0040	9
77	57745.7456	0.0025	0.0073	8
78	57745.7979	0.0015	0.0045	8
94	57746.6774	0.0019	0.0019	8
95	57746.7303	0.0012	-0.0004	8
96	57746.7867	0.0022	0.0009	8
109	57747.5020	0.0004	-0.0005	127
110	57747.5560	0.0004	-0.0016	127
111	57747.6057	0.0022	-0.0070	24
114	57747.7703	0.0043	-0.0078	9
119	57748.0504	0.0004	-0.0033	40
130	57748.6610	0.0024	0.0008	9
131	57748.7165	0.0026	0.0012	10
132	57748.7612	0.0032	-0.0093	10
133	57748.8224	0.0053	-0.0031	7
148	57749.6455	0.0028	-0.0070	10
149	57749.7037	0.0013	-0.0040	9
168	57750.7467	0.0015	-0.0084	10

\*BJD-2400000.

 $^\dagger$ Against max = 2457741.4933 + 0.055130E. $^\ddagger$ Number of points used to determine the maximum.**Fig. 95.** Ordinary superhumps in ASASSN-16os (2016). (Upper): PDM analysis. (Lower): Phase-averaged profile.

this  $P_{SH}$ . The period of stage A superhump in table 3 was determined by the PDM method for the data before BJD 2457728.7.

Short-term periodic oscillations were reported (vsnet-alert 20452, 20457). An analysis of the entire data confirmed the presence of a coherent signal with a period 0.0035420(2) d [306.03(2) s] as originally reported (vsnet-alert 20457) (figure 130). Given the sharpness (high coherence) of the signal, it may be an intermediate-polar (IP) signal rather than quasi-periodic oscillations (vsnet-alert 20458). Since IPs are relatively rare in SU UMa-type dwarf novae [see table 1 in Hameury and Lasota (2017); the only well-established SU UMa-type dwarf nova (not including WZ Sge-type one) is CC Scl (Kato et al. 2015b)], further confirmation of the signal in this system is desired.

### 3.101 MASTER OT J042609.34+354144.8

This object (hereafter MASTER J042609) was discovered as a transient at an unfiltered CCD magnitude of 12.9 on 2012 September 30 by the MASTER network (Denisenko et al. 2012). The SU UMa-type nature was confirmed during this superoutburst (Kato et al. 2014b). This object is

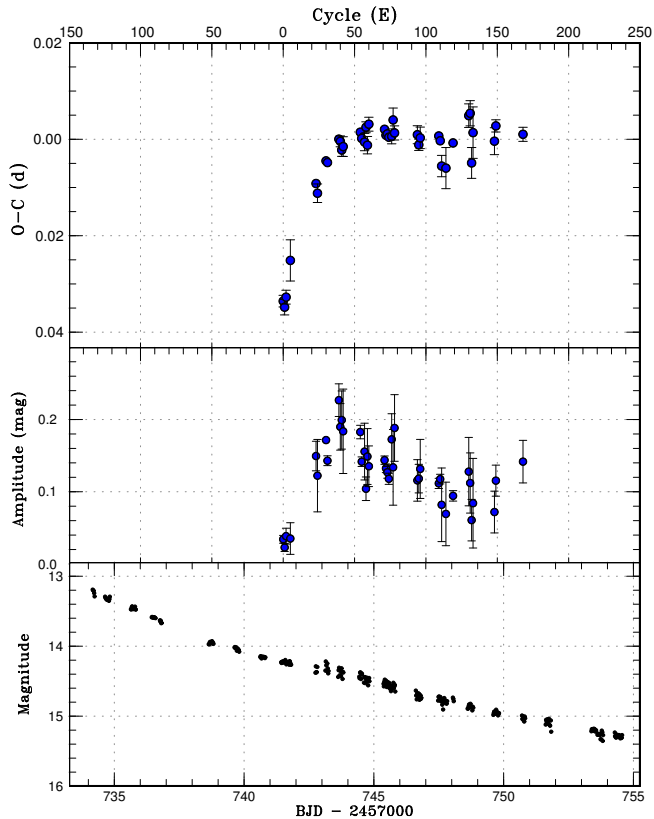


**Fig. 96.**  $O - C$  diagram of superhumps in ASASSN-16os (2016). (Upper:)  $O - C$  diagram. We used a period of 0.05499 d for calculating the  $O - C$  residuals. (Middle:) Amplitudes of superhumps. (Lower:) Light curve. The data were binned to 0.017 d.

also a grazing eclipser. For more information and history, see Kato et al. (2014b).

The 2016 superoutburst was detected by E. Muylaert at a visual magnitude of 13.8 on December 26. The last observation before this detection was on  $V=15.35$ – $15.51$  on December 23 (ASAS-SN). It was not clear when the outburst started. Superhumps were observed with a period change (vsnet-alert 20532, 20533). The times of superhump maxima are listed in table 98. The period change observed during the 2016 superoutburst probably reflected stage B-C transition (figure 131). Although the last two points may have been traditional late superhumps, no clear superhumps were observed after them despite relatively good observational coverage. Although no clear eclipses were visible during this superoutburst, a phase-averaged light curve with a period of 0.06550168 d and an epoch of BJD 2456276.6430 (Kato et al. 2014b) yielded a shallow eclipse (0.03 mag) at the expected phase (figure 132). We consider 0.06550168(1) d to be the refined orbital period.

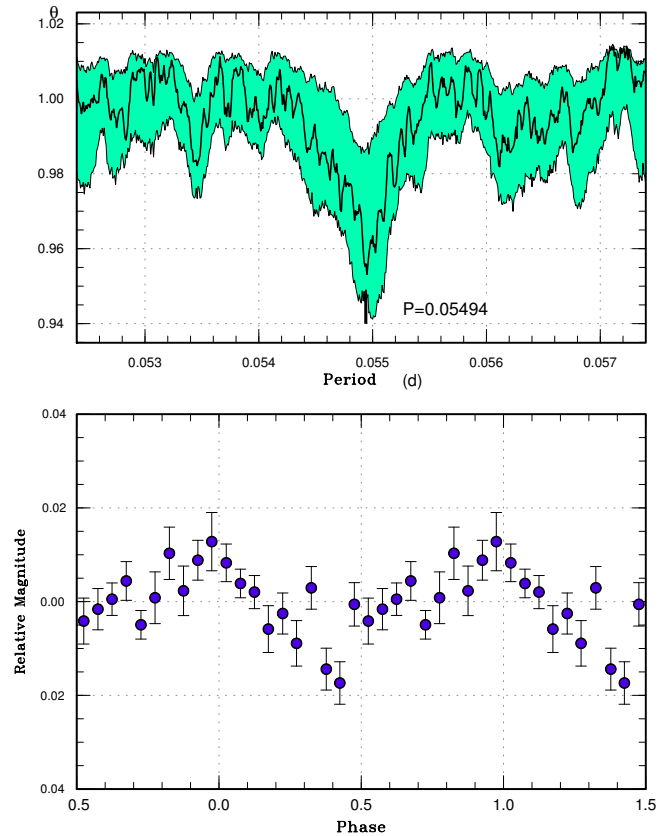


**Fig. 97.** Possible early superhumps in ASASSN-16os (2016). The segment of before BJD 2457741 was used. (Upper:) PDM analysis. (Lower:) Phase-averaged profile.

### 3.102 MASTER OT J043220.15+784913.8

This object (hereafter MASTER J043220) was discovered as a transient at an unfiltered CCD magnitude of 16.8 on 2013 December 12 by the MASTER network (Shurpakov et al. 2013a). The 2017 outburst was detected by the ASAS-SN team at  $V=16.29$  on January 25. The object was already seen in outburst at  $V=16.52$  in the ASAS-SN data. Subsequent observations detected superhumps (vsnet-alert 20614; figure 133). The times of superhump maxima were BJD 2457780.4941(5) ( $N=64$ ) and 2457780.5584(5) ( $N=64$ ). A PDM analysis yielded a period of 0.0640(6) d.

### 3.103 MASTER OT J043915.60+424232.3

This object (hereafter MASTER J043915) was discovered as a transient at an unfiltered CCD magnitude of 15.7 on 2014 January 21 by the MASTER network (Balanutsa et al. 2014). The SU UMa-type nature was confirmed during this superoutburst (Kato et al. 2015a). For more history, see Kato et al. (2015a).

The 2016 superoutburst was detected by the ASAS-SN

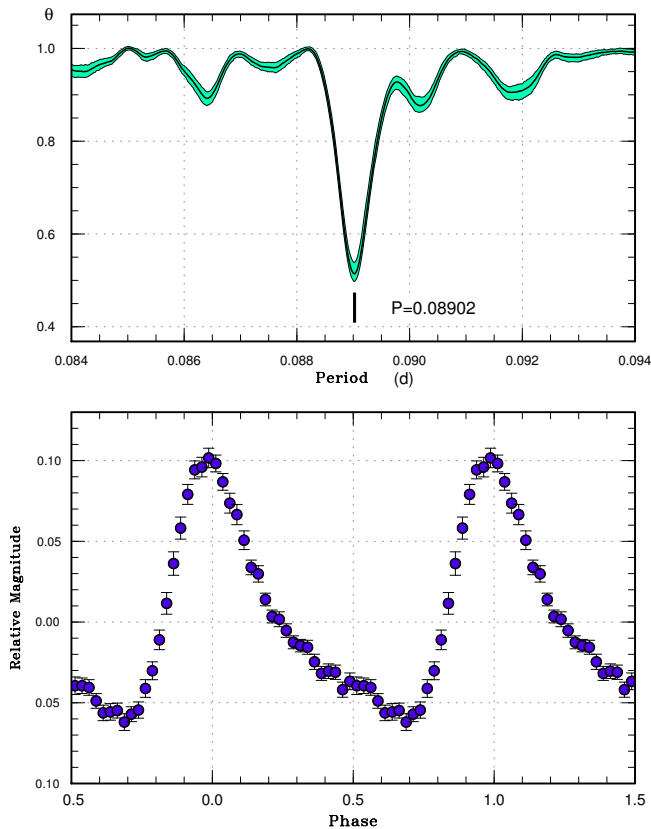


Fig. 98. Superhumps in ASASSN-16ow (2016). (Upper): PDM analysis. (Lower): Phase-averaged profile.

team at  $V=16.38$  on December 22. Superhumps were subsequently recorded (vsnet-alert 20509). The times of superhump maxima are listed in table 99. Although there were not disagreement between the 2014 and 2016 observations, we could not detect clear stages B and C, which are expected for this short  $P_{SH}$  (figure 134).

### 3.104 MASTER OT J054746.81+762018.9

This object (hereafter MASTER J054746) was discovered as a transient at an unfiltered CCD magnitude of 16.7 mag on 2016 October 12 by the MASTER network (Shumkov et al. 2016b). Subsequent observations detected superhumps (vsnet-alert 20227; figure 135). The times of superhump maxima are listed in table 100. The best superhump period with the PDM method is listed in table 3.

### 3.105 MASTER OT J055348.98+482209.0

This object (hereafter MASTER J055348) was discovered as a transient at an unfiltered CCD magnitude of 16.5 mag on 2014 March 13 by the MASTER network (Vladimirov et al. 2014). The 2017 outburst was detected by the ASAS-

Table 74. Superhump maxima of ASASSN-16ow (2016)

$E$	max*	error	$O - C^\dagger$	$N^\ddagger$
0	57737.5297	0.0003	-0.0078	147
1	57737.6182	0.0004	-0.0083	151
17	57739.0492	0.0004	-0.0015	175
18	57739.1439	0.0023	0.0041	61
21	57739.4039	0.0006	-0.0029	90
22	57739.4951	0.0012	-0.0007	52
29	57740.1203	0.0004	0.0014	138
30	57740.2094	0.0005	0.0015	213
31	57740.2984	0.0005	0.0015	275
34	57740.5679	0.0004	0.0040	86
35	57740.6541	0.0004	0.0012	88
40	57741.1031	0.0011	0.0051	92
55	57742.4369	0.0005	0.0037	43
56	57742.5257	0.0005	0.0035	83
57	57742.6176	0.0035	0.0064	21
62	57743.0572	0.0014	0.0010	87
66	57743.4140	0.0004	0.0017	109
67	57743.5031	0.0004	0.0018	117
68	57743.5939	0.0005	0.0036	81
79	57744.5678	0.0021	-0.0017	22
88	57745.3689	0.0005	-0.0017	96
89	57745.4573	0.0004	-0.0023	146
90	57745.5452	0.0004	-0.0034	162
96	57746.0808	0.0019	-0.0018	65
97	57746.1686	0.0010	-0.0031	77
100	57746.4366	0.0005	-0.0021	85
101	57746.5261	0.0007	-0.0016	106
102	57746.6155	0.0016	-0.0013	47

\*BJD-2400000.

†Against max = 2457737.5375 + 0.089011E.

‡Number of points used to determine the maximum.

SN team at  $V=16.52$  on February 16. Subsequent observations detected superhumps (vsnet-alert 20681). Although observations on two nights were reported, neither data were of sufficient quality to determine the superhump period (the object already faded below 17 mag). The period used to calculated epochs in table 101 was one of the possibilities giving smallest  $O - C$  residuals. Other candidate aliases were 0.0784(1) d and 0.0720(1) d (figure 136). The period of 0.0666 d reported in vsnet-alert 20681 could not express the second-night observation.

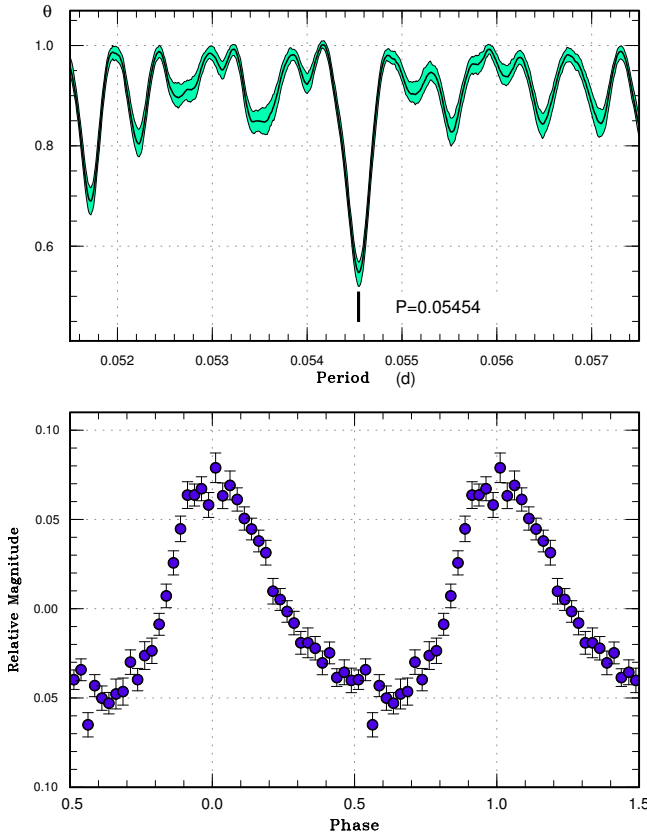


Fig. 99. Ordinary superhumps in ASASSN-17aa (2017). (Upper): PDM analysis. (Lower): Phase-averaged profile.

Table 75. Superhump maxima of ASASSN-17aa (2017)

$E$	max*	error	$O - C^\dagger$	$N^\ddagger$
0	57765.2954	0.0008	0.0036	106
1	57765.3520	0.0005	0.0056	126
2	57765.4052	0.0004	0.0041	104
51	57768.0754	0.0004	-0.0006	49
56	57768.3470	0.0005	-0.0019	125
57	57768.3998	0.0004	-0.0037	112
69	57769.0551	0.0006	-0.0035	49
70	57769.1111	0.0005	-0.0020	49
71	57769.1652	0.0007	-0.0026	49
72	57769.2200	0.0007	-0.0024	48
92	57770.3135	0.0023	-0.0007	78
93	57770.3664	0.0005	-0.0024	125
111	57771.3500	0.0006	-0.0013	101
112	57771.4045	0.0006	-0.0015	126
180	57775.1205	0.0016	0.0024	29
181	57775.1763	0.0009	0.0036	49
182	57775.2306	0.0008	0.0033	49

\*BJD-2400000.

$^\dagger$ Against max = 2457765.2918 + 0.054591E.

$^\ddagger$ Number of points used to determine the maximum.

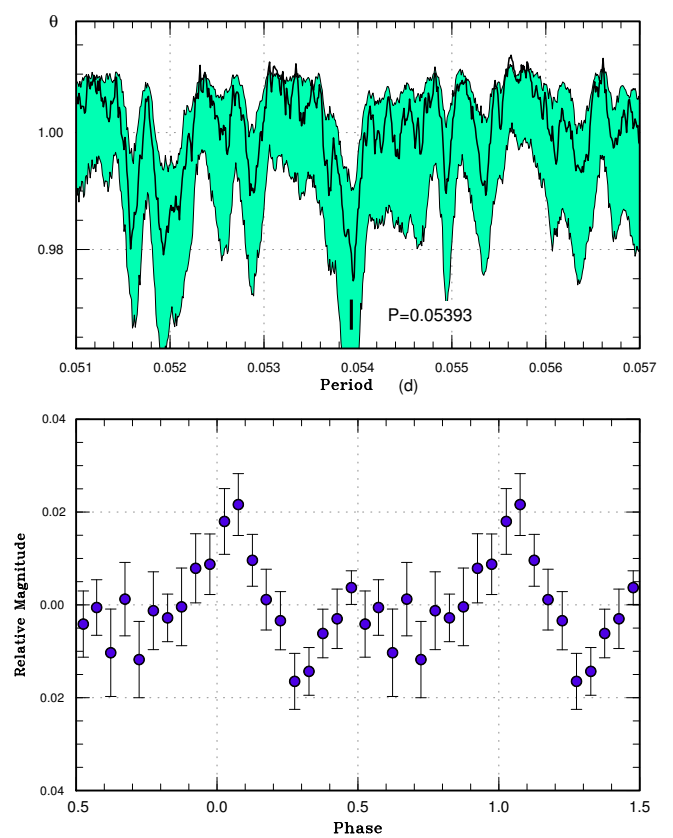


Fig. 100. Possible early superhumps in ASASSN-17aa (2017). (Upper): PDM analysis. (Lower): Phase-averaged profile.

Table 76. Superhump maxima of ASASSN-17ab (2017)

$E$	max*	error	$O - C^\dagger$	$N^\ddagger$
0	57756.6178	0.0026	-0.0016	9
1	57756.6869	0.0006	-0.0029	13
2	57756.7610	0.0004	0.0008	12
15	57757.6768	0.0009	0.0014	13
16	57757.7470	0.0008	0.0011	13
17	57757.8183	0.0003	0.0020	12
29	57758.6617	0.0006	0.0007	12
30	57758.7314	0.0008	-0.0001	13
31	57758.8006	0.0009	-0.0012	13
44	57759.7163	0.0010	-0.0007	13
45	57759.7882	0.0010	0.0009	13
86	57762.6714	0.0045	-0.0023	12
87	57762.7456	0.0013	0.0014	12
88	57762.8169	0.0013	0.0024	13
101	57763.7288	0.0015	-0.0009	11
102	57763.7990	0.0008	-0.0011	14

\*BJD-2400000.

$^\dagger$ Against max = 2457756.6194 + 0.070399E.

$^\ddagger$ Number of points used to determine the maximum.

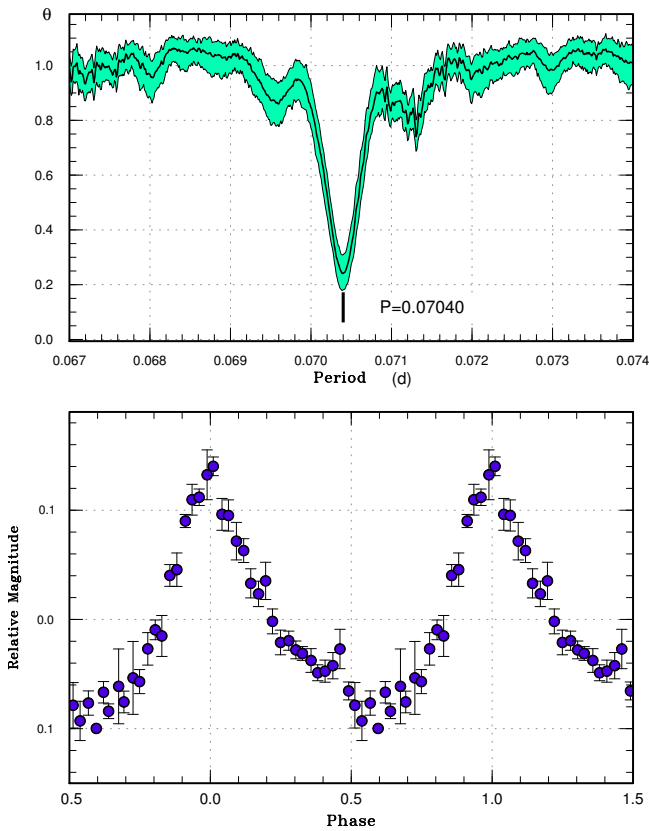


Fig. 101. Superhumps in ASASSN-17ab (2017). (Upper): PDM analysis. (Lower): Phase-averaged profile.

Table 77. Superhump maxima of ASASSN-17az (2017)

$E$	max*	error	$O - C^\dagger$	$N^\ddagger$
0	57783.3017	0.0005	-0.0006	130
1	57783.3594	0.0022	0.0006	76
35	57785.2807	0.0016	0.0012	82
36	57785.3348	0.0011	-0.0012	129

\*BJD-2400000.

†Against max = 2457783.3023 + 0.056492E.

‡Number of points used to determine the maximum.

Table 78. Superhump maxima of ASASSN-17bl (2017)

$E$	max*	error	$O - C^\dagger$	$N^\ddagger$
0	57788.6964	0.0020	-0.0151	10
1	57788.7494	0.0020	-0.0176	12
2	57788.8101	0.0046	-0.0123	12
35	57790.6538	0.0029	0.0035	9
36	57790.7135	0.0027	0.0078	8
37	57790.7666	0.0011	0.0055	9
38	57790.8238	0.0008	0.0073	9
43	57791.0939	0.0027	0.0004	12
53	57791.6557	0.0029	0.0083	9
54	57791.7093	0.0015	0.0065	8
55	57791.7620	0.0026	0.0039	8
56	57791.8193	0.0024	0.0057	8
71	57792.6505	0.0024	0.0060	9
72	57792.7069	0.0048	0.0071	9
73	57792.7601	0.0023	0.0049	9
74	57792.8141	0.0017	0.0035	10
75	57792.8664	0.0015	0.0004	6
79	57793.0867	0.0050	-0.0009	13
89	57793.6408	0.0022	-0.0007	10
90	57793.6989	0.0046	0.0020	9
91	57793.7539	0.0036	0.0016	9
92	57793.8126	0.0045	0.0049	10
93	57793.8611	0.0016	-0.0021	8
97	57794.0852	0.0004	0.0005	33
98	57794.1388	0.0006	-0.0013	35
99	57794.1944	0.0006	-0.0011	35
100	57794.2504	0.0006	-0.0005	34
110	57794.8038	0.0020	-0.0010	10
132	57796.0206	0.0012	-0.0029	31
133	57796.0729	0.0019	-0.0059	34
147	57796.8495	0.0019	-0.0049	35
162	57797.6856	0.0018	0.0004	8
163	57797.7424	0.0024	0.0017	10
164	57797.7939	0.0027	-0.0022	14
180	57798.6742	0.0036	-0.0082	9
182	57798.7861	0.0016	-0.0071	24
183	57798.8476	0.0022	-0.0009	17
189	57799.1785	0.0011	-0.0024	24
191	57799.2947	0.0045	0.0030	13
199	57799.7322	0.0022	-0.0026	10
200	57799.7852	0.0016	-0.0051	25
201	57799.8441	0.0035	-0.0015	20
204	57800.0146	0.0021	0.0028	9
217	57800.7303	0.0031	-0.0016	9
235	57801.7365	0.0044	0.0075	11
236	57801.7843	0.0029	-0.0001	18
237	57801.8429	0.0040	0.0031	16

\*BJD-2400000.

†Against max = 2457788.7115 + 0.055393E.

‡Number of points used to determine the maximum.

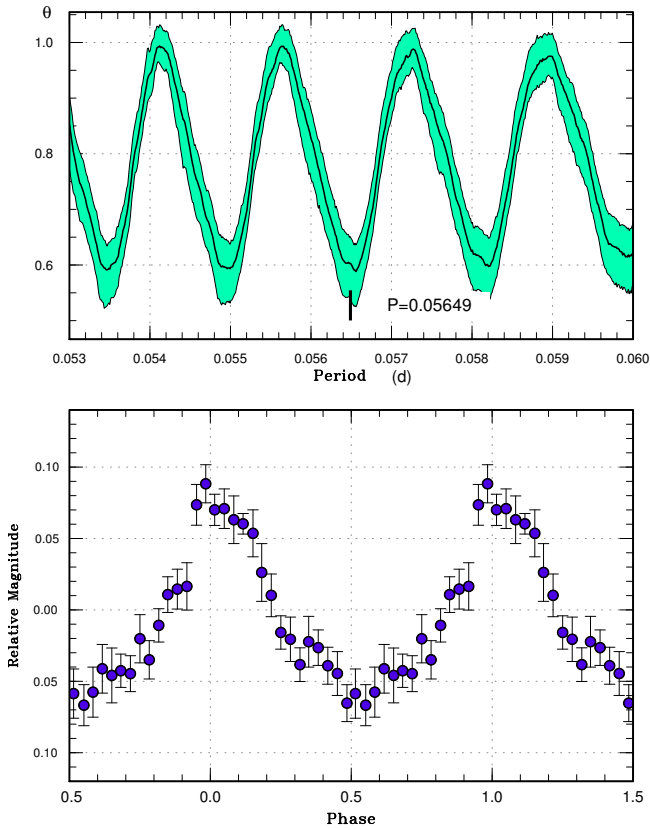


**Fig. 102.** Superhumps in ASASSN-17az (2017). (Upper): PDM analysis. The most likely alias based on  $O - C$  analysis was chosen. (Lower): Phase-averaged profile.

**Table 79.** Superhump maxima of ASASSN-17bm (2017)

$E$	max*	error	$O - C^\dagger$	$N^\ddagger$
0	57783.3970	0.0007	0.0005	152
24	57785.3910	0.0017	0.0018	155
25	57785.4720	0.0011	-0.0002	191
28	57785.7252	0.0039	0.0038	12
29	57785.7979	0.0058	-0.0065	15
52	57787.7031	0.0036	-0.0110	12
53	57787.8088	0.0073	0.0117	18

\*BJD-2400000.

$^\dagger$  Against max = 2457783.3965 + 0.083032E.

$^\ddagger$  Number of points used to determine the maximum.

**Table 80.** Superhump maxima of ASASSN-17bv (2017)

$E$	max*	error	$O - C^\dagger$	$N^\ddagger$
0	57787.7449	0.0007	-0.0074	18
1	57787.8269	0.0011	-0.0079	17
12	57788.7425	0.0015	-0.0007	17
13	57788.8231	0.0011	-0.0027	17
33	57790.4778	0.0013	0.0005	100
34	57790.5623	0.0005	0.0024	156
35	57790.6439	0.0015	0.0014	11
36	57790.7266	0.0019	0.0015	12
37	57790.8088	0.0012	0.0012	13
40	57791.0590	0.0003	0.0036	62
44	57791.3876	0.0007	0.0019	135
45	57791.4710	0.0005	0.0028	190
46	57791.5532	0.0005	0.0023	196
47	57791.6370	0.0018	0.0036	9
48	57791.7178	0.0020	0.0018	12
49	57791.8009	0.0017	0.0023	13
52	57792.0484	0.0008	0.0021	42
58	57792.5468	0.0025	0.0050	22
60	57792.7110	0.0023	0.0040	13
61	57792.7923	0.0016	0.0028	14
62	57792.8777	0.0032	0.0056	6
64	57793.0381	0.0003	0.0009	150
65	57793.1201	0.0004	0.0003	136
66	57793.2012	0.0004	-0.0012	148
67	57793.2832	0.0009	-0.0018	167
70	57793.5330	0.0009	0.0003	176
71	57793.6156	0.0012	0.0003	146
76	57794.0267	0.0004	-0.0014	124
77	57794.1092	0.0007	-0.0015	120
78	57794.1930	0.0006	-0.0004	148
79	57794.2704	0.0011	-0.0055	141
80	57794.3575	0.0016	-0.0010	187
81	57794.4385	0.0009	-0.0026	189
82	57794.5217	0.0012	-0.0020	189
88	57795.0138	0.0063	-0.0053	92
89	57795.1017	0.0036	0.0000	94
90	57795.1805	0.0011	-0.0037	148
91	57795.2671	0.0011	0.0003	110
96	57795.6842	0.0029	0.0045	10
97	57795.7538	0.0050	-0.0085	10
100	57796.0153	0.0024	0.0053	32
102	57796.1715	0.0033	-0.0037	44
103	57796.2583	0.0022	0.0005	46

\*BJD-2400000.

$^\dagger$  Against max = 2457787.7523 + 0.082578E.

$^\ddagger$  Number of points used to determine the maximum.

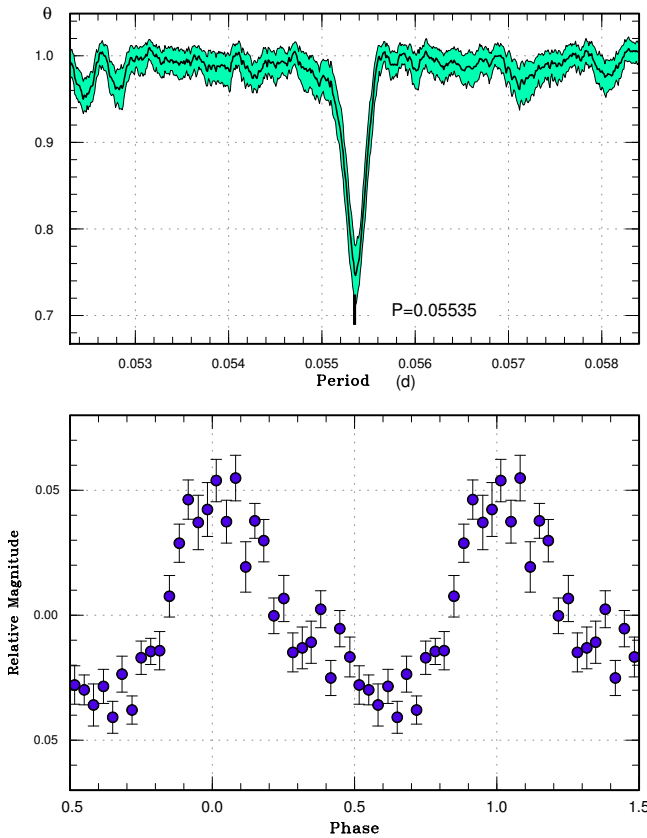


Fig. 103. Ordinary superhumps in ASASSN-17bl (2017). (Upper): PDM analysis. (Lower): Phase-averaged profile.

Table 81. Superhump maxima of ASASSN-17ce (2017)

$E$	max*	error	$O - C^\dagger$	$N^\ddagger$
0	57800.0338	0.0003	-0.0028	73
1	57800.1148	0.0002	-0.0026	73
4	57800.3530	0.0030	-0.0069	74
5	57800.4405	0.0004	-0.0003	186
6	57800.5221	0.0007	0.0005	128
21	57801.7390	0.0014	0.0047	17
22	57801.8220	0.0009	0.0069	24
26	57802.1414	0.0008	0.0029	25
59	57804.8064	0.0011	-0.0001	26
88	57807.1428	0.0018	-0.0083	50
89	57807.2411	0.0018	0.0092	45
90	57807.3114	0.0057	-0.0013	13
138	57811.1967	0.0051	0.0033	44
139	57811.2692	0.0065	-0.0051	47

\*BJD-2400000.

$^\dagger$ Against max = 2457800.0365 + 0.080847E.

$^\ddagger$ Number of points used to determine the maximum.

Table 82. Superhump maxima of ASASSN-17cn (2017)

$E$	max*	error	$O - C^\dagger$	$N^\ddagger$
0	57818.2910	0.0011	0.0081	113
1	57818.3398	0.0008	0.0030	124
2	57818.3934	0.0010	0.0026	123
3	57818.4483	0.0013	0.0033	95
19	57819.3097	0.0010	0.0004	124
20	57819.3626	0.0009	-0.0007	124
21	57819.4217	0.0014	0.0043	123
22	57819.4730	0.0014	0.0016	125
23	57819.5254	0.0008	-0.0000	124
37	57820.2801	0.0009	-0.0016	114
38	57820.3336	0.0009	-0.0022	124
39	57820.3899	0.0011	0.0001	124
40	57820.4428	0.0010	-0.0011	123
41	57820.4971	0.0008	-0.0007	124
42	57820.5506	0.0007	-0.0013	124
51	57821.0406	0.0030	0.0025	39
52	57821.0889	0.0007	-0.0032	52
53	57821.1420	0.0008	-0.0041	49
54	57821.1980	0.0005	-0.0021	49
55	57821.2512	0.0017	-0.0030	36
60	57821.5229	0.0014	-0.0014	26
63	57821.6834	0.0024	-0.0029	21
74	57822.2754	0.0015	-0.0053	120
75	57822.3341	0.0026	-0.0006	124
76	57822.3882	0.0017	-0.0005	124
77	57822.4413	0.0031	-0.0014	124
79	57822.5503	0.0017	-0.0004	125
81	57822.6557	0.0023	-0.0030	12
94	57823.3604	0.0012	-0.0007	124
95	57823.4122	0.0015	-0.0029	124
96	57823.4674	0.0014	-0.0018	124
97	57823.5220	0.0020	-0.0012	125
137	57825.6893	0.0031	0.0052	18
152	57826.5008	0.0018	0.0063	16
154	57826.6050	0.0030	0.0025	17
173	57827.6311	0.0024	0.0021	17

\*BJD-2400000.

$^\dagger$ Against max = 2457818.2828 + 0.054024E.

$^\ddagger$ Number of points used to determine the maximum.

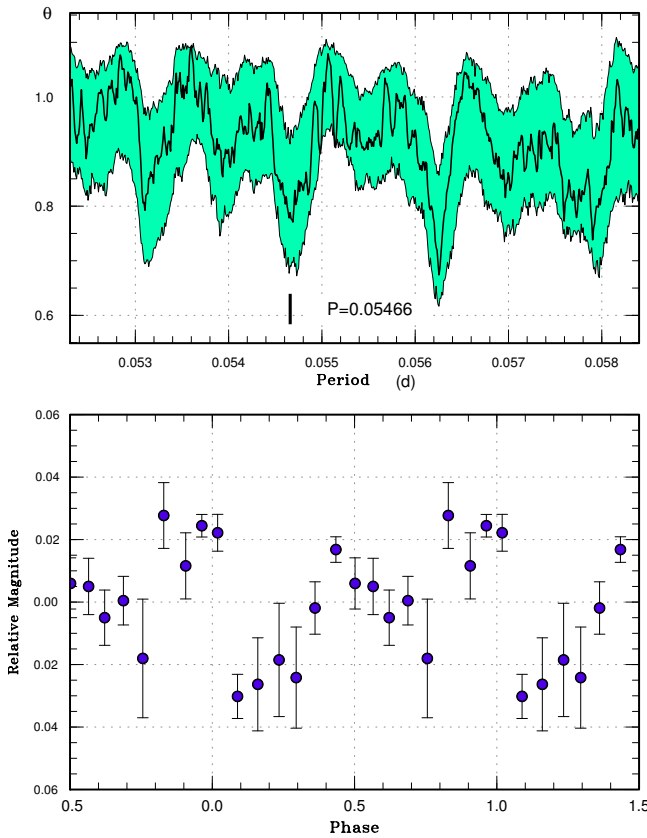


Fig. 104. Possible early superhumps in ASASSN-17bl (2017). (Upper): PDM analysis. (Lower): Phase-averaged profile.

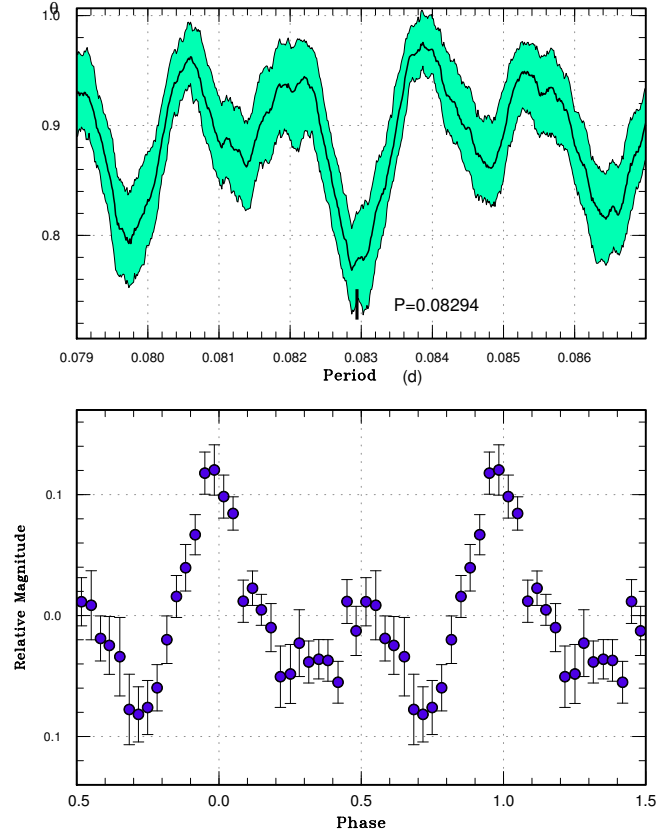


Fig. 105. Superhumps in ASASSN-17bm (2017). (Upper): PDM analysis. (Lower): Phase-averaged profile.

Table 83. Superhump maxima of ASASSN-17dg (2017)

$E$	max*	error	$O - C^\dagger$	$N^\ddagger$
0	57821.8464	0.0010	0.0006	26
3	57822.0427	0.0008	-0.0026	60
4	57822.1111	0.0006	-0.0006	60
5	57822.1761	0.0007	-0.0021	60
6	57822.2435	0.0007	-0.0012	60
8	57822.3801	0.0007	0.0025	154
9	57822.4440	0.0006	-0.0001	153
10	57822.5110	0.0005	0.0004	154
11	57822.5782	0.0005	0.0012	153
15	57822.8451	0.0014	0.0021	27
21	57823.2440	0.0010	0.0021	31
33	57824.0393	0.0010	-0.0003	60
34	57824.1098	0.0019	0.0037	60
35	57824.1679	0.0014	-0.0047	60
36	57824.2382	0.0011	-0.0009	60

\*BJD-2400000.

$^\dagger$ Against max = 2457821.8458 + 0.066482E.

$^\ddagger$ Number of points used to determine the maximum.

Table 84. Superhump maxima of ASASSN-17dq (2017)

$E$	max*	error	$O - C^\dagger$	$N^\ddagger$
0	57828.3203	0.0006	0.0010	113
1	57828.3769	0.0010	-0.0004	72
2	57828.4339	0.0011	-0.0014	103
38	57830.5179	0.0009	-0.0050	38
40	57830.6359	0.0015	-0.0028	21
55	57831.5074	0.0017	-0.0011	39
57	57831.6253	0.0015	0.0008	21
74	57832.6074	0.0030	-0.0029	21
90	57833.5426	0.0016	0.0045	14
91	57833.6081	0.0019	0.0120	15
92	57833.6552	0.0027	0.0012	15
93	57833.7177	0.0033	0.0056	7
108	57834.5796	0.0022	-0.0022	17
109	57834.6387	0.0023	-0.0011	18
110	57834.7000	0.0017	0.0022	16
142	57836.5428	0.0034	-0.0105	23

\*BJD-2400000.

$^\dagger$ Against max = 2457828.3194 + 0.057986E.

$^\ddagger$ Number of points used to determine the maximum.



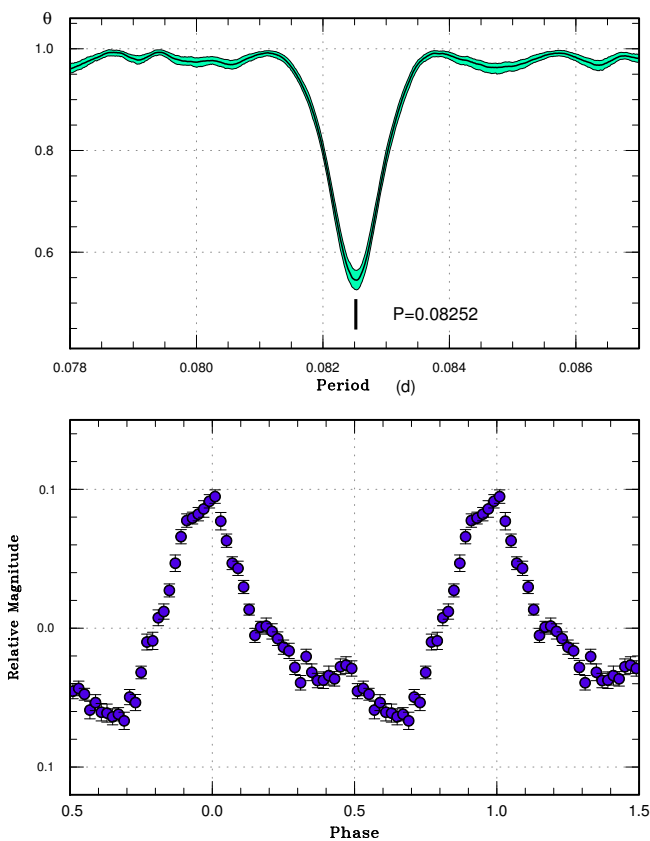


Fig. 106. Superhumps in ASASSN-17bv (2017). (Upper): PDM analysis. (Lower): Phase-averaged profile.

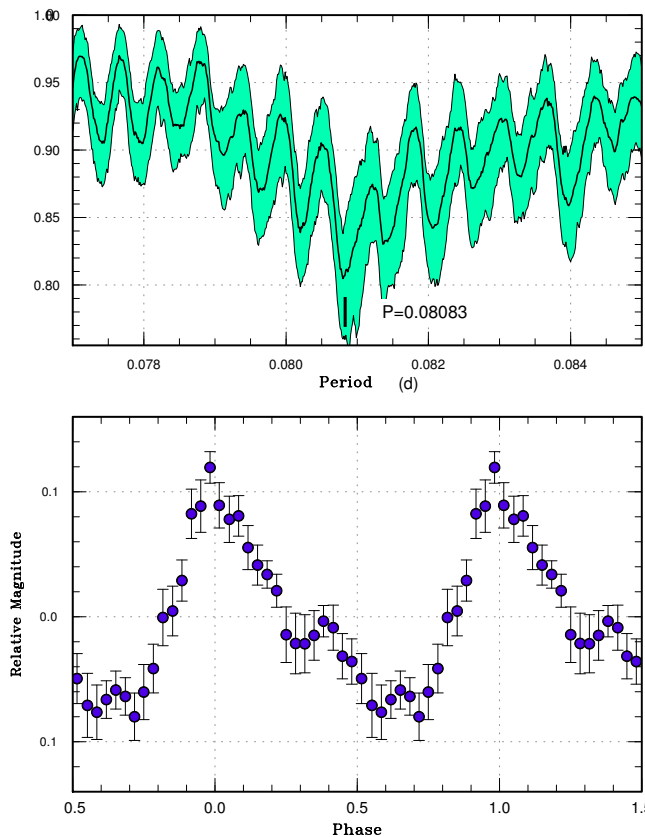


Fig. 107. Superhumps in ASASSN-17ce (2017). (Upper): PDM analysis. (Lower): Phase-averaged profile.

Table 85. Superhump maxima of CRTS J000130 (2016)

$E$	max*	error	$O - C^\dagger$	$N^\ddagger$
0	57639.5745	0.0003	0.0020	96
1	57639.6745	0.0009	0.0073	33
10	57640.5097	0.0031	-0.0103	34
11	57640.6146	0.0004	-0.0001	95
21	57641.5612	0.0005	-0.0010	96
22	57641.6603	0.0010	0.0033	54
30	57642.4117	0.0010	-0.0033	31
31	57642.5077	0.0011	-0.0021	26
41	57643.4551	0.0009	-0.0021	37
51	57644.4083	0.0009	0.0036	177
52	57644.4989	0.0014	-0.0005	102
53	57644.6001	0.0011	0.0060	97
63	57645.5388	0.0020	-0.0029	25

\*BJD-2400000.

$^\dagger$ Against max = 2457639.5725 + 0.094749E.

$^\ddagger$ Number of points used to determine the maximum.

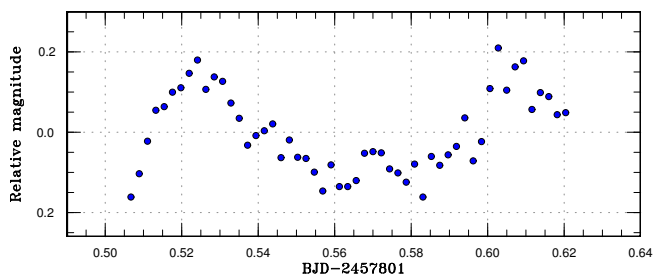


Fig. 108. Superhumps in ASASSN-17ck (2017).

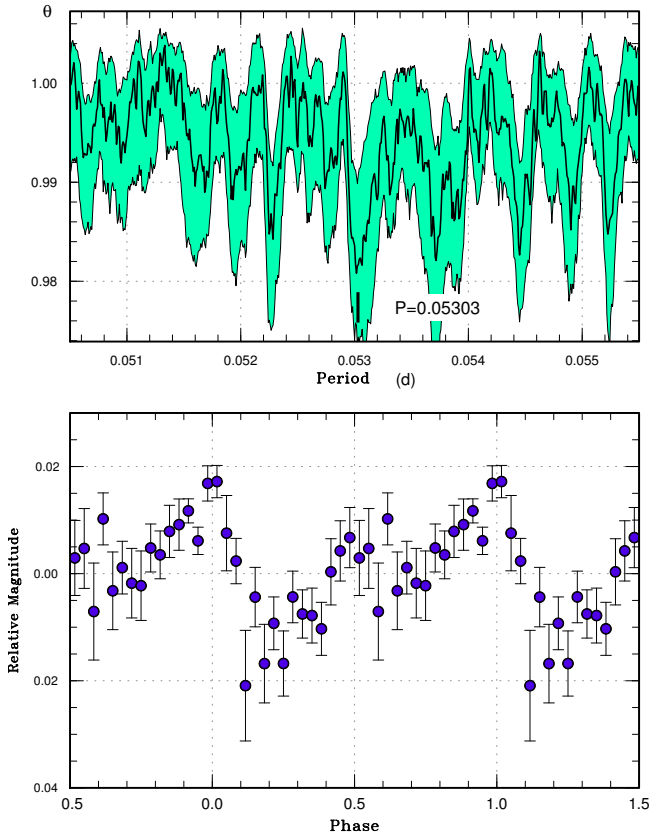


Fig. 109. Early superhumps in ASASSN-17cn (2017). (Upper): PDM analysis. (Lower): Phase-averaged profile.

Table 86. Superhump maxima of CRTS J023638 (2016)

$E$	max*	error	$O - C^\dagger$	$N^\ddagger$
0	57632.5227	0.0034	-0.0111	41
1	57632.5933	0.0003	-0.0138	73
14	57633.5485	0.0004	-0.0105	82
15	57633.6227	0.0006	-0.0095	52
28	57634.5818	0.0005	-0.0023	68
29	57634.6560	0.0004	-0.0014	49
40	57635.4657	0.0017	0.0029	21
41	57635.5409	0.0007	0.0049	29
42	57635.6194	0.0033	0.0101	11
55	57636.5723	0.0007	0.0111	69
56	57636.6441	0.0005	0.0097	48
68	57637.5268	0.0021	0.0137	27
68	57637.5267	0.0020	0.0136	27
80	57638.4083	0.0016	0.0166	27
137	57642.5488	0.0009	-0.0167	31
138	57642.6214	0.0013	-0.0173	25

\*BJD-2400000.

$^\dagger$ Against max = 2457632.5338 + 0.073224E.

$^\ddagger$ Number of points used to determine the maximum.

Table 87. Superhump maxima of CRTS J033349 (2016)

$E$	max*	error	$O - C^\dagger$	$N^\ddagger$
0	57718.0808	0.0038	0.0002	76
1	57718.1532	0.0011	-0.0036	166
5	57718.4653	0.0013	0.0039	154
6	57718.5405	0.0012	0.0030	127
8	57718.6937	0.0033	0.0039	19
9	57718.7615	0.0027	-0.0046	20
10	57718.8430	0.0058	0.0008	12
21	57719.6798	0.0024	-0.0002	24
22	57719.7597	0.0043	0.0036	25
23	57719.8323	0.0024	0.0001	19
31	57720.4414	0.0014	-0.0002	174
34	57720.6668	0.0020	-0.0032	27
35	57720.7436	0.0017	-0.0026	20
36	57720.8164	0.0039	-0.0060	20
47	57721.6592	0.0027	-0.0009	28
48	57721.7310	0.0032	-0.0052	20
49	57721.8172	0.0049	0.0047	20
60	57722.6564	0.0040	0.0062	27

\*BJD-2400000.

$^\dagger$ Against max = 2457718.0806 + 0.076159E.

$^\ddagger$ Number of points used to determine the maximum.

Table 88. List of superoutbursts of CRTS J033349

Year	Month	Day	max*	V-mag
2014	10	28	56959	14.26
2015	2	16	57070	14.49
2015	9	16	57282	14.50
2015	12	29	57386	14.38
2016	8	17	57618	14.41
2016	11	18	57711	14.46

\*JD-2400000.

Table 89. Superhump maxima of CRTS J085603 (2016)

$E$	max*	error	$O - C^\dagger$	$N^\ddagger$
0	57721.4212	0.0034	-0.0039	29
1	57721.4868	0.0005	0.0017	61
2	57721.5477	0.0004	0.0025	61
17	57722.4482	0.0041	0.0024	56
18	57722.5033	0.0017	-0.0026	57

\*BJD-2400000.

$^\dagger$ Against max = 2457721.4251 + 0.060043E.

$^\ddagger$ Number of points used to determine the maximum.

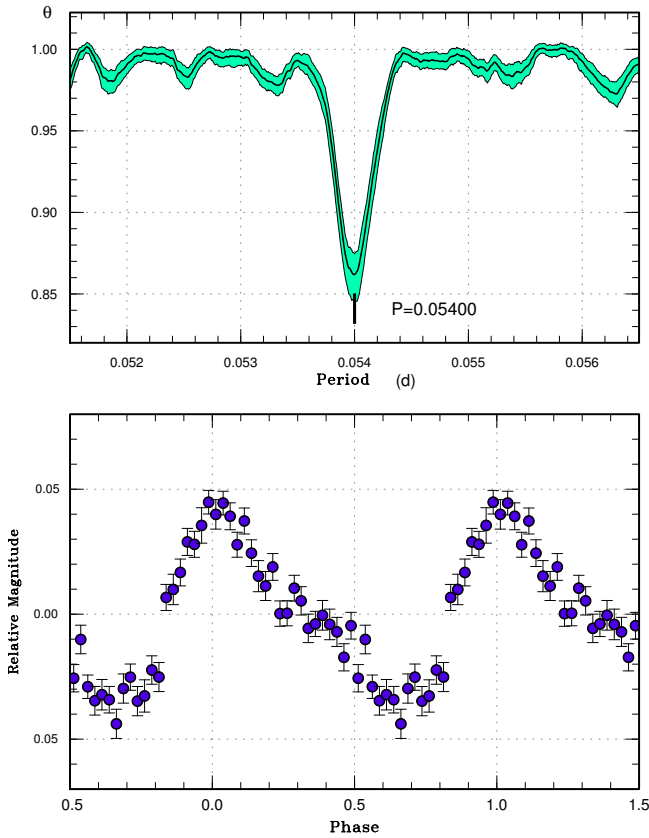


Fig. 110. Ordinary superhumps in ASASSN-17cn (2017). (Upper): PDM analysis. (Lower): Phase-averaged profile.

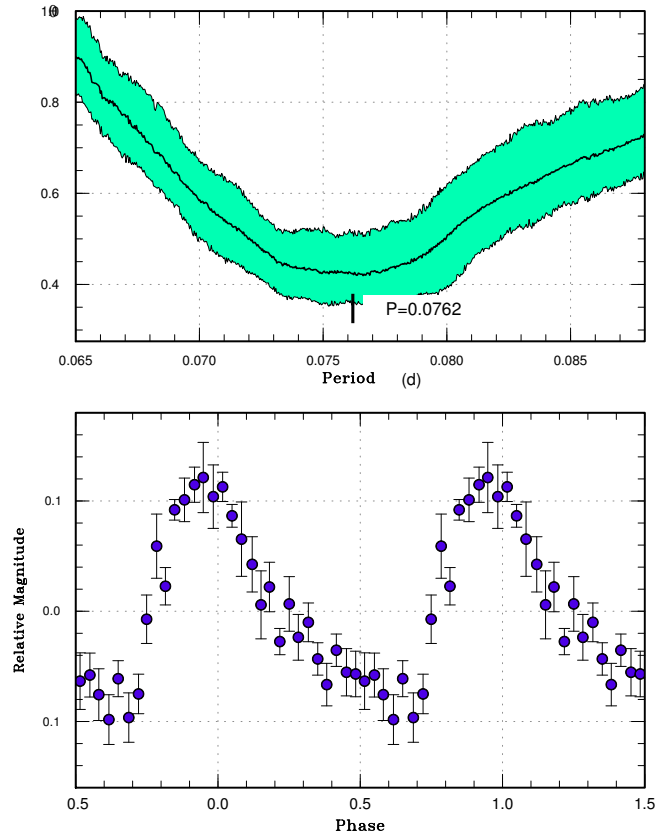


Fig. 111. Superhumps in ASASSN-17cx (2017). (Upper): PDM analysis. (Lower): Phase-averaged profile.

Table 90. List of likely superoutbursts of CRTS J085603

Year	Month	Day	max*	V-mag
2014	5	10	56788	15.67
2015	2	17	57071	15.67
2015	10	22	57317	15.61
2016	5	17	57526	15.75
2016	11	26	57718	16.62

\*JD-2400000.

Table 91. Superhump maxima of CRTS J164950 (2015)

E	max*	error	O - C <sup>†</sup>	N <sup>‡</sup>
0	57127.5058	0.0023	-0.0009	24
1	57127.5740	0.0004	0.0010	64
19	57128.7677	0.0002	-0.0007	93
20	57128.8353	0.0002	0.0006	111

\*BJD-2400000.

<sup>†</sup>Against max = 2457127.5067 + 0.066405E.

<sup>‡</sup>Number of points used to determine the maximum.

Table 92. Superhump maxima of CRTS J164950 (2016)

E	max*	error	O - C <sup>†</sup>	N <sup>‡</sup>
0	57636.3464	0.0016	-0.0034	15
1	57636.4151	0.0005	0.0004	61
30	57638.2969	0.0010	-0.0001	39
31	57638.3700	0.0015	0.0081	29
46	57639.3310	0.0010	-0.0044	66
60	57640.2493	0.0015	0.0052	38
61	57640.3032	0.0009	-0.0058	66

\*BJD-2400000.

<sup>†</sup>Against max = 2457636.3498 + 0.064905E.

<sup>‡</sup>Number of points used to determine the maximum.

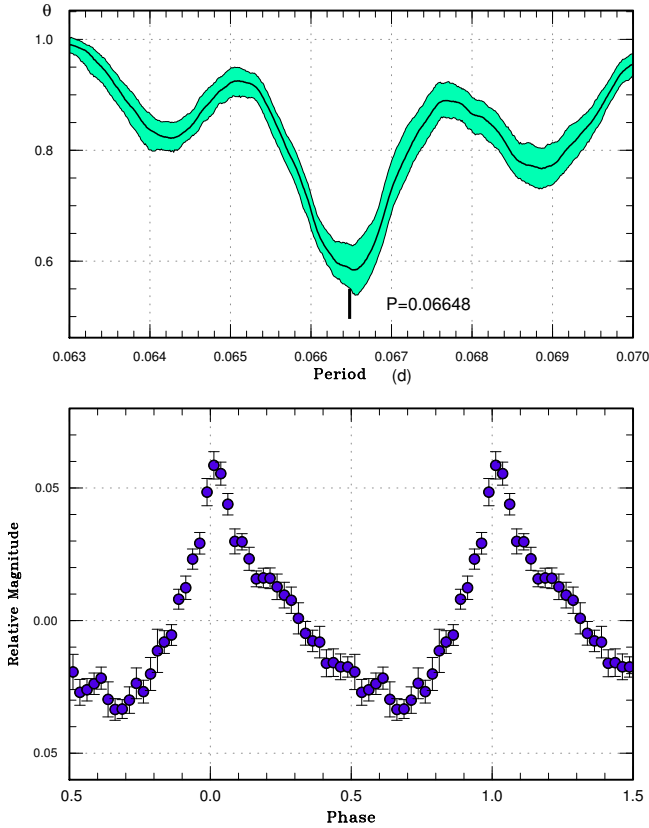


Fig. 112. Superhumps in ASASSN-17dg (2017). (Upper): PDM analysis. (Lower): Phase-averaged profile.

Table 93. Superhump maxima of CSS J062450 (2017)

$E$	max*	error	$O - C^\dagger$	$N^\ddagger$
0	57825.3383	0.0002	-0.0010	109
1	57825.4167	0.0003	-0.0002	109
2	57825.4944	0.0003	-0.0000	171
3	57825.5735	0.0009	0.0015	39
14	57826.4251	0.0006	-0.0003	88

\*BJD-2400000.

†Against max = 2457825.3393 + 0.077577E.

‡Number of points used to determine the maximum.

Table 94. List of likely superoutbursts of CSS J062450 in the ASAS-SN data

Year	Month	Day	max*	V-mag
2013	12	24	56651	14.31
2014	9	7	56908	14.61
2015	1	12	57035	14.70
2015	9	17	57283	14.79
2016	1	29	57416	14.74
2016	9	25	57657	14.94
2017	3	11	57823	14.59

\*JD-2400000.

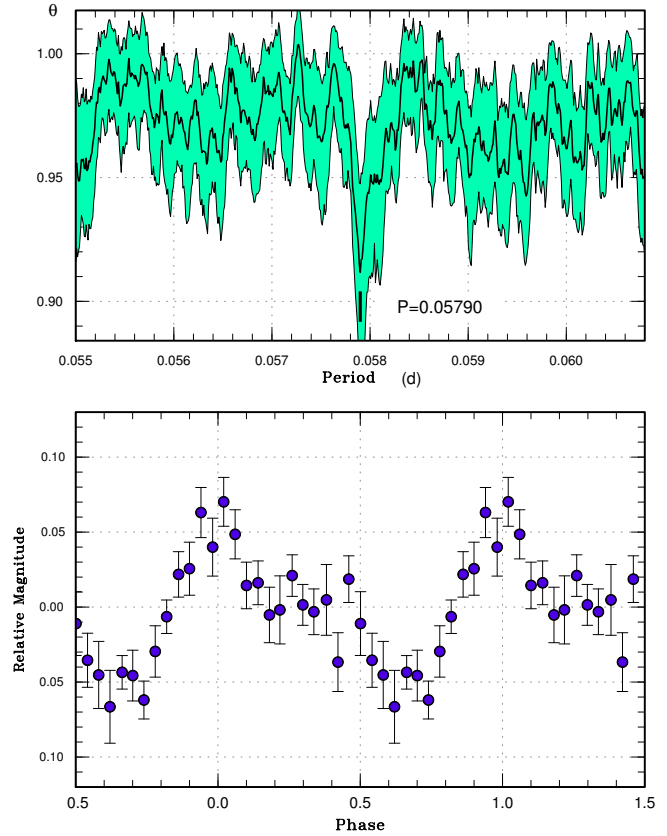


Fig. 113. Superhumps in ASASSN-17dq (2017). (Upper): PDM analysis. (Lower): Phase-averaged profile.

Table 95. Superhump maxima of DDE 26 (2016)

$E$	max*	error	$O - C^\dagger$	$N^\ddagger$
0	57605.5307	0.0011	0.0026	28
7	57606.1479	0.0011	-0.0018	96
8	57606.2347	0.0026	-0.0038	87
10	57606.4153	0.0011	-0.0008	107
11	57606.5091	0.0006	0.0042	128
33	57608.4582	0.0004	-0.0005	104
34	57608.5459	0.0004	-0.0016	104
44	57609.4372	0.0009	0.0017	186

\*BJD-2400000.

†Against max = 2457605.5281 + 0.088804E.

‡Number of points used to determine the maximum.

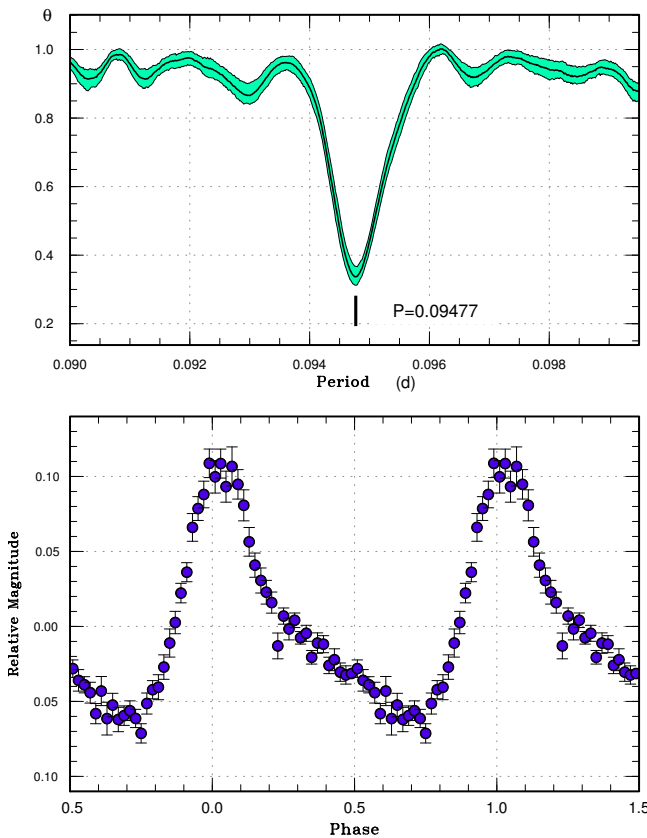


Fig. 114. Superhumps in CRTS J000130 (2016). (Upper): PDM analysis. (Lower): Phase-averaged profile.

Table 96. Superhump maxima of MASTER J021315

<i>E</i>	max*	error	<i>O</i> – <i>C</i> <sup>†</sup>	<i>N</i> <sup>‡</sup>
0	57665.4175	0.0008	–0.0077	84
1	57665.5308	0.0043	–0.0006	40
10	57666.4920	0.0012	0.0055	62
11	57666.5966	0.0006	0.0039	105
12	57666.7072	0.0046	0.0084	26
18	57667.3382	0.0009	0.0026	103
19	57667.4387	0.0009	–0.0031	98
20	57667.5458	0.0008	–0.0021	98
21	57667.6470	0.0010	–0.0069	100

\*BJD–2400000.

<sup>†</sup>Against max = 2457665.4252 + 0.106129*E*.

<sup>‡</sup>Number of points used to determine the maximum.

Table 97. Superhump maxima of MASTER J030205 (2016)

<i>E</i>	max*	error	<i>O</i> – <i>C</i> <sup>†</sup>	<i>N</i> <sup>‡</sup>
0	57728.2331	0.0010	–0.0010	94
1	57728.2942	0.0010	–0.0013	100
2	57728.3565	0.0008	–0.0006	92
3	57728.4166	0.0020	–0.0021	47
4	57728.4758	0.0055	–0.0044	21
6	57728.6009	0.0010	–0.0025	53
12	57728.9791	0.0005	0.0064	131
13	57729.0356	0.0004	0.0013	131
14	57729.1002	0.0003	0.0044	246
15	57729.1643	0.0014	0.0069	83
16	57729.2225	0.0009	0.0035	54
17	57729.2878	0.0008	0.0073	75
18	57729.3452	0.0003	0.0031	144
19	57729.4060	0.0003	0.0024	145
20	57729.4671	0.0003	0.0020	145
21	57729.5283	0.0006	0.0016	61
22	57729.5901	0.0006	0.0018	62
24	57729.7127	0.0005	0.0014	122
25	57729.7714	0.0006	–0.0015	122
26	57729.8386	0.0010	0.0041	88
34	57730.3253	0.0006	–0.0016	87
35	57730.3870	0.0004	–0.0014	119
36	57730.4466	0.0005	–0.0034	131
37	57730.5139	0.0009	0.0024	49
44	57730.9401	0.0004	–0.0024	131
45	57730.9987	0.0004	–0.0052	131
46	57731.0600	0.0003	–0.0055	129
50	57731.3076	0.0016	–0.0042	72
51	57731.3677	0.0012	–0.0056	72
52	57731.4258	0.0008	–0.0090	68
53	57731.4949	0.0011	–0.0015	72
54	57731.5572	0.0011	–0.0008	72
61	57731.9860	0.0011	–0.0029	135
62	57732.0482	0.0013	–0.0021	188
63	57732.1110	0.0006	–0.0009	175
64	57732.1765	0.0009	0.0030	99
65	57732.2313	0.0006	–0.0037	134
66	57732.3015	0.0012	0.0049	148
67	57732.3500	0.0010	–0.0081	129
68	57732.4179	0.0007	–0.0018	77
69	57732.4736	0.0008	–0.0077	132
70	57732.5429	0.0006	0.0001	127
71	57732.5997	0.0009	–0.0047	42
77	57732.9768	0.0011	0.0031	195
86	57733.5226	0.0006	–0.0051	77
87	57733.5912	0.0014	0.0019	40
92	57733.9053	0.0017	0.0083	79
93	57733.9625	0.0011	0.0039	131
94	57734.0291	0.0006	0.0090	131
95	57734.0879	0.0012	0.0062	130
96	57734.1450	0.0012	0.0018	94

\*BJD–2400000.

<sup>†</sup>Against max = 2457728.2340 + 0.061554*E*.

<sup>‡</sup>Number of points used to determine the maximum.

**Table 98.** Superhump maxima of MASTER J042609

<i>E</i>	max*	error	$O - C^\dagger$	phase <sup>‡</sup>	$N^\S$	<i>E</i>	max*	error	$O - C^\dagger$	phase <sup>‡</sup>	$N^\S$
1	57751.0076	0.0003	-0.0054	0.81	110	52	57754.4538	0.0003	0.0039	0.42	142
2	57751.0742	0.0004	-0.0062	0.82	123	53	57754.5229	0.0006	0.0056	0.47	142
3	57751.1419	0.0004	-0.0059	0.86	124	54	57754.5900	0.0005	0.0053	0.50	142
4	57751.2102	0.0011	-0.0050	0.90	87	55	57754.6570	0.0008	0.0049	0.52	130
5	57751.2779	0.0004	-0.0046	0.93	75	59	57754.9300	0.0005	0.0084	0.69	125
6	57751.3458	0.0004	-0.0042	0.97	159	60	57754.9956	0.0006	0.0066	0.69	170
7	57751.4152	0.0004	-0.0021	0.03	155	61	57755.0655	0.0007	0.0091	0.76	183
8	57751.4818	0.0005	-0.0029	0.05	141	62	57755.1309	0.0006	0.0071	0.75	198
9	57751.5504	0.0003	-0.0018	0.09	141	63	57755.1985	0.0007	0.0073	0.79	220
10	57751.6165	0.0004	-0.0030	0.10	139	64	57755.2694	0.0012	0.0108	0.87	78
15	57751.9509	0.0006	-0.0056	0.21	143	67	57755.4664	0.0020	0.0056	0.88	89
16	57752.0203	0.0005	-0.0036	0.27	192	68	57755.5360	0.0008	0.0078	0.94	133
17	57752.0878	0.0003	-0.0035	0.30	205	74	57755.9393	0.0006	0.0069	0.10	141
18	57752.1528	0.0003	-0.0059	0.29	208	75	57756.0042	0.0009	0.0043	0.09	180
19	57752.2207	0.0004	-0.0053	0.33	83	76	57756.0737	0.0008	0.0064	0.15	207
20	57752.2890	0.0003	-0.0044	0.37	353	77	57756.1393	0.0010	0.0047	0.15	206
21	57752.3566	0.0003	-0.0042	0.40	415	78	57756.2036	0.0008	0.0015	0.13	143
22	57752.4244	0.0004	-0.0038	0.44	360	89	57756.9424	0.0018	-0.0009	0.41	189
23	57752.4892	0.0005	-0.0064	0.42	412	90	57757.0174	0.0047	0.0067	0.56	194
24	57752.5560	0.0005	-0.0070	0.44	120	91	57757.0746	0.0028	-0.0035	0.43	204
30	57752.9671	0.0012	-0.0002	0.72	196	104	57757.9562	0.0011	0.0020	0.89	83
31	57753.0344	0.0011	-0.0003	0.75	188	105	57758.0257	0.0012	0.0042	0.95	131
32	57753.1046	0.0011	0.0025	0.82	208	106	57758.0938	0.0030	0.0048	0.99	203
33	57753.1710	0.0012	0.0015	0.83	83	107	57758.1676	0.0014	0.0112	0.12	122
34	57753.2392	0.0007	0.0023	0.88	260	108	57758.2239	0.0011	0.0002	0.98	80
35	57753.3059	0.0005	0.0017	0.89	259	111	57758.4286	0.0008	0.0027	0.10	45
36	57753.3736	0.0007	0.0019	0.93	291	112	57758.5044	0.0040	0.0111	0.26	38
44	57753.9145	0.0008	0.0037	0.18	124	113	57758.5567	0.0007	-0.0040	0.06	54
45	57753.9883	0.0018	0.0101	0.31	101	118	57758.8918	0.0006	-0.0059	0.17	96
46	57754.0502	0.0008	0.0047	0.26	179	119	57758.9642	0.0010	-0.0008	0.28	125
47	57754.1160	0.0008	0.0030	0.26	203	120	57759.0254	0.0009	-0.0070	0.21	109
48	57754.1820	0.0007	0.0017	0.27	228	121	57759.0969	0.0014	-0.0029	0.30	126
49	57754.2526	0.0003	0.0048	0.35	273	122	57759.1578	0.0013	-0.0093	0.23	123
50	57754.3206	0.0004	0.0054	0.38	207	126	57759.4043	0.0016	-0.0324	1.00	59
51	57754.3869	0.0004	0.0044	0.40	133	127	57759.4710	0.0039	-0.0331	0.01	74

\*BJD-2400000.

†Against max = 2457750.9456 + 0.067390*E*.

‡Orbital phase.

§Number of points used to determine the maximum.

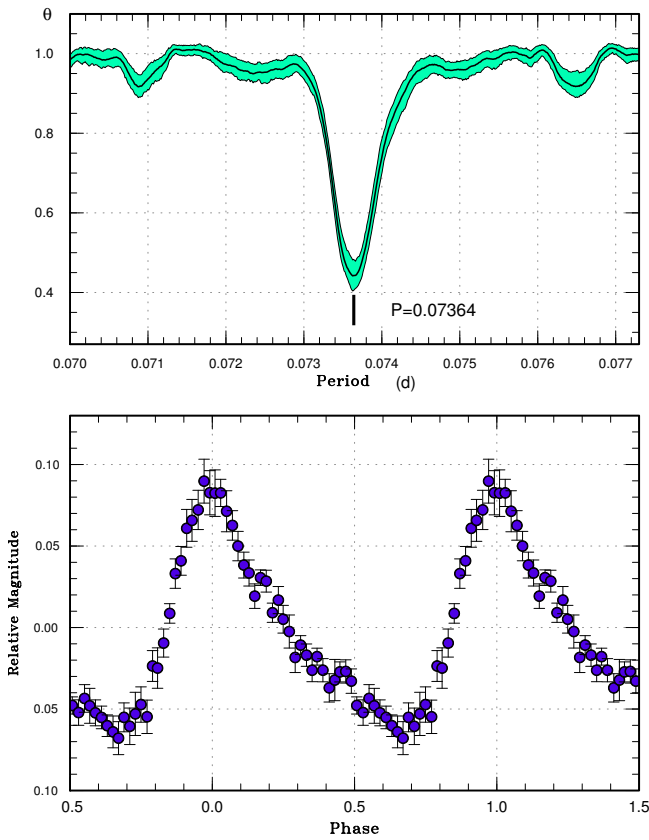


**Fig. 115.** Superhumps in CRTS J023638 (2016). (Upper): PDM analysis. The data during the superoutburst plateau (before BJD 2457641) were used. (Lower): Phase-averaged profile.

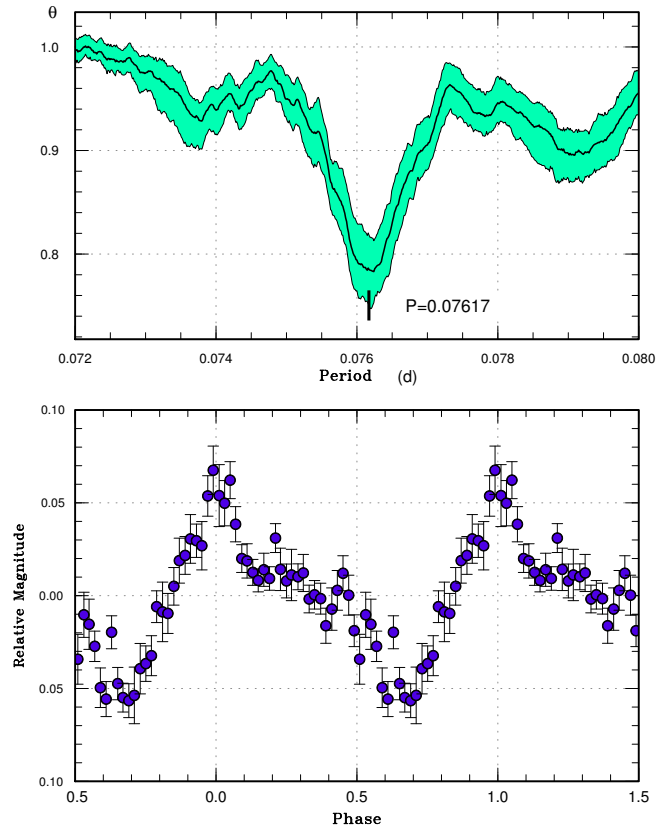


**Fig. 116.** Superhumps in CRTS J033349 (2016). (Upper): PDM analysis. (Lower): Phase-averaged profile.

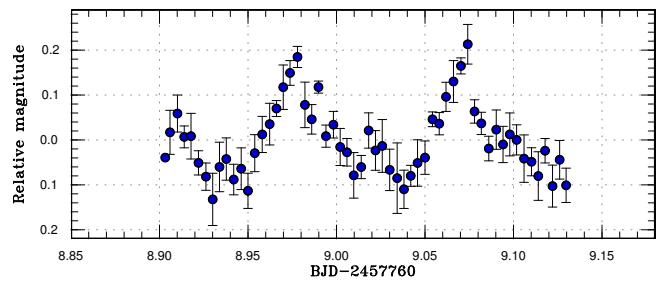


**Fig. 117.** Superhump in CRTS J044637 (2017). The data were binned to 0.004 d.

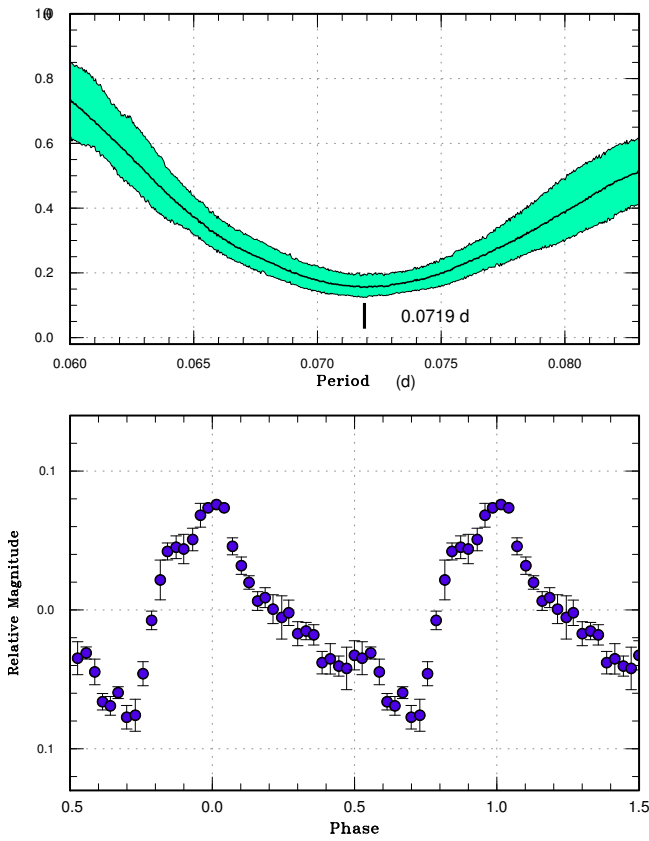


Fig. 118. Superhumps in CRTS J082603 (2017). (Upper): PDM analysis. (Lower): Phase-averaged profile.

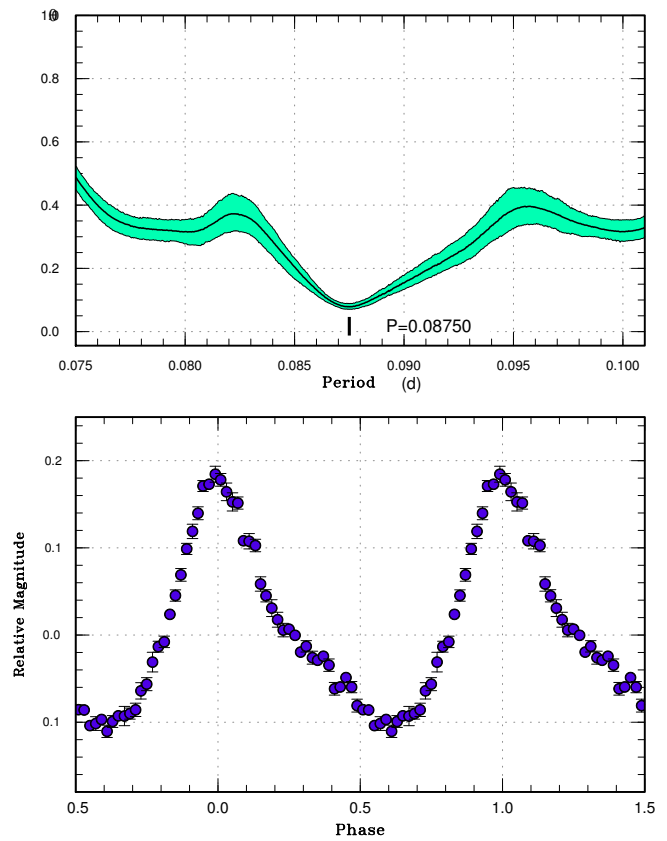


Fig. 120. Superhumps in CRTS J085113 (2016). (Upper): PDM analysis. (Lower): Phase-averaged profile.

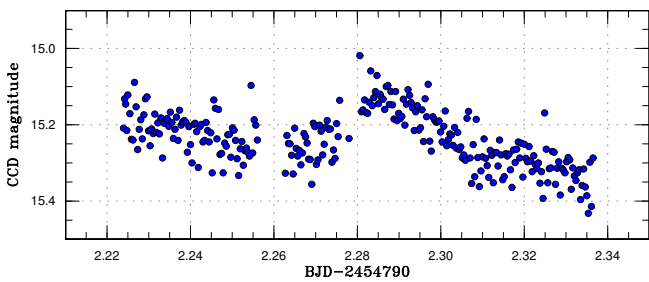


Fig. 119. Superhump in CRTS J085113 (2008).



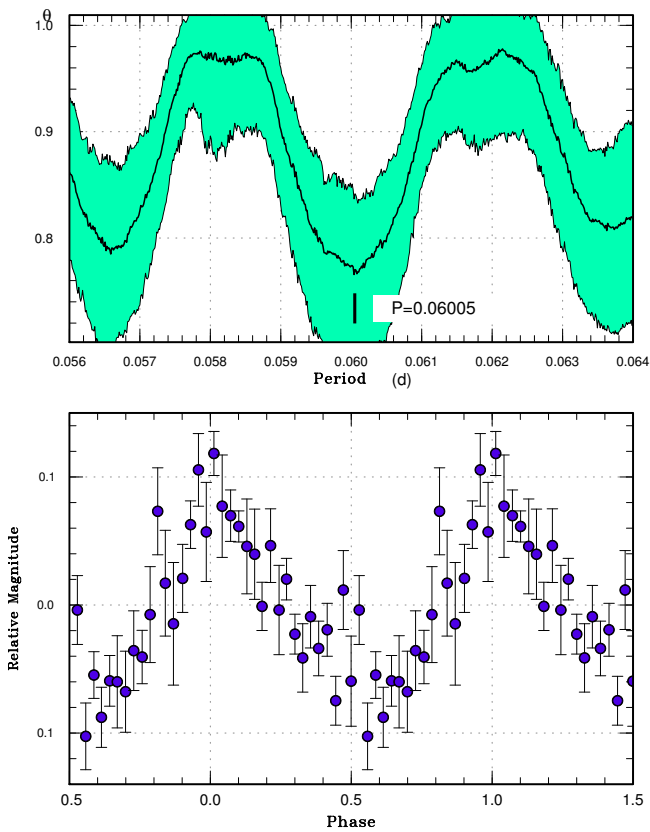


Fig. 121. Superhumps in CRTS J085603 (2016). (Upper): PDM analysis. (Lower): Phase-averaged profile.

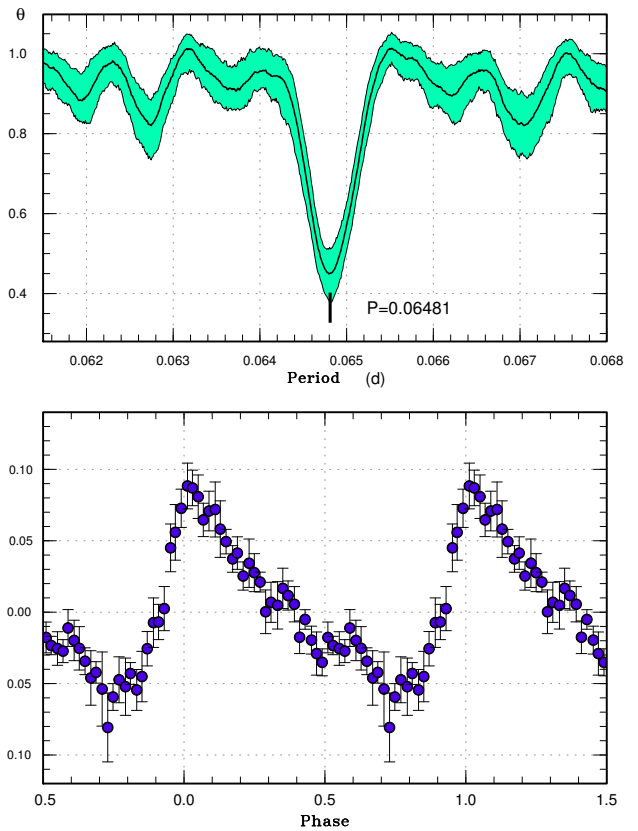


Fig. 123. Superhumps in CRTS J164950 (2016). (Upper): PDM analysis. (Lower): Phase-averaged profile.

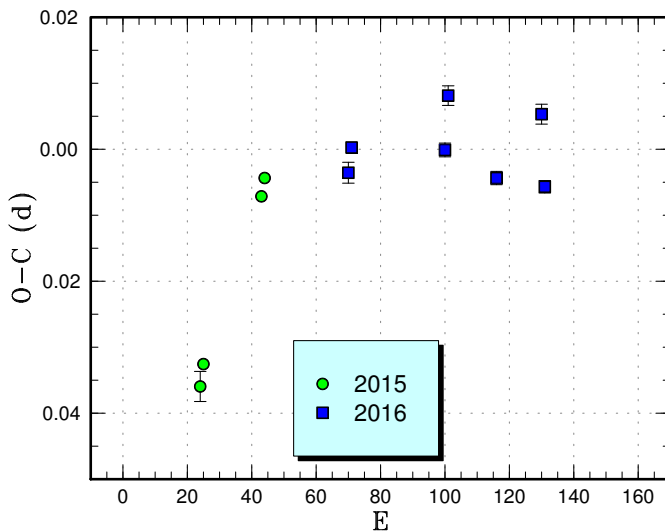


Fig. 122. Comparison of  $O - C$  diagrams of CRTS J164950 between different superoutbursts. A period of 0.06490 d was used to draw this figure. Approximate cycle counts ( $E$ ) after the start of the superoutburst were used.

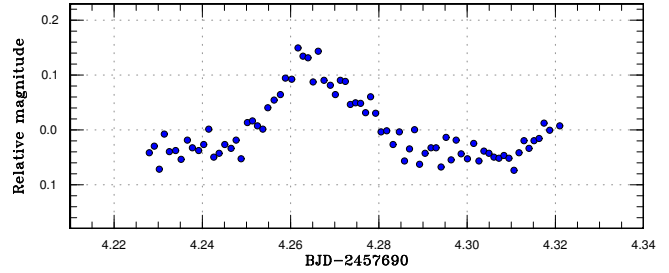
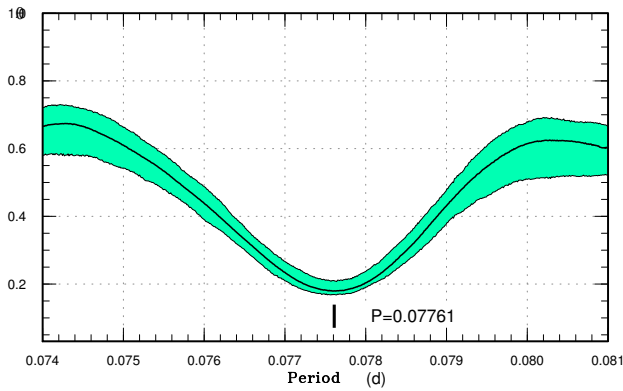


Fig. 126. Superhump in DDE 48 (2016).

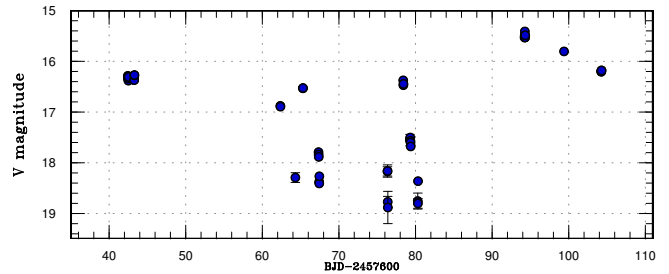
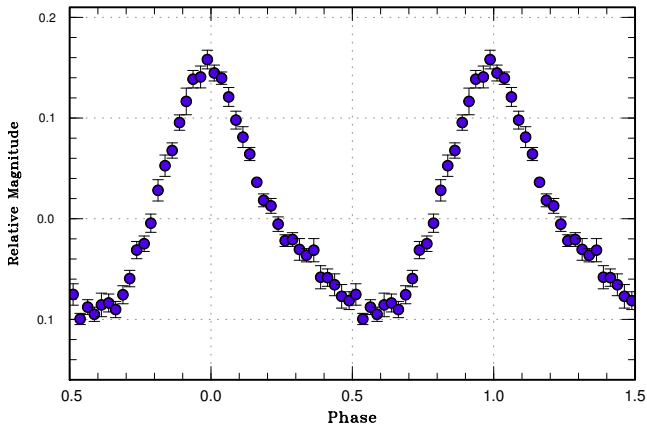


Fig. 127. Light curve of DDE 48 (2016). The data were binned to 0.002 d.

Fig. 124. Superhumps in CSS J062450 (2016). (Upper): PDM analysis. (Lower): Phase-averaged profile.

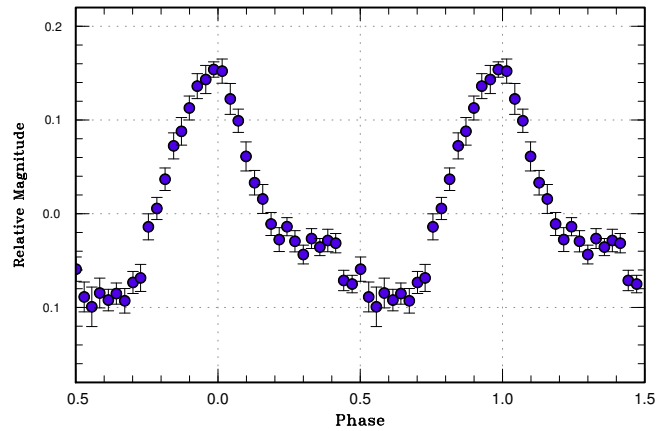
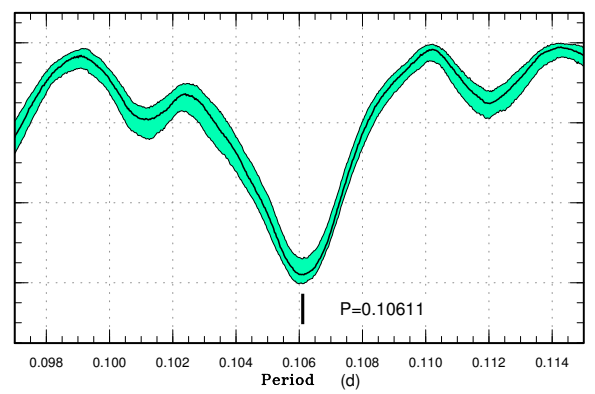


Fig. 128. Superhumps in MASTER J021315 (2016). (Upper): PDM analysis. (Lower): Phase-averaged profile.

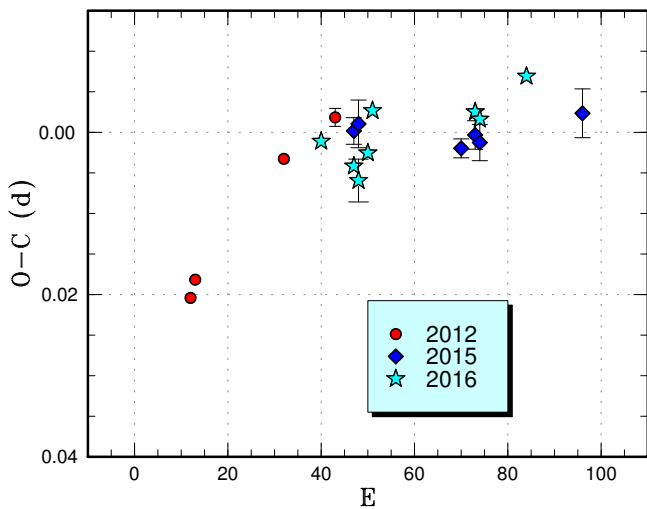


Fig. 125. Comparison of  $O - C$  diagrams of DDE 26 between different superoutbursts. A period of 0.08860 d was used to draw this figure. Approximate cycle counts ( $E$ ) after the start of the superoutburst were used.

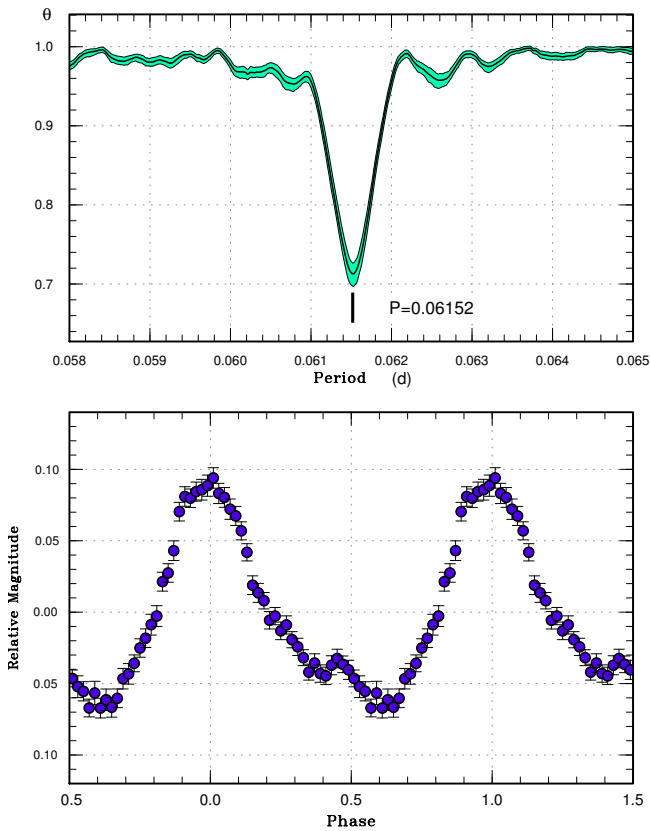


Fig. 129. Superhumps in MASTER J030205 (2016). (Upper): PDM analysis. (Lower): Phase-averaged profile.

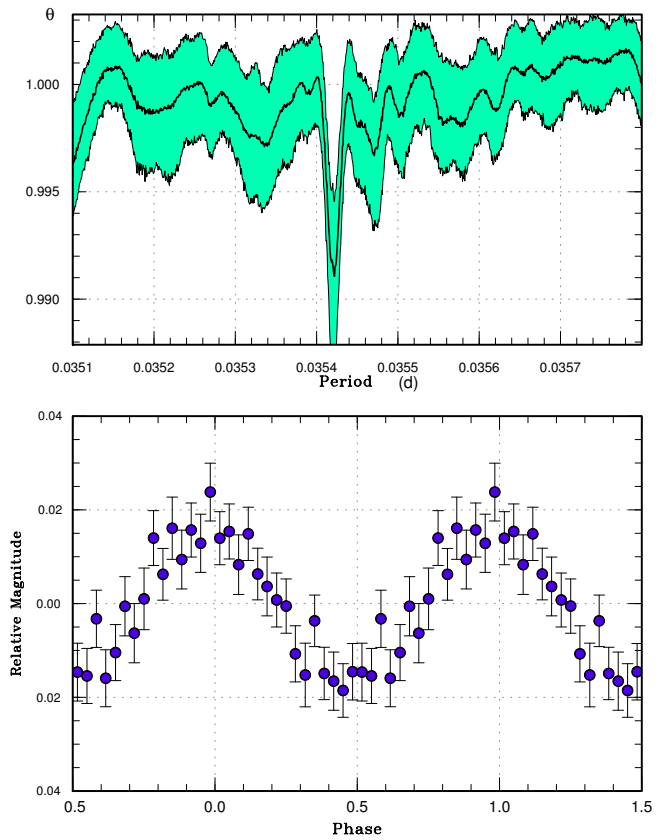


Fig. 130. Possible intermediate-polar-type signal in MASTER J030205 (2016). (Upper): PDM analysis. (Lower): Phase-averaged profile.

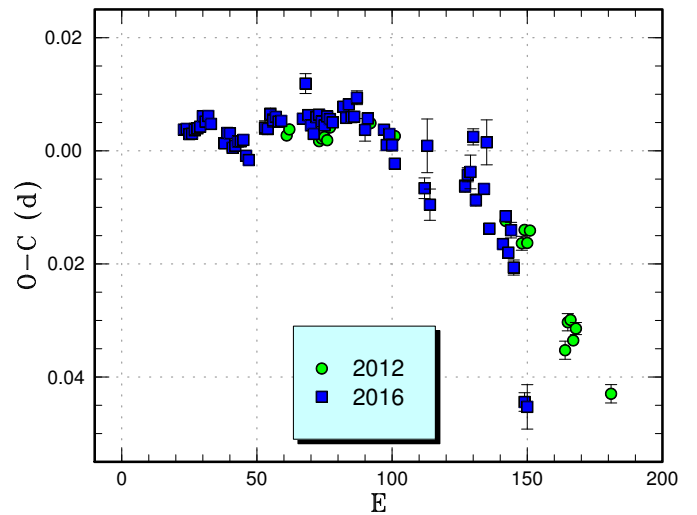


Fig. 131. Comparison of  $O - C$  diagrams of MASTER J042609 between different superoutbursts. A period of 0.06756 d was used to draw this figure. Approximate cycle counts ( $E$ ) after the outburst detection were used. The 2012 superoutburst was shifted by 20 cycles to match the 2016 one.

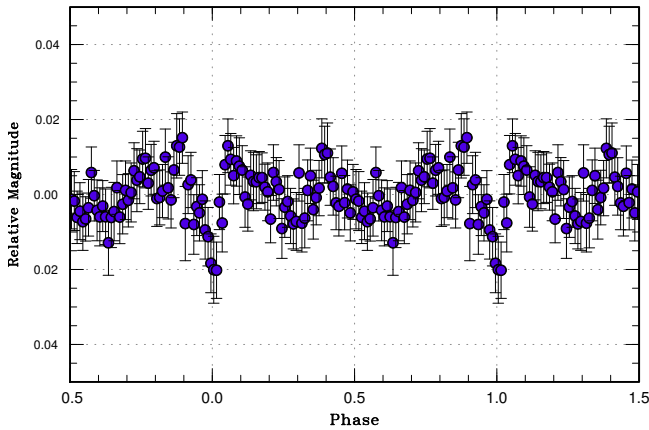


Fig. 132. Eclipse profile in MASTER J042609 (2016). The superhumps were mostly removed by using LOWESS. The phase-averaged profile was drawn against the ephemeris  $\text{BJD } 2456276.6430 + 0.06550168E$ .

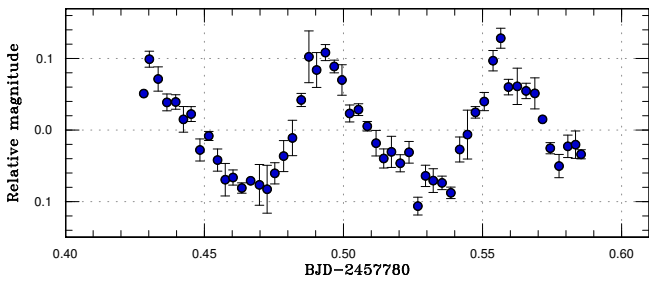


Fig. 133. Superhump in MASTER J043220 (2017). The data were binned to 0.003 d.

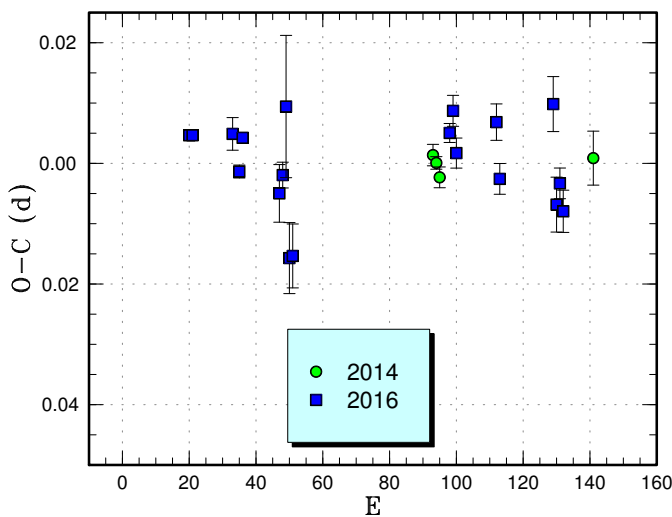


Fig. 134. Comparison of  $O - C$  diagrams of MASTER J043915 between different superoutbursts. A period of 0.06243 d was used to draw this figure. Approximate cycle counts ( $E$ ) after the start of the superoutburst were used.

Table 99. Superhump maxima of MASTER J043915 (2016)

$E$	max*	error	$O - C^\dagger$	$N^\ddagger$
0	57746.2392	0.0003	0.0045	150
1	57746.3016	0.0003	0.0045	149
13	57747.0510	0.0027	0.0048	47
15	57747.1696	0.0011	-0.0015	83
16	57747.2376	0.0004	0.0041	137
27	57747.9151	0.0048	-0.0050	42
28	57747.9806	0.0021	-0.0020	43
29	57748.0544	0.0118	0.0094	43
30	57748.0917	0.0059	-0.0158	42
31	57748.1545	0.0053	-0.0154	32
78	57751.1091	0.0016	0.0051	42
79	57751.1752	0.0026	0.0088	43
80	57751.2306	0.0025	0.0018	15
92	57751.9849	0.0030	0.0069	43
93	57752.0379	0.0026	-0.0025	43
109	57753.0492	0.0046	0.0100	24
110	57753.0950	0.0046	-0.0067	43
111	57753.1609	0.0025	-0.0032	42
112	57753.2187	0.0035	-0.0078	33

\*BJD-2400000.

†Against max =  $2457746.2346 + 0.062428E$ .

‡Number of points used to determine the maximum.

Table 100. Superhump maxima of MASTER J054746 (2016)

$E$	max*	error	$O - C^\dagger$	$N^\ddagger$
0	57674.4439	0.0012	0.0008	52
1	57674.4982	0.0016	-0.0008	44
2	57674.5539	0.0014	-0.0009	56
3	57674.6117	0.0015	0.0009	56

\*BJD-2400000.

†Against max =  $2457674.4430 + 0.055927E$ .

‡Number of points used to determine the maximum.

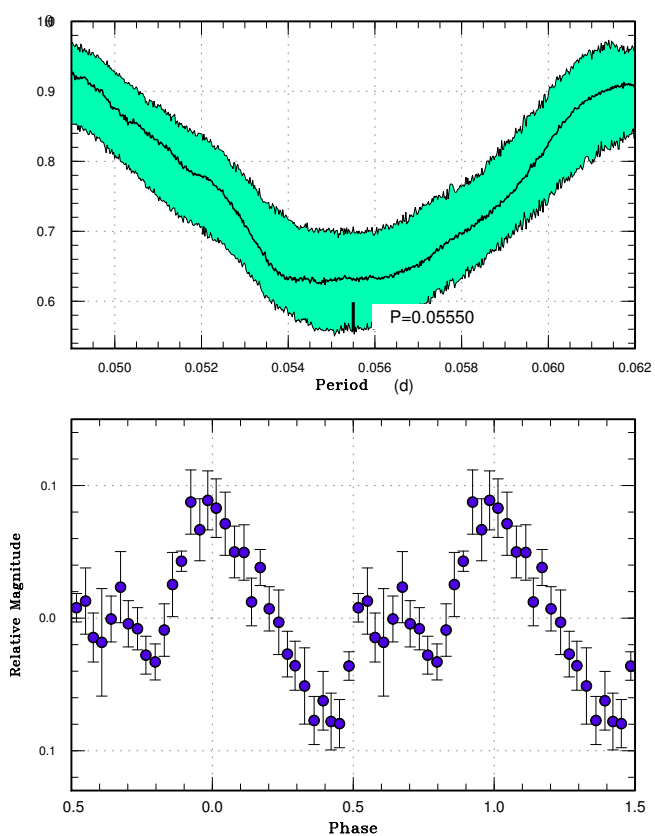


Fig. 135. Superhumps in MASTER J054746 (2016). (Upper): PDM analysis. (Lower): Phase-averaged profile.

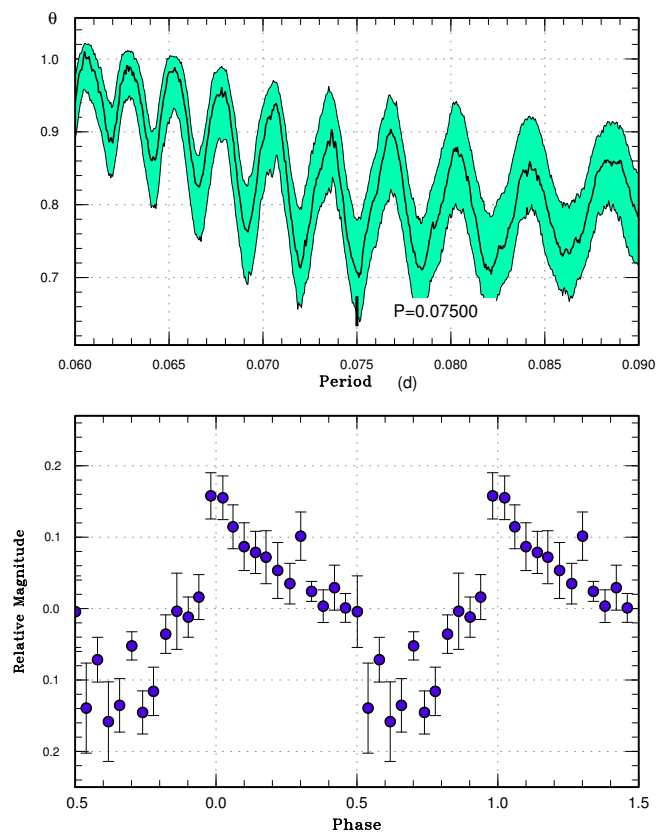


Fig. 136. Superhumps in MASTER J055348 (2017). (Upper): PDM analysis. The selected period was one of the possibilities. (Lower): Phase-averaged profile.

**Table 101.** Superhump maxima of MASTER J055348 (2017)

$E$	max*	error	$O - C^\dagger$	$N^\ddagger$
0	57803.3236	0.0010	0.0035	47
1	57803.3917	0.0010	-0.0035	53
23	57805.0467	0.0022	-0.0014	65
24	57805.1248	0.0028	0.0015	77

\*BJD-2400000.

 $^\dagger$ Against max = 2457803.3201 + 0.075130E. $^\ddagger$ Number of points used to determine the maximum.**Table 102.** Superhump maxima of MASTER J055845 (2016)

$E$	max*	error	$O - C^\dagger$	$N^\ddagger$
0	57647.5355	0.0018	0.0015	13
1	57647.5904	0.0016	-0.0017	35
17	57648.5226	0.0017	0.0009	42
18	57648.5800	0.0016	0.0001	30
19	57648.6370	0.0023	-0.0009	26

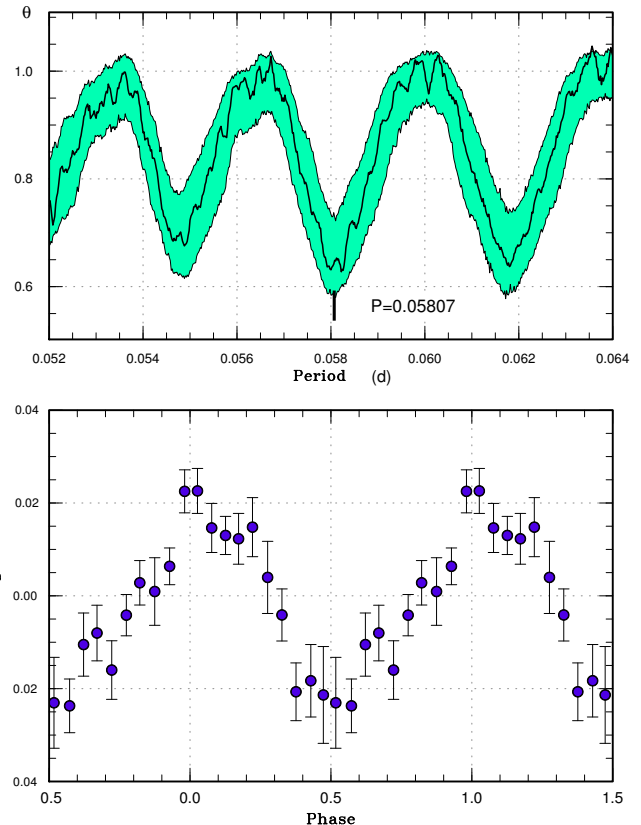
\*BJD-2400000.

 $^\dagger$ Against max = 2457647.5340 + 0.058102E. $^\ddagger$ Number of points used to determine the maximum.

### 3.106 MASTER OT J055845.55+391533.4

This optical transient (hereafter MASTER J055845) was detected on 2014 February 19 at a magnitude of 14.4 (Yecheistov et al. 2014). During the 2014 superoutburst, single-night observations detected superhumps (likely stage C ones) with a period of 0.0563(4) d (Kato et al. 2015a).

The 2016 outburst was detected by the ASAS-SN team at  $V=15.24$  on September 14. The object was on the rise at  $V=16.51$  on September 7. Rather queerly, the object was also detected at  $V=14.16$  on August 30. There were no observations between August 30 and September 7. Three-night observations starting on September 16 detected superhumps (vsnet-alert 20186). During these observations, the object brightened from 15.4 mag (September 16) to 15.2 mag (September 18). Superhumps were recorded on the first two nights (table 102). The period in table 3 was determined by the PDM method (figure 137). Since the recorded outburst behavior was rather strange, we could not determine the superhump stage. The reason of the large difference of superhump periods between 2014 and 2016 is unclear. The 2014 observations were single-night ones and there were no possibility of an alias and the 2014 period could not satisfy the 2016 data. More observations are apparently needed.

**Fig. 137.** Superhumps in MASTER J055845 (2016). (Upper): PDM analysis. (Lower): Phase-averaged profile.

### 3.107 MASTER OT J064725.70+491543.9

This object (hereafter MASTER J064725) was discovered as a transient at an unfiltered CCD magnitude of 13.2 mag on 2013 March 7 by the MASTER network (Tiurina et al. 2013). Subsequent observations detected superhumps (Kato et al. 2014b).

The 2016 superoutburst was detected by the ASAS-SN team at  $V=13.99$  on December 13. Time-resolved photometry started on December 17 and stage A superhumps were not recorded. The times of superhump maxima are listed in table 103. The 2016 observations, which were obtained in poorer conditions than in the 2013 observations, likely resulted a mixture of stages B and C (figure 138). Due to the limited number of superhumps maxima, we could not determine the periods for these stages individually.

### 3.108 MASTER OT J065330.46+251150.9

This object (hereafter MASTER J065330) was discovered as a transient at an unfiltered CCD magnitude of 15.9 mag on 2014 February 16 by the MASTER network (Echeistov

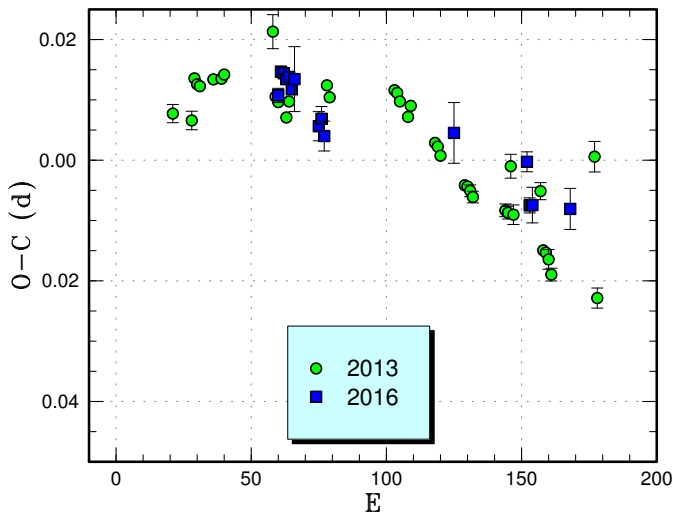


Fig. 138. Comparison of  $O - C$  diagrams of MASTER J064725 between different superoutbursts. A period of 0.06777 d was used to draw this figure. Approximate cycle counts ( $E$ ) after the start of the superoutburst were used.

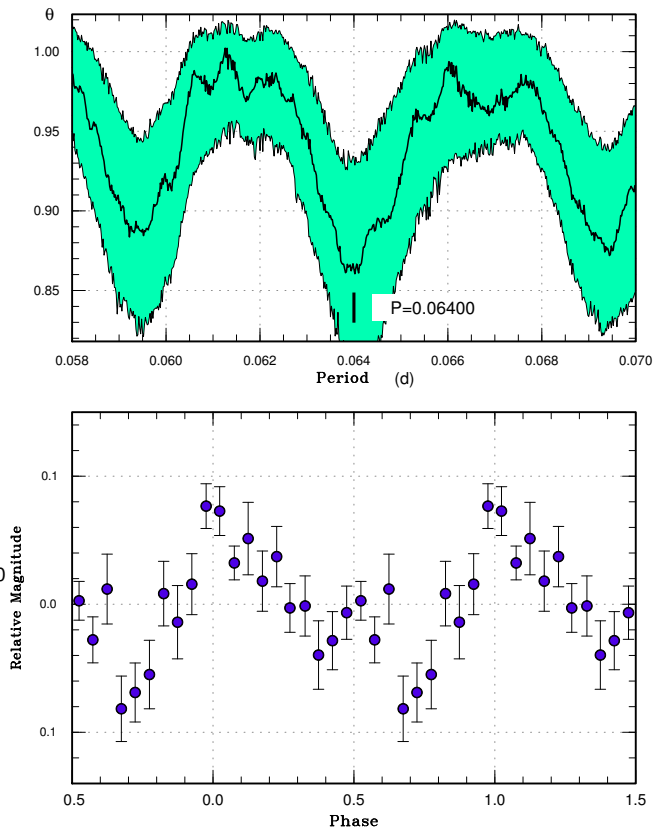


Fig. 139. Superhumps in MASTER J065330 (2017). (Upper): PDM analysis. (Lower): Phase-averaged profile.

Table 103. Superhump maxima of MASTER J064725 (2016)

$E$	max*	error	$O - C^\dagger$	$N^\ddagger$
0	57739.9678	0.0012	-0.0017	39
1	57740.0395	0.0007	0.0024	74
2	57740.1070	0.0007	0.0023	76
3	57740.1738	0.0008	0.0015	76
4	57740.2419	0.0008	0.0021	75
5	57740.3076	0.0008	0.0002	76
6	57740.3771	0.0054	0.0021	25
15	57740.9792	0.0024	-0.0040	58
16	57741.0482	0.0020	-0.0026	65
17	57741.1131	0.0025	-0.0053	67
65	57744.3666	0.0050	0.0042	49
92	57746.1916	0.0017	0.0044	21
93	57746.2522	0.0013	-0.0026	25
94	57746.3200	0.0030	-0.0024	20
108	57747.2681	0.0034	-0.0004	13

\*BJD-2400000.

$^\dagger$ Against max = 2457739.9695 + 0.067584E.

$^\ddagger$ Number of points used to determine the maximum.

Table 104. Superhump maxima of MASTER J065330 (2017)

$E$	max*	error	$O - C^\dagger$	$N^\ddagger$
0	57780.2944	0.0008	0.0004	64
1	57780.3575	0.0010	-0.0006	54
12	57781.0643	0.0128	0.0021	40
13	57781.1244	0.0027	-0.0018	67

\*BJD-2400000.

$^\dagger$ Against max = 2457780.2941 + 0.064012E.

$^\ddagger$ Number of points used to determine the maximum.

et al. 2014). The 2017 outburst was detected by the ASAS-SN team at  $V=15.89$  on January 23. Subsequent observations detected superhumps (vsnet-alert 20612; figure 139). The times of superhump maxima are listed in table 104. According to the ASAS-SN data, there was another long outburst (superoutburst) on 2015 September 17.

### 3.109 MASTER OT J075450.18+091020.2

This object (hereafter MASTER J075450) was discovered as a transient at an unfiltered CCD magnitude of 16.0 mag on 2013 November 7 by the MASTER network

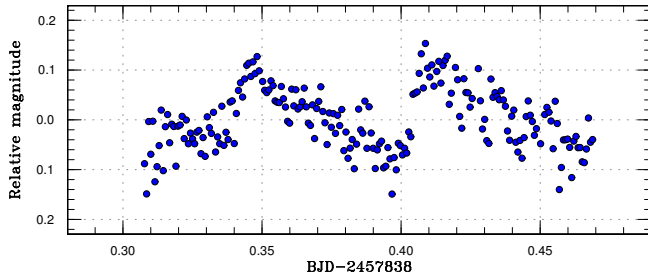


Fig. 140. Superhump in MASTER J075450 (2017).

Table 105. Superhump maxima of MASTER J150518 (2017)

$E$	max*	error	$O - C^\dagger$	$N^\ddagger$
0	57797.8081	0.0013	-0.0040	18
14	57798.8103	0.0011	0.0022	31
28	57799.8090	0.0026	0.0048	30
56	57801.7933	0.0038	-0.0030	23

\*BJD-2400000.

$^\dagger$  Against max = 2457797.8121 + 0.071145E.

$^\ddagger$  Number of points used to determine the maximum.

(Vladimirov et al. 2013). The 2017 outburst was detected by the ASAS-SN team at  $V=16.36$  on March 24. The object was then found to be already in outburst at  $V=16.39$  on March 22. Observations on March 25–26 detected superhumps (vsnet-alert 20821; figure 140). The times of superhump maxima were BJD 2457838.3515(8) ( $N=71$ ) and 2457838.4172(8) ( $N=68$ ). The superhump period determined by the PDM method was 0.0664(5) d. There was also a most likely superoutburst in the ASAS-SN data on 2015 January 20 with a maximum of  $V=16.08$ .

### 3.110 MASTER OT J150518.03–143933.6

This object (hereafter MASTER J150518) was discovered as a transient at an unfiltered CCD magnitude of 15.5 mag on 2017 February 8 by the MASTER network (Gress et al. 2017). This transient was also detected by the ASAS-SN team (ASASSN-17cb) at  $V=15.4$  on the same night, but the announcement was made after confirmation at  $V=15.1$  on February 11. Although only the late course of the outburst was observed, superhumps were recorded (vsnet-alert 20660). Since observations only recorded one superhump maximum on each night, the one-day alias could not be resolved. We selected one of them to minimize the  $\theta$  of the PDM analysis to make cycle counts in table 105. Although the large negative global  $P_{\text{dot}}$  may have reflected stage B-C transition, the quality of the data were insufficient to confirm it.

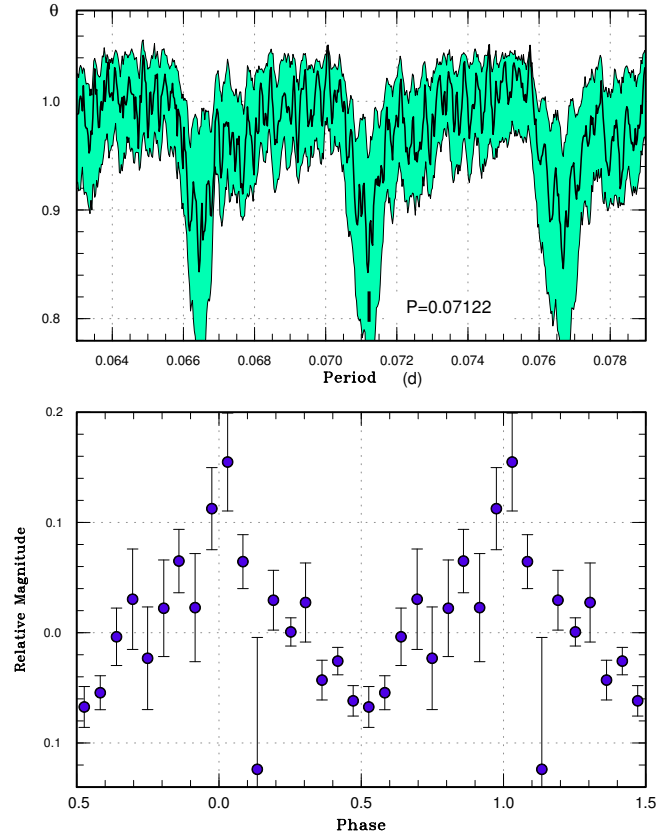


Fig. 141. Superhumps in MASTER J150518 (2017). (Upper): PDM analysis. (Lower): Phase-averaged profile.

### 3.111 MASTER OT J151126.74–400751.9

This object (hereafter MASTER J151126) was discovered as a transient at an unfiltered CCD magnitude of 14.0 mag on 2016 March 18 by the MASTER network (Popova et al. 2016). Subsequent observations detected superhumps (vsnet-alert 19614, 19630; figure 142). The times of superhump maxima are listed in table 106. We interpreted that most of our observations recorded stage B as judged from a positive  $P_{\text{dot}}$  expected for this  $P_{\text{SH}}$ . The outburst faded on April 3. The duration of the outburst was at least 16 d.

### 3.112 MASTER OT J162323.48+782603.3

This object (hereafter MASTER J162323) was detected as a transient at an unfiltered CCD magnitude of 13.2 mag on 2013 December 9 by the MASTER network (Denisenko et al. 2013a). The 2013 superoutburst was well observed (Kato et al. 2014a).

The 2015 superoutburst was detected at  $V=13.49$  on August 10 by the ASAS-SN team. Double-wave modulations were recorded on August 22 (vsnet-alert 19004).



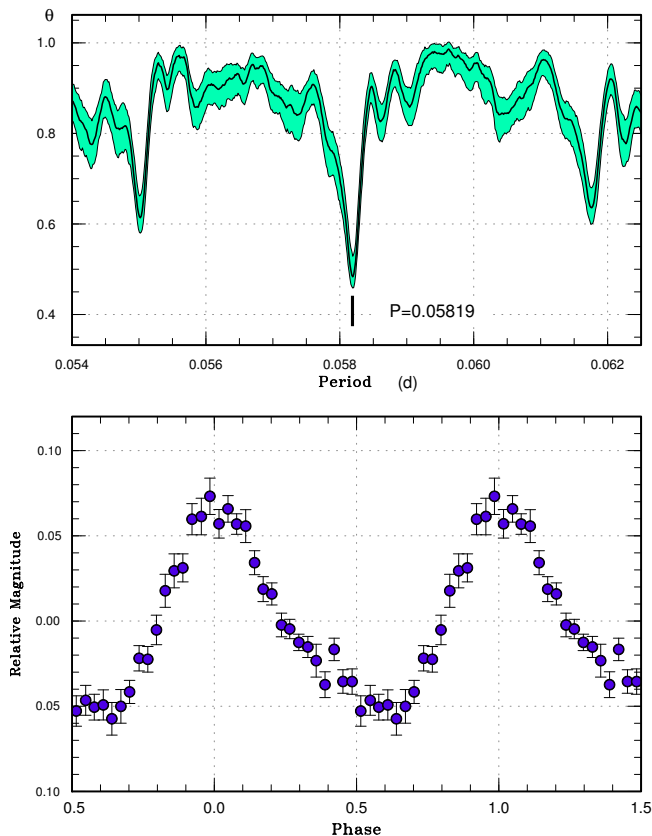


Fig. 142. Superhumps in MASTER J151126 (2016). (Upper): PDM analysis. The data during the superoutburst plateau (before BJD 2457480) were used. (Lower): Phase-averaged profile.

Table 106. Superhump maxima of MASTER J151126 (2016)

$E$	max*	error	$O - C^\dagger$	$N^\ddagger$
0	57468.8045	0.0006	-0.0032	14
16	57469.7426	0.0006	0.0039	28
17	57469.8009	0.0007	0.0039	19
30	57470.5560	0.0011	0.0027	72
31	57470.6139	0.0003	0.0023	134
32	57470.6697	0.0016	-0.0001	51
51	57471.7718	0.0009	-0.0036	25
84	57473.6907	0.0011	-0.0049	30
85	57473.7514	0.0011	-0.0023	30
102	57474.7389	0.0009	-0.0040	18
153	57477.7113	0.0014	0.0008	32
154	57477.7670	0.0056	-0.0018	18
170	57478.7027	0.0011	0.0029	32
171	57478.7614	0.0016	0.0035	19

\*BJD-2400000.

†Against max = 2457468.8077 + 0.058188E.

‡Number of points used to determine the maximum.

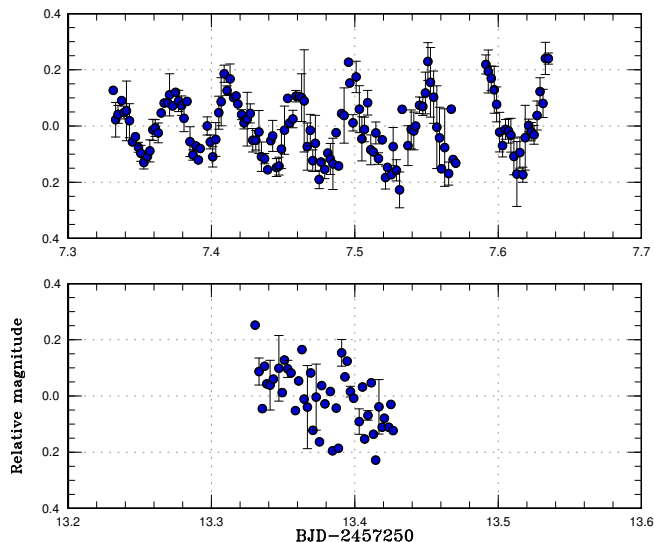


Fig. 143. Superhump-like double wave modulations in MASTER J162323 (2015). The data were binned to 0.002 d. The variations were only recorded on BJD 2457255 (August 22) and they disappeared 6 d later.

Table 107. Superhump maxima of MASTER J162323 (2016)

$E$	max*	error	$O - C^\dagger$	$N^\ddagger$
0	57659.3470	0.0001	0.0003	146
1	57659.4361	0.0003	-0.0004	77
4	57659.7062	0.0003	0.0001	174

\*BJD-2400000.

†Against max = 2457659.3467 + 0.089866E.

‡Number of points used to determine the maximum.

These variations disappeared 6 d later (see figure 143). Since these observations covered only the last (and likely post-superoutburst) phase of the superoutburst and the nature of humps is unclear, we did not use these data for comparison with other superoutbursts.

There was an outburst at  $V=13.46$  on 2016 April 22 (ASAS-SN detection). Subsequent observations did not detect superhumps (observers: Shugarov team and Akazawa). There was another outburst at  $V=13.34$  on 2016 September 26 (ASAS-SN detection). Three superhumps were recorded during this superoutburst (table 107). These superhumps were likely obtained around transition from stage A to B (figure 144) and the period [0.09013(7) d, PDM method] is not listed in table 3.

### 3.113 MASTER OT J165153.86+702525.7

This object (hereafter MASTER J165153) was detected as a transient at an unfiltered CCD magnitude of 15.9 on 2013 May 23 by the MASTER network (Shurpakov et al. 2013b).

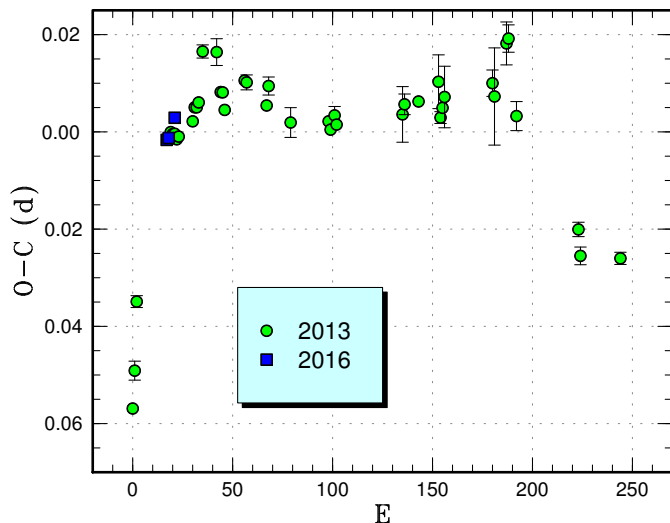


**Fig. 144.** Comparison of  $O - C$  diagrams of MASTER J162323 between different superoutbursts. A period of 0.08866 d was used to draw this figure. Approximate cycle counts ( $E$ ) after the start of the superoutburst were used. We shifted the 2016  $O - C$  diagram by 25 cycles to match the well-observed 2015 one.

**Table 108.** Superhump maxima of MASTER J165153 (2017)

$E$	max*	error	$O - C^\dagger$	$N^\ddagger$
0	57797.4370	0.0007	-0.0015	41
1	57797.5098	0.0004	-0.0007	65
2	57797.5817	0.0004	-0.0007	62
16	57798.5899	0.0009	0.0002	68
17	57798.6654	0.0007	0.0037	66
18	57798.7371	0.0022	0.0034	34
29	57799.5199	0.0044	-0.0052	24
30	57799.5975	0.0005	0.0005	71
31	57799.6694	0.0006	0.0004	71

\*BJD-2400000.

$^\dagger$ Against max = 2457797.4385 + 0.071951 $E$ .

$^\ddagger$ Number of points used to determine the maximum.

The 2017 outburst was detected by the ASAS-SN team at  $V=14.64$  on February 4. Subsequent observations detected superhumps (vsnet-alert 20659; figure 145). The times of superhump maxima are listed in table 108.

### 3.114 MASTER OT J174816.22+501723.3

This object (hereafter MASTER J174816) was discovered as a transient at an unfiltered CCD magnitude of 15.6 mag on 2013 June 28 by the MASTER network (Denisenko et al. 2013b). The object has a blue SDSS counterpart ( $g=17.59$ ). At least nine outbursts were recorded in the CRTS data. The object has a bright ( $J=15.55$ ) 2MASS counterpart, suggesting that the object was in outburst during 2MASS

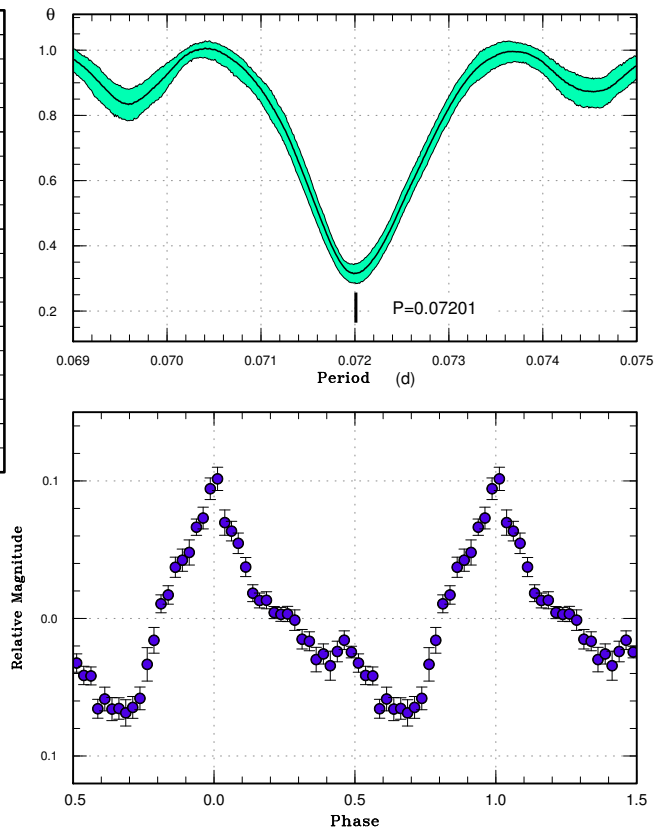


**Fig. 145.** Superhumps in MASTER J165153 (2017). (Upper): PDM analysis. (Lower): Phase-averaged profile.

**Table 109.** Superhump maxima of MASTER J174816 (2016)

$E$	max*	error	$O - C^\dagger$	$N^\ddagger$
0	57473.5497	0.0012	0.0012	83
1	57473.6305	0.0006	-0.0014	84
20	57475.2172	0.0016	0.0021	57
21	57475.2965	0.0017	-0.0019	73

\*BJD-2400000.

$^\dagger$ Against max = 2457473.5485 + 0.083328 $E$ .

$^\ddagger$ Number of points used to determine the maximum.

scans.

The 2016 outburst was detected by the ASAS-SN team at  $V=15.50$  on March 25. Subsequent observations detected superhumps (vsnet-alert 19642; figure 146). The times of superhump maxima are listed in table 109. Although we adopted a period of 0.08342(4) d (PDM method), an alias of 0.07950(4) d could not be excluded.

### 3.115 MASTER OT J211322.92+260647.4

This object (hereafter MASTER J211322) was discovered by the MASTER network at an unfiltered CCD mag-

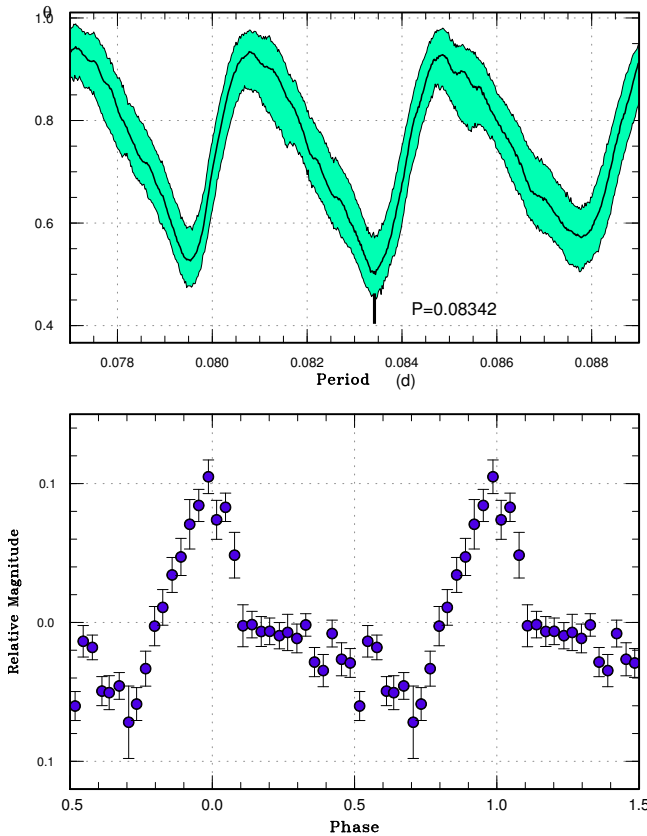


**Fig. 146.** Superhumps in MASTER J174816 (2016). (Upper): PDM analysis. (Lower): Phase-averaged profile.

nitude of 15.2 on 2012 December 21 (Shurpakov et al. 2012). The 2016 outburst was detected by the ASAS-SN team at  $V=15.53$  on November 24. There was another bright outburst reaching  $V=14.91$  on 2015 May 29 according to the ASAS-SN data. Subsequent observations detected superhumps (vsnet-alert 20453; figure 147). Although two superhump maxima were measured to be BJD 2457718.2276(8) ( $N=73$ ) and 2457720.2718(14) ( $N=66$ , the maximum was missed and was estimated by template fitting), only one superhump maximum was recorded on each night and the period is  $2.04(1)/n$ , where  $n$  is an integer.

### 3.116 MASTER OT J220559.40–341434.9

This object (hereafter MASTER J220559) was discovered by the MASTER network at an unfiltered CCD magnitude of 14.5 on 2016 September 19 (Pogrosheva et al. 2016a; correction in Pogrosheva et al. 2016b). The object was also detected by the ASAS-SN team (ASASSN-16kr) at  $V=14.3$  on September 11. The ASAS-SN detection was announced after the object brightened to  $V=13.9$  on September 22, 2 d after the MASTER announcement. Although the object

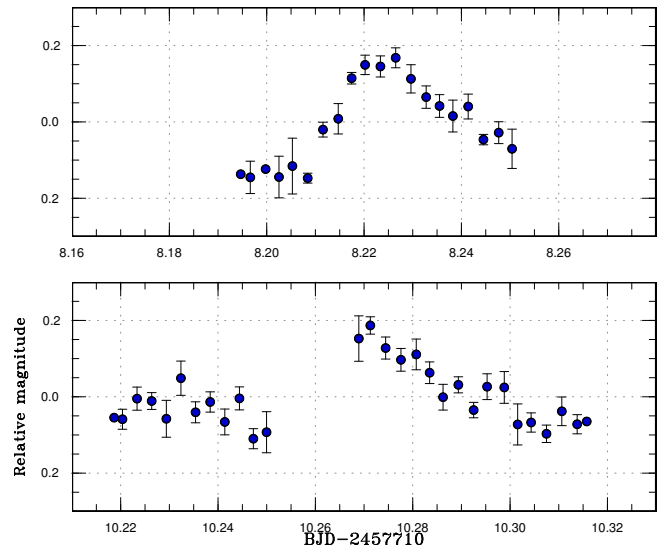


**Fig. 147.** Superhump in MASTER J211322 (2016).

was initially considered to be an SS Cyg-type object from the low outburst amplitude (cf. vsnet-alert 20189), time-resolved photometry detected superhumps and eclipses (vsnet-alert 20190, 20196, 20206; figure 148, figure 149).

We obtained the eclipse ephemeris using the MCMC analysis (Kato et al. 2013):

$$\text{Min(BJD)} = 2457658.72016(3) + 0.0612858(3)E. \quad (4)$$

This ephemeris is not intended for long-term prediction of eclipses. The epoch refers to the center of the observation. The times of superhump maxima outside the eclipses are listed in table 110. Although the  $O - C$  diagram suggests stage B-C transition, the periods and  $P_{\text{dot}}$  may have not been well determined since the actual start of the outburst was much earlier than the detection announcement and determination of superhump maxima should have been affected by overlapping eclipses and orbital humps in the late epochs. A large positive  $P_{\text{dot}}$ , however, is usual for such a short- $P_{\text{orb}}$  SU UMA-type dwarf nova.

The small outburst amplitude ( $\sim 4.5$  mag) was probably a result of the high orbital inclination. Since the object has deep eclipses and apparently shows a large positive  $P_{\text{dot}}$ , it surely deserves further detailed observations to clarify the origin of increasing  $P_{\text{SH}}$  during stage B. Observations of the early phase of a superoutburst are also desired to determine  $q$  by the stage A superhump method.

### 3.117 SBS 1108+574

This object (hereafter SBS 1108) was originally selected as an ultraviolet-excess object during the course of the

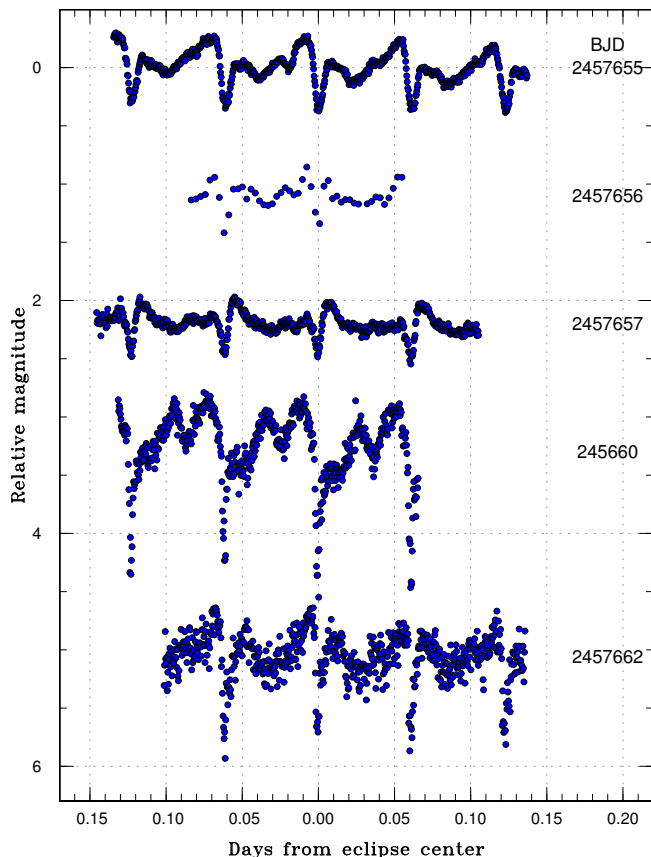


Fig. 148. Eclipses and superhumps in MASTER J220559.

Second Byurakan Survey (SBS, Markarian and Stepanian 1983). An outburst detected by CRTS on 2012 April 22 (=CSS120422:111127+571239) led to an identification as an SU UMa-type dwarf nova having a period below the period minimum (cf. Kato et al. 2013). Littlefield et al. (2013) studied this object by spectroscopy and found He I emission of comparable strength to the Balmer lines, indicating a hydrogen abundance less than 0.1 of ordinary hydrogen-rich CVs but still at least 10 times higher than that in AM CVn stars. The object received special attention since it is considered to be a candidate progenitor of an AM CVn system (also known as EI Psc-type objects) (Littlefield et al. 2013).

The 2016 outburst was detected by the ASAS-SN team at  $V=15.44$  on March 17. Although subsequent observations detected superhumps (vsnet-alert 19615, 19674), the 2016 outburst was not as well observed as in 2012 and superhumps were detected only on two nights (table 111). We could not make a comparison of  $O - C$  diagrams between the 2012 and 2016 observations due to the insufficiency of observations in 2016.

Table 110. Superhump maxima of MASTER J220559 (2016)

$E$	max*	error	$O - C^{\dagger}$	phase $^{\ddagger}$	$N^{\S}$
0	57655.2787	0.0007	0.0037	0.85	48
1	57655.3385	0.0004	0.0016	0.82	111
2	57655.4032	0.0006	0.0043	0.88	111
3	57655.4630	0.0004	0.0022	0.85	109
4	57655.5247	0.0003	0.0020	0.86	105
23	57656.6919	0.0026	-0.0077	0.90	13
32	57657.2503	0.0006	-0.0067	0.02	108
33	57657.3144	0.0006	-0.0046	0.06	111
34	57657.3758	0.0005	-0.0051	0.06	110
35	57657.4381	0.0005	-0.0048	0.08	111
71	57659.6648	0.0034	-0.0079	0.41	17
72	57659.7253	0.0032	-0.0093	0.40	16
81	57660.3019	0.0022	0.0099	0.81	111
82	57660.3663	0.0023	0.0123	0.86	111
83	57660.4333	0.0013	0.0174	0.95	88
87	57660.6702	0.0019	0.0065	0.82	13
88	57660.7305	0.0028	0.0049	0.80	14
113	57662.2699	0.0018	-0.0041	0.92	111
114	57662.3323	0.0007	-0.0037	0.94	110
115	57662.3961	0.0008	-0.0018	0.98	110
116	57662.4507	0.0018	-0.0092	0.87	100

\*BJD-2400000.

$^{\dagger}$ Against max = 2457655.2750 + 0.061939E.

$^{\ddagger}$ Orbital phase.

$^{\S}$ Number of points used to determine the maximum.

Table 111. Superhump maxima of SBS 1108 (2016)

$E$	max*	error	$O - C^{\dagger}$	$N^{\ddagger}$
0	57466.3045	0.0016	-0.0007	43
1	57466.3458	0.0015	0.0015	43
2	57466.3832	0.0010	-0.0001	43
3	57466.4223	0.0010	-0.0000	44
4	57466.4608	0.0008	-0.0007	37
69	57468.9995	0.0020	-0.0002	34
70	57469.0385	0.0014	-0.0003	125
71	57469.0774	0.0020	-0.0004	85
72	57469.1178	0.0031	0.0009	57

\*BJD-2400000.

$^{\dagger}$ Against max = 2457466.3052 + 0.039051E.

$^{\ddagger}$ Number of points used to determine the maximum.

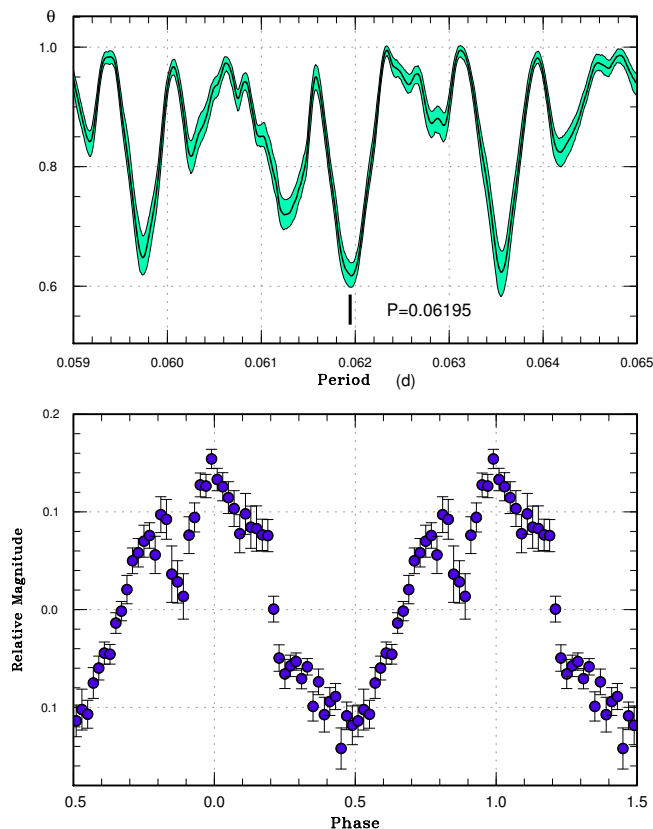


**Fig. 149.** Superhumps in MASTER J220559 (2016). (Upper): PDM analysis. The signal at 0.06129 d is the orbital period. Other signals are aliases and false ones produced in combination with orbital variations. (Lower): Phase-averaged profile.

### 3.118 SDSS J032015.29+441059.3

This object (hereafter SDSS J032015) was originally selected as a CV by Wils et al. (2010) based on SDSS variability. The SDSS colors suggested an object below the period gap (Kato et al. 2012b).

The 2016 outburst was detected by the ASAS-SN team at  $V=14.84$  on September 19. Subsequent observations detected superhumps (vsnet-alert 20209; figure 150). The times of superhump maxima are listed in table 112. Since the observations were obtained during the final part of the superoutburst, these superhumps probably consisted of both stage B and C ones.

Although there were single-night observations by C. Littlefield on 2014 October 3, the nature of this outburst and detected variations were unknown (cf. vsnet-alert 17801, 17818).

### 3.119 SDSS J091001.63+164820.0

This object (hereafter SDSS J091001) was originally selected as a CV by the SDSS (Szkody et al. 2009). The SDSS

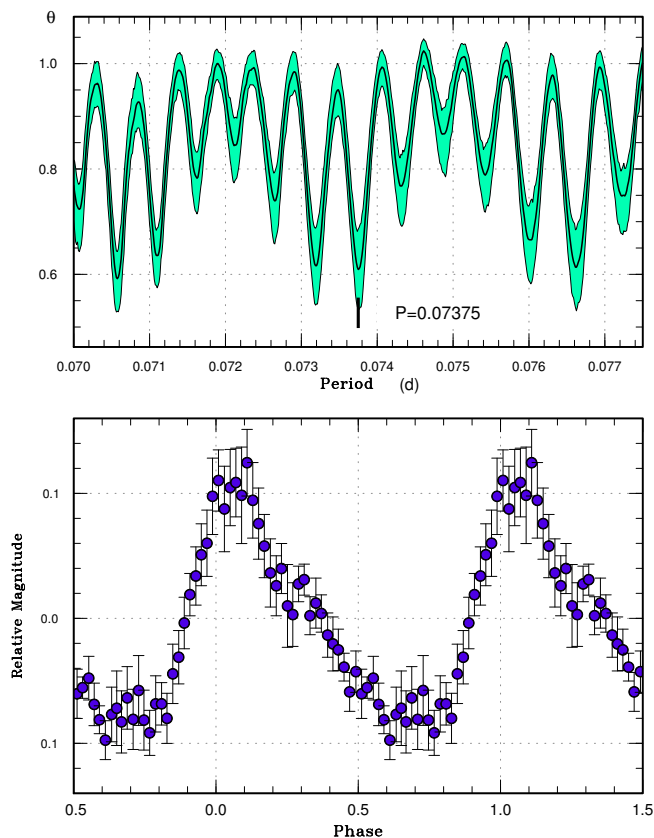


**Fig. 150.** Superhumps in SDSS J032015 (2016). (Upper): PDM analysis. The alias selection was based on  $O - C$  analysis and the single-night determination by I. Miller (vsnet-alert 20209). (Lower): Phase-averaged profile.

**Table 112.** Superhump maxima of SDSS J032015 (2016)

$E$	max*	error	$O - C^\dagger$	$N^\ddagger$
0	57653.5127	0.0031	-0.0045	24
1	57653.5964	0.0004	0.0054	70
2	57653.6674	0.0005	0.0027	51
26	57655.4311	0.0026	-0.0038	32
27	57655.5077	0.0005	-0.0009	73
134	57663.4055	0.0008	0.0049	55
136	57663.5504	0.0012	0.0023	73
137	57663.6156	0.0023	-0.0062	59

\*BJD-2400000.

$^\dagger$ Against max = 2457653.5172 + 0.073757E.

$^\ddagger$ Number of points used to determine the maximum.

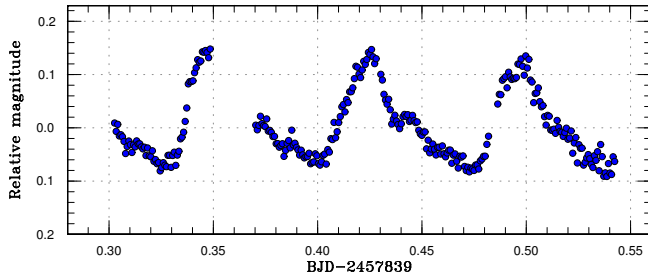


Fig. 151. Superhump in SDSS J091001 (2017).

colors suggested an object below the period gap (Kato et al. 2012b). There was an outburst in 2016 February–March (cf. vsnet-alert 19539), but CCD observations by T. Vanmunster and Y. Maeda showed that the outburst was a rapidly fading normal one.

The 2017 outburst was detected by the ASAS-SN team at  $V=14.39$  on March 25. The ASAS-SN data indicated that the outburst started at  $V=16.28$  on March 21 and peaked at  $V=14.04$  on March 23. Subsequent observations detected superhumps (vsnet-alert 20830). Three superhump maxima were recorded: BJD 2457839.3524(3) ( $N=50$ ), 2457839.4252(3) ( $N=76$ ) and 2457839.4980(3) ( $N=73$ ). The superhump period determined by the PDM method was 0.0734(2) d.

### 3.120 SDSS J113551.09+532246.2

This object (hereafter SDSS J113551) was reported as an outbursting object discovered by ROTSE-IIIb telescope at an unfiltered CCD magnitude of 15.1 on 2006 March 24 (Quimby and Mondol 2006). Kato et al. (2012b) expected an orbital period of 0.112(6) d based on SDSS colors.

The 2017 outburst was detected by the ASAS-SN team at  $V=15.34$  on February 16. Although observations on two nights were reported, neither data were of sufficient quality to determine the superhump period (due to cloud gaps). The period used to calculate epochs in table 113 was one of the possibilities giving smallest  $O - C$  residuals. Other candidate aliases were 0.1023(1) d and 0.0914(1) d (table 113). In any case, SDSS J113551 is in or close to the period gap and should be studied further. According to the ASAS-SN data, there were past (most likely) superoutbursts on 2012 March 10 ( $V=15.53$ ) and 2016 May 15 ( $V=15.68$ ). There were additional possible ones which were not well recorded. The frequency of superoutbursts was not probably especially low.

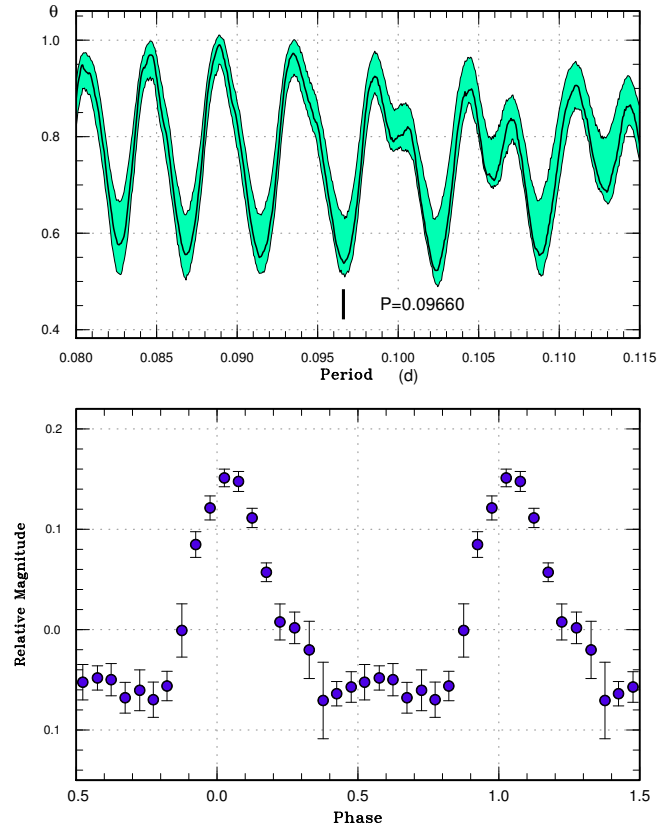


Fig. 152. Superhumps in SDSS J113551 (2017). (Upper): PDM analysis. The selected period was one of the possibilities. (Lower): Phase-averaged profile.

Table 113. Superhump maxima of SDSS J113551 (2017)

$E$	max*	error	$O - C^\dagger$	$N^\ddagger$
0	57803.4956	0.0004	0.0021	75
1	57803.5880	0.0007	-0.0023	51
18	57805.2362	0.0007	0.0001	181

\*BJD-2400000.

$^\dagger$ Against max = 2457803.4935 + 0.096810E.

$^\ddagger$ Number of points used to determine the maximum.

## 3.121 SDSS J115207.00+404947.8

This object (hereafter SDSS J115207) was originally selected as a CV by the SDSS (Szkody et al. 2007). Although Szkody et al. (2007) suspected an eclipsing system, its nature was established by Southworth et al. (2010), who determined the orbital period of 0.06770(28) d and an mass ratio of 0.14(3). Savoury et al. (2011) obtained further observations and refined the values to be 0.067721356(3) d and 0.155(6), respectively.

The object was confirmed to be an SU UMa-type dwarf nova by the detection of superhumps during the 2009 superoutburst (Kato et al. 2010). Due to the poor coverage of the 2009 superoutburst and the limited knowledge of the orbital period at that time, we could not determine superhump and orbital periods precisely in Kato et al. (2010).

The 2017 superoutburst was detected by the ASAS-SN team at  $V=15.51$  on February 14. Superhumps were subsequently detected (vsnet-alert 20664, 20671, 20688).

We noticed that the ephemeris by Savoury et al. (2011) could not express our eclipse observations and found that the period 0.0677497 d satisfy all the data (Southworth et al. 2010; Savoury et al. 2011; Kato et al. 2010 and the present observations). By using our data in 2009 and 2017, we have updated the eclipse ephemeris using the MCMC analysis (Kato et al. 2013):

$$\text{Min}(\text{BJD}) = 2457578.07695(6) + 0.0677497014(14)E. \quad (5)$$

The epoch corresponds to the center of the entire combined observation of 2009 and 2017. This period corresponds to 4797 cycles between Southworth et al. (2010) and Savoury et al. (2011), which was assumed to be 4799 cycles in Savoury et al. (2011). The  $O - C$  values against this ephemeris are listed in table 114. The times of eclipse centers by our observations in table 114 were determined by the same MCMC method against the data segments (2007 and 2017) by fixing the orbital period. The eclipse profiles used to determine these minima are shown in figure 153 and figure 154.

The times of superhump maxima are listed in table 115. Although superhumps were initially suspected to be stage A ones (vsnet-alert 20671), they were more likely already stage B ones (figure 155). Stage B-C transition occurred around  $E=52$ . We also provide an updated table of superhump maxima of the 2009 superoutburst in table 116. This table is based on the identification of the true superhump period and based on the updated orbital ephemeris. The 2009 observations likely recorded a combination of stages B and C.

**Table 114.** List of eclipse minima in SDSS J115207

$E$	BJD-2400000	$O - C$	Source*
-39831	54879.5387(2)	0.0001	1
-39830	54879.6065(2)	0.0002	1
-38125	54995.11953(6)	-0.00005	2
-35033	55204.601324(6)	-0.00034	3
3321	57803.07370(2)	-0.00001	2

\*1: Southworth et al. (2010), 2: this work, 3: Savoury et al. (2011)

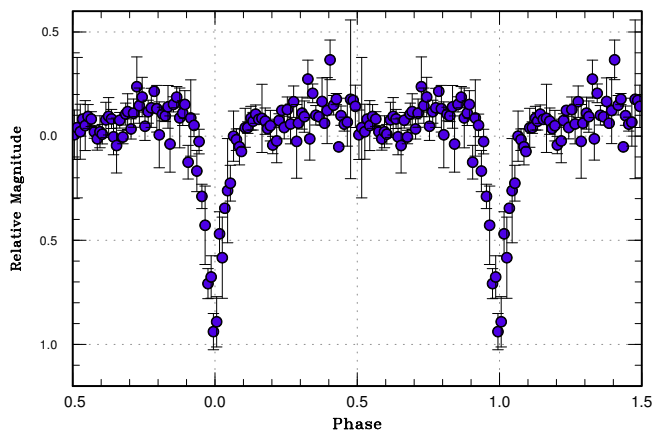


**Fig. 153.** Eclipse profile in SDSS J115207 (2009). The superhumps were mostly removed by using LOWESS. The phase-averaged profile was drawn against the ephemeris equation (5).

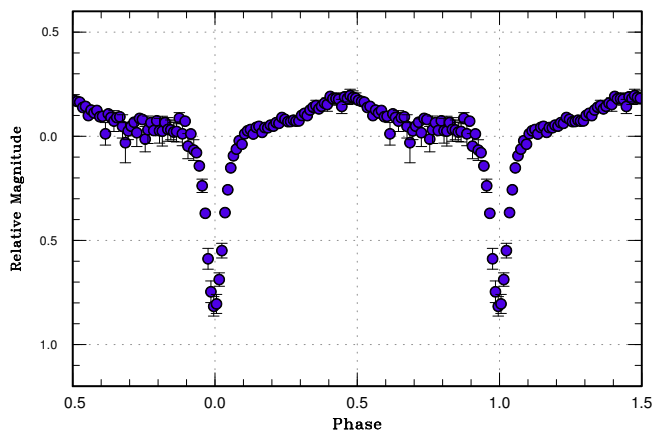


**Fig. 154.** Eclipse profile in SDSS J115207 (2017). The superhumps were mostly removed by using LOWESS. The phase-averaged profile was drawn against the ephemeris equation (5).

**Table 115.** Superhump maxima of SDSS J115207 (2017)

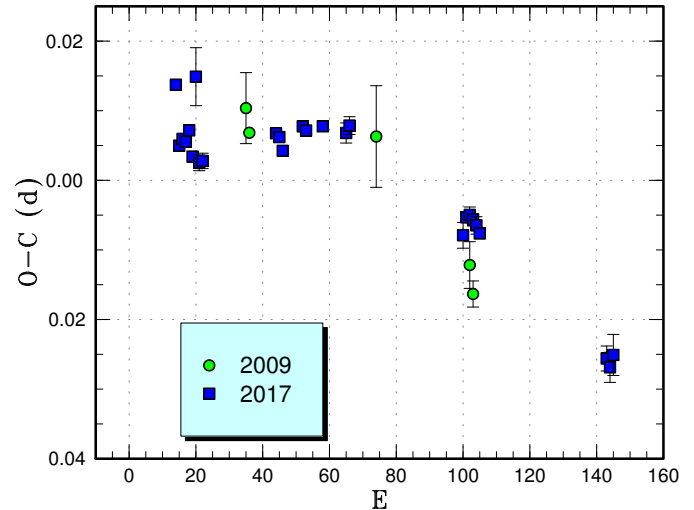
$E$	max*	error	$O - C^\dagger$	phase <sup>‡</sup>	$N^\S$
0	57799.9836	0.0007	0.0026	0.39	85
1	57800.0452	0.0008	-0.0059	0.30	124
2	57800.1165	0.0007	-0.0047	0.35	129
3	57800.1865	0.0003	-0.0049	0.38	167
4	57800.2585	0.0006	-0.0030	0.45	201
5	57800.3251	0.0007	-0.0066	0.43	95
6	57800.4069	0.0042	0.0051	0.64	40
7	57800.4649	0.0011	-0.0070	0.49	37
8	57800.5355	0.0011	-0.0065	0.54	35
30	57802.0874	0.0003	0.0024	0.44	135
31	57802.1572	0.0003	0.0021	0.47	212
32	57802.2256	0.0005	0.0004	0.48	100
38	57802.6513	0.0003	0.0053	0.77	137
39	57802.7211	0.0003	0.0049	0.79	180
44	57803.0735	0.0005	0.0066	1.00	85
51	57803.5650	0.0014	0.0073	0.25	29
52	57803.6365	0.0013	0.0085	0.31	30
86	57806.0129	0.0019	0.0005	0.38	21
87	57806.0859	0.0007	0.0033	0.46	36
88	57806.1566	0.0011	0.0039	0.50	37
89	57806.2262	0.0009	0.0034	0.53	91
90	57806.2958	0.0013	0.0028	0.56	87
91	57806.3650	0.0008	0.0019	0.58	43
129	57809.0207	0.0018	-0.0074	0.78	62
130	57809.0898	0.0022	-0.0085	0.80	61
131	57809.1619	0.0030	-0.0065	0.86	56

\*BJD-2400000.

<sup>†</sup>Against max = 2457799.9810 + 0.070133E.<sup>‡</sup>Orbital phase.<sup>§</sup>Number of points used to determine the maximum.**Table 116.** Superhump maxima of SDSS J115207 (2009)

$E$	max*	error	$O - C^\dagger$	phase <sup>‡</sup>	$N^\S$
0	54993.9978	0.0051	-0.0003	0.44	72
1	54994.0646	0.0007	-0.0035	0.43	136
39	54996.7378	0.0073	0.0086	0.88	9
67	54998.6894	0.0034	-0.0005	0.69	17
68	54998.7556	0.0019	-0.0044	0.67	31

\*BJD-2400000.

<sup>†</sup>Against max = 2454993.9981 + 0.070028E.<sup>‡</sup>Orbital phase.<sup>§</sup>Number of points used to determine the maximum.**Fig. 155.** Comparison of  $O - C$  diagrams of SDSS J115207 between different superoutbursts. A period of 0.07036 d was used to draw this figure. Approximate cycle counts ( $E$ ) after the start of the superoutburst were used.**Table 117.** Superhump maxima of SDSS J131432 (2017)

$E$	max*	error	$O - C^\dagger$	$N^\ddagger$
0	57842.5432	0.0004	0.0014	60
2	57842.6754	0.0005	0.0024	43
12	57843.3287	0.0004	-0.0005	54
13	57843.3928	0.0004	-0.0020	62
14	57843.4579	0.0004	-0.0026	56
53	57846.0226	0.0033	0.0030	86
54	57846.0845	0.0008	-0.0008	136
55	57846.1499	0.0009	-0.0009	102

\*BJD-2400000.

<sup>†</sup>Against max = 2457842.5418 + 0.065620E.<sup>‡</sup>Number of points used to determine the maximum.

### 3.122 SDSS J131432.10+444138.7

This object (hereafter SDSS J131432) was originally selected as a CV by Wils et al. (2010) based on SDSS colors and variability. The 2017 outburst was detected by the ASAS-SN team at  $V=15.63$  on March 28. Subsequent observations detected superhumps (vsnet-alert 20841; figure 156). The times of superhump maxima are listed in table 117.

### 3.123 SDSS J153015.04+094946.3

This object (hereafter SDSS J153015) was originally selected as a CV by the SDSS (Szkody et al. 2009). The dwarf nova-type variation was confirmed by CRTS observations (Drake et al. 2014). The 2017 outburst was detected by the ASAS-SN team at  $V=15.84$  on March 7. Based on ASAS-



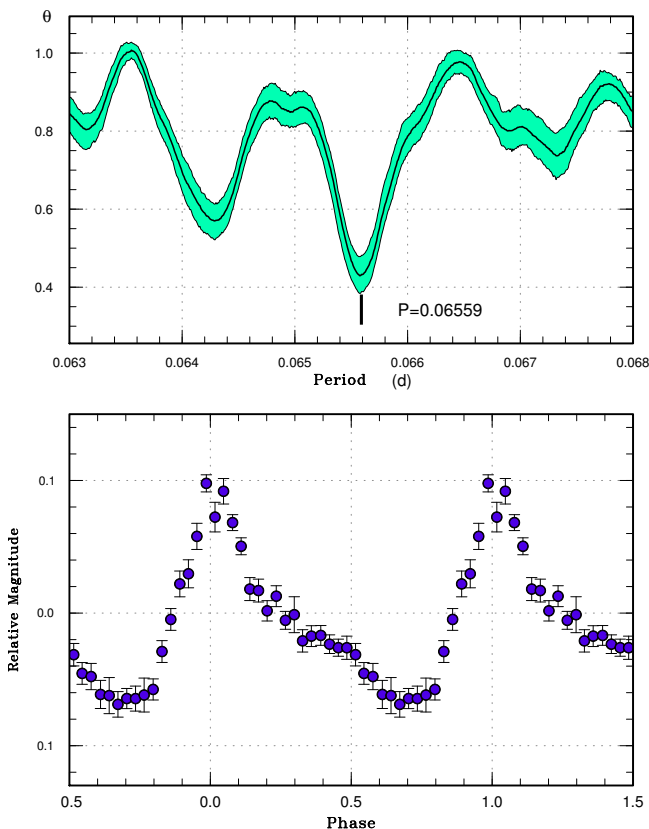


Fig. 156. Superhumps in SDSS J131432 (2017). (Upper): PDM analysis. (Lower): Phase-averaged profile.

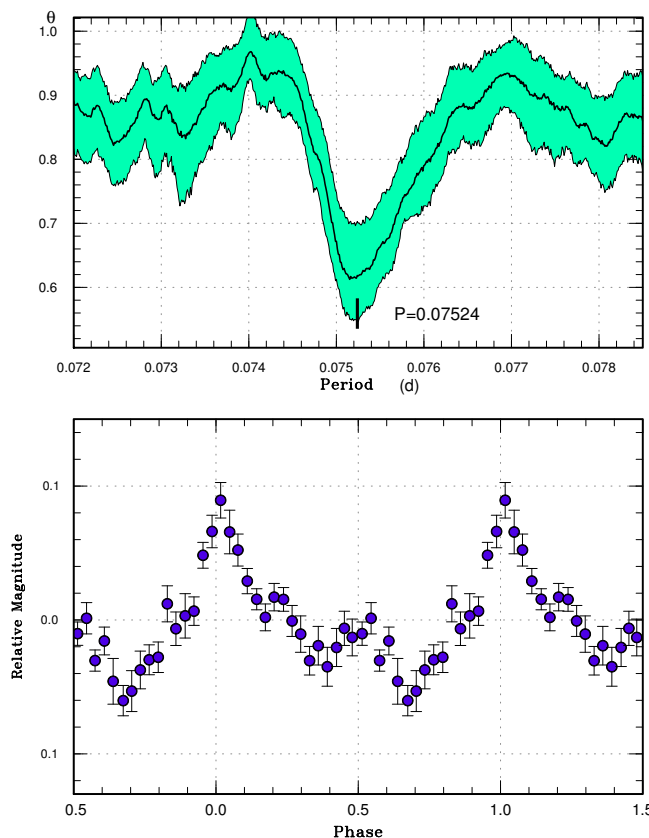


Fig. 157. Superhumps in SDSS J153015 (2017). (Upper): PDM analysis. (Lower): Phase-averaged profile.

SN observations, this outburst was likely a precursor one. The peak was observed on March 10. Subsequent observations detected superhumps (vsnet-alert 20769; figure 157). The times of superhump maxima are listed in table 118. The period in table 3 was obtained by the PDM analysis. Since these superhump observations were made during the early phase, the period may refer to that of stage A superhumps.

ASAS-SN observations indicate that this object shows superoutburst relatively regularly. The times of recent (likely) superoutburst are listed in table 119. Assuming that two superoutbursts were not recorded between 2016 July and 2017 March, all the superoutbursts were well expressed by a supercycle of 84.7(1.2) d with the maximum  $|O - C|$  of 18 d. The long-term light curve does not look like that of an ER UMa-type dwarf nova but resembles that of V503 Cyg (cf. subsections 3.14, 3.27 and 3.90). Further observations to search for negative superhumps are recommended.

Table 118. Superhump maxima of SDSS J153015 (2017)

$E$	max*	error	$O - C^\dagger$	$N^\ddagger$
0	57822.5636	0.0025	0.0023	36
13	57823.5380	0.0025	-0.0022	58
14	57823.6147	0.0011	-0.0007	74
15	57823.6903	0.0011	-0.0005	62
41	57825.6497	0.0018	0.0011	44

\*BJD-2400000.

$^\dagger$ Against max = 2457822.5613 + 0.075301E.

$^\ddagger$ Number of points used to determine the maximum.

Table 119. List of likely superoutbursts of SDSS J153015 since 2015

Year	Month	Day	max*	V-mag
2015	2	17	57070	15.93
2015	5	12	57155	15.79
2015	7	31	57235	15.57
2016	1	22	57409	15.97
2016	4	15	57493	15.91
2016	7	28	57597	15.77
2017	3	10	57823	15.76

\*JD-2400000.

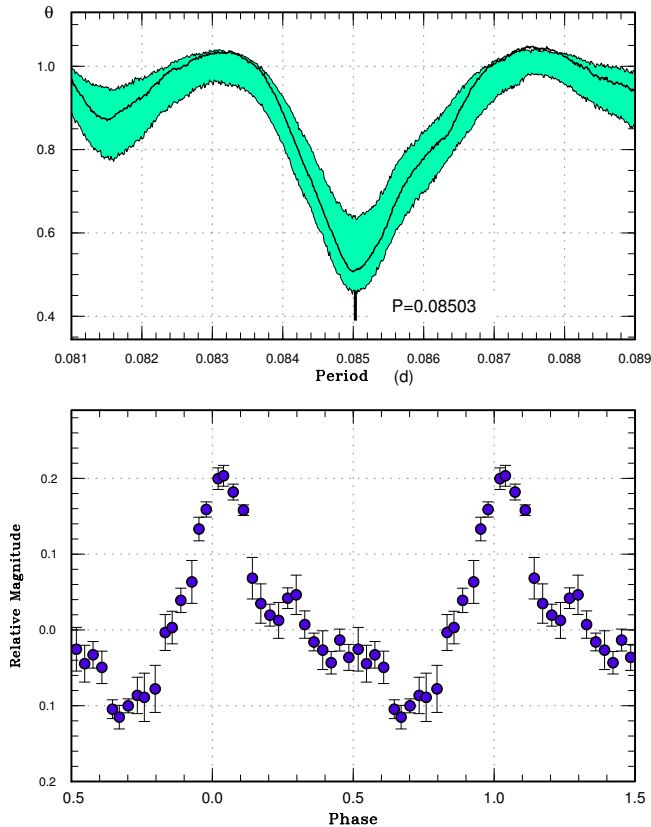


**Fig. 158.** Superhumps in SDSS J155720 (2016). (Upper): PDM analysis. The data segment BJD 2457467–2457471 was used. (Lower): Phase-averaged profile.

### 3.124 SDSS J155720.75+180720.2

This object (hereafter SDSS J155720) was originally selected as a CV by the SDSS (Szkody et al. 2009). The spectrum was that of a dwarf nova in quiescence and Szkody et al. (2009) suggested a period of  $\sim 2.1$  hr. There is an ROSAT X-ray counterpart of 1RXSJ155720.3+180715. The object was detected in outburst on 2007 June 12 (14.8 mag) and 2008 September 5 (16.1 mag) by the CRTS team<sup>19</sup>

The 2016 outburst was detected by the CRTS team at an unfiltered CCD magnitude of 15.37 on March 17 (=CSS160317:155721+180720) and by the ASAS-SN team at  $V=15.12$  on the same night. Subsequent observations detected superhumps (vsnet-alert 19613; figure 158). The times of superhump maxima are listed in table 120.

### 3.125 SSS J134850.1–310835

This object (hereafter SSS J134850) was discovered by Stan Howerton during the course of the CRTS SNHunt (super-

**Table 120.** Superhump maxima of SDSS J155720 (2016)

$E$	max*	error	$O - C^\dagger$	$N^\ddagger$
0	57467.7552	0.0050	0.0009	17
1	57467.8406	0.0004	0.0009	41
2	57467.9249	0.0025	-0.0005	12
12	57468.7812	0.0009	0.0002	17
13	57468.8640	0.0014	-0.0025	12
23	57469.7278	0.0030	0.0056	25
24	57469.8008	0.0009	-0.0070	30
29	57470.2381	0.0047	0.0025	93

\*BJD-2400000.

$^\dagger$ Against max = 2457467.7542 + 0.085565E.

$^\ddagger$ Number of points used to determine the maximum.

**Table 121.** Superhump maxima of SSS J134850 (2016)

$E$	max*	error	$O - C^\dagger$	$N^\ddagger$
0	57499.6580	0.0009	-0.0030	28
1	57499.7437	0.0009	-0.0018	20
12	57500.6755	0.0014	0.0002	29
13	57500.7634	0.0019	0.0035	10
24	57501.6888	0.0008	-0.0009	27
32	57502.3677	0.0003	0.0017	195
33	57502.4507	0.0004	0.0002	195
44	57503.3822	0.0003	0.0018	195
45	57503.4669	0.0003	0.0020	195
56	57504.3938	0.0003	-0.0010	179
67	57505.3233	0.0003	-0.0014	194
68	57505.4080	0.0003	-0.0013	195
69	57505.4916	0.0004	-0.0022	132
79	57506.3402	0.0003	0.0011	193
80	57506.4236	0.0005	-0.0001	163

\*BJD-2400000.

$^\dagger$ Against max = 2457499.6609 + 0.084534E.

$^\ddagger$ Number of points used to determine the maximum.

nova hunt)<sup>20</sup> The object showed a number of outbursts in the ASAS-3 data in the past.

The 2016 outburst was detected by R. Stubbings at a visual magnitude of 11.8 on April 17. Subsequent observations detected superhumps (vsnet-alert 19751; figure 159). The times of superhump maxima are listed in table 121. The period variation was rather smooth and we gave a global  $P_{\text{dot}}$  rather than giving stages. An analysis of the post-superoutburst data did not yield a superhump period.

<sup>20</sup><<https://www.aavso.org/sss1348501-310835-bright-dwarf-nova->

<sup>19</sup><<http://nessi.cacr.caltech.edu/catalina/20160317/1603171180824123493.html>>.centaurus>.

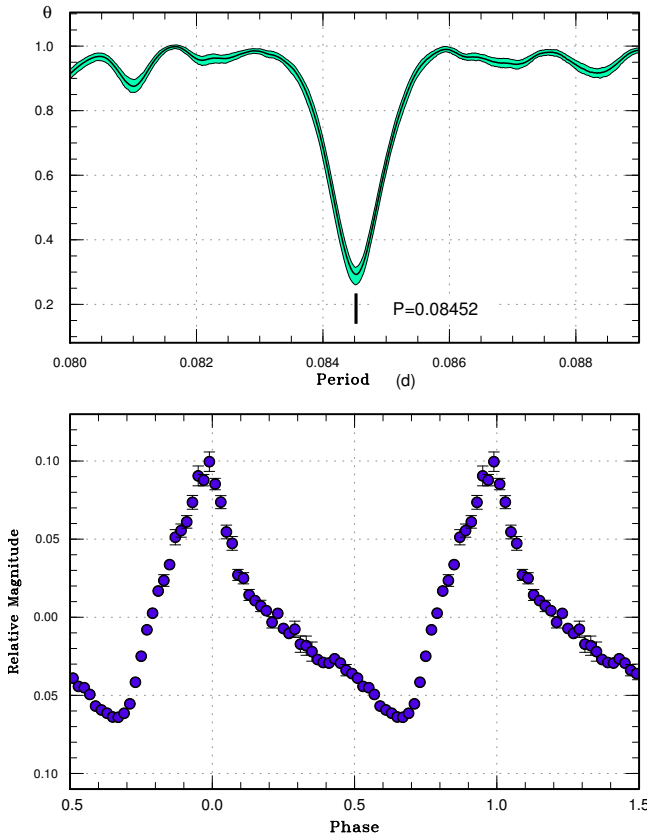


Fig. 159. Superhumps in SSS J134850 during the superoutburst plateau (2016). (Upper): PDM analysis. (Lower): Phase-averaged profile.

### 3.126 TCP J01375892+4951055

This object (hereafter TCP J013758) was discovered by K. Itagaki at an unfiltered CCD magnitude of 13.2 on 2016 October 19.<sup>21</sup> There is a blue SDSS counterpart ( $g=19.85$  and  $u - g=0.15$ ) and also a GALEX UV counterpart. The object was suspected to be a dwarf nova. Subsequent observations detected growing superhumps (vsnet-alert 20238). Superhumps with a stable period were observed 2 d after the discovery (vsnet-alert 20242, 20268; figure 160). The times of superhump maxima are listed in table 122. The data show clear stages A–C, with a positive  $P_{\text{dot}}$  for stage B characteristic to this short  $P_{\text{SH}}$  (figure 161). The period of stage A superhumps was not very well determined due to a gap around the stage A–B transition. The behavior suggests a typical SU UMa-type dwarf nova.

### 3.127 TCP J18001854–3533149

This object (hereafter TCP J180018) was discovered as a transient by K. Nishiyama and F. Kabashima at an unfiltered

Table 122. Superhump maxima of TCP J013758 (2016)

$E$	max*	error	$O - C^\dagger$	$N^\ddagger$
0	57681.5361	0.0011	-0.0179	52
9	57682.0851	0.0006	-0.0246	92
10	57682.1605	0.0008	-0.0109	115
11	57682.2268	0.0009	-0.0064	114
12	57682.2862	0.0012	-0.0088	93
14	57682.4183	0.0004	-0.0002	54
15	57682.4761	0.0006	-0.0042	68
31	57683.4787	0.0002	0.0104	50
32	57683.5401	0.0001	0.0100	144
33	57683.6015	0.0002	0.0097	96
34	57683.6623	0.0001	0.0087	96
35	57683.7237	0.0002	0.0083	74
43	57684.2157	0.0003	0.0063	77
44	57684.2781	0.0006	0.0070	40
45	57684.3399	0.0005	0.0071	26
46	57684.4011	0.0007	0.0065	24
47	57684.4575	0.0022	0.0011	13
48	57684.5246	0.0002	0.0065	99
49	57684.5847	0.0002	0.0049	95
50	57684.6469	0.0002	0.0053	96
51	57684.7078	0.0002	0.0044	96
59	57685.1987	0.0012	0.0013	15
60	57685.2604	0.0006	0.0013	22
61	57685.3220	0.0005	0.0011	24
62	57685.3817	0.0010	-0.0010	16
72	57685.9980	0.0005	-0.0022	82
73	57686.0596	0.0003	-0.0024	159
74	57686.1213	0.0003	-0.0024	184
75	57686.1829	0.0002	-0.0026	184
76	57686.2437	0.0003	-0.0035	185
77	57686.3063	0.0007	-0.0027	67
92	57687.2313	0.0006	-0.0040	43
93	57687.2939	0.0003	-0.0031	67
94	57687.3563	0.0004	-0.0024	58
110	57688.3457	0.0004	-0.0012	68
123	57689.1529	0.0006	0.0033	113
124	57689.2155	0.0006	0.0041	113
140	57690.2052	0.0004	0.0058	60
142	57690.3288	0.0009	0.0058	32
157	57691.2510	0.0006	0.0017	34
158	57691.3082	0.0020	-0.0028	17
208	57694.3812	0.0015	-0.0174	47

\*BJD-2400000.

<sup>†</sup>Against max = 2457681.5540 + 0.061753E.

<sup>‡</sup>Number of points used to determine the maximum.

<sup>21</sup><<http://www.cbat.eps.harvard.edu/unconf/followups/J01375892+4951055.html>>.

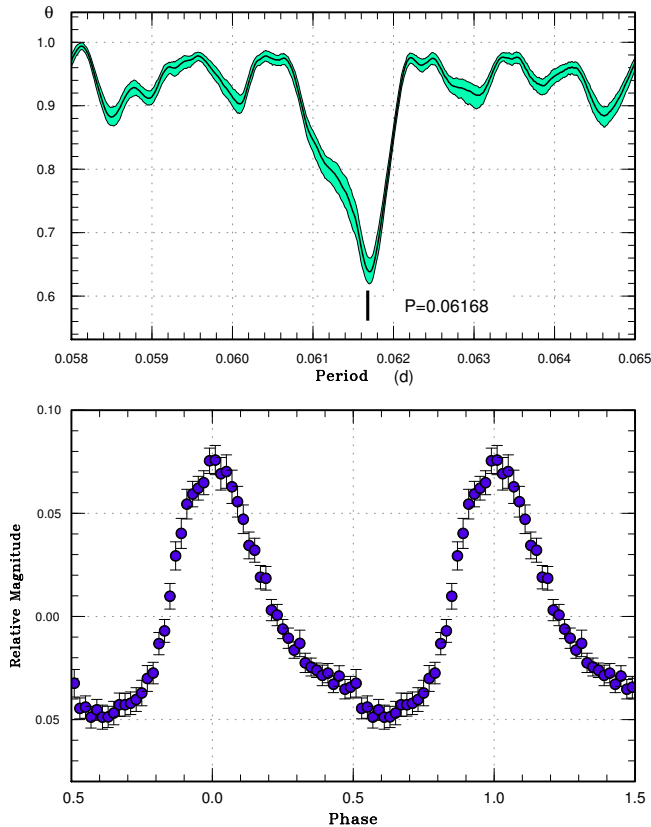


Fig. 160. Superhumps in TCP J013758 (2016). (Upper): PDM analysis. (Lower): Phase-averaged profile.

tered CCD magnitude of 12.2 on March 16.<sup>22</sup> Multicolor photometry by S. Kiyota showed a blue color, suggesting a dwarf nova-type outburst. A spectroscopic study by K. Ayani on March 20 showed Balmer absorption lines ( $H\beta$  to  $H\delta$ ). The  $H\alpha$  line was not clear probably because the absorption is filled with the emission. The spectrum indicated a dwarf nova in outburst. Subsequent observations detected superhumps (vsnet-alert 19635, 19646, 19662, 19684, 19703; figure 162). The times of superhump maxima are listed in table 123. There were clear stages A–C, with a positive  $P_{\text{dot}}$  for stage B, characteristic to a short- $P_{\text{SH}}$  SU UMa-type dwarf nova (figure 163).

The outburst faded on April 8 and the duration of the total outburst was at least 23 d. The object showed a single post-superoutburst rebrightening on April 25 at 14.5 mag (figure 163).

<sup>22</sup><<http://www.cbat.eps.harvard.edu/unconf/followups/J18001854-3533149.html>>.

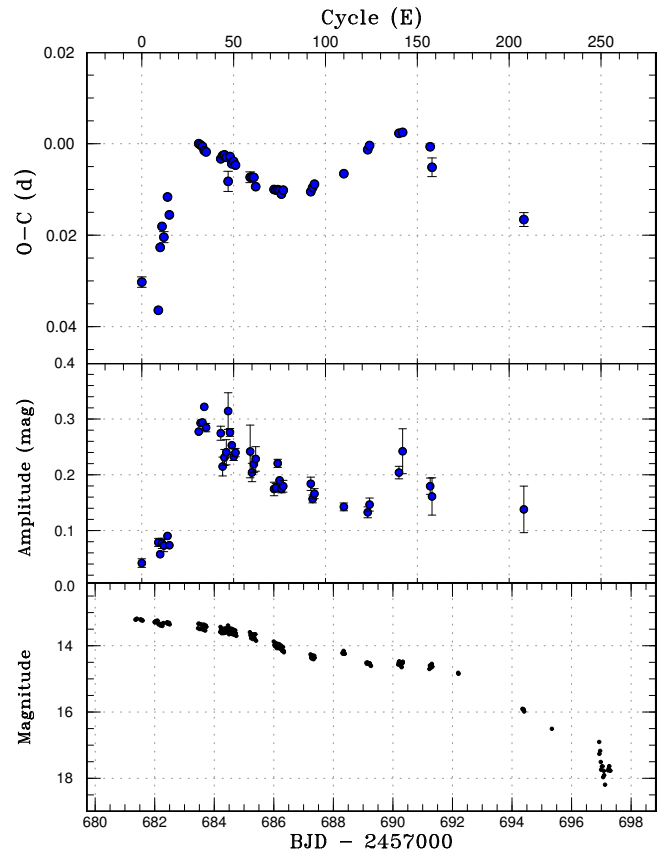


Fig. 161. O – C diagram of superhumps in TCP J013758 (2016). (Upper:) O – C diagram. We used a period of 0.06169 d for calculating the O – C residuals. (Middle:) Amplitudes of superhumps. (Lower:) Light curve. The data were binned to 0.021 d.

## 4 Discussion

### 4.1 Statistics of objects

Following Kato et al. (2015a) and Kato et al. (2016a), we present statistics of sources of the objects studied in our surveys (figure 164). Although ASAS-SN CVs remained the majority of the objects we studied, there have also been an increase in MASTER CVs and CRTS CVs. The noteworthy recent tendency is the increase of objects in the Galactic plane discovered by ASAS-SN. This region had usually been avoided by the majority of surveys (the best examples being SDSS and CRTS) and we can expect a great increase of dwarf novae if the Galactic plane is thoroughly surveyed by ASAS-SN. This increase of CV candidates in the Galactic plane, however, has made it difficult to distinguish dwarf novae and classical novae. Indeed, there have been four Galactic novae discovered by the ASAS-SN team: ASASSN-16ig = V5853 Sgr (Stanek et al. 2016a; Williams and Darnley 2016), ASASSN-16kb (Prieto et al. 2016), ASASSN-16kd (Stanek et al. 2016c; Bohlson 2016), and ASASSN-16ma = V5856 Sgr (Stanek

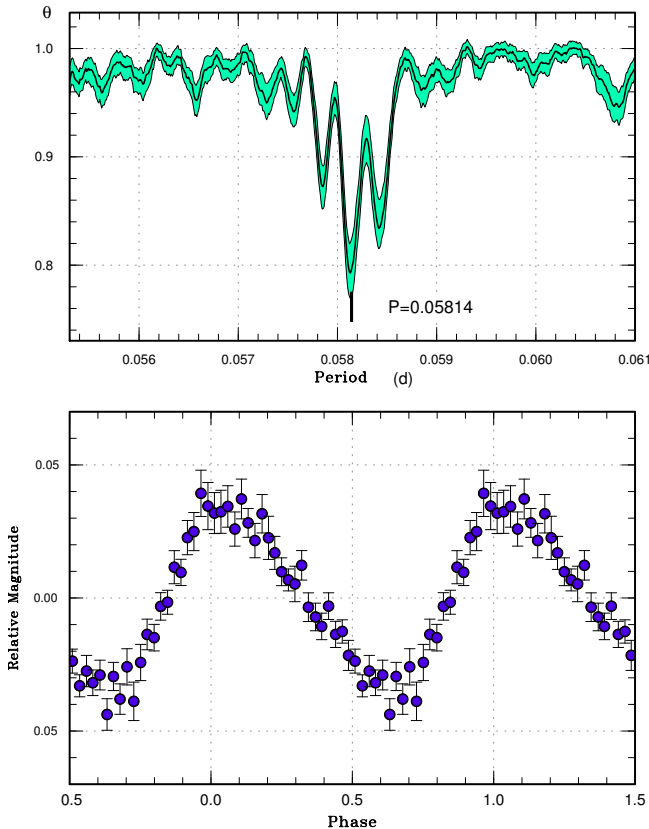


Fig. 162. Superhumps in TCP J180018 (2016). (Upper): PDM analysis. (Lower): Phase-averaged profile.

et al. 2016b; Luckas 2016) in 2016. Several dwarf novae studied in this paper were also flagged as “could also be a nova” on the ASAS-SN Transients page. Some objects in this paper (ASASSN-16jb and ASASSN-16ow) were initially suspected to be Galactic novae. Although they have not been a serious problem in studying dwarf novae, the supposed nova classification might cause a delay in time-resolved photometry to detect superhumps in the earliest phase, and observers should keep in mind the dwarf nova-type possibilities of nova candidate in the Galactic plane.

#### 4.2 Period distribution

In figure 165, we give distributions of superhump and estimated orbital periods (see the caption for details) since Kato et al. (2009). For readers’ convenience, we also listed ephemerides of eclipsing systems newly determined or used in this study in table 124. When there are multiple observations of superoutbursts of the same object, we adopted an average of the measurements. This figure can be considered to be a good representation of the distribution of orbital periods for non-magnetic CVs below the

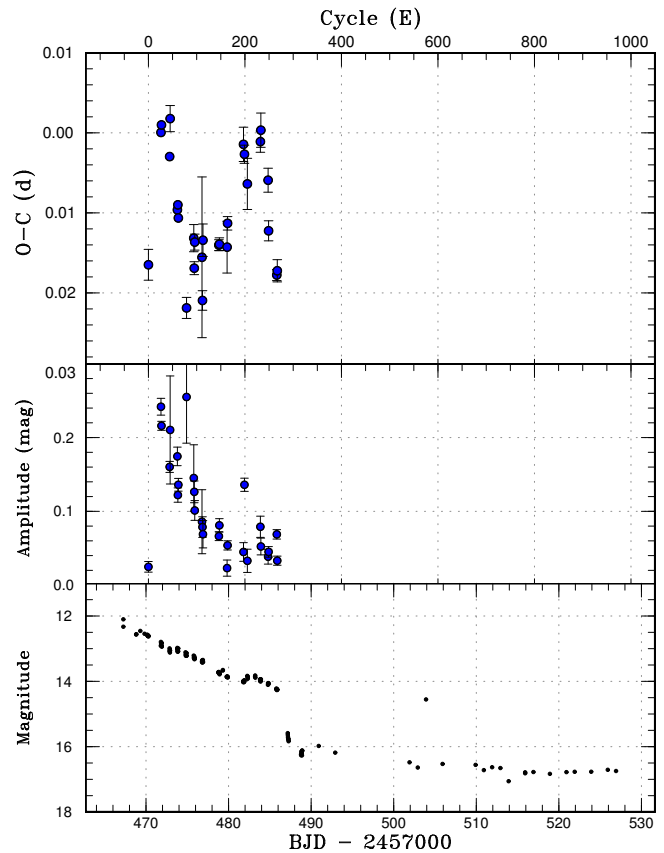


Fig. 163.  $O - C$  diagram of superhumps in TCP J180018 (2016). (Upper:)  $O - C$  diagram. We used a period of 0.05844 d for calculating the  $O - C$  residuals. (Middle:) Amplitudes of superhumps. (Lower:) Light curve. The data were binned to 0.019 d.

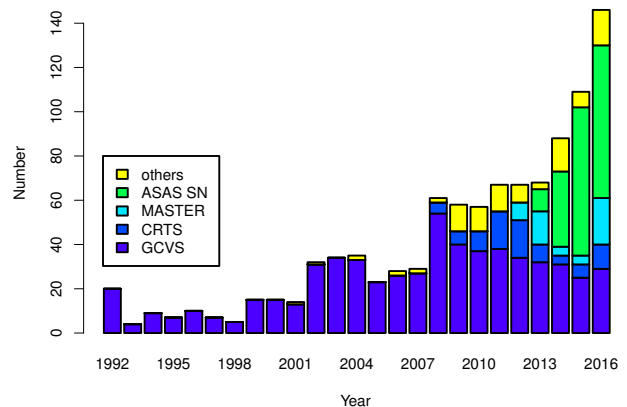


Fig. 164. Object categories in our survey. Superoutbursts with measured superhump periods are included. The year represents the year of outburst. The year 1992 represents outbursts up to 1992 and the year 2016 includes the outbursts in 2017, respectively. The category GCVS includes the objects named in the General Catalog of Variable Stars Kholopov et al. (1985) in the latest version and objects named in New Catalog of Suspected Variable Stars (NSV: Kukarkin et al. 1982). The categories CRTS, MASTER, ASAS-SN represent objects which were discovered in respective surveys. A fraction of objects discovered by these surveys are already named in GCVS and are included in the category GCVS.

**Table 123.** Superhump maxima of TCP J180018 (2016)

$E$	max*	error	$O - C^\dagger$	$N^\ddagger$
0	57470.2775	0.0019	-0.0068	71
26	57471.8134	0.0003	0.0098	50
27	57471.8728	0.0002	0.0107	68
44	57472.8624	0.0003	0.0068	280
45	57472.9255	0.0016	0.0116	78
60	57473.7907	0.0005	0.0002	50
61	57473.8498	0.0005	0.0008	62
62	57473.9066	0.0005	-0.0008	44
79	57474.8888	0.0013	-0.0120	16
94	57475.7742	0.0017	-0.0033	26
95	57475.8288	0.0008	-0.0070	50
96	57475.8905	0.0010	-0.0038	48
111	57476.7652	0.0100	-0.0056	30
112	57476.8183	0.0012	-0.0110	50
113	57476.8843	0.0020	-0.0035	50
146	57478.8122	0.0007	-0.0040	52
147	57478.8707	0.0008	-0.0039	50
163	57479.8054	0.0032	-0.0042	52
164	57479.8668	0.0008	-0.0013	50
197	57481.8052	0.0021	0.0087	34
199	57481.9208	0.0011	0.0074	12
205	57482.2678	0.0032	0.0037	31
232	57483.8509	0.0013	0.0091	70
233	57483.9108	0.0021	0.0105	42
248	57484.7812	0.0015	0.0043	60
249	57484.8333	0.0013	-0.0020	52
266	57485.8212	0.0007	-0.0075	72
267	57485.8802	0.0014	-0.0070	70

\*BJD-2400000.

 $^\dagger$ Against max = 2457470.2843 + 0.058438E. $^\ddagger$ Number of points used to determine the maximum.

period gap, since the majority of CVs below the period gap are SU UMa-type dwarf novae. The following features reported in Kato et al. (2016a) are apparent: (1) the sharp cut-off at a period of 0.053 d and (2) accumulation of objects (“period spike”) just above the cutoff.

We determined the location of the sharp cut-off (period minimum) by using the Bayesian approach. We assumed the following period distribution  $D(P_{\text{orb}})$ :

$$D(P_{\text{orb}}) \propto \begin{cases} c_1, & (P_{\text{orb}} \leq P_{\text{min}}) \\ 1/(P_{\text{orb}} - c_2), & (P_{\text{orb}} > P_{\text{min}}). \end{cases} \quad (6)$$

$P_{\text{min}}$  is the cut-off and  $c_1, c_2$  are parameters to be determined. We defined the likelihood to obtain the entire sample of our SU UMa-type dwarf novae by using this distribution (the distribution is normalized for a range of 0.01–0.13 d). We obtained the parameters by the MCMC

**Table 124.** Ephemerides of eclipsing systems.

Object	Epoch (BJD)	Period (d)
OY Car	2457120.49413(2)	0.0631209131(5)
GP CVn	2455395.37115(4)	0.0629503676(9)
V893 Sco	2454173.3030(3)	0.0759614600(16)
MASTER J220559	2457658.72016(3)	0.0612858(3)
SDSS J115207	2457578.07695(6)	0.0677497014(14)

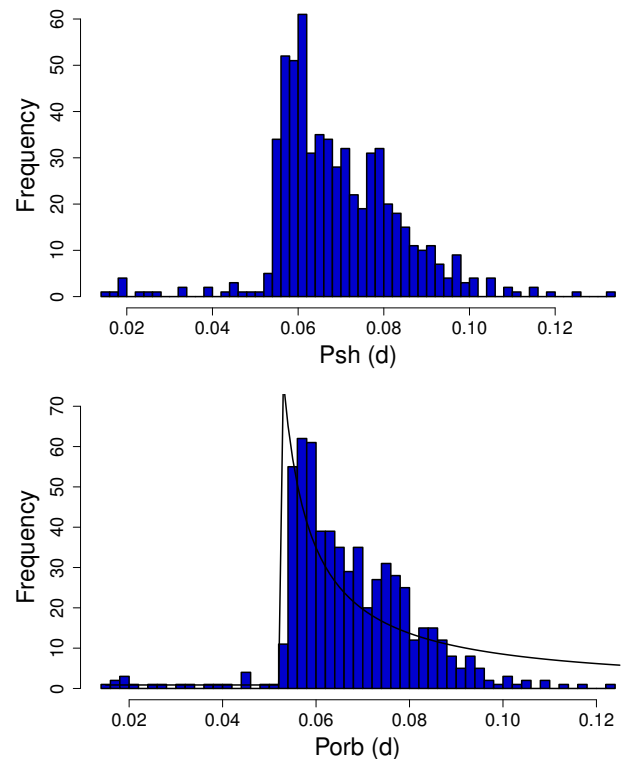


**Fig. 165.** Distribution of superhump periods in this survey. The data are from Kato et al. (2009), Kato et al. (2010), Kato et al. (2012a), Kato et al. (2013), Kato et al. (2014b), Kato et al. (2014a), Kato et al. (2015a), Kato et al. (2016a) and this paper. The mean values are used when multiple superoutbursts were observed. (Upper) distribution of superhump periods. (Lower) distribution of orbital periods. For objects with superhump periods shorter than 0.053 d, the orbital periods were assumed to be 1% shorter than superhump periods. For objects with superhump periods longer than 0.053 d, we used the calibration in Kato et al. (2012a) to estimate orbital periods. The line is the model distribution to determine the period minimum (equation 6, see text for the details).

method as follows:  $c_1 = 1.93(25)$ ,  $c_2 = 0.0471(7)$  and  $P_{\text{min}} = 0.052897(16)$ . The value of  $P_{\text{min}}$  is insensitive to the functional form above  $P_{\text{min}}$ . The resulting distribution is drawn as a line in the lower panel of figure 165.

Although the model does not properly reproduce the location of the period spike, the numbers of dwarf novae are lower than the best fit curve above  $P_{\text{orb}} \sim 0.09$  d. This appears to correspond to the period gap, contrary to our finding in Kato et al. (2016a).

### 4.3 Period derivatives during stage B

Figure 166 represents updated relation between  $P_{\text{dot}}$  for stage B versus  $P_{\text{orb}}$ . We have omitted poor quality observation (quality C) since Kato et al. (2016a) and simplified the symbols. The majority of new objects studied in this paper follow the trend presented in earlier papers.

### 4.4 Mass ratios from stage A superhumps

We list new estimates for  $q$  from stage A superhumps (Kato and Osaki 2013) in table 125. This table includes measurements of the objects in separate papers, which are listed in table 1. In table 126, we list all stage A superhumps recorded in the present study.

An updated distribution of mass ratios is shown in figure 167 [for the list of objects, see Kato and Osaki (2013), Kato et al. (2015a) and Kato et al. (2016a)]. We have newly added SDSS J105754.25+275947.5 (hereafter SDSS J105754) with  $P_{\text{orb}}=0.062792$  d and  $q=0.0546(20)$  (McAllister et al. 2017b, eclipse observation) and ASASSN-14ag with  $P_{\text{orb}}=0.060311$  d and  $q=0.149(16)$  (McAllister et al. 2017a, eclipse observation). It would be worth mentioning that McAllister et al. (2017b) classified SDSS J105754 as a period bouncer and we have two objects (ASASSN-16dt and ASASSN-16js) near the location of SDSS J105754. Both objects are likely identified as period bouncers and these detections demonstrate the efficiency of the stage A superhump method. The present study has strengthened the concentration of WZ Sge-type dwarf novae around  $q = 0.07$  just above the period minimum, as reported in Kato et al. (2015a) and Kato et al. (2016a).

### 4.5 WZ Sge-type objects

WZ Sge-type dwarf novae are a subclass of SU UMa-type dwarf novae characterized by the presence of early superhumps (Kato et al. 1996a; Kato 2002; Ishioka et al. 2002; see a recent review Kato 2015). They are seen during the earliest stages of a superoutburst, and have period almost equal to the orbital periods.

These early superhumps are considered to be a result of the 2:1 resonance (Osaki and Meyer 2002). These objects usually show very rare outbursts (once in several years to decades) with large outburst amplitudes (6–9 mag or even more, Kato 2015) and often have complex light curves (Kato 2015). The WZ Sge-type dwarf novae are of special astrophysical interest for several reasons. We list two of them: (1) From the point of view of outburst physics, the origin of the complex light curves, including repetitive rebrightenings, is not well understood. They

**Table 125.** New estimates for the binary mass ratio from stage A superhumps

Object	$\epsilon^*$ (stage A)	$q$ from stage A
HT Cas	0.0566(5)	0.171(2)
GS Cet	0.0288(8)	0.078(2)
GZ Cnc	0.081(3)	0.27(2)
IR Gem	0.068(11)	0.22(4)
HV Vir	0.034(1)	0.093(3)
ASASSN-16da	0.042(2)	0.12(1)
ASASSN-16dt	0.0135(7)	0.036(2)
ASASSN-16eg	0.0552(6)	0.166(2)
ASASSN-16hj	0.034(7)	0.09(2)
ASASSN-16iw	0.029(1)	0.079(2)
ASASSN-16jb	0.0321(5)	0.088(1)
ASASSN-16js	0.0213(16)	0.056(5)
ASASSN-16oi	0.033(2)	0.091(7)
ASASSN-16os	0.018(1)	0.047(3)
ASASSN-17bl	0.0235(9)	0.062(3)

are also considered to be analogous to black-hole X-ray transients which often show rebrightenings (cf. Kuulkers et al. 1996) and there may be common underlying physics between WZ Sge-type dwarf novae and black-hole X-ray transients. (2) From the point of view of CV evolution, they are considered to represent the terminal stage of CV evolution and they may have brown-dwarf secondaries. Studies of WZ Sge-type dwarf novae are indispensable when discussing the terminal stage of CV evolution, such as the period minimum and period bouncers (e.g. Knigge 2006; Knigge et al. 2011; Patterson 2011; Kato 2015). We used the period of early superhumps as the approximate orbital period (Kato et al. 2014a; Kato 2015; labeled as ‘E’ in table 3). In table 127, we list the parameters of WZ Sge-type dwarf novae (including likely ones).

It has been known that  $P_{\text{dot}}$  and  $P_{\text{orb}}$  are correlated with the rebrightening type [starting with figure 36 in Kato et al. 2009 and refined in Kato et al. (2009)–Kato et al. (2015a) and Kato (2015), and updated in Kato et al. (2016a)]. The five types of outbursts based on rebrightenings are: type-A outbursts [long-duration rebrightening; we include type-A/B introduced in Kato (2015)], type-B outbursts (multiple rebrightenings), type-C outbursts (single rebrightening), type-D outbursts (no rebrightening) and type-E outbursts (double superoutburst, with ordinary superhumps only during the second one). In figure 168, we show the updated result up to this paper. In this figure, we also added objects without known rebrightening types. These objects have been confirmed to follow the same trend, which we consider to represent the evolutionary track [see subsection 7.6 in Kato (2015)]. The

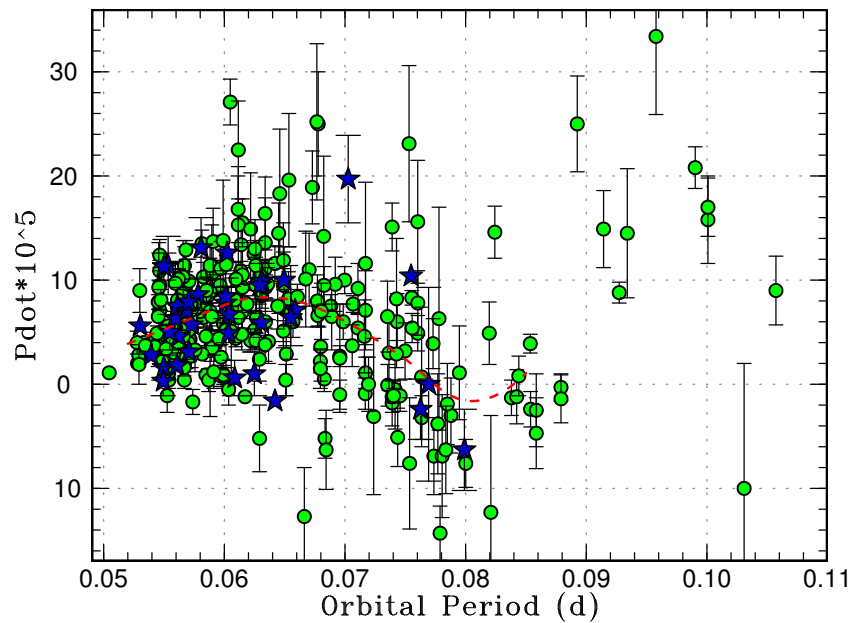


**Fig. 166.**  $P_{\dot{}}$  for stage B versus  $P_{orb}$ . Filled circles and filled stars represent samples in Kato et al. (2009)–Kato et al. (2016a) and this paper, respectively. The curve represents the spline-smoothed global trend.

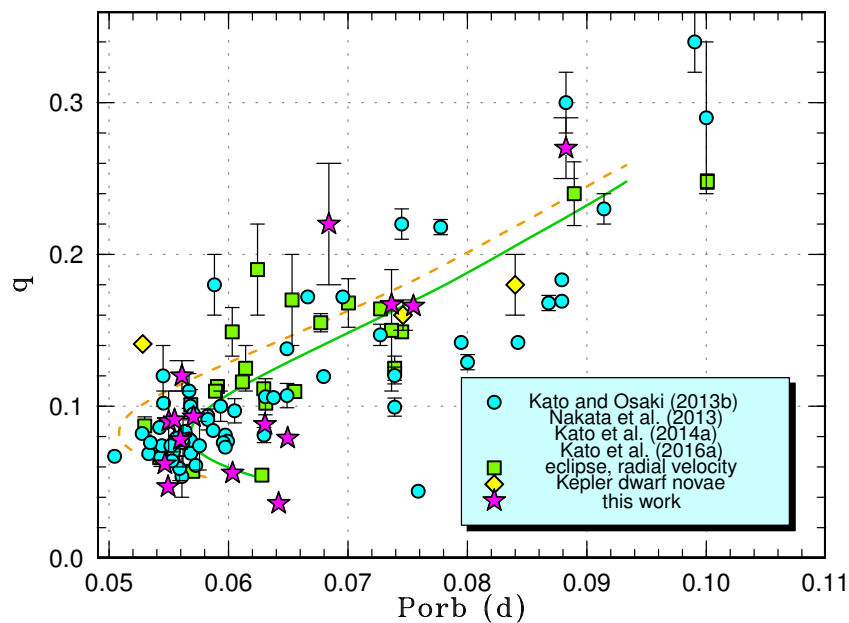


**Fig. 167.** Mass ratio versus orbital period. The dashed and solid curves represent the standard and optimal evolutionary tracks in Knigge et al. (2011), respectively. The filled circles, filled squares, filled stars, filled diamonds represent  $q$  values from a combination of the estimates from stage A superhumps published in four preceding sources (Kato and Osaki 2013; Nakata et al. 2013; Kato et al. 2014b; Kato et al. 2014a; Kato et al. 2015a; Kato et al. 2016a and references therein), known  $q$  values from quiescent eclipses or radial-velocity study,  $q$  estimated in this work and dwarf novae in the Kepler data (see text for the reference), respectively. The objects in “this work” includes objects studied in separate papers but listed in table 1.



**Table 126.** Superhump Periods during Stage A

Object	Year	period (d)	err
BB Ari	2016	0.07514	0.00007
HT Cas	2016	0.07807	0.00004
GS Cet	2016	0.05763	0.00027
GZ Cnc	2017	0.09599	–
V1113 Cyg	2016	0.08030	0.00018
IR Gem	2017	0.07315	0.00000
HV Vir	2016	0.05824	0.00001
ASASSN-13ak	2016	0.08884	0.00047
ASASSN-15cr	2017	0.06258	0.00014
ASASSN-16da	2016	0.05858	0.00010
ASASSN-16ds	2016	0.06856	0.00015
ASASSN-16dt	2016	0.06512	0.00001
ASASSN-16eg	2016	0.07989	0.00004
ASASSN-16hj	2016	0.05691	0.00031
ASASSN-16ib	2016	0.06036	0.00007
ASASSN-16ik	2016	0.06656	0.00010
ASASSN-16iw	2016	0.06691	0.00012
ASASSN-16jb	2016	0.06514	0.00003
ASASSN-16jd	2016	0.05840	0.00012
ASASSN-16js	2016	0.06165	0.00010
ASASSN-16ob	2016	0.05785	0.00016
ASASSN-16oi	2016	0.05738	0.00009
ASASSN-16os	2016	0.05596	0.00006
ASASSN-17bl	2017	0.05599	0.00004
CRTS J164950	2015	0.06641	0.00006
MASTER J021315	2016	0.10712	0.00025
MASTER J030205	2016	0.06275	0.00015
OT J002656	2016	0.13320	0.00003
TCP J013758	2016	0.06290	0.00056

outlier around  $P_{\text{orb}}=0.050$  d is ASASSN-15po, the object below the period minimum (Namekata et al. 2017). The two points around  $P_{\text{orb}}=0.079$  d is RZ Leo. As shown in subsection 3.17 in Kato et al. (2016a), the two superoutbursts in 2000 and 2016 were not sufficiently covered and  $P_{\text{dot}}$  values had large errors and we consider that these points are not very reliable.

#### 4.6 Objects with Very Short Supercycles

In this study, there were a group of four object with very short supercycles: NY Her [supercycle 63.5(2) d, subsection 3.14], 1RXS J161659 [89(1) d, subsection 3.27], CRTS J033349 [108(1) d, subsection 3.90] and SDSS J153015 [84.7(1.2) d, subsection 3.123]. We are not aware whether such a large number of detections were by chance or as a result of the recent change in detection policies of transients such as ASAS-SN. The most notable common fea-

tures of these objects are the small number of normal outbursts. Since the short supercycle reflects the high mass-transfer rate (cf. Osaki 1996), the small number of normal outbursts is unexpected.

A likely solution to this apparent inconsistency is the disk tilt, which would prevent the accreted matter accumulating in the outer edge of the disk and it would suppress normal outbursts (Ohshima et al. 2012; Osaki and Kato 2013a; Osaki and Kato 2013b). It has been also demonstrated that the prototypical example V503 Cyg (supercycle 89 d) showed negative superhumps (Harvey et al. 1995), which are considered to be a consequence of a disk tilt (e.g. Wood and Burke 2007; Montgomery and Bisikalo 2010). The temporary emergence of frequent normal outbursts in V503 Cyg (Kato et al. 2002b) also suggests that normal outbursts were somehow suppressed, most likely by a disk tilt. More recent examples in Kepler dwarf novae V1504 Cyg and V344 Lyr in relation to transiently appearing negative superhumps were discussed in Osaki and Kato (2013a), Osaki and Kato (2013b) and it has become more evident that the state with negative superhumps (i.e. the disk is likely tilted) is associated with the reduced number of normal outbursts.

It has been proposed that a high mass-transfer rate is prone to produce a disk tilt in a hydrodynamical model (Montgomery and Martin 2010). If it is indeed the case, the large number of SU UMa-type dwarf novae with few normal outbursts but with short supercycles may be a result of easy occurrence of a disk tilt in high-mass transfer systems and may not be surprising. A search for negative superhumps in the four systems reported in this paper is recommended. Long-term monitoring is also encouraged to see whether these objects switch the outburst mode as in V503 Cyg.

We should make a comment on another SU UMa-type dwarf nova V4140 Sgr with a short supercycle (80–90 d, Borges and Baptista 2005). Borges and Baptista (2005) and Baptista et al. (2016) used the eclipse mapping method and derived a conclusion that the distribution of the disk temperature in quiescence is incompatible with the disk-instability model and they interpreted that the outbursts in this object are caused by mass-transfer bursts from the secondary. We noticed that, despite its short supercycle, this object rarely shows normal outbursts (for example, there were no outburst between 2017 March 12 and April 16, observations by J. Hamsch). The object appears to be a V503 Cyg-like one and we can expect a disk tilt. The apparent deviation of the distribution of the disk temperature may have been caused by an accretion stream hitting the inner parts of the disk when the disk is tilted and may not be contradiction with the picture of the disk-

**Table 127.** Parameters of WZ Sge-type superoutbursts.

Object	Year	$P_{\text{SH}}^*$	$P_{\text{orb}}^\dagger$	$P_{\text{dot}}^\ddagger$	$\text{err}^\ddagger$	$\epsilon$	Type <sup>§</sup>	$N_{\text{reb}}^\parallel$	delay <sup>#</sup>	Max	Min
GS Cet	2016	0.056645	0.05597	6.3	0.6	0.012	–	–	8	13.0	20.4
ASASSN-16da	2016	0.057344	0.05610	7.5	0.9	0.022	–	–	5	15.1	21.5
ASASSN-16dt	2016	0.064507	0.064197	–1.6	0.5	0.005	E+C	2	23	13.4	21.1:
ASASSN-16eg	2016	0.077880	0.075478	10.4	0.8	0.032	C	1	6	12.7	19.4
ASASSN-16fu	2016	0.056936	0.05623	4.6	0.6	0.013	–	–	6	13.9	21.6
ASASSN-16gh	2016	0.061844	–	6.7	2.7	–	–	–	12	14.3	[22
ASASSN-16gj	2016	0.057997	–	7.0	1.0	–	A:	1	$\leq 9$	]13.3	21.3
ASASSN-16hg	2016	0.062371	–	0.6	1.7	–	A:	1	$\geq 6$	]14.1	21.6:
ASASSN-16hj	2016	0.055644	0.05499	11.3	1.3	0.012	A+B?	3	9	14.2	21.1:
ASASSN-16ia	2016	–	0.05696	–	–	–	–	–	–	14.6	[22
ASASSN-16is	2016	0.058484	0.05762	4.2	1.7	0.015	–	–	11	14.9	20.4
ASASSN-16iw	2016	0.065462	0.06495	10.0	3.2	0.008	B	5	7	13.9	21.9
ASASSN-16jb	2016	0.064397	0.06305	5.9	0.7	0.021	–	–	7	13.3	[21
ASASSN-16js	2016	0.060934	0.06034	4.9	1.0	0.010	–	–	10	13.0	20.1
ASASSN-16lo	2016	0.054608	0.05416	–	–	0.008	–	–	11	14.3	20.7:
ASASSN-16ob	2016	0.057087	–	1.8	0.5	–	–	–	13	13.8	[22
ASASSN-16oi	2016	0.056241	0.05548	5.0	1.7	0.014	–	–	8	13.4	22.0:
ASASSN-16os	2016	0.054992	0.05494	0.3	1.4	0.001	–	–	8	13.6	21.4:
ASASSN-17aa	2017	0.054591	0.05393	2.8	0.3	0.012	–	–	9	13.9	[22
ASASSN-17bl	2017	0.055367	0.05467	3.6	0.6	0.013	–	–	11	13.7	[22
ASASSN-17cn	2017	0.053991	0.05303	5.6	0.8	0.018	–	–	$\geq 9$	13.2	[22

\*Representative value ( $P_1$ ).

<sup>†</sup>Period of early superhumps.

<sup>‡</sup>Unit  $10^{-5}$ .

<sup>§</sup>A: long-lasting rebrightening; B: multiple rebrightenings; C: single rebrightening; D: no rebrightening.

<sup>||</sup>Number of rebrightenings.

<sup>#</sup>Days before ordinary superhumps appeared.

instability model. Since no other V503 Cyg-like objects are eclipsing, we have had no observation about the structure of the disk in V503 Cyg-like objects. We propose to study V4140 Sgr more closely for detecting negative superhumps, and searching for a switch in the outburst mode to test the possibility of the V503 Cyg-like nature.

## 5 Summary

We provided updated statistics of the period distribution. We obtained the period minimum of 0.05290(2) d and confirmed the presence of the period gap above  $P_{\text{orb}} \sim 0.09$  d. We refined the  $P_{\text{orb}}-P_{\text{dot}}$  relation of SU UMa-type dwarf novae, the updated evolutionary track using stage A superhumps and refined relationship between  $P_{\text{orb}}-P_{\text{dot}}$  versus the rebrightening type in WZ Sge-type dwarf novae. We also provide basic observational data of superoutbursts we studied for SU UMa-type dwarf novae.

The objects of special interest in this paper can be summarized as follows:

- Four objects (NY Her, 1RXS J161659, CRTS J033349 and SDSS J153015) have supercycles shorter than 100 d. These objects do not resemble ER UMa-type dwarf novae but show infrequent normal outbursts as in V503 Cyg. We consider that these properties may be caused by a tilted disk and we expect to detect negative superhumps in these systems.
- DDE 48 is likely an ER UMa-type dwarf nova. NSV 2026 also has a short supercycle but with frequent normal outbursts.
- ASASSN-16ia and ASASSN-16js are WZ Sge-type dwarf novae with large-amplitude early superhumps.
- ASASSN-16ia showed a precursor outburst prior to the WZ Sge-type superoutburst. This is the first certain case of such a precursor outburst in a WZ Sge-type superoutburst.
- ASASSN-16js has a low mass ratio and is most likely a period bouncer. ASASSN-16gh is also a candidate for a period bouncer.
- ASASSN-16iw is a WZ Sge-type dwarf nova with five

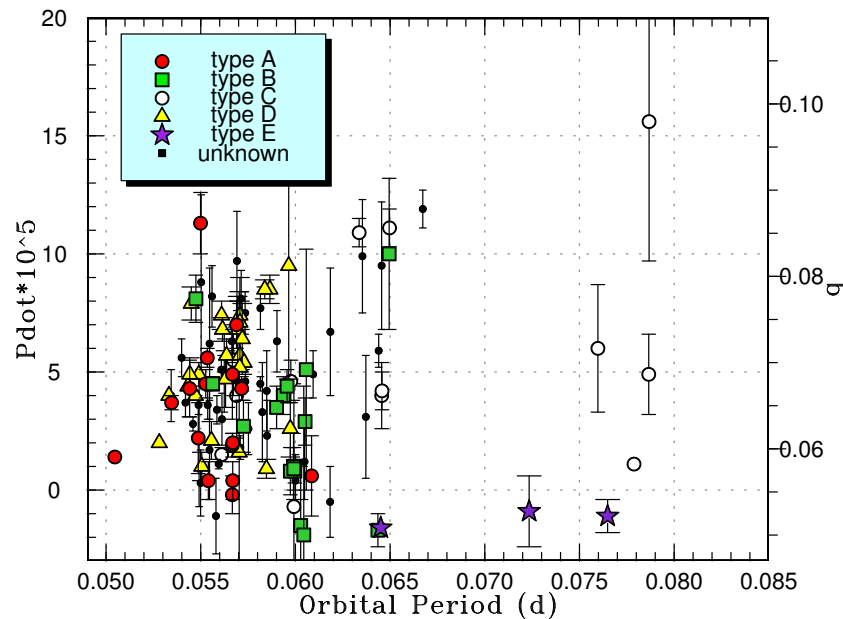


**Fig. 168.**  $P_{\text{dot}}$  versus  $P_{\text{orb}}$  for WZ Sge-type dwarf novae. Symbols represent the type of outburst: type-A (filled circles), type-B (filled squares), type-C (filled triangles), type-D (open circles) and type-E (filled stars) (see text for details). On the right side, we show mass ratios estimated using equation (6) in Kato (2015). We can regard this figure as to represent an evolutionary diagram.

post-superoutburst rebrightenings.

- MASTER J021315 is located in the period gap. This object likely showed long-lasting phase of stage A. Outbursts in this system were relatively rare and it should have a low mass-transfer rate.
- ASASSN-16kg, ASASSN-16ni, CRTS J000130 and SDSS J113551 are also SU UMa-type dwarf novae in the period gap. ASASSN-16ni is possibly an SU UMa-type dwarf nova in or above the period gap.
- ASASSN-16kg and ASASSN-16ni have large outburst amplitudes. ASASSN-16kg showed a rebrightening. These properties are uncommon among dwarf novae in the period gap.
- MASTER J030205 showed a likely spin period and it is likely a rare intermediate polar among SU UMa-type dwarf novae.
- Five objects OY Car, GP CVn, V893 Sco, MASTER J220559 and SDSS J115207 are eclipsing and we present refined eclipse ephemerides for some of them.

## Acknowledgements

This work was supported by the Grant-in-Aid “Initiative for High-Dimensional Data-Driven Science through Deepening of Sparse Modeling” (25120007) from the Ministry of Education, Culture, Sports, Science and Technology (MEXT) of Japan. This work was also partially supported by Grant VEGA 2/0008/17 and APVV-15-0458 (by Shugarov, Chochol, Sekeráš), NSH-

9670.2016.2 (Voloshina, Katysheva) RFBR 17-52-175300 (Voloshina), RSF-14-12-00146 (Golysheva for processing observations data from Slovak Observatory) and APVV-15-0458 (Dubovsky, Kudzej). ASAS-SN is supported by the Gordon and Betty Moore Foundation through grant GBMF5490 to the Ohio State University and NSF grant AST-1515927. The authors are grateful to observers of VSNET Collaboration and VSOLJ observers who supplied vital data. We acknowledge with thanks the variable star observations from the AAVSO International Database contributed by observers worldwide and used in this research. We are also grateful to the VSOLJ database. This work is helped by outburst detections and announcement by a number of variable star observers worldwide, including participants of CVNET and BAA VSS alert. The CCD operation of the Bronberg Observatory is partly sponsored by the Center for Backyard Astrophysics. We are grateful to the Catalina Real-time Transient Survey team for making their real-time detection of transient objects and the past photometric database available to the public. We are also grateful to the ASAS-3 team for making the past photometric database available to the public. This research has made use of the SIMBAD database, operated at CDS, Strasbourg, France. This research has made use of the International Variable Star Index (VSX) database, operated at AAVSO, Cambridge, Massachusetts, USA.

## Supporting information

(In the PASJ version): Additional supporting information can be found in the online version of this article: Tables. Figures.

Supplementary data is available at PASJ Journal online.

## References

- Ahn, C. P., et al. 2012, *ApJS*, 203, 21
- Antipin, S. V. 1999, *IBVS*, 4673, 1
- Arenas, J., & Mennickent, R. E. 1998, *A&A*, 337, 472
- Balanutsa, P., Denisenko, D., Gorbovskey, E., & Lipunov, V. 2013, *Perem. Zvezdy*, submitted (arXiv/1307.7396)
- Balanutsa, P., et al. 2014, *Astron. Telegram*, 5787
- Balanutsa, P., et al. 2016a, *Astron. Telegram*, 9174
- Balanutsa, P., et al. 2016b, *Astron. Telegram*, 9824
- Baptista, R., Borges, B. W., & Oliveira, A. S. 2016, *MNRAS*, 463, 3799
- Barwig, H., Mantel, K. H., & Ritter, H. 1992, *A&A*, 266, L5
- Belyavskii, S. I. 1936, *Perem. Zvezdy*, 5, 36
- Bernhard, K., Lloyd, C., Berthold, T., Kriebel, W., & Renz, W. 2005, *IBVS*, 5620, 1
- Bohlsen, T. 2016, *Astron. Telegram*, 9477
- Bond, H. E. 1978, *PASP*, 90, 526
- Borges, B. W., & Baptista, R. 2005, *A&A*, 437, 235
- Boyce, E. H. 1942, *Annals of the Astron. Obs. of Harvard Coll.* 109, 11
- Boyd, D., Krajci, T., Shears, J., & Poyner, G. 2007, *J. Br. Astron. Assoc.*, 117, 198
- Bruch, A., Steiner, J. E., & Gneiding, C. D. 2000, *PASP*, 112, 237
- Burenkov, A. N., & Voikhanskaia, N. F. 1979, *Soviet Astronomy Letters*, 5, 452
- Cleveland, W. S. 1979, *J. Amer. Statist. Assoc.*, 74, 829
- Coppejans, D. L., K rding, E. G., Knigge, C., Pretorius, M. L., Woudt, P. A., Groot, P. J., Van Eck, C. L., & Drake, A. J. 2016, *MNRAS*, 456, 4441
- Cutri, R. M., et al. 2003, *2MASS All Sky Catalog of point sources (NASA/IPAC Infrared Science Archive)*
- Davis, A. B., Shappee, B. J., Archer Shappee, B., & ASAS-SN 2015, *American Astron. Soc. Meeting Abstracts*, 225, #344.02
- Denisenko, D., et al. 2013a, *Astron. Telegram*, 5643
- Denisenko, D., et al. 2012, *Astron. Telegram*, 4441
- Denisenko, D., et al. 2013b, *Astron. Telegram*, 5182
- Denisenko, D. V. 2012, *Astron. Lett.*, 38, 249
- Drake, A. J., et al. 2009, *ApJ*, 696, 870
- Drake, A. J., et al. 2014, *MNRAS*, 441, 1186
- Drake, A. J., Mahabal, A., Djorgovski, S. G., Graham, M. J., Williams, R., Beshore, E. C., Larson, S. M., & Christensen, E. 2008, *Astron. Telegram*, 1479
- Duerbeck, H. W. 1984, *IBVS*, 2502
- Duerbeck, H. W. 1987, *Space Sci. Rev.*, 45, 1
- Echeistov, V., et al. 2014, *Astron. Telegram*, 5898
- Feinswog, L., Szkody, P., & Garnavich, P. 1988, *AJ*, 96, 1702
- Fernie, J. D. 1989, *PASP*, 101, 225
- Gaia Collaboration 2016, *VizieR Online Data Catalog*, 1337
- Gorbovskey, E. S., et al. 2013, *Astron. Rep.*, 57, 233
- Gress, O., et al. 2017, *Astron. Telegram*, 61
- Hameury, J.-M., & Lasota, J.-P. 2017, *A&A*, in press (arXiv/1703.03563)
- Han, Z.-T., Qian, S.-B., Fern andez Laj us, E., Liao, W.-P., & Zhang, J. 2015, *New Astron.*, 34, 1
- Harvey, D., Skillman, D. R., Patterson, J., & Ringwald, F. A. 1995, *PASP*, 107, 551
- Hirose, M., & Osaki, Y. 1990, *PASJ*, 42, 135
- Hirose, M., & Osaki, Y. 1993, *PASJ*, 45, 595
- Hoffleit, D. 1935, *Harvard Coll. Obs. Bull.*, 901, 20
- Hoffmeister, C. 1949, *Erg. Astron. Nachr.*, 12, 12
- Hoffmeister, C. 1964, *Astron. Nachr.*, 288, 49
- Hoffmeister, C. 1966, *Astron. Nachr.*, 289, 139
- Howell, S. B., Szkody, P., Kreidl, T. J., Mason, K. O., & Puchnarewicz, E. M. 1990, *PASP*, 102, 758
- Imada, A., et al. 2009, *PASJ*, 61, L17
- Imada, A., et al. 2006, *PASJ*, 58, 143
- Ishioka, R., Kato, T., Uemura, M., Iwamatsu, H., Matsumoto, K., Martin, B. E., Billings, G. W., & Novak, R. 2001, *PASJ*, 53, L51
- Ishioka, R., et al. 2003, *PASJ*, 55, 683
- Ishioka, R., Sekiguchi, K., & Maehara, H. 2007, *PASJ*, 59, 929
- Ishioka, R., et al. 2002, *A&A*, 381, L41
- Kapusta, A. B., & Thorstensen, J. R. 2006, *PASP*, 118, 1119
- Kato, T. 1994, *IBVS*, 4136
- Kato, T. 2001, *IBVS*, 5122
- Kato, T. 2002, *PASJ*, 54, L11
- Kato, T. 2015, *PASJ*, 67, 108
- Kato, T., et al. 2014a, *PASJ*, 66, 90
- Kato, T., et al. 2015a, *PASJ*, 67, 105
- Kato, T., et al. 2002a, *A&A*, 396, 929
- Kato, T., et al. 2013, *PASJ*, 65, 23
- Kato, T., et al. 2014b, *PASJ*, 66, 30
- Kato, T., et al. 2016a, *PASJ*, 68, 65
- Kato, T., Hamsch, F.-J., Oksanen, A., Starr, P., & Henden, A. 2015b, *PASJ*, 67, 3
- Kato, T., Hanson, G., Poyner, G., Muylaert, E., Reszelski, M., & Dubovsky, P. A. 2000, *IBVS*, 4932
- Kato, T., Haseda, K., Takamizawa, K., Kazarovets, E. V., & Samus, N. N. 1998, *IBVS*, 4585
- Kato, T., et al. 2009, *PASJ*, 61, S395
- Kato, T., Ishioka, R., & Uemura, M. 2002b, *PASJ*, 54, 1029
- Kato, T., & Kunjaya, C. 1995, *PASJ*, 47, 163
- Kato, T., et al. 2012a, *PASJ*, 64, 21
- Kato, T., Maehara, H., & Uemura, M. 2012b, *PASJ*, 64, 62
- Kato, T., et al. 2010, *PASJ*, 62, 1525
- Kato, T., Nogami, D., Baba, H., Matsumoto, K., Arimoto, J., Tanabe, K., & Ishikawa, K. 1996a, *PASJ*, 48, L21
- Kato, T., Nogami, D., Masuda, S., & Hirata, R. 1996b, *PASJ*, 48, 45
- Kato, T., & Osaki, Y. 2013, *PASJ*, 65, 115
- Kato, T., et al. 2016b, *PASJ*, 68, L4
- Kato, T., Sekine, Y., & Hirata, R. 2001, *PASJ*, 53, 1191
- Kato, T., Stubbings, R., Pearce, A., Nelson, P., & Monard, B. 2001a, *IBVS*, 5119, 1
- Kato, T., et al. 2017, *PASJ*, in press (arXiv/1703.00650)
- Kato, T., Uemura, M., Buczynski, D., & Schmeer, P. 2001b, *IBVS*, 5123
- Kato, T., Uemura, M., Ishioka, R., Nogami, D., Kunjaya, C., Baba, H., & Yamaoka, H. 2004, *PASJ*, 56, S1

- Kholopov, P. N., et al. 1985, General Catalogue of Variable Stars, fourth edition (Moscow: Nauka Publishing House)
- Kimura, M., et al. 2017, PASJ, submitted
- Kimura, M., et al. 2016, PASJ, 68, L2
- Knigge, C. 2006, MNRAS, 373, 484
- Knigge, C., Baraffe, I., & Patterson, J. 2011, ApJS, 194, 28
- Kukarkin, B. V., et al. 1982, New Catalogue of Suspected Variable Stars (Moscow: Nauka Publishing House)
- Kuulkers, E., Howell, S. B., & van Paradijs, J. 1996, ApJ, 462, L87
- Lasker, B., Lattanzi, M. G., McLean, B. J., & et al. 2007, VizieR Online Data Catalog, 1305
- Lazaro, C., Martinez-Pais, I. G., Arevalo, M. J., & Solheim, J. E. 1991, AJ, 101, 196
- Lázaro, C., Martinez-Pais, I. G., Solheim, J. E., & Arévalo, M. J. 1990, Ap&SS, 169, 257
- Leibowitz, E. M., Mendelson, H., Bruch, A., Duerbeck, H. W., Seitter, W. C., & Richter, G. A. 1994, ApJ, 421, 771
- Littlefair, S. P., Dhillon, V. S., Marsh, T. R., Gänsicke, B. T., Southworth, J., Baraffe, I., Watson, C. A., & Copperwheat, C. 2008, MNRAS, 388, 1582
- Littlefield, C., et al. 2013, AJ, 145, 145
- Liu, Wu., Hu, J. Y., Li, Z. Y., & Cao, L. 1999, ApJS, 122, 257
- Lubow, S. H. 1991, ApJ, 381, 259
- Lubow, S. H. 1992, ApJ, 401, 317
- Luckas, P. 2016, Astron. Telegram, 9678
- Markarian, B. E., & Stepanian, D. A. 1983, Astrofizika, 19, 639
- Mason, E., & Howell, S. 2003, A&A, 403, 699
- Matsumoto, K., Mennickent, R. E., & Kato, T. 2000, A&A, 363, 1029
- Mayall, M. W. 1968, JRASC, 62, 141
- Maza, J., Hamuy, M., Wischnjewsky, M., Wells, L., Phillips, M., & Barros, S. 1990, IAU Circ., 5073
- McAllister, M. J., et al. 2017a, MNRAS, 464, 1353
- McAllister, M. J., et al. 2017b, MNRAS, 467, 1024
- Meinunger, L. 1976, Mitteil. Veränderl. Sterne, 7
- Mennickent, R. E., Nogami, D., Kato, T., & Worraker, W. 1996, A&A, 315, 493
- Miller, W. J. 1971, Ricerche Astronomiche, 8, 167
- Montgomery, M. M. 2001, MNRAS, 325, 761
- Montgomery, M. M., & Bisikalo, D. V. 2010, MNRAS, 405, 1397
- Montgomery, M. M., & Martin, E. L. 2010, ApJ, 722, 989
- Morgenroth, O. 1933, Astron. Nachr., 250, 75
- Murray, J. R. 1998, MNRAS, 297, 323
- Nakata, C., et al. 2013, PASJ, 65, 117
- Namekata, K., et al. 2017, PASJ, 69, 2
- Niels Bohr Institute, U. o. C., Institute of Astronomy, UK, C., & Real Instituto y Observatorio de La Armada en San Fernando 2014, VizieR Online Data Catalog, 1327
- Ohshima, T., et al. 2012, PASJ, 64, L3
- Olech, A., Mularczyk, K., Kędzierski, P., Złoczewski, K., Wiśniewski, M., & Szaruga, K. 2006, A&A, 452, 933
- Olech, A., Złoczewski, K., Mularczyk, K., Kędzierski, P., Wiśniewski, M., & Stachowski, G. 2004, Acta Astron., 54, 57
- Osaki, Y. 1989, PASJ, 41, 1005
- Osaki, Y. 1996, PASP, 108, 39
- Osaki, Y., & Kato, T. 2013a, PASJ, 65, 50
- Osaki, Y., & Kato, T. 2013b, PASJ, 65, 95
- Osaki, Y., & Meyer, F. 2002, A&A, 383, 574
- Otulakowska-Hypka, M., Olech, A., de Miguel, E., Rutkowski, A., Koff, R., & Bakakowska, K. 2013, MNRAS, 429, 868
- Pastukhova, E. N. 1988, Astron. Tsirk., 1534, 17
- Patterson, J. 2011, MNRAS, 411, 2695
- Patterson, J., Bond, H. E., Grauer, A. D., Shafter, A. W., & Mattei, J. A. 1993, PASP, 105, 69
- Patterson, J., McGraw, J. T., Coleman, L., & Africano, J. L. 1981, ApJ, 248, 1067
- Patterson, J., et al. 2003, PASP, 115, 1308
- Pearson, K. J. 2006, MNRAS, 371, 235
- Pogrosheva, T., et al. 2016a, Astron. Telegram, 9509
- Pogrosheva, T., et al. 2016b, Astron. Telegram, 9510
- Pojmański, G. 2002, Acta Astron., 52, 397
- Popova, A. 1960, Mitteil. Veränderl. Sterne, 464
- Popova, E., et al. 2016, Astron. Telegram, 8843
- Popowa, M. 1961, Astron. Nachr., 286, 81
- Pretorius, M. L., Woudt, P. A., Warner, B., Bolt, G., Patterson, J., & Armstrong, E. 2004, MNRAS, 352, 1056
- Prieto, J. L., Chomiuk, L., Strader, J., Morrell, N., Stanek, K. Z., & Shappee, B. J. 2016, Astron. Telegram, 9479
- Prieto, J. L., et al. 2013, Astron. Telegram, 5102
- Quimby, R., & Mondol, P. 2006, Astron. Telegram, 787
- Robertson, J. W., Honeycutt, R. K., & Turner, G. W. 1995, PASP, 107, 443
- Ross, F. E. 1927, AJ, 37, 155
- Satyvoldiev, V. 1972, Astron. Tsirk., 711, 7
- Savoury, C. D. J., et al. 2011, MNRAS, 415, 2025
- Schmeer, P., Hurst, G. M., Kilmartin, P. M., & Gilmore, A. C. 1992, IAU Circ., 5502
- Schneller, H. 1931, Astron. Nachr., 243, 335
- Shafter, A. W., Cowley, A. P., & Szkody, P. 1984, ApJ, 282, 236
- Shappee, B. J., et al. 2014, ApJ, 788, 48
- Shears, J., Brady, S., Foote, J., Starkey, D., & Vanmunster, T. 2008, J. Br. Astron. Assoc., 118, 288
- Shumkov, V., et al. 2016a, Astron. Telegram, 9470
- Shumkov, V., et al. 2016b, Astron. Telegram, 9616
- Shurpakov, S., et al. 2012, Astron. Telegram, 4675
- Shurpakov, S., et al. 2013a, Astron. Telegram, 5657
- Shurpakov, S., et al. 2013b, Astron. Telegram, 5083
- Simonsen, M. 2011, J. American Assoc. Variable Star Obs., 39, 66
- Siviero, A., & Munari, U. 2016, Astron. Telegram, 9862
- Smart, R. L. 2013, VizieR Online Data Catalog, 1324
- Southworth, J., Copperwheat, C. M., Gänsicke, B. T., & Pyrzas, S. 2010, A&A, 510, A100
- Southworth, J., Marsh, T. R., Gänsicke, B. T., Aungwerowjit, A., Hakala, P., de Martino, D., & Lehto, H. 2007, MNRAS, 382, 1145
- Stanek, K. Z., et al. 2016a, Astron. Telegram, 9343
- Stanek, K. Z., et al. 2016b, Astron. Telegram, 9669
- Stanek, K. Z., et al. 2016c, Astron. Telegram, 9469
- Stanek, K. Z., et al. 2013, Astron. Telegram, 5082
- Stellingwerf, R. F. 1978, ApJ, 224, 953
- Szkody, P., et al. 2002, AJ, 123, 430
- Szkody, P., et al. 2009, AJ, 137, 4011
- Szkody, P., et al. 2003, AJ, 126, 1499
- Szkody, P., et al. 2006, AJ, 131, 973
- Szkody, P., et al. 2005, AJ, 129, 2386
- Szkody, P., et al. 2007, AJ, 134, 185
- Szkody, P., & Howell, S. B. 1992, ApJS, 78, 537

- Szkody, P., Ingram, D., Schmeer, P., Midtskogen, O., Dahle, H., & Bortle, J. E. 1992, IAU Circ., 5516
- Tappert, C., & Bianchini, A. 2003, A&A, 401, 1101
- Thorstensen, J. R., Fenton, W. H., Patterson, J. O., Kemp, J., Krajci, T., & Baraffe, I. 2002, ApJ, 567, L49
- Thorstensen, J. R., Taylor, C. J., Peters, C. S., Skinner, J. N., Southworth, J., & Gänsicke, B. T. 2015, AJ, 149, 128
- Tiurina, N., et al. 2013, Astron. Telegram, 4871
- Tsevevich, V. P. 1967, Second Supplement to General Catalogue of Variable Stars, second edition (Moscow: Astronomical Council of the Academy of Sciences in the USSR)
- Uemura, M., et al. 2002, PASJ, 54, L15
- Uemura, M., Mennickent, R., & Stubbings, R. 2004, IBVS, 5569
- Vladimirov, V., et al. 2013, Astron. Telegram, 5585
- Vladimirov, V., et al. 2014, Astron. Telegram, 5983
- Vogt, N. 1983, A&A, 118, 95
- Vogt, N., & Bateson, F. M. 1982, A&AS, 48, 383
- Wakamatsu, Y., et al. 2017, PASJ, submitted
- Walker, A. D., & Olmsted, M. 1958, PASP, 70, 495
- Warner, B. 1985, in *Interacting Binaries*, ed. P. P. Eggleton, & J. E. Pringle (Dordrecht: D. Reidel Publishing Company), p. 367
- Warner, B. 1995, *Cataclysmic Variable Stars* (Cambridge: Cambridge University Press)
- Wenzel, W. 1993a, *Mitteil. Veränderl. Sterne*, 12, 153
- Wenzel, W. 1993b, IBVS, 3921
- Whitehurst, R. 1988, MNRAS, 232, 35
- Williams, G. 1983, ApJS, 53, 523
- Williams, S. C., & Darnley, M. J. 2016, Astron. Telegram, 9375
- Wils, P., Gänsicke, B. T., Drake, A. J., & Southworth, J. 2010, MNRAS, 402, 436
- Witham, A. R., Knigge, C., Drew, J. E., Greimel, R., Steeghs, D., Gänsicke, B. T., Groot, P. J., & Mampaso, A. 2008, MNRAS, 384, 1277
- Wolf, M., & Wolf, G. 1906, *Astron. Nachr.*, 170, 361
- Wood, M. A., & Burke, C. J. 2007, ApJ, 661, 1042
- Wood, M. A., Still, M. D., Howell, S. B., Cannizzo, J. K., & Smale, A. P. 2011, ApJ, 741, 105
- Yamaoka, H., Itagaki, K., Kaneda, H., Jacques, C., Pimentel, E., Maehara, H., & Bolt, G. 2008, *Cent. Bur. Electron. Telegrams*, 1463
- Yecheistov, V., et al. 2013, Astron. Telegram, 5536
- Yecheistov, V., et al. 2014, Astron. Telegram, 5905
- Zengin Çamurdan, D., Ibanoglu, C., & M., Çamurdan C. 2010, *New Astron.*, 15, 476
- Zwitter, T., & Munari, U. 1996, A&AS, 117, 449

